



Universiteit
Leiden
The Netherlands

Dynamics and regulation of the oxidative stress response upon chemical exposure

Bischoff, L.J.M.

Citation

Bischoff, L. J. M. (2022, January 12). *Dynamics and regulation of the oxidative stress response upon chemical exposure*. Retrieved from <https://hdl.handle.net/1887/3249612>

Version: Publisher's Version

License: [Licence agreement concerning inclusion of doctoral thesis in the Institutional Repository of the University of Leiden](#)

Downloaded from: <https://hdl.handle.net/1887/3249612>

Note: To cite this publication please use the final published version (if applicable).

Dynamics and regulation of the oxidative stress response upon chemical exposure

Luc Bischoff

Cover design: L.J.M. Bischoff. Image based on Akiyoshi Kitaoka

Thesis lay-out: Douwe Oppewal

Printing: Ipskamp Printing, Enschede

ISBN: 978-94-6421-590-8

© Copyright, Luc Bischoff, 2021

All rights reserved. No part of this book may be reproduced in any form or by any means without permission of the author.

Dynamics and regulation of the oxidative stress response upon chemical exposure

Proefschrift

ter verkrijging van
de graad van doctor aan de Universiteit Leiden,
op gezag van rector magnificus prof. dr. ir. H. Bijl,
volgens besluit van het college voor promoties
te verdedigen op woensdag 12 januari 2022
klokke 11:15 uur

door
Lucas Jacobus Marie Bischoff
geboren te Boxmeer, Nederland,
in 1984

Promotor:

Prof. Dr. B. van de Water (Universiteit Leiden / LACDR)

Co-promotor:

Dr. D. Noort (TNO, Rijswijk)

Dr. J.P. Langenberg (TNO, Rijswijk)

Promotiecommissie:

Prof. Dr. H. Irth (Universiteit Leiden/ LACDR) (voorzitter)

Prof. Dr. J.A. Bouwstra (Universiteit Leiden/LACDR) (secretaris)

Prof. Dr. P. Jennings (VU Amsterdam)

Prof. Dr. E.C.M. de Lange (Universiteit Leiden/LACDR)

Dr. H. Vrieling (Leids Universitair Medisch Centrum)

The research described in this thesis was performed at the division of Drug Discovery & Safety of the Leiden Academic Centre for Drug Research (LACDR), Leiden University (Leiden, The Netherlands). The research was financially supported by the Ministry of Defence of the Netherlands and the European Commission Horizon2020 EU-ToxRisk project (Grant nr 681002).

INDEX

CHAPTER 1

General introduction and aim of the thesis 7

CHAPTER 2

MicroRNA patterns as biomarkers for chemical exposure and disease 21

CHAPTER 3

Screening the microRNA landscape of Nrf2 pathway modulation 45
Identifies miR-6499-3p as a novel modulator of the anti-oxidant response through targeting of KEAP1

CHAPTER 4

A systematic analysis of Nrf2 pathway activation dynamics during repeated xenobiotic exposure 95

CHAPTER 5

A systematic high throughput transcriptomics and phenotypic screening approach to classify the pro-oxidant mode-of-action of a large class of phenolic compounds 125

CHAPTER 6

General discussion and future prospects 155

CHAPTER 7

Appendices 169

1

General introduction and aim of the thesis

There is an increasing number of chemicals that enters the society, including drugs, environmental chemicals and cosmetics, combined also referred as the chemical exposome. Likewise there is an increased hazard for chemically-induced health effects. Chemicals can interfere with biological systems and induce compound specific responses, either related to the pharmacological on- or off-target effects. In particular compounds with (in)direct electrophilic reactivity are of direct harm to cells. Such compounds will interfere with normal cellular physiological processes and activate adaptive cellular stress responses that try to repair the cellular injury. Understanding the fundamental relationship between activation of these cellular stress responses and ultimate onset of cytotoxicity can be used for constructing mechanism-based biomarkers.

CLASSIFICATION AND USE OF BIOMARKERS

To establish whether exposure to a certain chemical or drug did or did not occur, or what the unwanted consequences are from exposure to a chemical or drug, appropriate biomarkers are needed. The broad definition of a biomarker, as stated by the World Health Organization (WHO), is: a biomarker is almost any measurement reflecting an interaction between a biological system and an environmental agent, which may be chemical, physical or biological (WHO, 1993). A more specific definition of a biomarker given by the WHO is: a biomarker is any substance, structure or process that can be measured in the body or its products and influence or predict the incidence or outcome of disease (WHO, 2001). The role of a biomarker can be interpreted as a “fingerprint” left behind in the body after exposure (with the analogy of the body as a “crime scene”). Many different classification systems of biomarkers are described in literature based on the information they provide or their intended use. Although classification of biomarkers in certain categories might be useful, one has to keep in mind that biomarkers might fit in different categories, depending on the knowledge we have regarding their link to the chemical exposure or disease mechanisms, as well as their intended use in a particular situation.

Manno et al. (2010), describes a classification system where biomarkers are divided in three different groups depending on their toxicological significance: biomarkers of susceptibility, biomarkers of exposure and biomarkers of effect (Manno et al. 2010). Another method of classification is described by Baker et al. (2005), who classifies biomarkers concerning their applications, for example: disease biomarkers and toxicity biomarkers (Baker 2005). Furthermore, with advancement in technology and knowledge of biological pathways and disease mechanisms, came the use of

biomarker panels, constructed of multiple biomarkers e.g. multiple genes or proteins representing a specific stress pathway, like for example inflammation. Based on this, Robinson et al. (2013), introduced the concept of “actionable” biomarkers, biomarkers that can be used to guide clinical management of disease and could even be used to diagnose diseases in their early, asymptomatic state (Robinson et al. 2013) (Figure 1). Two types of “actionable” biomarkers described by Robinson et al. (2013), are mechanistic biomarkers, which play a role in the mechanism of the disease, and descriptive biomarkers, which are not directly involved in the mechanism of disease, but are rather products of the disease or the damage induced by the disease. Antoine et al. (2013), describe a mechanistic biomarker for early and sensitive detection of acetaminophen-induced acute liver injury. They described a plasma derived biomarker panel consisting of miR-122, a microRNA highly specific for the liver, high mobility group box 1 (HMGB1) a marker of necrosis, and caspase-cleaved keratin-18 (K18) a marker of necrosis and apoptosis (Antoine et al. 2013). This biomarker panel proved to be more sensitive than the measurement of alanine transaminase (ALT) a well-established biomarker for assessing the health status of the liver. This indicates that mechanistic biomarkers existing of several proteins and microRNAs related to certain stress response pathways, can provide information concerning the molecular mechanisms of action of a chemical upon exposure. In the field of pharmacology, there is great need for mechanistic biomarkers, as these markers might have the ability to predict the response of a drug and thereby provide information which can be used to develop personal-based medicine approaches (Amadoz et al. 2015). However, it might be clear that for the construction of these (mechanistic) biomarker panels a greater understanding is needed regarding the different players (proteins, genes, microRNAs) of the different stress response pathways, as well as their interactions and changes over time (dynamics of the stress response pathway). Therefore, guided by the advancement in omics techniques, much research is targeted on unraveling the mechanisms of stress response pathways such as the DNA-damage response, unfolded protein response, and oxidative stress response. Moreover, microRNAs are promising small non-coding RNAs that could serve as biomarkers for small injury and can also modulate cellular biology including toxic responses. Since oxidative stress and microRNAs are central in this thesis, below these topics will be specifically addressed in some detail.

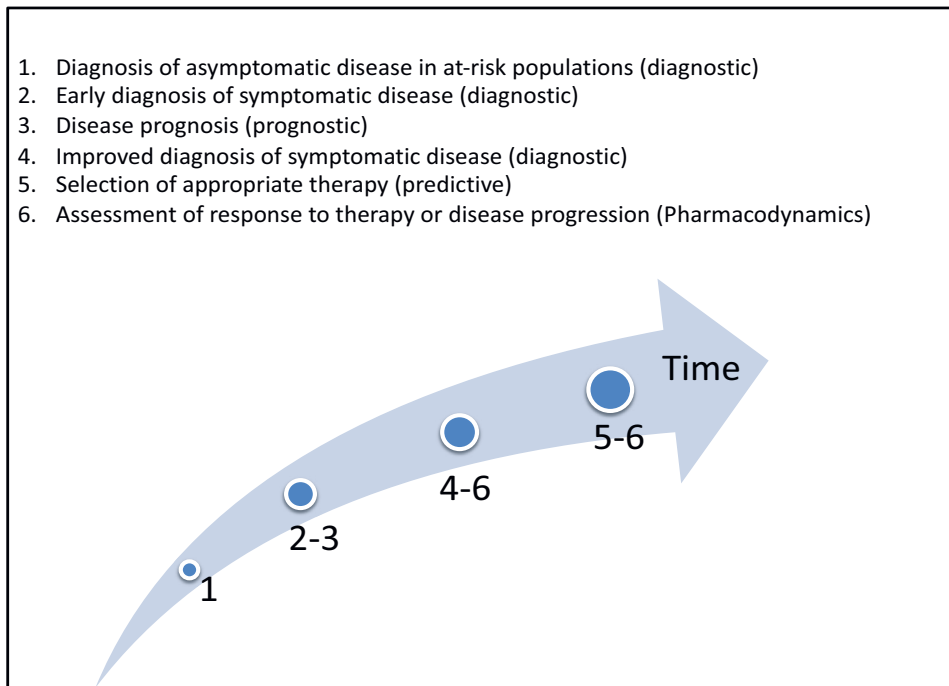


Figure 1. Use of actionable biomarkers over time.

(Modified from Robinson et al. 2013).

THE OXIDATIVE STRESS RESPONSE PATHWAY

In a cell there is a continuous production of reactive oxygen (ROS) and nitrogen species (RNS) (Finkel and Holbrook 2000). ROS and RNS are generated as a result of internal metabolism, for example aerobic respiration in mitochondria, and exposure to exogenous toxicants (Filomeni et al. 2015; Ma 2013; Turrens 2003). A controlled production of ROS and RNS has been described in literature to contribute to the regulation of various physiological processes in the cell like proliferation, autophagy and inflammation (Finkel 2011). However, uncontrolled production of ROS and RNS, called oxidative stress, can result in inflammatory responses and eventually lead to pathological conditions like cancer and neurodegenerative disorders (Prasad et al. 2017).

To overcome oxidative stress, a cell has several mechanisms to protect itself against oxidative stress. One of the most important mechanisms against oxidative stress is the Nrf2 pathway (Figure 2), named after its transcription factor, nuclear factor erythroid 2-related factor 2 (Nrf2). Not surprisingly, the Nrf2 pathway plays a role

in many diseases including cancer and neurodegenerative diseases like Alzheimer's disease (Bryan et al. 2013; Deshmukh et al. 2017). It is reported that in many different tumor cells Nrf2 is overexpressed, consequently making these cells less vulnerable for chemotherapy (Kensler and Wakabayashi 2010; Ren et al. 2011; Tang et al. 2011; Wang et al. 2008).

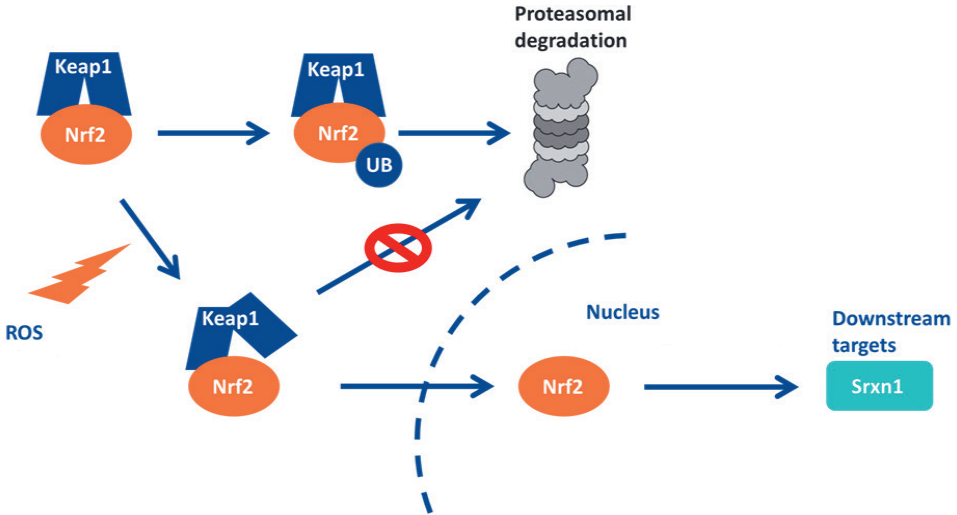


Figure 2. The Nrf2 pathway: the “cyclic sequential attachment and regeneration” model.

Nuclear factor E2-related factor 2 (Nrf2) is a transcription factor that upregulates expression of a battery of genes to combat oxidative and electrophilic stress. Modification of Kelch-like ECH-associated protein 1 (Keap1) by reactive oxygen species stabilizes Nrf2 by escaping from degradation. Nrf2 then is able to move freely to the nucleus, where it activates many different antioxidants like Srxn1.

Canonical activation of the Nrf2 pathway

In basal conditions, Nrf2 is bound in the cytoplasm to two Kelch-like ECH-associated protein 1 proteins (Keap1) (Keum and Choi 2014; Zipper and Mulcahy 2002). Nrf2 consists of seven functional domains (Neh1 – Neh7). Of these domains Neh2 contains seven lysine residues, which plays a role in the ubiquitination of Nrf2 (Itoh et al. 1999; Zhang et al. 2004), which facilitates the destruction of Nrf2 via the ubiquitin-26S proteasomal pathway (Kobayashi et al. 2004). Furthermore, the Neh2 domain contains two binding sites which interact with Keap1. These are the ETGE and DLG motives (McMahon et al. 2006).

Keap1 is an adaptor for Cullin-3 (Cul3)-based E3 ubiquitin ligase, which facilitates poly-ubiquitin conjugation to Nrf2, and therefore degradation by the proteasome

(Kobayashi et al. 2004). Keap1 consists of three functional domains. A broad complex/tramtrack/bric-a-brac (BTB) domain, which binds to Cul3 and is required for the dimerization of Keap1 (Zipper and Mulcahy 2002). An intervening region (IVR), and a kelch/double glycine repeat (DGR) domain, which interacts with the Neh2 domain of Nrf2 (Canning et al. 2015). Furthermore, human Keap1 contains 27 cysteine residues (Zhang and Hannink 2003). These cysteine residues can interact with ROS and electrophilic compounds, leading to Nrf2 pathway activation. Interestingly, chemicals show different affinity for the different cysteine groups (Takaya et al. 2012).

In literature, different models can be found describing how, upon activation, Nrf2 enters the nucleus to bind to the antioxidant response element (ARE) and starts the transcription of different antioxidants. Early models described total dissociation of Nrf2 from Keap1, but latest understanding suggest models like the 'two-site recognition hinge-and-latch' and abandoned the idea of total dissociation of Nrf2 from Keap1. The two-site recognition hinge-and-latch model, is named after the Nrf2 motives ETGE (hinge) and DLG (latch) (Tong et al. 2006b). Keap1 has a higher affinity for the hinge than for the latch (Tong et al. 2006a). Subsequently, Keap1 binds first to the ETGE domain and after the connection is established to the DLG domain.

Covalent binding of ROS or reactive metabolites to one of the cysteine groups of Keap1 is thought to induce a conformational change in the IVR domain of Keap1, decreasing the binding from Keap1 with Cul3 and dissociation of the DLG domain (Cleasby et al. 2014). The ETGE domain, which has a tighter interaction than the DLG domain, does not dissociate from Keap1 (Suzuki and Yamamoto 2015; Tong et al. 2007). Moreover, because of the dissociation of the DLG domain, Nrf2 is not targeted for degradation. As a consequence, *de novo* synthesized Nrf2 is able to translocate to the nucleus. In the nucleus Nrf2 will bind to the ARE, together with members of the masculoaponeurotic fibrosarcoma (Maf) proteins (MafF, MafG and MafK), which facilitates binding to the ARE. Binding to the ARE results in the transcription of different cytoprotective genes involved in e.g. glutathione metabolism, phase 2 drug-metabolizing enzymes and antioxidant response proteins as, for example, sulfiredoxin1 (Srxn1), hemeoxygenase 1 (Hmox1), and NAD(P)H-quinone oxidoreductase 1 (Nqo1) (Hayes et al. 2010; Zhang and Gordon 2004).

In parallel with the above described inhibition of ubiquitination of Nrf2, binding of an electrophilic compound can trigger the ubiquitination of Keap1 by the Cul3-Rbx1 complex decreasing the levels of Keap1, resulting in the movement of *de novo* synthesized Nrf2 into the nucleus (Hong et al. 2005). Unlike degradation of ubiquitinated Nrf2, Keap1 degradation is independent of the proteasome pathway (Zhang et al. 2005).

Different mechanisms of Nrf2 pathway termination are described in literature. Sun et al. (2007), suggest a mechanism whereby Nrf2 is transported back to the cytoplasm by Keap1, which has a nuclear export sequence (Sun et al. 2007). Furthermore, transcription regulator protein Bach1 can bind to the ARE and is therefore able to compete with Nrf2 (Tkachev et al. 2011). Kaspar and Jaiswal (2010), describes that Nrf2 regulates its own degradation through increasing Cul3-Rbx1 expression upon binding to the ARE and thereby inducing promoter activity of Cul3-Rbx1 genes (Kaspar and Jaiswal 2010).

Interactions with other adaptive pathways: non-canonical Nrf2 pathway activation

Numerous studies describe the interaction of the Nrf2 pathway with other adaptive stress response pathways like, for example, the DNA-damage response, the unfolded protein response and the NF- κ B-signaling pathway.

Interaction with the DNA damage response

Faraonio et al. (2006), showed that p53, a key player in the DNA damage response, negatively regulates Nrf2-mediated gene transcription (Faraonio et al. 2006). However, the KRR motif in p21, a downstream target of p53, is able to bind to the DLG and ETGE motifs within Nrf2, blocking the binding of Nrf2 with Keap1. Consequently, ubiquitination cannot take place, which in turn leads to activation of the Nrf2 pathway (Chen et al. 2009).

Interaction with the unfolded protein response

Oxidative stress can result in endoplasmic reticulum stress (ERS) (Digaleh et al. 2013). ERS might in turn lead to activation of the unfolded protein response (UPR). The UPR roughly exists of three major branches, which consists of three transmembrane sensors: transcription factor 6 (ATF6), inositol-requiring enzyme-1 α (IRE1) and protein kinase-like ER kinase (PERK) (Hetz 2012). PERK-dependent phosphorylation promotes the dissociation of Nrf2 from Keap1, and therefore activation of the Nrf2 pathway (Cullinan et al. 2003; Zhu et al. 2015).

Interaction with the NF- κ B-signaling pathway

Wardyn et al. (2015), described the crosstalk between NF- κ B and Nrf2, with increased activity of NF- κ B in the absence of Nrf2 (Wardyn et al. 2015). Furthermore, ROS can oxidize cysteine residues in the DNA binding domain of NF- κ B (Hirota et al. 1999). Moreover, I κ B kinase β (IKK β) is a substrate analogue of Keap1 (Kim et al. 2010). Jiang et al. (2013), found that, like Nrf2, IKK β has a ETGE motif (Jiang et al. 2013). This makes it possible for IKK β to bind to Keap1, and therefore to compete with Nrf2. Consequently, Keap1 is responsible for IKK β ubiquitination and therefore

degradation, and therefore downregulation of NF- κ B (Lee et al. 2009). Furthermore, AP-1 factors as c-Fos and Jun-D are also known to bind to the ARE. Binding of these factors blocks the binding site of the ARE for Nrf2 resulting in a decrease of its downstream targets (Li and Jaiswal 1992; Venugopal and Jaiswal 1996; Wilkinson et al. 1998). Recently it became clear that besides genes and proteins another class of signaling molecules play an important role in the regulation of stress response pathways: microRNAs.

MICRORNAS

MicroRNAs (miRNAs or miRs) are small (~22-nt) non-coding RNAs (Starega-Roslan et al. 2010). MicroRNAs regulate gene expression at the post-transcriptional level and are involved in many biological processes. MicroRNA target sites are typically located on the 3'untranslated region of their target mRNAs. These target sites only need to be partially complementary to the microRNA (Lam et al. 2015), which leads to target mRNA translational repression or degradation (Djuranovic et al. 2012; Filipowicz et al. 2008). A single microRNA can have about 100 target sites (Brennecke et al. 2005), and mRNAs can be targeted by more than one single microRNA (Peter 2010; Wu et al. 2010).

MicroRNAs are involved in many physiological processes including the immune response, metabolism, and development (Hou et al. 2011). Furthermore, microRNAs are involved in toxicological responses (Mendell and Olson 2012) including activation/inhibition of stress response pathways (Bartoszewska et al. 2013). Therefore microRNAs also play a role in diseases like, for example, (various types of) cancer (Meng et al. 2016) and other pathologies like acute myocardial infarction (Devaux et al. 2012). Moreover, some microRNAs exist which are highly "tissue specific", meaning they are abundantly present in a certain tissue type, as for example miR-122 is tissue specific for the liver. Measurement of these microRNAs might provide information regarding the organs which are damaged upon chemical exposure, because of their high concentration in the bloodstream after tissue damage occurred (Laterza et al. 2009). Altogether, these features make microRNAs interesting candidates for biomarkers for exposure and disease.

Understanding the fundamental relationship between activation of cellular stress responses and ultimate onset of cytotoxicity is of critical importance. As described above, knowledge of stress pathway behavior on protein, gene, and microRNA level can be applied in the construction of a mechanistic biomarker fingerprint.

THESIS OUTLINE

1

The focus of the described research in this thesis is on the oxidative stress response (Nrf2 pathway). The aim of the research presented in this thesis is to obtain more information concerning microRNAs which are involved in the Nrf2 pathway to determine and evaluate the application of microRNAs for the construction of novel mechanistic biomarkers. Furthermore, we aimed to obtain a better understanding with respect to the dynamics of the Nrf2 pathway to repeated xenobiotic exposure. In **Chapter 2**, microRNAs are introduced and their utility as biomarkers of chemical exposure and disease (effect) is reviewed in respect to the current knowledge of this upcoming field. As shown in **Chapter 2**, exposure to chemicals can lead to overexpression of certain microRNAs. In **Chapter 3**, to investigate the effect of overexpression of microRNAs on the Nrf2 pathway response in general and in combination with chemical exposure, a microRNA mimic screen was performed. In this screen overexpression of microRNAs was induced by using synthetic microRNA mimics. Since repeated exposure may drive adaptation programs and may lead to different responses between single and repeated exposures, in **Chapter 4** the effect of a second exposure on the dynamics of the Nrf2 pathway activation was conducted. In **Chapter 5** results of a study are shown where a panel of structurally different phenolic compounds were used to demonstrate the proof-of-concept that Nrf2 pathway reporters can successfully be applied as biomarkers to characterize the specific pro-oxidant responses of chemicals. Finally, in **Chapter 6** the findings of the studies described in this thesis are discussed and an overview is provided concerning future perspectives and implications of the included studies.

REFERENCES

- Amadoz A, Sebastian-Leon P, Vidal E, Salavert F, Dopazo J (2015) Using activation status of signaling pathways as mechanism-based biomarkers to predict drug sensitivity. *Sci Rep* 5:18494 doi:10.1038/srep18494
- Antoine DJ, Dear JW, Lewis PS, et al. (2013) Mechanistic biomarkers provide early and sensitive detection of acetaminophen-induced acute liver injury at first presentation to hospital. *Hepatology* 58(2):777-87 doi:10.1002/hep.26294
- Baker M (2005) In biomarkers we trust? *Nature Biotechnology* 23(3):297-304 doi:10.1038/nbt0305-297
- Bartoszewska S, Kochan K, Madanecki P, et al. (2013) Regulation of the unfolded protein response by microRNAs. *Cell Mol Biol Lett* 18(4):555-578 doi:10.2478/s11658-013-0106-z
- Brennecke J, Stark A, Russell RB, Cohen SM (2005) Principles of microRNA-target recognition. *PLoS Biol* 3(3):e85 doi:10.1371/journal.pbio.0030085
- Bryan HK, Olayanju A, Goldring CE, Park BK (2013) The Nrf2 cell defence pathway: Keap1-dependent and -independent mechanisms of regulation. *Biochem Pharmacol* 85(6):705-17 doi:10.1016/j.bcp.2012.11.016
- Canning P, Sorrell FJ, Bullock AN (2015) Structural basis of Keap1 interactions with Nrf2. *Free Radic Biol Med* 88(Pt B):101-107 doi:10.1016/j.freeradbiomed.2015.05.034
- Chen W, Sun Z, Wang XJ, et al. (2009) Direct interaction between Nrf2 and p21(Cip1/WAF1) upregulates the Nrf2-mediated antioxidant response. *Mol Cell* 34(6):663-73 doi:10.1016/j.molcel.2009.04.029
- Cleasby A, Yon J, Day PJ, et al. (2014) Structure of the BTB domain of Keap1 and its interaction with the triterpenoid antagonist CDDO. *PLoS One* 9(6):e98896 doi:10.1371/journal.pone.0098896
- Cullinan SB, Zhang D, Hannink M, Arvisais E, Kaufman RJ, Diehl JA (2003) Nrf2 Is a Direct PERK Substrate and Effector of PERK-Dependent Cell Survival. *Molecular and Cellular Biology* 23(20):7198-7209 doi:10.1128/mcb.23.20.7198-7209.2003
- Deshmukh P, Unni S, Krishnappa G, Padmanabhan B (2017) The Keap1-Nrf2 pathway: promising therapeutic target to counteract ROS-mediated damage in cancers and neurodegenerative diseases. *Biophys Rev* 9(1):41-56 doi:10.1007/s12551-016-0244-4
- Devaux Y, Vausort M, Goretti E, et al. (2012) Use of Circulating MicroRNAs to Diagnose Acute Myocardial Infarction. *Clinical Chemistry* 58(3):559 doi:10.1373/clinchem.2011.173823
- Digaleh H, Kiaei M, Khodagholi F (2013) Nrf2 and Nrf1 signaling and ER stress crosstalk: implication for proteasomal degradation and autophagy. *Cellular and Molecular Life Sciences* 70(24):4681-4694 doi:10.1007/s00018-013-1409-y
- Djuranovic S, Nahvi A, Green R (2012) miRNA-Mediated Gene Silencing by Translational Repression Followed by mRNA Deadenylation and Decay. *Science* 336(6078):237 doi:10.1126/science.1215691
- Faraonio R, Vergara P, Di Marzo D, et al. (2006) p53 suppresses the Nrf2-dependent transcription of antioxidant response genes. *J Biol Chem* 281(52):39776-84 doi:10.1074/jbc.M605707200
- Filipowicz W, Bhattacharyya SN, Sonenberg N (2008) Mechanisms of post-transcriptional regulation by microRNAs: are the answers in sight? *Nature Reviews Genetics* 9(2):102-114 doi:10.1038/nrg2290
- Filomeni G, De Zio D, Cecconi F (2015) Oxidative stress and autophagy: the clash between damage and metabolic needs. *Cell Death Differ* 22(3):377-388 doi:10.1038/cdd.2014.150
- Finkel T (2011) Signal transduction by reactive oxygen species. *The Journal of Cell Biology* 194(1):7 doi:10.1083/jcb.201102095

- Finkel T, Holbrook NJ (2000) Oxidants, oxidative stress and the biology of ageing. *Nature* 408(6809):239-247 doi:10.1038/35041687
- Hayes JD, McMahon M, Chowdhry S, Dinkova-Kostova AT (2010) Cancer Chemoprevention Mechanisms Mediated Through the Keap1–Nrf2 Pathway. *Antioxidants & Redox Signaling* 13(11):1713-1748 doi:10.1089/ars.2010.3221
- Hetz C (2012) The unfolded protein response: controlling cell fate decisions under ER stress and beyond. *Nature Reviews Molecular Cell Biology* 13(2):89-102 doi:10.1038/nrm3270
- Hirota K, Murata M, Sachi Y, et al. (1999) Distinct Roles of Thioredoxin in the Cytoplasm and in the Nucleus: A TWO-STEP MECHANISM OF REDOX REGULATION OF TRANSCRIPTION FACTOR NF- κ B. *Journal of Biological Chemistry* 274(39):27891-27897 doi:10.1074/jbc.274.39.27891
- Hong F, Sekhar KR, Freeman ML, Liebler DC (2005) Specific patterns of electrophile adduction trigger Keap1 ubiquitination and Nrf2 activation. *J Biol Chem* 280(36):31768-75 doi:10.1074/jbc.M503346200
- Hou L, Wang D, Baccarelli A (2011) Environmental chemicals and microRNAs. *Mutat Res* 714(1-2):105-12 doi:10.1016/j.mrfmmm.2011.05.004
- Itoh K, Wakabayashi N, Katoh Y, et al. (1999) Keap1 represses nuclear activation of antioxidant responsive elements by Nrf2 through binding to the amino-terminal Neh2 domain. *Genes & Development* 13(1):76-86 doi:10.1101/gad.13.1.76
- Jiang Z-Y, Chu H-X, Xi M-Y, et al. (2013) Insight into the Intermolecular Recognition Mechanism between Keap1 and IKK β Combining Homology Modelling, Protein-Protein Docking, Molecular Dynamics Simulations and Virtual Alanine Mutation. *PLOS ONE* 8(9):e75076 doi:10.1371/journal.pone.0075076
- Kaspar JW, Jaiswal AK (2010) An autoregulatory loop between Nrf2 and Cul3-Rbx1 controls their cellular abundance. *J Biol Chem* 285(28):21349-58 doi:10.1074/jbc.M110.121863
- Kensler TW, Wakabayashi N (2010) Nrf2: friend or foe for chemoprevention? *Carcinogenesis* 31(1):90-9 doi:10.1093/carcin/bgp231
- Keum YS, Choi BY (2014) Molecular and chemical regulation of the Keap1-Nrf2 signaling pathway. *Molecules* 19(7):10074-89 doi:10.3390/molecules190710074
- Kim J-E, You D-J, Lee C, Ahn C, Seong JY, Hwang J-I (2010) Suppression of NF- κ B signaling by KEAP1 regulation of IKK β activity through autophagic degradation and inhibition of phosphorylation. *Cellular Signalling* 22(11):1645-1654 doi:https://doi.org/10.1016/j.cellsig.2010.06.004
- Kobayashi A, Kang MI, Okawa H, et al. (2004) Oxidative stress sensor Keap1 functions as an adaptor for Cul3-based E3 ligase to regulate proteasomal degradation of Nrf2. *Mol Cell Biol* 24(16):7130-9 doi:10.1128/MCB.24.16.7130-7139.2004
- Lam JKW, Chow MYT, Zhang Y, Leung SWS (2015) siRNA Versus miRNA as Therapeutics for Gene Silencing. *Molecular Therapy - Nucleic Acids* 4:e252 doi:https://doi.org/10.1038/mtna.2015.23
- Laterza OF, Lim L, Garrett-Engle PW, et al. (2009) Plasma MicroRNAs as Sensitive and Specific Biomarkers of Tissue Injury. *Clinical Chemistry* 55(11):1977 doi:10.1373/clinchem.2009.131797
- Lee D-F, Kuo H-P, Liu M, et al. (2009) KEAP1 E3 Ligase-Mediated Downregulation of NF- κ B Signaling by Targeting IKK β . *Molecular Cell* 36(1):131-140 doi:https://doi.org/10.1016/j.molcel.2009.07.025
- Li Y, Jaiswal AK (1992) Regulation of human NAD(P)H:quinone oxidoreductase gene. Role of AP1 binding site contained within human antioxidant response element. *Journal of Biological Chemistry* 267(21):15097-104
- Ma Q (2013) Role of Nrf2 in Oxidative Stress and Toxicity. *Annual Review of Pharmacology and Toxicology* 53(1):401-426 doi:10.1146/annurev-pharmtox-011112-140320

- Manno M, Viau C, in collaboration w, et al. (2010) Biomonitoring for occupational health risk assessment (BOHRA). *Toxicol Lett* 192(1):3-16 doi:10.1016/j.toxlet.2009.05.001
- McMahon M, Thomas N, Itoh K, Yamamoto M, Hayes JD (2006) Dimerization of substrate adaptors can facilitate cullin-mediated ubiquitylation of proteins by a "tethering" mechanism: a two-site interaction model for the Nrf2-Keap1 complex. *J Biol Chem* 281(34):24756-68 doi:10.1074/jbc.M601119200
- Mendell JT, Olson EN (2012) MicroRNAs in stress signaling and human disease. *Cell* 148(6):1172-87 doi:10.1016/j.cell.2012.02.005
- Meng X, Müller V, Milde-Langosch K, Trillsch F, Pantel K, Schwarzenbach H (2016) Diagnostic and prognostic relevance of circulating exosomal miR-373, miR-200a, miR-200b and miR-200c in patients with epithelial ovarian cancer. *Oncotarget* 7(13):16923-16935 doi:10.18632/oncotarget.7850
- Peter ME (2010) Targeting of mRNAs by multiple miRNAs: the next step. *Oncogene* 29(15):2161-2164 doi:10.1038/onc.2010.59
- Prasad S, Gupta SC, Tyagi AK (2017) Reactive oxygen species (ROS) and cancer: Role of antioxidative nutraceuticals. *Cancer Lett* 387:95-105 doi:10.1016/j.canlet.2016.03.042
- Ren D, Villeneuve NF, Jiang T, et al. (2011) Brusatol enhances the efficacy of chemotherapy by inhibiting the Nrf2-mediated defense mechanism. *Proc Natl Acad Sci U S A* 108(4):1433-8 doi:10.1073/pnas.1014275108
- Robinson WH, Lindstrom TM, Cheung RK, Sokolove J (2013) Mechanistic biomarkers for clinical decision making in rheumatic diseases. *Nat Rev Rheumatol* 9(5):267-76 doi:10.1038/nrrheum.2013.14
- Starega-Roslan J, Krol J, Koscianska E, et al. (2010) Structural basis of microRNA length variety. *Nucleic Acids Research* 39(1):257-268 doi:10.1093/nar/gkq727
- Sun Z, Zhang S, Chan JY, Zhang DD (2007) Keap1 controls postinduction repression of the Nrf2-mediated antioxidant response by escorting nuclear export of Nrf2. *Mol Cell Biol* 27(18):6334-49 doi:10.1128/MCB.00630-07
- Suzuki T, Yamamoto M (2015) Molecular basis of the Keap1-Nrf2 system. *Free Radic Biol Med* 88(Pt B):93-100 doi:10.1016/j.freeradbiomed.2015.06.006
- Takaya K, Suzuki T, Motohashi H, et al. (2012) Validation of the multiple sensor mechanism of the Keap1-Nrf2 system. *Free Radic Biol Med* 53(4):817-27 doi:10.1016/j.freeradbiomed.2012.06.023
- Tang X, Wang H, Fan L, et al. (2011) Luteolin inhibits Nrf2 leading to negative regulation of the Nrf2/ARE pathway and sensitization of human lung carcinoma A549 cells to therapeutic drugs. *Free Radic Biol Med* 50(11):1599-609 doi:10.1016/j.freeradbiomed.2011.03.008
- Tkachev VO, Menshchikova EB, Zenkov NK (2011) Mechanism of the Nrf2/Keap1/ARE signaling system. *Biochemistry (Moscow)* 76(4):407-422 doi:10.1134/s0006297911040031
- Tong KI, Katoh Y, Kusunoki H, Itoh K, Tanaka T, Yamamoto M (2006a) Keap1 recruits Neh2 through binding to ETGE and DLG motifs: characterization of the two-site molecular recognition model. *Mol Cell Biol* 26(8):2887-900 doi:10.1128/MCB.26.8.2887-2900.2006
- Tong KI, Kobayashi A, Katsuoka F, Yamamoto M (2006b) Two-site substrate recognition model for the Keap1-Nrf2 system: a hinge and latch mechanism. *Biol Chem* 387(10-11):1311-20 doi:10.1515/BC.2006.164
- Tong KI, Padmanabhan B, Kobayashi A, et al. (2007) Different electrostatic potentials define ETGE and DLG motifs as hinge and latch in oxidative stress response. *Mol Cell Biol* 27(21):7511-21 doi:10.1128/MCB.00753-07
- Turrens JF (2003) Mitochondrial formation of reactive oxygen species. *J Physiol* 552(Pt 2):335-44 doi:10.1113/jphysiol.2003.049478

- Venugopal R, Jaiswal AK (1996) Nrf1 and Nrf2 positively and c-Fos and Fra1 negatively regulate the human antioxidant response element-mediated expression of NAD(P)H:quinone oxidoreductase₁ gene. *Proceedings of the National Academy of Sciences* 93(25):14960 doi:10.1073/pnas.93.25.14960
- Wang XJ, Sun Z, Villeneuve NF, et al. (2008) Nrf2 enhances resistance of cancer cells to chemotherapeutic drugs, the dark side of Nrf2. *Carcinogenesis* 29(6):1235-43 doi:10.1093/carcin/bgn095
- Wardyn JD, Ponsford AH, Sanderson CM (2015) Dissecting molecular cross-talk between Nrf2 and NF- κ B response pathways. *Biochem Soc Trans* 43(4):621-626 doi:10.1042/BST20150014
- Wilkinson J, Radjendirane V, Pfeiffer GR, Jaiswal AK, Clapper ML (1998) Disruption of c-Fos Leads to Increased Expression of NAD(P)H:Quinone Oxidoreductase1 and GlutathioneS-Transferase. *Biochemical and Biophysical Research Communications* 253(3):855-858 doi:https://doi.org/10.1006/bbrc.1998.9804
- Wu S, Huang S, Ding J, et al. (2010) Multiple microRNAs modulate p21Cip1/Waf1 expression by directly targeting its 3' untranslated region. *Oncogene* 29(15):2302-2308 doi:10.1038/onc.2010.34
- Zhang DD, Hannink M (2003) Distinct Cysteine Residues in Keap1 Are Required for Keap1-Dependent Ubiquitination of Nrf2 and for Stabilization of Nrf2 by Chemopreventive Agents and Oxidative Stress. *Molecular and Cellular Biology* 23(22):8137-8151 doi:10.1128/mcb.23.22.8137-8151.2003
- Zhang DD, Lo SC, Cross JV, Templeton DJ, Hannink M (2004) Keap1 is a redox-regulated substrate adaptor protein for a Cul3-dependent ubiquitin ligase complex. *Mol Cell Biol* 24(24):10941-53 doi:10.1128/MCB.24.24.10941-10953.2004
- Zhang DD, Lo SC, Sun Z, Habib GM, Lieberman MW, Hannink M (2005) Ubiquitination of Keap1, a BTB-Kelch substrate adaptor protein for Cul3, targets Keap1 for degradation by a proteasome-independent pathway. *J Biol Chem* 280(34):30091-9 doi:10.1074/jbc.M501279200
- Zhang Y, Gordon GB (2004) A strategy for cancer prevention: Stimulation of the Nrf2-ARE signaling pathway. *Molecular Cancer Therapeutics* 3(7):885
- Zhu YF, Li XH, Yuan ZP, et al. (2015) Allicin improves endoplasmic reticulum stress-related cognitive deficits via PERK/Nrf2 antioxidative signaling pathway. *Eur J Pharmacol* 762:239-46 doi:10.1016/j.ejphar.2015.06.002
- Zipper LM, Mulcahy RT (2002) The Keap1 BTB/POZ dimerization function is required to sequester Nrf2 in cytoplasm. *J Biol Chem* 277(39):36544-52 doi:10.1074/jbc.M206530200

2

MicroRNA patterns as biomarkers for chemical exposure and disease

Luc J.M. Bischoff¹, Jan P. Langenberg², Daan Noort², Bob van de Water¹

¹Division of Drug Discovery and Safety, Leiden Academic Centre for Drug Research, Leiden University, Leiden, The Netherlands

²Department of CBRN Protection, TNO Defence, Safety and Security, Rijswijk, The Netherlands

Manuscript in preparation

ABSTRACT

MicroRNAs are small non-coding RNAs. They regulate gene expression at the post-transcriptional level and are involved in many biological processes. Recent studies indicate that circulating microRNAs are stable and can be assessed in a non-invasive manner, making microRNAs interesting biomarker candidates. Furthermore, microRNA expression changes are linked to various diseases like liver disease and cancer. In this review, changes in microRNA expression after chemical exposure are described. A literature study was conducted to obtain information related to microRNA up/down regulation after exposure to a diverse panel of chemicals. Interesting, the microRNAs most frequently found to be dysregulated are also found to play a role in various diseases linked to chemical exposure. Although microRNA expression changes show great potential as biomarkers, questions concerning biomarker robustness, biological functionality and adverse outcome causality of the response still remain.

INTRODUCTION

MicroRNA (or miRNA) is one of many types of non-coding RNA. MicroRNAs are small, around 22 nucleotides in length, and single stranded in their active mature form. Biogenesis of microRNAs contains multiple different steps. First, primary microRNA transcripts (pri-miRNA) are transcribed in the nucleus by RNA polymerase II or III. Next, each pri-microRNA is cleaved into hairpin loop structures (precursor microRNA or pre-miRNA) by the microprocessor complex DGCR8. The pre-miRNA is transported to the cytoplasm by Exportin-5 and cleaved into an imperfectly double-stranded microRNA by the RNase III protein Dicer. The passenger strand is degraded and the guide strand is incorporated into a RNA-Induced Silencing Complex (RISC). MicroRNAs regulate gene expression at the post-transcriptional level through sequence-specific binding to target mRNAs (Pogribny et al. 2016). MicroRNAs are involved in many physiological processes including the immune response, metabolism, and development (Hou et al. 2011). Furthermore, microRNAs are involved in toxicological responses and disease. Moreover, microRNAs are highly conserved among species (Lewis et al. 2003). Because of their imperfect complementary binding to mRNA, a single microRNA is able to target many different mRNAs (Bolley et al. 2015; Mohr and Mott 2015). Although the function of microRNAs is mostly described as downregulation of their target genes, microRNA binding will frequently not result in complete silencing of genes. In fact, sometimes only minor changes in protein response can be observed (Cech and Steitz 2014). Therefore microRNAs might be better described as “fine-tuners” of biological processes. The fact that the working mechanism of microRNAs is not a simple matter of on-off, complicates matters concerning their role in health and disease. Furthermore, a single microRNA might have opposing functions in different systems (Mohr and Mott 2015). Another aspect worth mentioning here is that different microRNAs can “work together” in downregulating one single mRNA target (Mohr and Mott 2015). For example, miR-375, miR-124, and let-7b were found to work together in enhancing myotrophin targeting in the pancreas, resulting in greater repression of the corresponding mRNA target (Krek et al. 2005).

Because of their role in a broad range of physiological processes, microRNAs can provide us with numerous information. Concerning chemical exposure, microRNAs might provide an indication of the working mechanism (mode-of-action) of the chemical. Since some microRNAs demonstrate highly “tissue specific” expression, measurement of these microRNAs as surrogate biomarkers in medium in *in vitro* test systems or plasma in experimental animal models and humans might provide information regarding the target organs that are damaged upon chemical exposure and ensuring release in extracellular fluids (Laterza et al. 2009). Also, different microRNAs are described in literature which are related to (various types of) cancer

Table 1. MicroRNA patterns after chemical exposure.

MicroRNAs specific for the target organ are depicted in green. MicroRNAs known to be organ specific, but not for the organ/tissue where they have been measured are depicted in red. ↑ = upregulated, ↓ = downregulated.

Chemical compound	Species	Tissue/cell type/ body fluid	Altered miRNA	References
Ethanol	Rhesus macaques	PBMC	181a↑, 221↑	(Asquith et al. 2014)
		Colon	155↑	(Asquith et al. 2014)
	Rat	Gastric tissue	145↑, 17↓, 19a↓, 21↓, 181a↓, 200c↓	(Luo et al. 2013)
	Mouse	Liver	132↑, 155↑	(Bala and Szabo 2012)
	Rat	Liver	34a↑, 103↑, 107↑, 122↑, 19b↓	(Dippold et al. 2013)
	Mouse	Liver	34a↑	(Meng et al. 2012)
	Human	Hepatobiliary cell lines	34a↑	(Meng et al. 2012)
	Human	HEK239T cells	7↑, 144↑, 203↑, 15b↓	(van Steenwyk et al. 2013)
	Mouse	Cerebellum	132↑, 155↑	(Lippai et al. 2013)
	Human	Monocytes	27a↑	(Saha et al. 2015)
	Human	SH-SY5Y neuroblastomal cells	302b↑, 497↑	(Yadav et al. 2011)
	Mouse	AML-12 hepatocytes and liver	217↑	(Yin et al. 2012)
	Human	Caco-2, intestinal epithelial cell	212↑	(Tang et al. 2008)
Aflatoxin	C57BL/6 mouse	Liver	705↑, 1224↑, 182↓, 183↓, 199a-3p↓	(Dolganiciu et al. 2009)
	Rat	Liver	34a↑, 92↓	(Yang et al. 2014)
	Human	Chang liver	33a-5p↑	(Fang et al. 2013)
Arsenic	Human	HepG2 liver carcinoma cells	33a-5p↑	(Fang et al. 2013)
	Human	Jurkat leukemic T cell	30d↑, 142-5p↑, 150↑, 181a↑, 222↑, 638↑, 663↑	(Sturchio et al. 2014)
	Human	HXO-RB44 Retinoblastoma cells	34a↑, 125a-3p, 129-5p↑, 181b↑, 425↑, 628-3p↑, 649↑, 890↑, 943↑, let-7b↓, 220b↓, 376a↓, 524-5p↓	(Zhang et al. 2013)
	Human	HUVEC	19b↑, 21↑, 24↑, 29b↑, 33a↑, 301a↑, 874↑, 198↓, 508-5p↓, 1252↓	(Li et al. 2012)
	Human	T24 bladder carcinoma cells	222↑, 19a↓	(Cao et al. 2011)
	Human	HepG2 liver carcinoma cells	24↑, 29a↑, 30a↑, 210↑, 886-3p↑, 296-5p↓, 663↓, 675↓, 744↓	(Meng et al. 2011)

Chemical compound	Species	Tissue/cell type/ body fluid	Altered miRNA	References
	Rat	Liver	151↑, 183↑, 26a↓, 423↓	(Ren et al. 2015)
	Human	Bronchial epithelial cell	21↑	(Luo et al. 2015)
	Human	A549 lung cell	98↑	(Gao et al. 2014)
	Human	NB4 acute promyelocytic leukemia cell	125↑, 126↑, 193b↑, 215↑, 335↑	(Ghaffari et al. 2012)
			372↓	(Ghaffari et al. 2012)
	Human	Hepatocellular carcinoma cells	491↑	(Jiang et al. 2014)
	Human	Hepatocellular carcinoma cells	491↑	(Wang et al. 2014)
	Guinea pig	Myocardium	1↑, 133↑	(Shan et al. 2013)
Acetaminophen	Human	Bronchial epithelial cells	190↑	(Beezhold et al. 2011)
	Porcine	Plasma	122↑, 124-1↑, 192↑	(Baker et al. 2015)
	Human	Serum	9-3p↑, 30d-5p↑, 122↑, 125b-5p↑, 204-5p↑, 423-5p↑, 574-3p↑, 4732-5p↑	(Yang et al. 2015)
	Human	Urine	302a↑, 357↑, 940↑, Let-7d*↑, 188-5p↑, 197↑	(Yang et al. 2015)
	Mouse	Liver	207↑, 297a↑, 297b-3p, 328↑, 466c-5p↑, 466d-3p↑, 466f-3p↑, 466g↑, 466g↑, 467a*↑, 467b*↑, 467e*↑, 468↑, 574-5p↑, 574-3p↑, 483↑, 483*↑, 485*↑, 669a↑, 669c↑, 671-5p↑, 672↑, 689↑, 709↑, 710↑, 711↑, 721↑, 877*↑, 1224↑, Let-7b↓, 29b↓, 29c↓, 30a↓, 101b↓, 212↓, 122↓, 129↓, 130a↓, 192↓, 194↓, 487b↓	(Wang et al. 2009)
			Let-7d*↑, Let-7g↑, 15a↑, 19b↑, 21↑, 22↑, 27b↑, 29a↑, 29b↑, 29c↑, 30a↑, 30c↑, 30e↑, 101b↑, 107↑, 122↑, 129↑, 130a↑, 148a↑, 192↑, 294*↑, 365↑, 574-5p↑, 680↑, 685↑, 23a↓, 26a↓, 124↓, 125a-3p↓, 125b-5p↓, 133a↓, 133b↓, 135a*↓, 202-3p↓, 205↓, 451↓, 468↓	(Wang et al. 2009)

Chemical compound	Species	Tissue/cell type/ body fluid	Altered miRNA	References
Benzo(a)pyrene			483↓, 710↓, 711↓, 712↓, 720↓, 721↓, 1224↓	
	Human	Blood	19a↑, 19b↑, 374a↑	(Jetten et al. 2012)
	Rat	Liver	298↓, 370↓	(Fukushima et al. 2007)
	Human	HepG2 liver carcinoma cells	26a-1↑, 29b↑, 140-5p↑, 181a↑, 542-5p↑, 1271↑, 1973↑, 122↓, 448↓, 518e↓, 518e↓, 582-3p↓, 591↓, 2276↓	(Lizarraga et al. 2012)
	Human	HepG2 liver carcinoma cells	181a-3p↑	(Caiment et al. 2015)
	Rat	Liver	29b↑, 34b-5p↑, 34c↑, 21↓, 122↓, 142-5p↓, 221↓, 222↓, 429↓	(Chanyshev et al. 2014)
	Rat	Ovary	21↑	(Chanyshev et al. 2014)
	Mouse	Liver	34a↑	(Malik et al. 2012)
	Mouse	Liver	140↑, 207↑, 290↑, 291a- 3p↑, 346↑, 376b↑, 483↑, 292-3p↓, 433-5p↓, 489↑, 434-3p↓, 546↓	(Zuo et al. 2014)
	Mouse	Colon	290↑, 291b-5p↑, 292- 5p↑, 298↑, 351↑, 433-5p↑, 503↑, 546↑	(Zuo et al. 2014)
	Mouse	Glandular stomach	207↑, 290↑, 291b-5p↑, 292-5p↑, 298↑, 346↑, 351↑, 433-5p↑, 503↑	(Zuo et al. 2014)
	Mouse	Lung	207↑, 290↑, 291a-3p↑, 291a-5p↑, 376b↑, 434-3p↑, 489↑, 291b- 5p↓, 292-5p↓, 433-5p↓	(Zuo et al. 2014)
	Mouse	Spleen	207↑, 290↑, 291b-5p↑, 292-5p↑, 298↑, 376b↑, 346↑, 351↑, 542-5p↑, 464↓	(Zuo et al. 2014)
	Mouse	Forestomach	291b-5p↑, 292-5p↑, 298↑, 346↑, 351↑, 503↑, 546↑, 140↓, 199b↓, 207↓, 433-5p↓, 489↓	(Zuo et al. 2014)
	Mouse	Lung	150↓	(Halappanavar et al. 2011)

(Meng et al. 2016) and other pathologies like acute myocardial infarction (Devaux et al. 2012). Altogether, these features make microRNAs interesting candidates for biomarkers for chemical exposure and related pathological outcomes.

With respect to the use of microRNAs as biomarkers of chemical exposure and adverse outcomes, we questioned whether exposure to a chemical would display a compound specific (microRNA) response, providing information about the chemical mode-of-action, or that the microRNA would merely reflect a general target organ toxicity response. We reasoned that in case of a general toxicity response, some microRNAs linked to general toxicity outcomes such as cell apoptosis, will be frequently found to be differently expressed across different studies using different chemicals and *in vitro/in vivo* systems. Another question we wanted to address was whether the microRNAs that are differently expressed after chemical exposure are more specific to the test system than to the type of chemical exposure.

To answer these questions, we performed a systematic literature study to obtain information related to changes in microRNA expression after exposure to chemical compounds. We focused on several compounds for which sufficient microRNA expression information in diverse tissues and/or test systems is available in the literature and these included: ethanol, aflatoxin B1, arsenic, paracetamol (acetaminophen), and benzo(a)pyrene. We did exclude literature describing exposure to mixtures or teratogenic effects. Sources used are PubMed and Science Direct. Keywords for literature searches simply involved microRNA and the individual compound name. We further only focused on microRNAs that were additionally validated by qRT-PCR experimentation.

MICRORNA CHANGES AFTER CHEMICAL EXPOSURE, LEAKAGE FROM DAMAGED CELLS OR FUNCTIONAL RESPONSE?

From our literature search we obtained in total 39 manuscripts that fulfilled our criteria. We did not take any consideration on dose and time point along; this will be discussed later. In Table 1 all the results on microRNA expression after treatment to the five selected chemicals are summarized from these manuscripts. Data were obtained from *in vitro* human test systems and *in vivo* experiments in rodents. We also observed a diversity of target tissues, with arsenic being tested in various cell types *in vitro*, and benzo(a)pyrene being assessed in different tissues *in vivo*.

We further evaluated this combined dataset and as a first step we investigated the commonality in microRNA expression changes by the five chemicals. Table 2 summarizes the microRNAs that were differentially expressed upon exposure to at least two different study compounds. We observed at least seven microRNAs, miR-21, miR-34, miR-19, miR-26, miR-29, miR-122 and miR-181, that were affected by at least three of the five chemicals. Remarkably, miR-21 and miR-34 were differentially expressed after exposure to four of the five chemicals included in this study, suggesting that these microRNAs are part of general cellular stress response pathways that are modulated after cell injury upon chemical exposure. Interestingly, these microRNAs are extensively studied in relation to cancer: miR-21 is found to regulate processes like cell proliferation and apoptosis where overexpression of miR-21 increases cell viability (Tong et al. 2015), suggesting a role in a protective adaptive response upon chemical exposure. For some microRNAs that were in overlap between multiple compounds, we observed opposite effects by the different compounds. For example, ethanol showed increased expression of miR-122 in rat liver, yet was down-regulated in rat liver after acetaminophen; the latter coincided with increase of miR-122 in plasma. These contrasting effects might be due to severe liver cell damage, which results in leakage or active transport of miR-122 out of the cells. Given that miR-122 is a highly expressed liver specific microRNA (Wang et al. 2021), miR-122 is likely not directly involved in the damage response itself.

Expression changes are known to depend on chemical class and cell type or tissue (Rodrigues et al. 2011). To answer the question whether or not the microRNA changes found in this meta-analysis are tissue specific, the TSmiR (Tissue-Specific microRNA) database was used (<http://bioeng.swjtu.edu.cn/TSmiR>) (Guo et al. 2014). This database only contains information of human microRNAs, but considering the fact that Shan et al. (2013) found upregulation of miR-1 and miR-133, two microRNAs known to be tissue specific for heart tissue, in Guinea pig myocard tissue, might indicate that at least some of the tissue specific microRNAs are consistent across different species (Shan et al. 2013). MicroRNAs known to be specific for the following tissues were incorporated: bone, brain, heart, kidney, liver, lung, pancreas, skeletal muscle, spleen, and thymus. We observed a few tissue specific microRNAs that were affected by the compounds, including miR-1 and miR-133 for myocard, and miR-483 and miR-192 for liver (see Table 1, marked in green). The list of microRNAs known to be tissue specific, but observed in other tissues (see Table 1, marked in red), was more numerous and included microRNAs that were observed either in cell lines *in vitro*, possibly because of higher sensitivity due to a single cell type as compared to tissue with mixed cell types. In addition, we observed such tissue specific microRNAs in serum, e.g. miR-9-3p, miR-124, miR-125b-5p and miR-192 or urine including miR-302a. These observations were particular made for acetaminophen which induces

hepatotoxicity. The liver injury biomarker miR-122 was not part of the list; this is likely due to low levels of miR-122 that are released from the liver into the blood under normal physiological conditions. If microRNAs leaked from severe damaged tissue are collected in the blood, they will be present in a higher amount than normal. Therefore, these microRNAs are likely good candidates for a biomarker of exposure. For example, a chemical substance known to be hepatotoxic, will damage the liver and in turn the blood will be enriched for liver specific microRNAs, such as miR-122 (Wang et al. 2021). Interestingly, Wang et al. (2009), found some microRNAs to be upregulated in mouse plasma, but down regulated in mouse liver after acetaminophen exposure (Wang et al. 2009). Furthermore, they also found microRNAs which were down regulated in plasma but upregulated in liver. The authors stated that their findings could be the result of cellular damage, but do not rule out the possibility of a specific transport mechanism. We speculate that most of the microRNAs that are released in the blood and urine, and derived from damaged tissues are not directly functionally involved in the damage response. Yet, there are indications that such microRNAs present in exosomes may indirectly impact the biology of the same tissue or cells in other tissues (Rahman et al. 2020). Altogether, these liver specific microRNAs that are released in the blood after acetaminophen might be used as biomarkers of exposure to hepatotoxic substances (Llewellyn et al. 2021; Wang et al. 2021).

Table 2. Differently expressed microRNAs by at least two different study compounds.

In this table subgroups of microRNAs are taken together. For example: miR-19a and miR-19b are shown as miR-19. Other subtypes are: 34a (all compounds except acetaminophen). 34b-5p benzo(a)pyrene. 34c benzo(a)pyrene. All miR-34 subtypes where found to be upregulated. miR-26: 26a/b, 26a alone and 26a-1. For miR-21 no subtypes were described in the used literature. miR-21 was down regulated in ethanol (rat gastric tissue) 1x up and 1x down regulated in acetaminophen and benzo(a)pyrene (mouse/rat tissue). Concerning arsenic exposure, three studies using different types of lung cells, all found miR-21 to be upregulated. MicroRNA shown are the microRNAs differently expressed by the chemical compound.

MicroRNA	EtOH	AFB1	As	APAP	BaP	Total nr. of chemicals
miR-21	✓		✓	✓	✓	4
miR-34	✓	✓	✓		✓	4
miR-19	✓		✓	✓		3
miR-26			✓	✓	✓	3
miR-29			✓	✓	✓	3
miR-122	✓			✓	✓	3
miR-181	✓		✓		✓	3
Let-7			✓	✓		2
miR-27	✓			✓		2
miR-30			✓	✓		2
miR-33		✓	✓			2
miR-92	✓	✓				2
miR-107	✓			✓		2
miR-125			✓	✓		2
miR-133			✓	✓		2
miR-142			✓		✓	2
miR-150			✓		✓	2
miR-183	✓		✓			2
miR-193			✓	✓		2
miR-199	✓				✓	2
miR-207				✓	✓	2
miR-212	✓			✓		2
miR-221	✓				✓	2
miR-222			✓		✓	2
miR-298				✓	✓	2
miR-302	✓			✓		2
miR-376			✓		✓	2
miR-423			✓	✓		2
miR-483				✓	✓	2
miR-1224	✓			✓		2

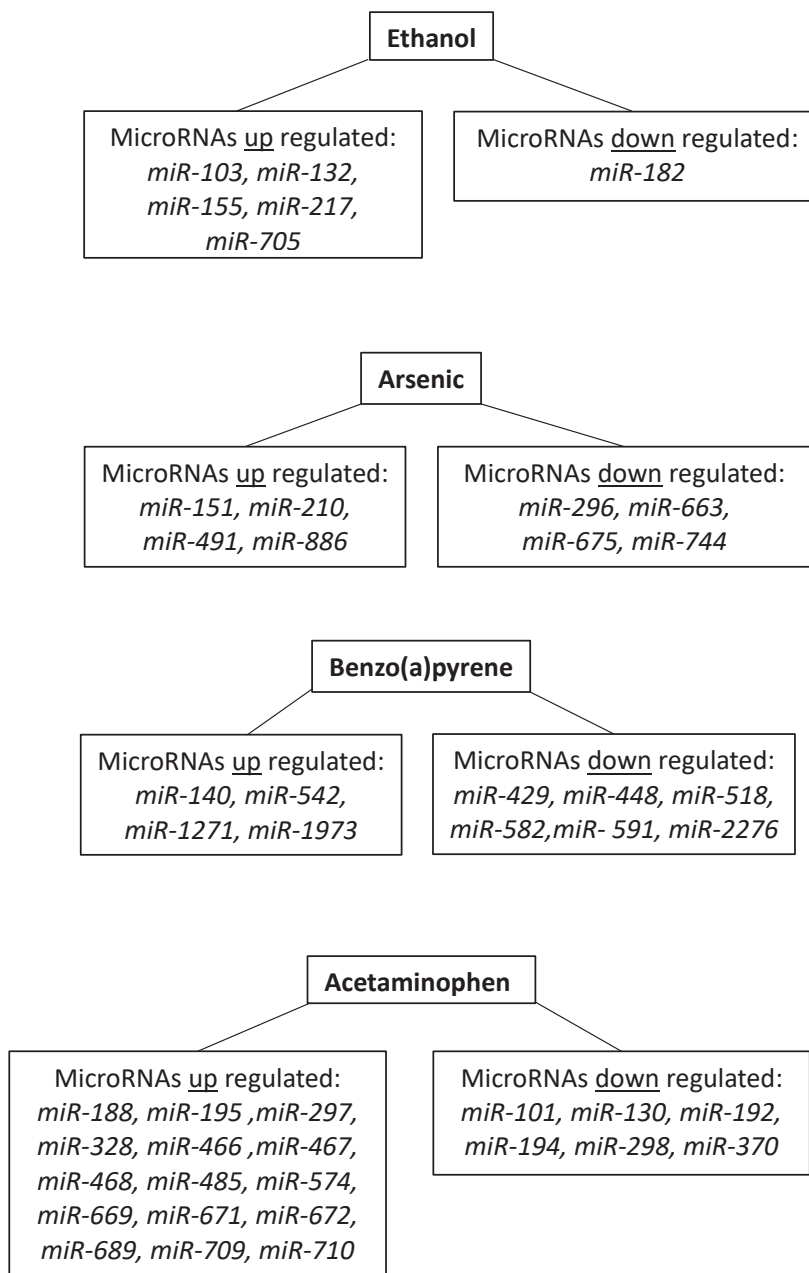


Figure 1. Up/down regulated microRNAs in liver tissue (human or animal) and *in vitro* liver models.

MicroRNAs depicted were only found to be dysregulated by only one of the five compounds. For aflatoxin, no unique microRNAs were found in liver tissue/cells.

UNIQUE EXPRESSED MICRORNAS AS BIOMARKERS OF EXPOSURE

Given the limited overlap in microRNAs that are in common between the five toxicants, we further focused on the compound specific microRNAs to derive an improved indication about the (specific) mode-of-action of the compounds. Since microRNAs will affect gene expression and thereby the overall biology, we selected up- and down-regulation for microRNAs which were only found to be differentially expressed by exposure to one single compound (Figure 1). Since liver was most studied, only results derived from *in vivo* liver tissue (human, rat or mouse) or *in vitro* liver models were combined. In these liver samples we observed highly treatment specific differentially expressed microRNAs patterns for the five compounds. To determine the feasibility to uncover biological connections of these compound specific microRNAs we performed a target prediction analysis. For this we focused on benzo(a)pyrene since its reactive metabolites will lead to covalent modification of DNA and consequently activate a DNA damage response. The target genes of the microRNAs found to be differentially expressed due to exposure to benzo(a)pyrene were determined in mirDB (<http://www.mirdb.org/miRDB/>). Only target genes with a target score of 100 were included. Next, the function of these target genes was derived using the NCBI gene database (<https://www.ncbi.nlm.nih.gov/>). While we identified four upregulated and six downregulated microRNAs, for only in total four we could derive predictions for target genes. For the upregulated microRNAs, miR-140 and miR-1271, only one and three target genes were predicted, and for miR-140 no biological information on this target gene was uncovered (see Figure 2). Interestingly, three genes, *ZEB1*, *ZEB2* and *TRIM33* reported to play a role in the DNA damage response, were found to be targeted by miR-249, one of the six downregulated miRNAs after Benzo(a)pyrene exposure (Kulkarni et al. 2013; Sayan et al. 2009).

This example of benzo(a)pyrene demonstrates the complex relationship between exposure, microRNA pattern changes, and changes at gene level, to provide mechanistic insight on the adverse effects. Also the lack of data, and the fact that there is no 100 % target score available for all microRNAs, makes it difficult to interpret the data from a mechanistic perspective. We are fully aware that interpreting and comparing microRNA data from different papers is still difficult because of the use of different biological test systems, different exposure times, compound concentrations and of course different microRNA analysis platforms and data normalization approaches. This also indicates the requirement that information obtained from different databases has to be combined. Given these constraints, there is a considerable uncertainty that the microRNAs we defined based on our

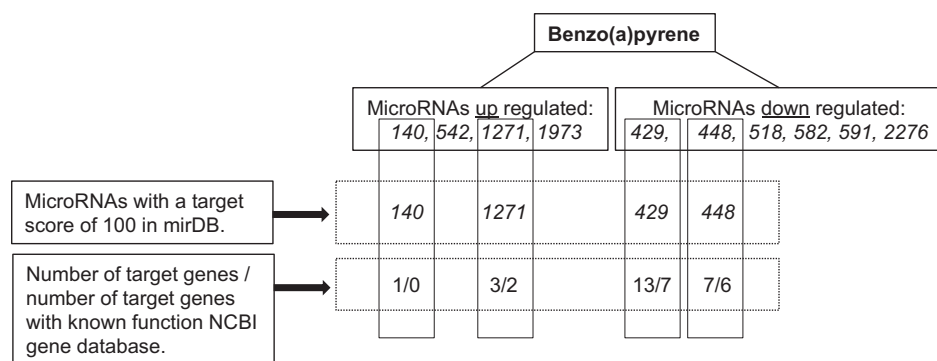


Figure 2. Overview of microRNAs differently expressed after benzo(a)pyrene exposure linked to information found in target prediction databases and NCBI.

MicroRNAs target genes with a target score of 100 found in mirDB. Their function is derived from the NCBI gene database. Not for all the target genes with a score of 100 a function was available in the NCBI database.

systematic meta-analysis may not be specific for the mode-of-action of the chemical compound. In addition, the identified single miRNA could have no relationship with the direct biological transcriptional and biological reprogramming after the chemical exposure in the target cells of toxicity. Firstly, the chemical of interest might indirectly impact the production and maturation process of microRNAs. This could be particularly true under conditions of severe cell injury that would disrupt normal cellular homeostasis and transcriptional processing. Secondly, microRNAs are thought to function by fine-tuning numerous processes (Mendell and Olson 2012). This implicates that the effect of a single microRNA will probably result in only a moderate effect at protein level. The effect of microRNAs will therefore rather be the resultant of a complex mechanism involving a set of different microRNAs. Lastly, microRNAs might have an indirect effect on their target genes (Lee et al. 2013). Once released from injured cells in the blood circulation, microRNAs may impact on the systemic biology through other means. Specific microRNAs, i.e. miR-21 and miR-29, can then bind to the toll-like receptor, triggering pro-inflammatory responses (Fabbri et al. 2012). Also, in plasma, microRNAs can be found encapsulated in vesicles and as Argonaute2 complexes (Arroyo et al. 2011). Argonaute2 proteins are the key effector proteins in microRNA-mediated silencing (Bartel 2018; Golden et al. 2017). Furthermore, microRNAs can also be delivered to recipient cells by high-density lipoproteins (Vickers et al. 2011). This alternative indirect biological effects of microRNAs make it difficult to interpret the specific functionality and, or causality of the microRNA response in relation to mechanisms of toxicity.

MICRORNA EXPRESSION PATTERNS AS BIOMARKERS OF DISEASE

Above we summarized the effect of five often studied chemicals on microRNA expression. Next, we questioned whether some of the key microRNAs found in our study are also known to be differentially expressed in diseases/adverse outcomes linked to the chemicals selected in this study. In the next session we focus on liver disease (ethanol, acetaminophen) and cancer (arsenic, benzo(a)pyrene, aflatoxin B1).

Liver disease

One of the most differently expressed microRNAs described after acetaminophen and also ethanol exposure is miR-122 (Figure 1 and 2) with a decrease in liver and coinciding increase in plasma and serum. miR-122 is the most abundant microRNA in human liver (Jopling 2012) and has therefore been proposed as a novel liver injury specific biomarker. miR-122 has specific biological activities. Thus, miR-122 plays a role in various processes like lipid, cholesterol metabolism and cell differentiation. Furthermore, miR-122 is found to suppress cell proliferation (Hu et al. 2012) and to promote hepatitis C virus replication (Hsu et al. 2012). Hepatocellular carcinoma cells have reduced levels of miR-122. Interestingly, HepG2 cells, a human hepatocellular carcinoma cell-line, known to be miR-122 deficient, was found to be able to take up exosomal miR-122 released by Huh7 cells when cultured together, reducing cell growth and proliferation in HepG2 cells (Basu and Bhattacharyya 2014); high levels of miR-122 in the liver hepatocytes may therefore maintain a non-proliferative differentiated phenotype. miR-122 also plays a role in inflammation: it downregulates cytokines like IL-6 and IL-1 β in human hepatic stellate cells (HSCs) which is associated with an inhibition of the NF- κ B nuclear translocation in human HSCs (Nakamura et al. 2015). Interestingly, miR-122 knock out results in the upregulation of the immunomodulating transcription factor RelB in the liver (Hsu et al. 2020). While miR-122 has been suggested as a single translational biomarker for liver injury; we also observed other microRNAs that show a decrease in liver and an increase in plasma after acetaminophen treatment, including miR-192 (Krauskopf et al. 2015). Furthermore, the use of a biomarker panel for drug induced liver injury consisting of miR-122 complemented with miR-192 and miR-193 is described (Su et al. 2012). Moreover, a broader “microRNA-based composite biomarker” for nonalcoholic steatohepatitis was suggested, containing ALT and miR-192, miR-21, and miR-505 (Liu et al. 2018), although we did not find these microRNAs together as a panel in any of the chemical treatments in our analysis. A recent study on the validation of various candidate liver injury biomarkers indicates the use of a combination of miR-122 with cytokeratin 18 (K18) and glutamate dehydrogenase (GLDH) in human subjects with liver injury (Llewellyn et al. 2021).

Cancer

In cancer, microRNAs might be separated into two groups: tumor-suppressive microRNAs and oncogenic microRNAs (Gao and Liu 2011). The various studies demonstrate in particular modulation of miR-34 and miR-21.

In our analysis, miR-34 was affected by four chemicals. miR-34 is a direct p53 target (Tian et al. 2014) and involved in stabilization of the p53 response to genotoxic stress and as such functions as a tumor-suppressive microRNA (Bommer et al. 2007; Navarro and Lieberman 2015). Three homologues of miR-34 are known: miR-34a, miR-34b, and miR-34c. In particular upregulation of different miR-34 homologues was observed in livers of rat and mouse after treatment with DNA damaging agents aflatoxin B1 and benzo(a)pyrene but not acetaminophen (see Table 1).

miR-21 was affected by ethanol, acetaminophen, arsenic and benzo(a)pyrene. miR-21 is one of the most studied oncogenic microRNAs. miR-21 is found to be upregulated in most cancer types (Kumarswamy et al. 2011). The enhanced expression of miR-21 in cancer cells has suggested this microRNA as a biomarker for malignancy in various tissues. miR-21 has a direct impact on the cytoprotection of cells to stress. Chan et al. (2005), found that knockdown of miR-21 in glioblastoma cells leads to the activation of different caspases and eventually to increased apoptosis and cell death (Chan et al. 2005). Although miR-21 clearly plays a role in many types of cancer, another function of miR-21 is related to signal transduction in T-lymphocyte, where miR-21 is a negative modulator of T-cell activation and its expression is induced in memory cells compared to naïve T-cells (Carissimi et al. 2014). Furthermore, miR-21 is found to be induced by inflammatory stimuli, like for example TGF- β 1 (Haakensen et al. 2016; Wang et al. 2018). The p53 target gene B cell translocation gene 2 (BTG2) is a target for miR-21, and a possible mechanism by which cardiomyocytes are protected against doxorubicin, a cytostatic compound used for chemotherapy in the treatment of cancer (Tong et al. 2015). Moreover, Thum et al. (2008), investigated the role of miR-21 in cardiac fibroblasts and found that inhibiting miR-21 results in an increase in apoptosis. Overexpression of miR-21 showed the opposite result. As an explanation they propose a mechanism whereby miR-21 negatively regulates SPRY1, which leads to an increase of ERK activation, which in turn leads to cell survival (Thum et al. 2008).

Consistent with the above observations is that miR-21 and miR-34 can be used to differentiate between genotoxic and non-genotoxic carcinogenicity in mouse hepatocytes (Marrone et al. 2016; Rieswijk et al. 2015). Yet, caution should be taken since there is no strong consistency in direction and magnitude of microRNA expression changes after chemical exposure. Furthermore, these changes might also reflect general toxicity rather than a mechanism eventually leading towards

cancer. Moreover, Lu et al. (2005), hypothesize that, because in healthy tissues the overall expression of microRNAs seems to be higher compared to tumors, the global microRNA expression reflects the state of cellular differentiation (Lu et al. 2005).

DISCUSSION AND FUTURE CHALLENGES

We conducted a literature study in order to obtain learnings concerning the overlap and specificity of differential expression of microRNAs upon chemical exposure. We have observed a diversity of microRNAs for our selected five chemicals that have been investigated most. For some microRNAs overlap between expression was observed with miR-21 and miR-34 as important examples with modulation by four out of five compounds, which can partly be linked to either a DNA-damage stress response by e.g. benzo(a)pyrene, aflatoxin B1 and arsenic or a more general cellular stress response by ethanol and acetaminophen. The current studies prohibit to link any of the microRNA expression patterns to a specific type of chemical exposure. While integration of microRNA and mRNA for mechanistic interpretation has been applied for improved mechanistic understanding (Caiment et al. 2015; Rieswijk et al. 2015), experimentally validating the mechanistic hypothesis on such causative relationships has so far been lacking.

The use of microRNAs as biomarkers of exposure or disease looks promising. First of all because of the fact that microRNAs can easily be obtained in different body fluids like blood (serum/plasma), urine and saliva and are highly stable. Secondly, because microRNAs are conserved across species making it easier to extrapolate findings in animals to humans. Thirdly, because of the existence of “tissue specific” microRNAs providing information about which tissue might be damaged. Measurement of these microRNAs might be taken along to assess the target organ. Obviously, in this example microRNAs are used as biomarkers of effect, such as plasma miR-122 as a marker of liver injury. Moreover, these microRNAs might be used as a panel of different microRNAs to obtain knowledge of the presence of an adverse effect. Additionally, proteins of interest might also (still) be part of this biomarker panel as demonstrated recently (Llewellyn et al. 2021).

While mRNA expression profiling has been applied more routinely in toxicogenomics-based mechanistic understanding of toxic responses, this has so far been limited for microRNA profiling. Our systematic analysis of the current literature has identified several considerations that can explain the variety of responses: i) use of different *in vitro* test systems with different degrees of differentiation status and involving both primary cells and cell lines; ii) different target organs assessed for miRNA expression;

iii) different time points were considered for evaluation of microRNA expression; iv) different concentration or dosing regimens applied in the various studies; v) lack of anchoring microRNA changes to adverse endpoints.

To make further progress on the application of microRNA profiling in mechanistic toxicology we have the following recommendations. Firstly, there is a need for more detailed concentration- time course data of microRNA expression after chemical exposure. This information will provide detailed insight in the consistency of microRNA changes over time. Secondly, studies should include diverse sets of chemicals with similar mode-of-action. This could include sets of compounds that impact on e.g. mitochondrial respiratory chain, DNA damage, oxidative stress, unfolded protein response, cytoskeletal damage, cyclin dependent kinase, etc. Thirdly, by integrating such larger miRNA expression datasets from the same test system, microRNA co-expression networks could be defined to provide learning on co-regulation of microRNA. When paralleled with mRNA transcriptional datasets, this information could then improve the integration of microRNA and mRNA data based on their co-expression (Callegaro et al. 2021). Fourthly, such studies should preferably be performed in highly differentiated human test systems representing the critical target organs for toxicity such as liver, kidney, heart and the neuronal systems. To increase the cost effectiveness of these studies, we propose the implementation of targeted microRNA sequencing approaches (Yeakley et al. 2017) limiting the overall costs for sequencing. Ultimately, identification of miRNAs that provide information on mode-of-action might be included in a plasma miRNA biomarker panel. Together, these suggested avenues for toxicological microRNA research will pave the way for microRNAs to be widely used as mechanistic biomarkers of chemical exposure as well as disease.

ACKNOWLEDGEMENTS

This work was supported by the Ministry of Defence of the Netherlands, the European Commission Horizon2020 EU-ToxRisk project (grant nr 681002) and the European Commission Horizon2020 Innovative Medicine Initiative 2 Joint Undertaking TransBioLine project (grant 821283).

REFERENCES

- Arroyo JD, Chevillet JR, Kroh EM, et al. (2011) Argonaute2 complexes carry a population of circulating microRNAs independent of vesicles in human plasma. *Proc Natl Acad Sci U S A* 108(12):5003-8 doi:10.1073/pnas.1019055108
- Asquith M, Pasala S, Engelmann F, et al. (2014) Chronic ethanol consumption modulates growth factor release, mucosal cytokine production, and microRNA expression in nonhuman primates. *Alcohol Clin Exp Res* 38(4):980-93 doi:10.1111/acer.12325
- Baker LA, Lee KC, Palacios Jimenez C, et al. (2015) Circulating microRNAs Reveal Time Course of Organ Injury in a Porcine Model of Acetaminophen-Induced Acute Liver Failure. *PLoS One* 10(5):e0128076 doi:10.1371/journal.pone.0128076
- Bala S, Szabo G (2012) MicroRNA Signature in Alcoholic Liver Disease. *Int J Hepatol* 2012:498232 doi:10.1155/2012/498232
- Bartel DP (2018) Metazoan MicroRNAs. *Cell* 173(1):20-51 doi:10.1016/j.cell.2018.03.006
- Basu S, Bhattacharyya SN (2014) Insulin-like growth factor-1 prevents miR-122 production in neighbouring cells to curtail its intercellular transfer to ensure proliferation of human hepatoma cells. *Nucleic Acids Res* 42(11):7170-85 doi:10.1093/nar/gku346
- Beezhold K, Liu J, Kan H, et al. (2011) miR-190-mediated downregulation of PHLPP contributes to arsenic-induced Akt activation and carcinogenesis. *Toxicol Sci* 123(2):411-20 doi:10.1093/toxsci/kfr188
- Bollegyn J, De Kock J, Rodrigues RM, Vinken M, Rogiers V, Vanhaecke T (2015) MicroRNAs as key regulators of xenobiotic biotransformation and drug response. *Arch Toxicol* 89(9):1523-41 doi:10.1007/s00204-014-1314-7
- Bommer GT, Gerin I, Feng Y, et al. (2007) p53-mediated activation of miRNA34 candidate tumor-suppressor genes. *Current biology : CB* 17(15):1298-307 doi:10.1016/j.cub.2007.06.068
- Caiment F, Gaj S, Claessen S, Kleinjans J (2015) High-throughput data integration of RNA-miRNA-circRNA reveals novel insights into mechanisms of benzo[a]pyrene-induced carcinogenicity. *Nucleic Acids Res* 43(5):2525-34 doi:10.1093/nar/gkv115
- Callegaro G, Kunnen SJ, Trairatphisan P, et al. (2021) The human hepatocyte TXG-MAPr: WGCNA transcriptomic modules to support mechanism-based risk assessment. *bioRxiv:2021.05.17.444463* doi:10.1101/2021.05.17.444463
- Cao Y, Yu SL, Wang Y, Guo GY, Ding Q, An RH (2011) MicroRNA-dependent regulation of PTEN after arsenic trioxide treatment in bladder cancer cell line T24. *Tumour Biol* 32(1):179-88 doi:10.1007/s13277-010-0111-z
- Carissimi C, Carucci N, Colombo T, et al. (2014) miR-21 is a negative modulator of T-cell activation. *Biochimie* 107 Pt B:319-26 doi:10.1016/j.biochi.2014.09.021
- Cech TR, Steitz JA (2014) The Noncoding RNA Revolution-Trashing Old Rules to Forge New Ones. *Cell* 157(1):77-94 doi:10.1016/j.cell.2014.03.008
- Chan JA, Krichevsky AM, Kosik KS (2005) MicroRNA-21 is an antiapoptotic factor in human glioblastoma cells. *Cancer Res* 65(14):6029-33 doi:10.1158/0008-5472.Can-05-0137
- Chanyshv MD, Kosorotikov NI, Titov SE, Kolesnikov NN, Gulyaeva LF (2014) Expression of microRNAs, CYP1A1 and CYP2B1 in the livers and ovaries of female rats treated with DDT and PAHs. *Life Sci* 103(2):95-100 doi:10.1016/j.lfs.2014.03.031
- Devaux Y, Vausort M, Goretti E, et al. (2012) Use of Circulating MicroRNAs to Diagnose Acute Myocardial Infarction. *Clinical Chemistry* 58(3):559 doi:10.1373/clinchem.2011.173823
- Dippold RP, Vadigepalli R, Gonye GE, Patra B, Hoek JB (2013) Chronic ethanol feeding alters miRNA expression dynamics during liver regeneration. *Alcohol Clin Exp Res* 37 Suppl 1:E59-69 doi:10.1111/j.1530-0277.2012.01852.x

- Dolganiuc A, Petrasek J, Kodys K, et al. (2009) MicroRNA expression profile in Lieber-DeCarli diet-induced alcoholic and methionine choline deficient diet-induced nonalcoholic steatohepatitis models in mice. *Alcohol Clin Exp Res* 33(10):1704-10 doi:10.1111/j.1530-0277.2009.01007.x
- Fabbri M, Paone A, Calore F, et al. (2012) MicroRNAs bind to Toll-like receptors to induce prometastatic inflammatory response. *Proc Natl Acad Sci U S A* 109(31):E2110-6 doi:10.1073/pnas.1209414109
- Fang Y, Feng Y, Wu T, et al. (2013) Aflatoxin B1 negatively regulates Wnt/beta-catenin signaling pathway through activating miR-33a. *PLoS One* 8(8):e73004 doi:10.1371/journal.pone.0073004
- Fukushima T, Hamada Y, Yamada H, Horii I (2007) Changes of micro-RNA expression in rat liver treated by acetaminophen or carbon tetrachloride--regulating role of micro-RNA for RNA expression. *The Journal of toxicological sciences* 32(4):401-9 doi:10.2131/jts.32.401
- Gao J, Liu QG (2011) The role of miR-26 in tumors and normal tissues (Review). *Oncol Lett* 2(6):1019-1023 doi:10.3892/ol.2011.413
- Gao SY, Zhou X, Li YJ, et al. (2014) Arsenic trioxide prevents rat pulmonary fibrosis via miR-98 overexpression. *Life Sci* 114(1):20-8 doi:10.1016/j.lfs.2014.07.037
- Ghaffari SH, Bashash D, Dizaji MZ, Ghavamzadeh A, Alimoghaddam K (2012) Alteration in miRNA gene expression pattern in acute promyelocytic leukemia cell induced by arsenic trioxide: a possible mechanism to explain arsenic multi-target action. *Tumour Biol* 33(1):157-72 doi:10.1007/s13277-011-0259-1
- Golden RJ, Chen B, Li T, et al. (2017) An Argonaute phosphorylation cycle promotes microRNA-mediated silencing. *Nature* 542(7640):197-202 doi:10.1038/nature21025
- Guo Z, Maki M, Ding R, Yang Y, Zhang B, Xiong L (2014) Genome-wide survey of tissue-specific microRNA and transcription factor regulatory networks in 12 tissues. *Sci Rep* 4:5150 doi:10.1038/srep05150
- Haakensen VD, Nygaard V, Greger L, et al. (2016) Subtype-specific micro-RNA expression signatures in breast cancer progression. *International journal of cancer* 139(5):1117-28 doi:10.1002/ijc.30142
- Halappanavar S, Wu D, Williams A, et al. (2011) Pulmonary gene and microRNA expression changes in mice exposed to benzo(a)pyrene by oral gavage. *Toxicology* 285(3):133-41 doi:10.1016/j.tox.2011.04.011
- Hou L, Wang D, Baccarelli A (2011) Environmental chemicals and microRNAs. *Mutat Res* 714(1-2):105-12 doi:10.1016/j.mrfmmm.2011.05.004
- Hsu KH, Wei CW, Su YR, et al. (2020) Upregulation of RelB in the miR-122 knockout mice contributes to increased levels of proinflammatory chemokines/cytokines in the liver and macrophages. *Immunology letters* 226:22-30 doi:10.1016/j.imlet.2020.06.015
- Hsu SH, Wang B, Kota J, et al. (2012) Essential metabolic, anti-inflammatory, and anti-tumorigenic functions of miR-122 in liver. *The Journal of clinical investigation* 122(8):2871-83 doi:10.1172/jci63539
- Hu J, Xu Y, Hao J, Wang S, Li C, Meng S (2012) MiR-122 in hepatic function and liver diseases. *Protein & cell* 3(5):364-71 doi:10.1007/s13238-012-2036-3
- Jetten MJ, Gaj S, Ruiz-Aracama A, et al. (2012) 'Omics analysis of low dose acetaminophen intake demonstrates novel response pathways in humans. *Toxicol Appl Pharmacol* 259(3):320-8 doi:10.1016/j.taap.2012.01.009
- Jiang F, Wang X, Liu Q, et al. (2014) Inhibition of TGF-beta/SMAD3/NF-kappaB signaling by microRNA-491 is involved in arsenic trioxide-induced anti-angiogenesis in hepatocellular carcinoma cells. *Toxicol Lett* 231(1):55-61 doi:10.1016/j.toxlet.2014.08.024

- Jopling C (2012) Liver-specific microRNA-122: Biogenesis and function. *RNA Biol* 9(2):137-42 doi:10.4161/rna.18827
- Krauskopf J, Caiment F, Claessen SM, et al. (2015) Application of high-throughput sequencing to circulating microRNAs reveals novel biomarkers for drug-induced liver injury. *Toxicol Sci* 143(2):268-76 doi:10.1093/toxsci/kfu232
- Krek A, Grün D, Poy MN, et al. (2005) Combinatorial microRNA target predictions. *Nat Genet* 37(5):495-500 doi:10.1038/ng1536
- Kulkarni A, Oza J, Yao M, et al. (2013) Tripartite Motif-containing 33 (TRIM33) protein functions in the poly(ADP-ribose) polymerase (PARP)-dependent DNA damage response through interaction with Amplified in Liver Cancer 1 (ALC1) protein. *J Biol Chem* 288(45):32357-32369 doi:10.1074/jbc.M113.459164
- Kumarswamy R, Volkmann I, Thum T (2011) Regulation and function of miRNA-21 in health and disease. *RNA Biol* 8(5):706-13 doi:10.4161/rna.8.5.16154
- Laterza OF, Lim L, Garrett-Engele PW, et al. (2009) Plasma MicroRNAs as Sensitive and Specific Biomarkers of Tissue Injury. *Clinical Chemistry* 55(11):1977 doi:10.1373/clinchem.2009.131797
- Lee CC, Yen CJ, Liu T (2013) Prediction of personalized microRNA activity. *Gene* 518(1):101-6 doi:10.1016/j.gene.2012.11.068
- Lewis BP, Shih IH, Jones-Rhoades MW, Bartel DP, Burge CB (2003) Prediction of mammalian microRNA targets. *Cell* 115(7):787-98 doi:10.1016/s0092-8674(03)01018-3
- Li X, Shi Y, Wei Y, Ma X, Li Y, Li R (2012) Altered expression profiles of microRNAs upon arsenic exposure of human umbilical vein endothelial cells. *Environ Toxicol Pharmacol* 34(2):381-387 doi:10.1016/j.etap.2012.05.003
- Lippai D, Bala S, Csak T, Kurt-Jones EA, Szabo G (2013) Chronic alcohol-induced microRNA-155 contributes to neuroinflammation in a TLR4-dependent manner in mice. *PLoS One* 8(8):e70945 doi:10.1371/journal.pone.0070945
- Liu J, Xiao Y, Wu X, et al. (2018) A circulating microRNA signature as noninvasive diagnostic and prognostic biomarkers for nonalcoholic steatohepatitis. *BMC Genomics* 19(1):188 doi:10.1186/s12864-018-4575-3
- Lizarraga D, Gaj S, Brauers KJ, Timmermans L, Kleinjans JC, van Delft JH (2012) Benzo[a]pyrene-induced changes in microRNA-mRNA networks. *Chem Res Toxicol* 25(4):838-49 doi:10.1021/tx2003799
- Llewellyn HP, Vaidya VS, Wang Z, et al. (2021) Evaluating the Sensitivity and Specificity of Promising Circulating Biomarkers to Diagnose Liver Injury in Humans. *Toxicol Sci* 181(1):23-34 doi:10.1093/toxsci/kfab003
- Lu J, Getz G, Miska EA, et al. (2005) MicroRNA expression profiles classify human cancers. *Nature* 435(7043):834-8 doi:10.1038/nature03702
- Luo F, Ji J, Liu Y, et al. (2015) MicroRNA-21, up-regulated by arsenite, directs the epithelial-mesenchymal transition and enhances the invasive potential of transformed human bronchial epithelial cells by targeting PDCD4. *Toxicol Lett* 232(1):301-9 doi:10.1016/j.toxlet.2014.11.001
- Luo XJ, Liu B, Dai Z, et al. (2013) Expression of apoptosis-associated microRNAs in ethanol-induced acute gastric mucosal injury via JNK pathway. *Alcohol* 47(6):481-93 doi:10.1016/j.alcohol.2013.05.005
- Malik AI, Williams A, Lemieux CL, White PA, Yauk CL (2012) Hepatic mRNA, microRNA, and miR-34a-target responses in mice after 28 days exposure to doses of benzo(a)pyrene that elicit DNA damage and mutation. *Environ Mol Mutagen* 53(1):10-21 doi:10.1002/em.20668
- Marrone AK, Tryndyak V, Beland FA, Pogribny IP (2016) MicroRNA Responses to the Genotoxic Carcinogens Aflatoxin B1 and Benzo[a]pyrene in Human HepaRG Cells. *Toxicol Sci* 149(2):496-502 doi:10.1093/toxsci/kfv253

- Mendell JT, Olson EN (2012) MicroRNAs in stress signaling and human disease. *Cell* 148(6):1172-87 doi:10.1016/j.cell.2012.02.005
- Meng F, Glaser SS, Francis H, et al. (2012) Epigenetic regulation of miR-34a expression in alcoholic liver injury. *Am J Pathol* 181(3):804-17 doi:10.1016/j.ajpath.2012.06.010
- Meng X, Müller V, Milde-Langosch K, Trillsch F, Pantel K, Schwarzenbach H (2016) Diagnostic and prognostic relevance of circulating exosomal miR-373, miR-200a, miR-200b and miR-200c in patients with epithelial ovarian cancer. *Oncotarget* 7(13):16923-16935 doi:10.18632/oncotarget.7850
- Meng XZ, Zheng TS, Chen X, et al. (2011) microRNA expression alteration after arsenic trioxide treatment in HepG-2 cells. *J Gastroenterol Hepatol* 26(1):186-93 doi:10.1111/j.1440-1746.2010.06317.x
- Mohr A, Mott J (2015) Overview of MicroRNA Biology. *Seminars in Liver Disease* 35(01):003-011 doi:10.1055/s-0034-1397344
- Nakamura M, Kanda T, Sasaki R, et al. (2015) MicroRNA-122 Inhibits the Production of Inflammatory Cytokines by Targeting the PKR Activator PACT in Human Hepatic Stellate Cells. *PLoS One* 10(12):e0144295 doi:10.1371/journal.pone.0144295
- Navarro F, Lieberman J (2015) miR-34 and p53: New Insights into a Complex Functional Relationship. *PLoS One* 10(7):e0132767 doi:10.1371/journal.pone.0132767
- Pogribny IP, Beland FA, Rusyn I (2016) The role of microRNAs in the development and progression of chemical-associated cancers. *Toxicol Appl Pharmacol* 312:3-10 doi:10.1016/j.taap.2015.11.013
- Rahman MA, Patters BJ, Kodidela S, Kumar S (2020) Extracellular Vesicles: Intercellular Mediators in Alcohol-Induced Pathologies. *Journal of neuroimmune pharmacology : the official journal of the Society on NeuroImmune Pharmacology* 15(3):409-421 doi:10.1007/s11481-019-09848-z
- Ren X, Gaile DP, Gong Z, et al. (2015) Arsenic responsive microRNAs in vivo and their potential involvement in arsenic-induced oxidative stress. *Toxicol Appl Pharmacol* 283(3):198-209 doi:10.1016/j.taap.2015.01.014
- Rieswijk L, Brauers KJ, Coonen ML, van Breda SG, Jennen DG, Kleijnans JC (2015) Evaluating microRNA profiles reveals discriminative responses following genotoxic or non-genotoxic carcinogen exposure in primary mouse hepatocytes. *Mutagenesis* 30(6):771-84 doi:10.1093/mutage/gev036
- Rodrigues AC, Li X, Radecki L, et al. (2011) MicroRNA expression is differentially altered by xenobiotic drugs in different human cell lines. *Biopharmaceutics & drug disposition* 32(6):355-67 doi:10.1002/bdd.764
- Saha B, Bruneau JC, Kodys K, Szabo G (2015) Alcohol-induced miR-27a regulates differentiation and M2 macrophage polarization of normal human monocytes. *J Immunol* 194(7):3079-87 doi:10.4049/jimmunol.1402190
- Sayan AE, Griffiths TR, Pal R, et al. (2009) SIP1 protein protects cells from DNA damage-induced apoptosis and has independent prognostic value in bladder cancer. *Proc Natl Acad Sci U S A* 106(35):14884-9 doi:10.1073/pnas.0902042106
- Shan H, Zhang Y, Cai B, et al. (2013) Upregulation of microRNA-1 and microRNA-133 contributes to arsenic-induced cardiac electrical remodeling. *Int J Cardiol* 167(6):2798-805 doi:10.1016/j.ijcard.2012.07.009
- Sturchio E, Colombo T, Boccia P, et al. (2014) Arsenic exposure triggers a shift in microRNA expression. *Sci Total Environ* 472:672-80 doi:10.1016/j.scitotenv.2013.11.092
- Su YW, Chen X, Jiang ZZ, et al. (2012) A panel of serum microRNAs as specific biomarkers for diagnosis of compound- and herb-induced liver injury in rats. *PLoS One* 7(5):e37395 doi:10.1371/journal.pone.0037395

- Tang Y, Banan A, Forsyth CB, et al. (2008) Effect of alcohol on miR-212 expression in intestinal epithelial cells and its potential role in alcoholic liver disease. *Alcohol Clin Exp Res* 32(2):355-64 doi:10.1111/j.1530-0277.2007.00584.x
- Thum T, Gross C, Fiedler J, et al. (2008) MicroRNA-21 contributes to myocardial disease by stimulating MAP kinase signalling in fibroblasts. *Nature* 456(7224):980-4 doi:10.1038/nature07511
- Tian Q, Jia J, Ling S, Liu Y, Yang S, Shao Z (2014) A causal role for circulating miR-34b in osteosarcoma. *Eur J Surg Oncol* 40(1):67-72 doi:10.1016/j.ejso.2013.08.024
- Tong Z, Jiang B, Wu Y, et al. (2015) MiR-21 Protected Cardiomyocytes against Doxorubicin-Induced Apoptosis by Targeting BTG2. *Int J Mol Sci* 16(7):14511-25 doi:10.3390/ijms160714511
- van Steenwyk G, Janeczek P, Lewohl JM (2013) Differential Effects of Chronic and Chronic-Intermittent Ethanol Treatment and Its Withdrawal on the Expression of miRNAs. *Brain Sci* 3(2):744-56 doi:10.3390/brainsci3020744
- Vickers KC, Palmisano BT, Shoucri BM, Shamburek RD, Remaley AT (2011) MicroRNAs are transported in plasma and delivered to recipient cells by high-density lipoproteins. *Nat Cell Biol* 13(4):423-33 doi:10.1038/ncb2210
- Wang K, Zhang S, Marzolf B, et al. (2009) Circulating microRNAs, potential biomarkers for drug-induced liver injury. *Proc Natl Acad Sci U S A* 106(11):4402-7 doi:10.1073/pnas.0813371106
- Wang W, Liu R, Su Y, Li H, Xie W, Ning B (2018) MicroRNA-21-5p mediates TGF-beta-regulated fibrogenic activation of spinal fibroblasts and the formation of fibrotic scars after spinal cord injury. *Int J Biol Sci* 14(2):178-188 doi:10.7150/ijbs.24074
- Wang X, He Y, Mackowiak B, Gao B (2021) MicroRNAs as regulators, biomarkers and therapeutic targets in liver diseases. *Gut* 70(4):784-795 doi:10.1136/gutjnl-2020-322526
- Wang X, Jiang F, Mu J, et al. (2014) Arsenic trioxide attenuates the invasion potential of human liver cancer cells through the demethylation-activated microRNA-491. *Toxicol Lett* 227(2):75-83 doi:10.1016/j.toxlet.2014.03.016
- Yadav S, Pandey A, Shukla A, et al. (2011) miR-497 and miR-302b regulate ethanol-induced neuronal cell death through BCL2 protein and cyclin D2. *J Biol Chem* 286(43):37347-57 doi:10.1074/jbc.M111.235531
- Yang W, Lian J, Feng Y, et al. (2014) Genome-wide miRNA-profiling of aflatoxin B1-induced hepatic injury using deep sequencing. *Toxicol Lett* 226(2):140-9 doi:10.1016/j.toxlet.2014.01.021
- Yang X, Salminen WF, Shi Q, et al. (2015) Potential of extracellular microRNAs as biomarkers of acetaminophen toxicity in children. *Toxicol Appl Pharmacol* 284(2):180-7 doi:10.1016/j.taap.2015.02.013
- Yeakley JM, Shepard PJ, Goyena DE, VanSteenhouse HC, McComb JD, Seligmann BE (2017) A trichostatin A expression signature identified by TempO-Seq targeted whole transcriptome profiling. *PLoS One* 12(5):e0178302 doi:10.1371/journal.pone.0178302
- Yin H, Hu M, Zhang R, Shen Z, Flatow L, You M (2012) MicroRNA-217 promotes ethanol-induced fat accumulation in hepatocytes by down-regulating SIRT1. *J Biol Chem* 287(13):9817-9826 doi:10.1074/jbc.M111.333534
- Zhang Y, Wu JH, Han F, et al. (2013) Arsenic trioxide induced apoptosis in retinoblastoma cells by abnormal expression of microRNA-376a. *Neoplasia* 60(3):247-53 doi:10.4149/neo_2013_033
- Zuo J, Brewer DS, Arlt VM, Cooper CS, Phillips DH (2014) Benzo pyrene-induced DNA adducts and gene expression profiles in target and non-target organs for carcinogenesis in mice. *BMC Genomics* 15(1):880 doi:10.1186/1471-2164-15-880

3

Screening the microRNA landscape of Nrf2 pathway modulation identifies miR-6499-3p as a novel modulator of the anti-oxidant response through targeting of KEAP1

Luc J.M. Bischoff¹, Nanette G. Vrijenhoek¹, Johannes P. Schimming¹, Anke H.W. Essing¹, Lukas S. Wijaya¹, Jan P. Langenberg², Daan Noort², Bob van de Water¹

¹ Division of Drug Discovery and Safety, Leiden Academic Centre for Drug Research, Leiden University, Leiden, The Netherlands

² Department of CBRN Protection, TNO Defence, Safety and Security, Rijswijk, The Netherlands

Manuscript in preparation

ABSTRACT

The Keap1/Nrf2 anti-oxidant response pathway is of critical importance for the adaptive cell physiology during both (patho)-physiological circumstances and exposure to xenobiotics. The Nrf2 pathway is controlled by various kinases, ubiquitinases and transcriptional co-regulators. So far, a systematic analysis of the functional role of all known microRNAs on the Nuclear factor-erythroid-2-related factor 2 (Nrf2) pathway is lacking. Here we screened a panel of ~2600 individual microRNA mimics for modulation of Nrf2 pathway activation using an endogenous Nrf2 target *Srxn1*-GFP HepG2 reporter cell line in combination with high throughput live confocal imaging after treatment with CDDO-Me. We identified a panel of 16 microRNAs that enhance (including miR-3165, miR-1909-3p, miR-1293, and miR-6499-3p) and 10 microRNAs that inhibit (including miR-200a-3p, miR-363-3p, miR-502-5p, and miR-25-3p) CDDO-Me-induced *Srxn1*-GFP expression. Overall these microRNAs had minimal effects on the activation of other cellular stress response pathways. Transcriptome analysis demonstrated a direct effect of the candidate inhibiting and enhancing microRNAs on Nrf2 target genes, reflecting the direct effect of Nrf2 and Keap1 depletion, respectively. MicroRNAs with identical seed regions showed a large overlap in differential gene expression. Target prediction models identified miR-6499-3p as a modulator of *KEAP1*. miR-6499-3p suppressed *KEAP1* expression and promoted Nrf2 stability and strongly enhanced *Srxn1*-GFP expression in association with protection against oxidative stress-induced cell death. In conclusion, we identified various microRNAs that control the Nrf2 pathway and which might be relevant biomarkers and/or provide alternative therapeutic modalities to modulate Nrf2 pathway activity in health and disease.

INTRODUCTION

There is increasing evidence that microRNAs are of critical importance in the modulation of chemical-induced drug responses (Balasubramanian et al. 2020). MicroRNAs (miRNAs or miRs) are small ~22-nt non-coding RNAs (Almeida et al. 2011; Lee et al. 1993; Starega-Roslan et al. 2010) and ~2000 human microRNA sequences have been determined (miRBase release 22). The biogenesis of microRNAs consists of multiple different steps (Hou et al. 2011; Lewis et al. 2003). First, pri-miRNA (primary miRNA transcripts) are transcribed in the nucleus by mainly RNA polymerase II or in some cases polymerase III (Borchert et al. 2006; Lee et al. 2004). Next, these pri-miRNAs are cleaved forming precursor microRNA (pre-miRNA) by microprocessor. This microprocessor complex is formed by DROSHA, a double-stranded RNase III enzyme, and its essential cofactor, the double-stranded RNA (dsRNA)-binding protein DiGeorge syndrome critical region 8 (DGCR8) (Lin and Gregory 2015). The pre-miRNA is transported to the cytoplasm by Exportin-5 and cleaved into an imperfectly double-stranded miRNA by the RNase III protein Dicer. The small RNA duplex generated by dicer is loaded onto an AGO protein (AGO2 being the most important), forming a RNA-Induced Silencing Complex (RISC). In RISC, both ends of the microRNA are protected by AGO proteins making them highly stable.

MicroRNAs regulate gene expression at the post-transcriptional level. The microRNA target sites are typically located on the 3'untranslated region of their target mRNAs. These target sites only need to be partially complementary to the microRNA (Lam et al. 2015), which leads to target mRNA translational repression or degradation (Djuranovic et al. 2012; Filipowicz et al. 2008). MicroRNAs can have 100 target sites per microRNA (Brennecke et al. 2005), and mRNAs can be targeted by more than one microRNA (Peter 2010; Wu et al. 2010). MicroRNAs are involved in many physiological processes including the immune response, metabolism, and development (Hou et al. 2011). Furthermore, microRNAs are involved in toxicological responses and disease (Mendell and Olson 2012) including activation and inhibition of various cellular stress response pathways (Bartoszewska et al. 2013).

A critical cellular stress response pathway is the anti-oxidant Nrf2 pathway, named after its transcription factor nuclear factor erythroid 2-related factor 2 (Nrf2). Under basal conditions Nrf2 is bound in the cytoplasm to two Kelch-like ECH-associated protein 1 proteins (Keum and Choi 2014; Zipper and Mulcahy 2002). Nrf2 consist of seven functional domains (Neh1 – Neh7). Of these domains Neh2 contains seven lysine residues which plays a role in the ubiquitination of Nrf2 (Itoh et al. 1999; Zhang et al. 2004), which facilitates the destruction of Nrf2 via the ubiquitin-26S proteasomal pathway (Kobayashi et al. 2004). Furthermore, Neh2 contains two binding sites which

interact with Keap1. These are the ETGE and DLG motives (McMahon et al. 2006). Binding of reactive oxygen species (ROS) or reactive metabolites to one of the cysteine groups of Keap1 is thought to induce a conformational change in Keap1, resulting in the detachment of Nrf2 of the DLG-motif. As a result, ubiquitination cannot take place. Newly produced Nrf2 translocates to the nucleus where, together with members of the masculoaponeurotic fibrosarcoma (Maf) proteins (MafF, MafG and MafK), it binds to the antioxidant response element (ARE). Binding to the ARE results in the transcription of different cytoprotective genes involved in e.g. glutathione metabolism, phase 2 drug-metabolizing enzymes and antioxidant response proteins as, for example, sulfiredoxin1 (Srxn1), hemeoxygenase 1 (Hmox1), and NAD(P)H-quinone oxidoreductase 1 (Nqo1) (Hayes et al. 2010; Zhang and Gordon 2004).

The Nrf2 pathway is critical in health and disease. Ischemic-reperfusion injury leads to strong activation of the Nrf2 pathway in e.g. liver, kidney and heart (Dodson et al. 2019). Xenobiotic exposure leads to the activation of the Nrf2 pathway in various target tissues, including various hepato- and nephrotoxic drugs (Copples et al. 2019; Herpers et al. 2016; Hiemstra et al. 2019; Wink et al. 2018). Therapeutic modulation of the Nrf2 pathway has been an important strategy to protect tissue for detrimental levels of oxidative stress under various pathological circumstances, including CDDO-Me (Cuadrado et al. 2018). Moreover, given the sustained activation of Nrf2 signaling in various types of cancer (Dodson et al. 2019), suppression of Nrf2 activity will be of critical importance to overcome the resistance to various anticancer therapeutics.

The Nrf2 pathway is controlled by various signal transduction components. Protein kinases can modulate both Keap1 and Nrf2 post-translational modification involving PKC and PERK (Baird and Yamamoto 2020). Ubiquitination is critical to modulate Nrf2 degradation and involves the KEAP1-CUL3-RBX1 complex (Baird and Yamamoto 2020). Transcriptional co-activators of the MAF family are critical to modulate Nrf2 transcriptional activity (Yamamoto et al. 2018). More recently various microRNAs including miR-200a were identified that modulate the levels of Nrf2 activity through direct modulation of Nrf2 levels (Cheng et al. 2013). Given the opportunities of microRNAs as candidate (mechanistic) biomarkers and therapeutic modulators, so far a systematic evaluation of the role of microRNAs in the control of Nrf2 signaling is lacking. Here the objective was to systematically uncover the microRNA landscape of Nrf2 pathway modulation through a whole genome microRNA mimic arrayed phenotypic high content imaging screen.

METHODS

Reagents

A human miRIDIAN miRNA Mimic Library 19.0 + 21.0 Supplement (2 nmol) was obtained from Dharmacon, USA. Upon arrival, plates were resuspended following the manufacture's description. MicroRNAs were diluted in 1x siRNA buffer (Dharmacon, USA) to a final concentration of 1 μ M. 5 μ L microRNA solution/well (96-well plate) was used giving a final concentration of 50 nM/well. siRNAs were obtained from Dharmacon and resuspended in a similar matter. Interferin (Westburg/PolyPlus, NL) was used as a transfection agent.

The following chemicals were used to induce cellular stress response activation: CDDO-Me (CAS: 218600-53-4) was purchased from Cayman Chemicals, USA. Diethyl maleate (CAS: 141-05-9), tert-butylhydroquinone (CAS: 1948-33-0), etoposide (CAS: 33419-42-0) and tunicamycin (CAS:11089-65-9) were purchased from Sigma-Aldrich, USA and dissolved in 100% dimethyl sulfoxide (CAS: 67-68-5) purchased from Sigma-Aldrich, USA. Antibodies were acquired from Santa Cruz (GAPDH: sc-32233 and Cell Signaling (GFP: #2956).

Cell culture, microRNA transfection, and immunofluorescence

A human hepatoma HepG2 cell line was obtained from American Type Culture Collection (ATCC® HB-8065™, Wesel, Germany). Previously, HepG2-GFP reporter cells were developed and characterized for Keap1, Nrf2, Srxn1, Hmox1, p21 and Chop/DDIT3 (Wink et al. 2017). Briefly, cell lines were constructed with green fluorescent protein (GFP) reporter genes located on bacterial artificial chromosomes (BACs) that encode C-terminal GFP-tagged fusion proteins, following 500 μ g/mL G-418. For more information see (Poser et al. 2008). Cells were grown in Dulbecco's Modified Eagle Medium (DMEM) high glucose, supplemented with 10% (v/v) fetal bovine serum (FBS), 25 U/mL penicillin and 25 μ g streptomycin. Cells were used for experiments until passage 20.

For experiments, 23,000 cells/well were seeded and transfected in a 96-well plate. 72 h after transfection, cells were exposed to different chemicals. After exposure, the plates were measured making use of confocal microscopy (Figure 1A).

For immunofluorescence analysis of the p62 (SQSTM1) protein, plates containing HepG2-Keap1-GFP cells were used. These cells were transfected with microRNAs for 72 hours and exposed to CDDO-Me (30 nM) for 24 h. After this period, cells were washed with PBS and stained with formaldehyde. For immunofluorescence measurement, fixed cells were permeabilized followed by primary antibody SQSTM1/

p62 staining (D5L7G; Cell Signaling, USA); IgG goat anti mouse linked to Cy-3 was used for secondary staining (Jackson ImmunoResearch, NL). Immunofluorescence was evaluated by confocal microscopy as described below.

Live confocal imaging

Live cell confocal imaging of GFP reporter HepG2 cells was performed on a Nikon Eclipse Ti confocal microscope equipped with four lasers: 366, 408, 488 and 561 nm. A 20x dry PlanApo VC NA 0.75 with 1x zoom was used. Prior to exposure, Hoechst³³³⁴² 100 ng/mL was added to the wells to stain nuclei and propidium iodide (PI) was added to measure cell death. For miRNA screens images were taken at specific time points; for validation screens live cell imaging was performed for a total period of 24 h with 1 hour time intervals. Microscopy images were further analyzed using Cell Profiler and R to define GFP reporter intensity at the single cell level. The fraction of GFP positive cells was calculated by counting the amount of cells with a GFP-value two times above baseline (DMSO control) level.

Viability assessment

To further explore the impact of microRNA overexpression on cell viability, HepG2-WT were transfected with miRNAs or siRNA controls for 72 h followed by co-staining with Hoechst 33342 and propidium iodide and then treated with 278 or 600 μ M nitrofurantoin (CAS: 67-20-9, Sigma Aldrich, #N7878) followed by high content imaging of cytotoxicity as previously described (Schimming et al. 2019).

Western blot

HepG2-WT cells were seeded 200,000 cells/well and transfected in a 24-well plate. After 72 h cells were exposed to different concentrations of CDDO-Me. Cells were lysed after 7 h with direct lysis buffer (70 μ L/well, 2x SPB (sample buffer: bromophenol blue solution) lysis buffer + 10% β -mercaptoethanol) and stored at -20°C. Proteins were separated on acrylamide gels (7.5%, 15% for SRXN1) and blotted on PVDF membranes. Membranes were blocked with 5% BSA (bovine serum albumine) in Tris-buffered saline (TBS)/0.05% Tween for 1 h at RT. Staining with antibodies (1:1000) was done overnight at 4°C in 1% BSA in TBS/Tween. After washing the membranes were exposed to HRP (GFP) or Cy-5 (housekeeping gene GAPDH) in 1% BSA in TBS/Tween for 1 h at RT. The membrane was exposed to ECL reagent for 5 minutes followed by immunoluminescence detection with ImageQuant™ LAS 4000 (GE Healthcare). Image analysis was done in imageJ.

Targeted RNA sequencing and bioinformatics

To determine gene expression changes after microRNA transfection, HepG2-WT (wild type) cells were used. The HepG2-WT cells were plated in 96-well plates (23,000

cells/well) and transfected as described above with selected microRNAs. siKEAP, siNFE2L2/Nrf2, mock control, and medium control were taken along as controls. After 72 h of transfection, wells were washed with 200 μ L PBS and lysed with 50 μ L TempO-Seq lysis buffer (BioSpyder, USA) for 5 minutes at room temperature. Lysate plates were sealed and immediately frozen at -80 °C. Experiments were performed as three biological replicates. The lysate plates were shipped on dry ice to Bioclavis (Glasgow, Scotland) followed by whole transcriptome TempO-Seq targeted RNAseq analysis (Yeakley et al. 2017).

Differentially expressed genes ($p_{adj} < 0.05$) were identified by the DESeq2 method (Love et al. 2014) using the therein described R package DESeq2. The mock transfection treatment was used as a control and the cutoff for sample exclusion was a total read count of 100,000. Pathway analysis was performed using IPA (QIAGEN Inc., <https://www.qiagenbioinformatics.com/products/ingenuitypathway-analysis>). Pathway enrichment analysis was performed leveraging the function of TXG-MAPr - PHH platform (https://txg-mapr.eu/WGCNA_PHH/TGGATES_PHH/ (Callegaro et al. 2021)). The log2 fold change values obtained from high throughput targeted sequencing (TempO-Seq) was uploaded to the online platform after eliminating probes measuring non-expressed genes (base mean = 0). Additionally, we only selected one probe per gene so that for probes which are measuring the expression of similar genes, we only selected one with the least adjusted p-value per condition. The gene expression values measured from TempO-Seq data were plotted according to the gene network model (modules) within the platform. The eigengene scores (EGS) for each module were calculated based on the z-score derived from the log2 fold change values of the genes consisting the network (module membership).

For microRNA target prediction, three different databases were used: IPA, mirDB (<http://www.mirdb.org>), (Wong and Wang 2015), and TargetScanHuman version 7.1 (http://www.targetscan.org/vert_71) (Agarwal et al. 2015). These sites both use an own bioinformatics algorithm to predict possible microRNA targets. For MiRDB we used a prediction score of >80. For Targetscan we used the cumulative context++ score, which estimates the total repression expected from multiple sites of the same microRNA, for each mRNA target predicted (Riffo-Campos et al. 2016).

Data analysis

Biological replicates were performed 3 times or more as indicated in the figure legends. Statistical analysis was performed in R. Figures were made in R, and Venn diagrams were made with the online tool Venny2.1 (<http://bioinfogp.cnb.csic.es/tools/venny/index.html>).

RESULTS

MicroRNA screen for Nrf2 pathway modulation

Here we systematically screened for microRNAs that affect Nrf2 pathway activation. For this we used the BAC-GFP-Srxn1 HepG2 reporter cells where Srxn1-GFP expression is dependent on Nrf2 activity (Wink et al. 2017). In total we screened the effect of expression of ~2600 individual miRNA mimetics. We used CDDO-Me (30 nM) to induce Nrf2 activation and measured the effect of microRNA expression on GFP-Srxn1 levels after 7 h. Since CDDO-Me-induced Srxn1-GFP expression takes ~4 h for onset we could use the 1 h time point as the miRNA only effect (Figure 1B and C). We observed numerous microRNAs affected Srxn1-GFP at 1 h or 7 h after CDDO-Me treatment. Remarkably, the performance on the effect of various microRNAs was stronger than the effect of siKEAP1 (enhancing Srxn1-GFP induction) and siNFE2L2 (suppressing Srxn1-GFP expression), supporting the likely strong effect of individual microRNAs on Nrf2 signaling. For further studies, we focused on the top 100 overlapping microRNAs at both time points, for both Srxn1-GFP enhancing (Figure 1D) and inhibiting (Figure 1E) microRNAs.

Next, we conducted a secondary screen for three biological replicates to validate the hits found in the primary screen (one biological replicate). We selected in total 134 Srxn1-GFP enhancing microRNAs: the top 100 enhancers found 1 h after exposure and the additional 34 microRNAs found in the top 100 after 7 h CDDO-Me exposure. In addition, we selected the top 100 microRNAs that did inhibit the Srxn1-GFP response after 7 h. Most of the 134 Srxn1-GFP enhancing microRNAs promoted the Srxn1-GFP intensity compared to the mock condition as well as the fraction of Srxn1-GFP positive cells (Figure 2A-D and Suppl. Figure 1). Interestingly, some microRNAs displayed a similar enhancement of Srxn1-GFP response as siKEAP1, including miR-3165, miR-1909-3p, miR-1293, and miR-6499-3p. Furthermore, most of the 100 inhibiting microRNAs used in the secondary screen, led to a lower Srxn1-GFP intensity associated with limited number of Srxn1-GFP positive cells (Figure 2E and F). For some microRNAs the effect on inhibition of CDDO-Me-induced Srxn1-GFP expression was stronger than siNFE2L2, including miR-200a-3p, miR-363-3p, miR-502-5p, and miR-25-3p. For follow up experiments, based on the comparison on the effect of siKEAP1 and siNFE2L2, we selected the top 16 Srxn1-GFP enhancing microRNAs and the top 10 Srxn1-GFP inhibiting microRNAs (Figure 2G and H). We screened for Nrf2 modulating microRNAs using CDDO-Me as a potent pharmacological activator of Nrf2 signaling through its modification of Keap1. To exclude the context dependency of our results, we verified the effect of the candidate microRNAs also in the context of tert-butylhydroquinone (tBHQ; 100 μ M) and diethyl maleate (DEM; 100 μ M), two known inducers of the Nrf2 pathway, but with a different mode of action (Casey et

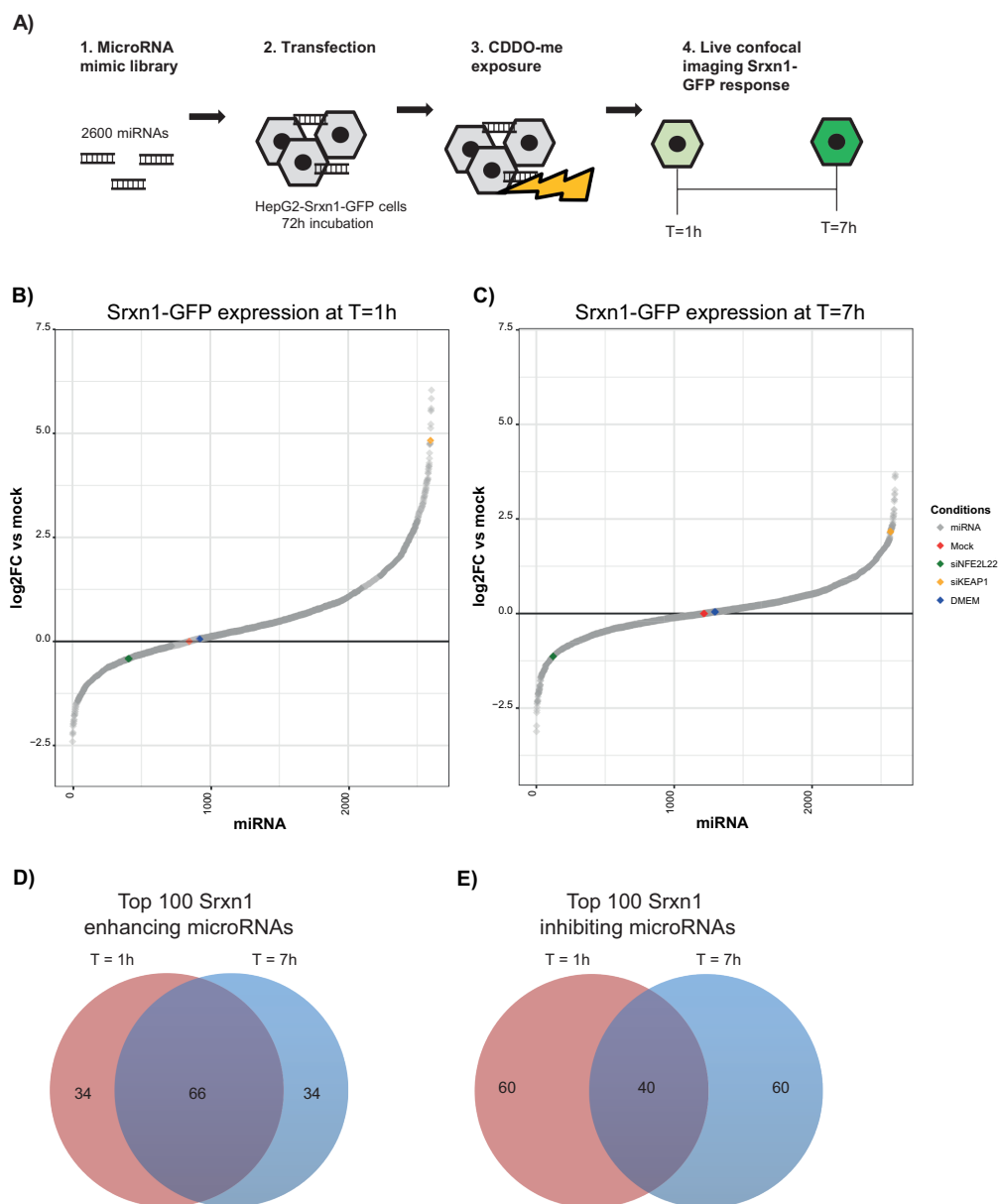


Figure 1. Systematic screen for microRNA mimetics on Nrf2 activation.

A) Schematic overview of the used *in vitro* method. **B)** Ranked distribution of the microRNAs to their GFP-intensity (\log_2FC vs mock) 1 h after exposure to 30 nM CDDO-Me. **C)** Ranked distribution of the microRNAs to their GFP-intensity (\log_2FC vs mock) 7 h after exposure to 30 nM CDDO-Me. **D)** Top 100 Srxn1 enhancing microRNAs for each time point, showing a 66 % overlap between 1 h and 7 h after 30 nM CDDO-Me exposure. **E)** Top 100 Srxn1 inhibiting microRNAs for each time point, showing a 40 % overlap between 1 h and 7 h after 30 nM CDDO-Me exposure.

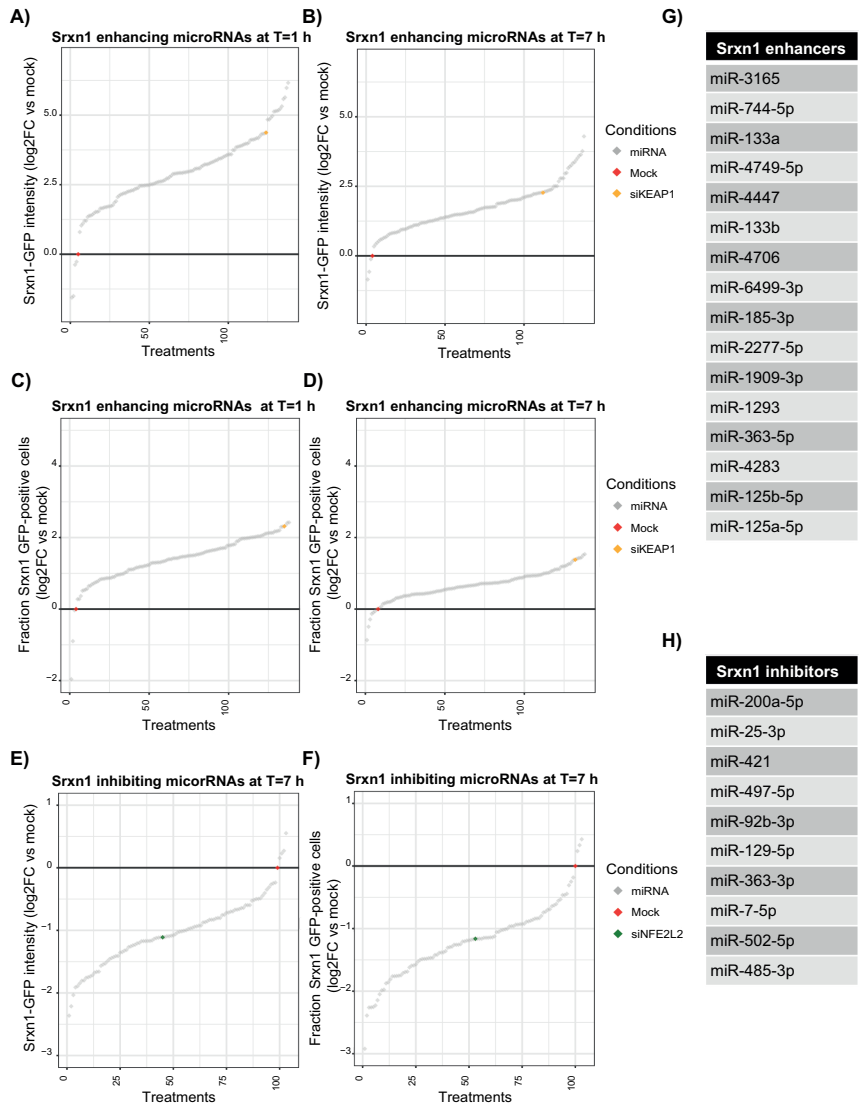


Figure 2. Validation of candidate Nrf2 signaling modulating microRNAs.

A) Ranked distribution of the 134 selected Srnx1 enhancing microRNAs, including mock and siKEAP1 control, to their Srnx1-GFP intensity (log2FC vs mock) after 1 h 30 nM CDDO-Me exposure. **B)** Ranked distribution of the 134 selected Srnx1 enhancing microRNAs, including mock and siKEAP1 control, to their Srnx1-GFP intensity (log2FC vs mock) after 7 h 30 nM CDDO-Me exposure. **C)** Ranked distribution of the 134 selected Srnx1 enhancing microRNAs, including mock and siKEAP1 control, to the amount of Srnx1 GFP-positive cells (log2FC vs mock) after 1 h 30 nM CDDO-Me exposure. **D)** Ranked distribution of the 134 selected Srnx1 enhancing microRNAs, including mock and siKEAP1 control, to the amount of GFP-positive cells (log2FC vs mock) after 7 h 30 nM CDDO-Me exposure. **E)** Ranked distribution of the 100 selected Srnx1 inhibiting microRNAs, including mock and siNFE2L2 control, to their Srnx1-GFP intensity (log2FC vs mock) after 7 h 30 nM CDDO-Me exposure. **F)** Ranked distribution of the 100 selected Srnx1 inhibiting microRNAs, including mock and siNFE2L2 control, to the amount of Srnx1 GFP-positive cells (log2FC vs mock) after 7 h 30 nM CDDO-Me exposure. **G)** selected Srnx1 enhancing microRNAs. **H)** Selected Srnx1 inhibiting microRNAs.

al. 2002; Priya et al. 2014; Yamauchi et al. 2011, Imhoff and Hansen 2010, Abiko et al 2011, Weber et al 1990) (Suppl. Figure 2).

Effects of candidate microRNAs on the dynamics of Nrf2 pathway activation

To further increase our understanding of the effect of the selected validated candidate microRNAs on the Nrf2 pathway, we tested the effect of the 16 Srxn1-GFP enhancing and 10 Srxn1-GFP inhibiting microRNAs on Nrf2 activation and Keap1 behavior using our previously established BAC-GFP-Nrf2 and Keap1-GFP HepG2 reporter cell lines. For this we followed the dynamics of the Nrf2-GFP and Keap1-GFP using 24 h live confocal imaging (Figure 3A). We observed strong overall enhancement of Srxn1-GFP activation with some microRNAs already demonstrating Srxn1-GFP expression prior to CDDO-Me addition and with limited enhancement (e.g. miR-6499-3p) or with further strong enhancement of Srxn1-GFP (e.g. miR-4749-5p; Figure 3B). Typically the response of the enhancer was much stronger than for CDDO-Me alone. Interestingly, for some of the enhancing microRNAs, the effect was associated with strongly enhanced Nrf2-GFP nuclear expression levels (e.g. miR-3165; Figure 3C) and was associated with later onset of Keap1-GFP translocation to autophagosome foci (e.g. miR-2277-5p) (Figure 3D and Suppl. Figure 3). Overall, the effect of the validated candidates on the different Nrf2 pathway components was microRNA specific, suggesting different functions of the various microRNAs in modulating the Nrf2 pathway.

Effects of microRNAs on other generic cellular stress response pathways

MicroRNAs can target multiple genes and therefore potentially affect various cellular stress response pathways. Alternatively, the expression of microRNA mimetics may trigger a general cellular stress response and activate e.g. also an unfolded protein response or the DNA damage response (Figure 4A). Therefore, first we evaluated the effect of the candidate microRNAs on the expression of Hmox1, a stress response gene that is activated upon oxidative stress in various tissues and under the control of AP-1 transcription factors (Medina et al. 2020). While CDDO-Me (30 nM) caused strong activation of the Nrf2-dependent Srxn1-GFP expression, no major induction of Hmox1-GFP was observed. MicroRNAs that did promote Srxn1-GFP induction did not per se affect Hmox1-GFP reporter activation after CDDO-Me treatment, except for miR-2277-5p. Interestingly, miR-485-3p transfection led to a strong Hmox1 activation, irrespective of CDDO-Me treatment (Figure 4B). An explanation for this might be that miR-485-3p is related to the iron-responsive regulation of ferroportin, a cellular iron exporter (Sangokoya et al. 2013). None of the microRNAs caused induction of p21-GFP expression caused by p53 activation, indicating that these microRNAs do

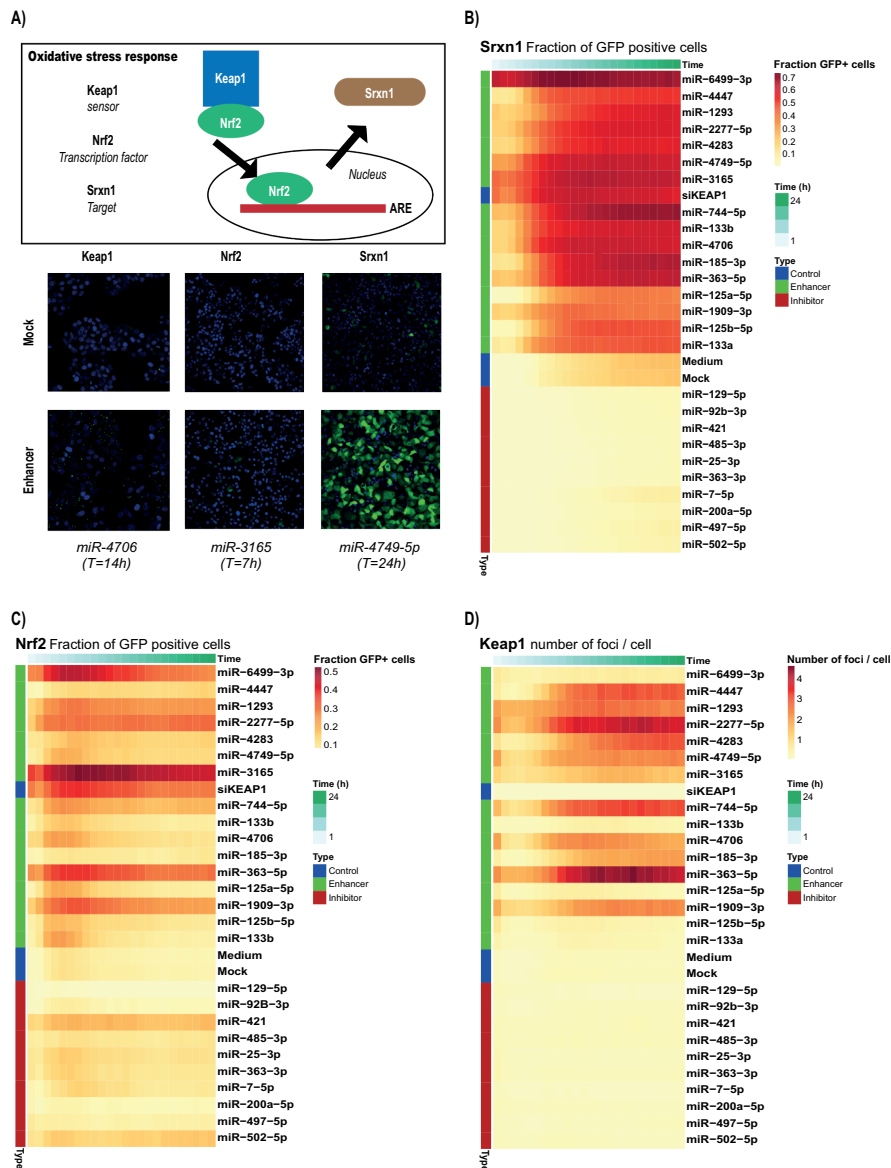


Figure 3. Effect of candidate microRNAs on the dynamics of Nrf2 pathway activation by CDDO-Me.

A) Schematic overview of the Nrf2 pathway and the corresponding microscope images (mock condition and examples of Srxn1-enhancing microRNAs **B)** Heatmap showing the fraction of Srxn1-GFP positive cells after transfection (72 h) of the different selected Srxn1-enhancing and Srxn1-inhibiting microRNAs over a 24 h timespan after exposure to 30 nM CDDO-Me. **C)** Heatmap showing the fraction of Nrf2-GFP positive cells after transfection (72 h) of the different selected Srxn1-enhancing and Srxn1-inhibiting microRNAs over a 24 h timespan after exposure to 30 nM CDDO-Me. **D)** Heatmap showing the number of Keap1 foci after transfection (72 h) of the different selected Srxn1-enhancing and Srxn1-inhibiting microRNAs over a 24 h timespan after exposure to 30 nM CDDO-Me. Values in all heatmaps are mean values from three different experiments.

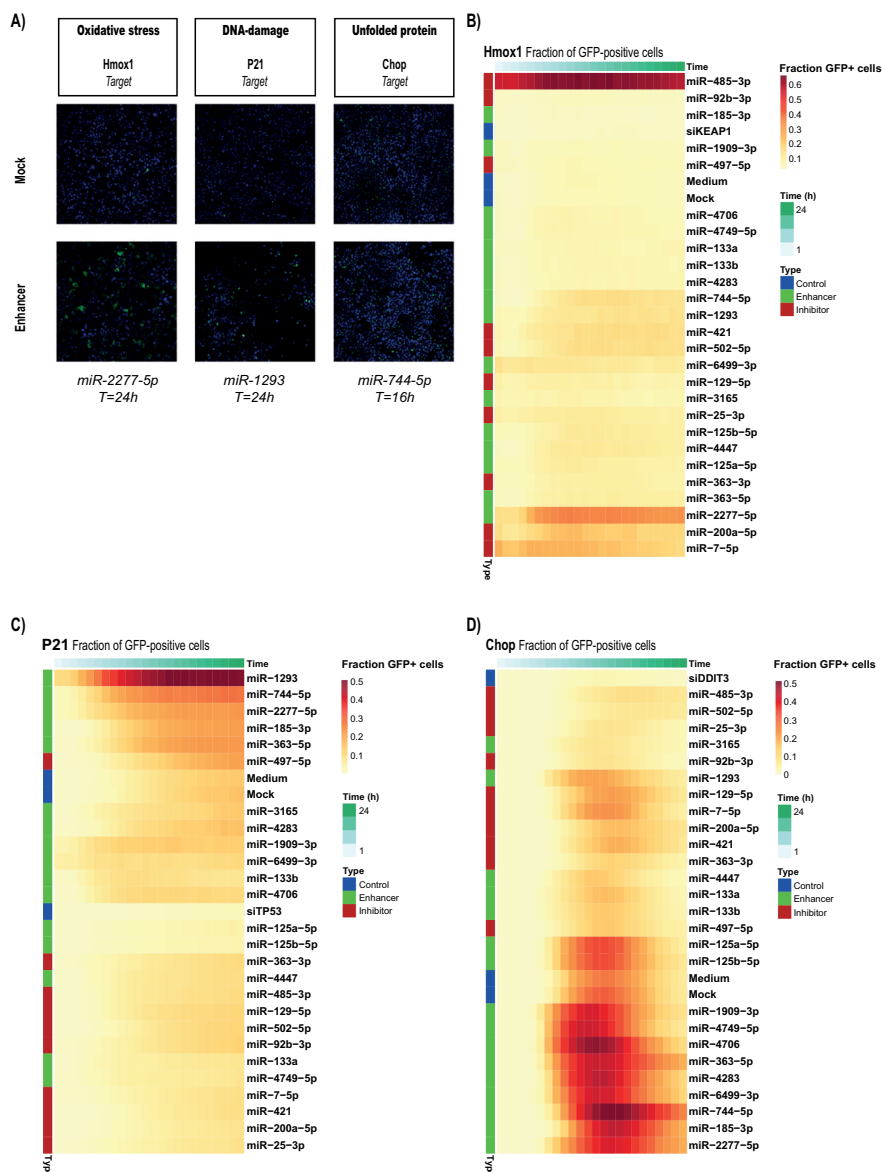


Figure 4. Effect of candidate microRNAs on cellular stress response pathway activation.

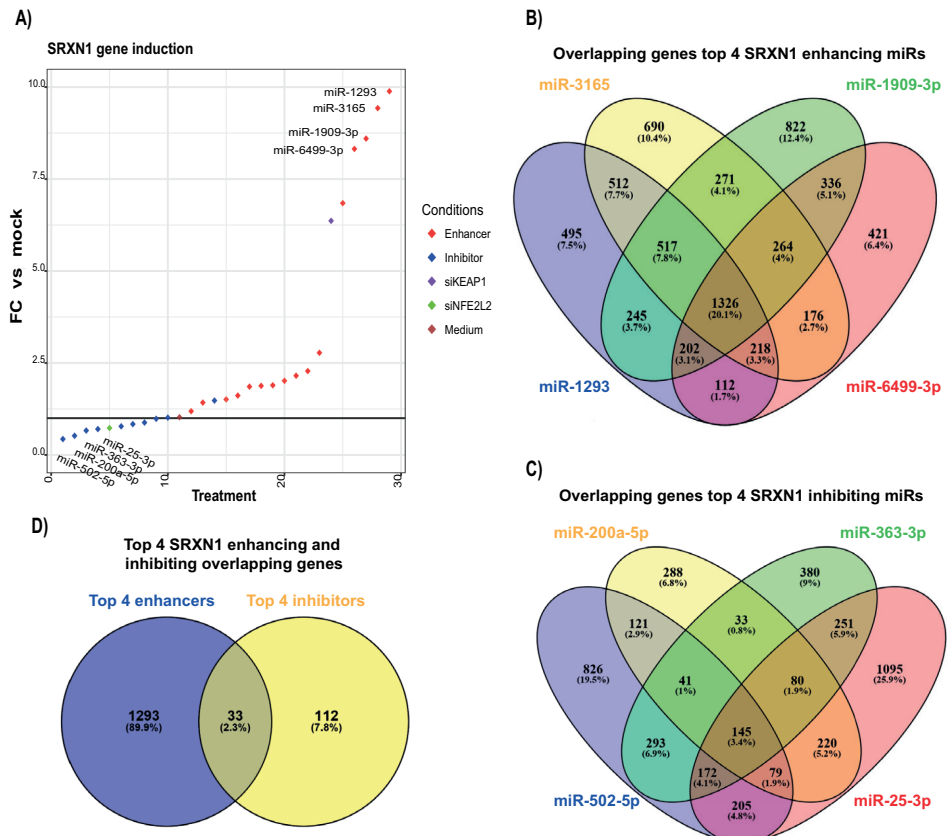
A) Microscope images of HepG2 Hmx1-GFP, p21-GFP and Chop-GFP cells (mock condition and examples of *Srxn1* enhancing microRNAs). **B)** Heatmap showing the fraction of Hmx1-GFP positive cells after transfection (72 h) of the different selected *Srxn1*-enhancing and *Srxn1* inhibiting microRNAs over a 24 h timespan after 30 nM CDDO-Me exposure. **C)** Heatmap showing the fraction of p21-GFP positive cells after transfection (72 h) of the different selected *Srxn1* enhancing and *Srxn1* inhibiting microRNAs over a 24 h timespan after exposure to 25 μ M etoposide. **D)** Heatmap showing the number of Chop-GFP positive cells after transfection (72 h) of the different selected *Srxn1* enhancing and *Srxn1* inhibiting microRNAs over a 24 h timespan after exposure to 6 μ M tunicamycin. Values in all heatmaps are mean values from three different experiments.

likely not impact on DNA damage response signaling or modulation of the cell cycle. Yet, we found that in particular some of the Nrf2 pathway enhancing microRNAs did also enhance the induction of p21-GFP reporter activity caused by etoposide, with a remarkable effect by miR-1293. Also some Nrf2 pathway suppressing microRNAs did enhance the etoposide response, including miR-497-5p (Figure 4C). In previous studies we observed that *Srxn1*-GFP activation by drugs that have a liability for drug-induced liver injury is associated with the activation of the unfolded protein response that is represented by the upregulation of the unfolded protein response marker CHOP/DDIT3 (Wink et al. 2018). While siCHOP/DDIT3 abolished the Chop-GFP induction by tunicamycin, microRNAs that caused enhancement of Nrf2 pathway activation did not affect the dynamics of the induction of Chop-GFP. Moreover, none of the microRNAs did affect Chop-GFP levels by itself (Figure 4D).

Nrf2 pathway modulating microRNA mimic transcriptomic responses of KEAP1 depletion

As a next step we aimed to get more insight on the overall regulation of gene expression profiles of our candidate microRNAs. Therefore we established transcriptome analysis using whole genome targeted RNAseq analysis based on the TempO-Seq approach (Yeakley et al. 2017). We established the transcriptome for all candidate enhancers and suppressors as well as siNFE2L2 (Nrf2) and siKEAP1 as controls, in the absence of any treatment (Figure 5). We observed the suppression and enhancement of basal *Srxn1* expression by the respective candidate microRNAs, with several microRNAs being as potent enhancers as siKEAP1 (i.e. miR-1293, miR-3165, miR-1909-3p and miR-6499-3p), and a panel of repressors as potent as siNFE2L2 (i.e. miR-502-5p, miR-200a-5p, miR-363-3p and miR-25-3p) (Figure 5A). Overall, we did not observe major changes in the expression of the critical Nrf2 pathway components *KEAP1* and *NFE2L2* (see Suppl. Figure 4). We anticipated that the microRNAs that showed similar effects on *Srxn1* expression would have similar gene expression modulation. Therefore, we compared the transcriptome of the top 4 enhancing microRNAs and the top 4 inhibiting microRNAs, based on their ability to induce or repress *SRXN1* and compared their significantly ($\text{padj} \leq 0.05$) differentially expressed (DE) genes (Fig. 5B and C). The top 4 enhancing microRNAs had 20.1 % (1326) DE genes in common, whereas the top 4 inhibiting microRNAs had only 3.4 % DE genes in common. 33 DE expressed genes were found in both the top 4 enhancing and the top 4 inhibiting microRNAs (Figure 5D; Suppl. Table 1). Next, we assessed whether the enhancing and inhibiting miRNAs shared similar pathway modulation as siKEAP1 or siNFE2L2, respectively. We used pathway analysis software to define the top 20 (10 up and 10 down) differentially expressed canonical pathways after siKEAP1 transfection and directly compared these with all the 16 candidate enhancing microRNAs. The effect of most microRNAs were highly comparable

to siKEAP1, with miR-6499-3p being most similar. Importantly, as expected, all candidate enhancing microRNAs showed an upregulation of the Nrf2 signaling pathway. Moreover, also most microRNAs did affect Rho-GTPase signaling pathways comparable to *KEAP1* depletion. Strikingly, various microRNAs did activate the LXR/RXR pathway, which was downregulated by siKEAP1, demonstrating differential regulation (Figure 5E). The suppressing microRNAs showed similar overall Nrf2 signaling pathway suppression as siNFE2L2, except for miR-25-3p. While, miR-363-3p showed most comparable pathway modulation for down regulated pathway, it did not affect the pathways that were strongest upregulated after Nrf2 depletion (Figure 5F). Some pathways were differentially affected by Nrf2 pathway suppressors and enhancers (marked in bold) although not in opposite directions, suggesting to be due to experimental conditions, e.g. transfection reagents. Particularly, the LXR/RXR pathway was strongly activated, possibly due to transactivation by transfection lipids.



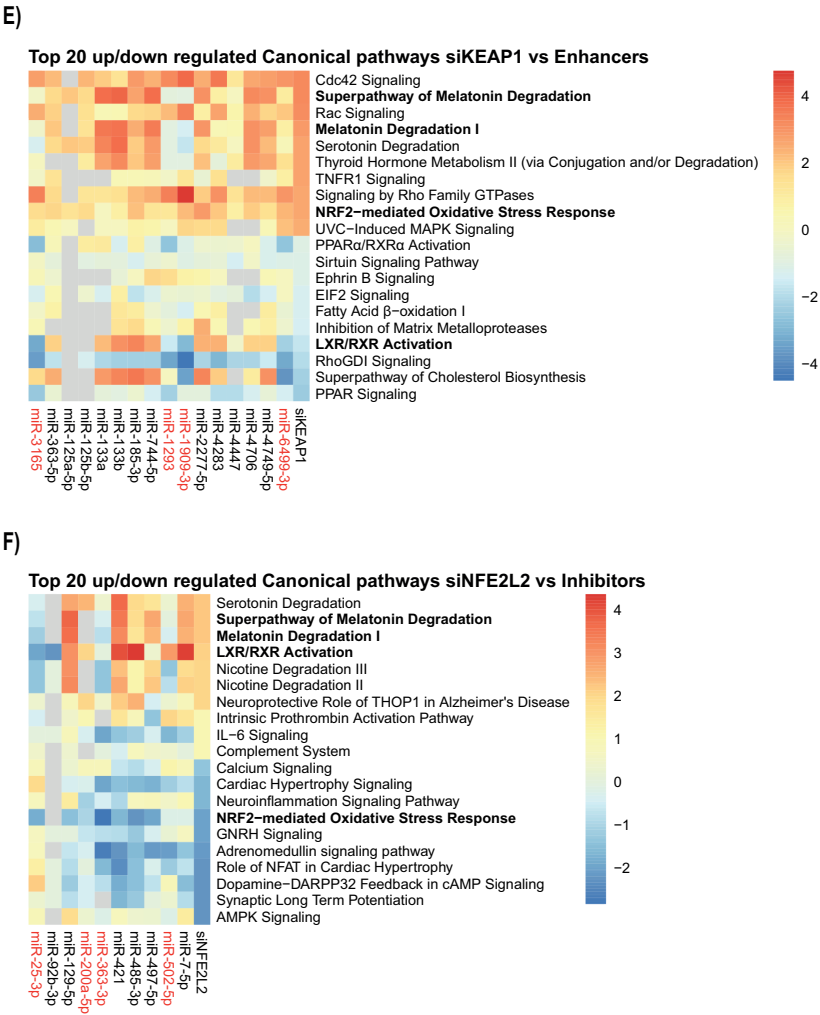


Figure 5. Effect of candidate Nrf2 pathway modulating miRNA on gene expression.

A) Ranked distribution of the selected microRNAs (enhancer, inhibitor), siKEAP1, siNFE2L2 and medium control for SRXN1 gene induction in HepG2 cells 72 hour after microRNA transfection. **B)** Venn diagram showing the overlapping genes of the top 4 Srxn1 enhancing microRNAs. Percentages are calculated from the total gene-set. **C)** Venn diagram showing the overlapping genes of the top 4 Srxn1 inhibiting microRNAs. Percentages are calculated from the total gene-set. **D)** Venn diagram showing the amount of overlapping DE genes between the overlapping top 4 Srxn1 enhancing and top 4 Srxn1 inhibiting genes. **E)** Heatmap showing clustering of the top 10 upregulated pathways and top 10 downregulated pathways after siKEAP1 transfection compared with the 16 selected enhancing microRNAs. Top 4 is shown in red. **F)** Heatmap showing clustering of the top 10 upregulated pathways and top 10 downregulated pathways after siNFE2L2 transfection compared with the 10 selected inhibiting microRNAs. Gene samples for this measurement were taken after 72 h transfection. Pathway analysis was performed using IPA software. Top 4 is shown in red.

To further assess the impact of the candidate microRNAs on the Nrf2 transcriptional network, we used the siNFE2L2 and siKEAP1 treatments to define the gene set that is under direct control of KEAP1/Nrf2 regulation (Figure 6A). We included genes that were upregulated after *KEAP1* depletion and downregulated after Nrf2 depletion (Figure 6B and Suppl. Table 2), or downregulated by depletion of *KEAP1* and upregulated after depletion of Nrf2 (Figure 6C and Suppl. Table 3). Next, we defined the common denominators of these gene sets and the common genes from the top microRNA candidates. Due to the stringent filtering procedure no genes were observed in overlap for all four groups. *KEAP1* depletion caused the most prominent gene expression changes in concordance with Nrf2 depletion (Figure 6D), therefore we further focused on the genes associated with *KEAP1* depletion and looked for overlap with candidate microRNAs. The genes involved in this group included *bona fide* Nrf2 target genes including *GCLM* and *NQO1*. *SRXN1* and *SQSTM1* were not part of this group, likely because the basic levels are low and are not significantly affected by Nrf2 depletion. We further looked at overlapping genes between the common genes of the top 4 enhancer microRNAs and siKEAP1 (Figure 6E) as well as the overlapping genes between the common genes of the top 4 inhibitors and the siNFE2L2 DE genes (Figure 6F). Enhancer microRNAs showed 397 genes in overlap with siKEAP1 and inhibitor microRNAs showed 24 genes in overlap with siNFE2L2 (see Suppl. Table 4 and 5). *GPF15*, *TRO*, *FRMD4B*, *SPP1*, and *LEAP2* were found in both sets. Together, these respective 397 and 24 overlapping genes represent various well-established Nrf2 target genes, including *NQO1*, *GCLM* and *GCLC*, thus further supporting the direct modulation of the Nrf2 program by the candidate microRNAs.

To get further quantitative information on gene network activation by the candidate microRNAs we made advantage of co-regulated gene network analysis using our previously established toxicogenomic map tool (https://txg-mapr.eu/WGCNA_PHH/TGGATEs_PHH/ (Callegaro et al. 2021; Langfelder and Horvath 2008; Sutherland et al. 2018)). Here we focused on the 397 genes (478 probes) that were in overlap between the top 4 *Srxn1* enhancing microRNAs (miR-1909-3p, miR-6499-3p, miR-1293, and miR-3165) and siKEAP1 (Figure 6E and Suppl. Table 4) for which similar patterns in gene expression were observed (Figure 7A; Suppl. Figure 5). The fold change expression data for these genes was used to calculate the gene network module activation score, eigengene score (EGS), of each module (Figure 7B). A cluster of modules was strongly enhanced by these microRNAs and siKEAP1 representing two oxidative stress gene network modules: Module 144 and Module 325. Module 144 contained *SRXN1* as well as other Nrf2 target genes including *TXRDN1* and *GCLM* and was strongly activated by all four enhancing microRNAs and siKEAP1 (Figure 7C). The pattern of expression of genes within both Module 144 and Module 325 was similar for these microRNAs and siKEAP1 (Figure 7C and Suppl. Figure 6).

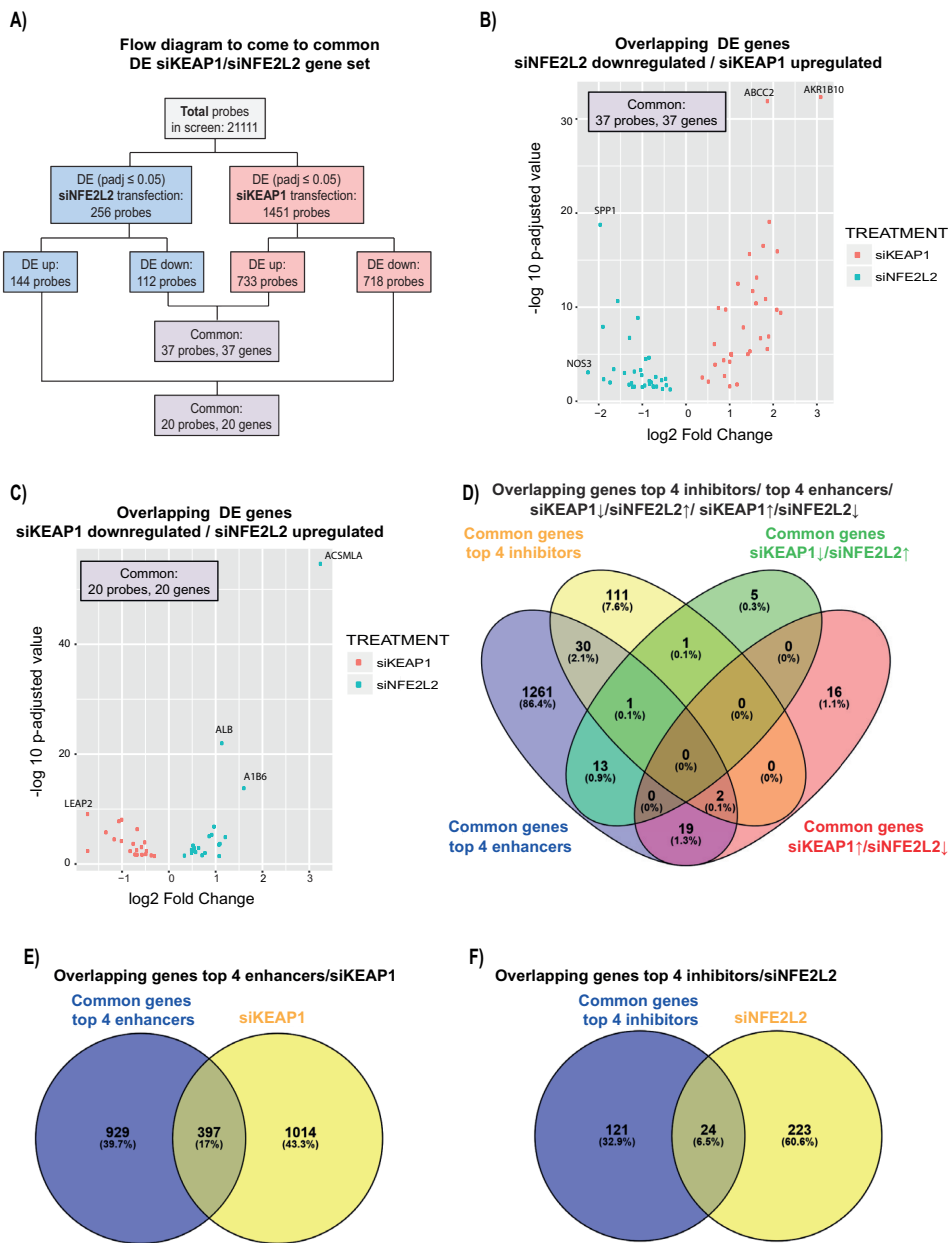
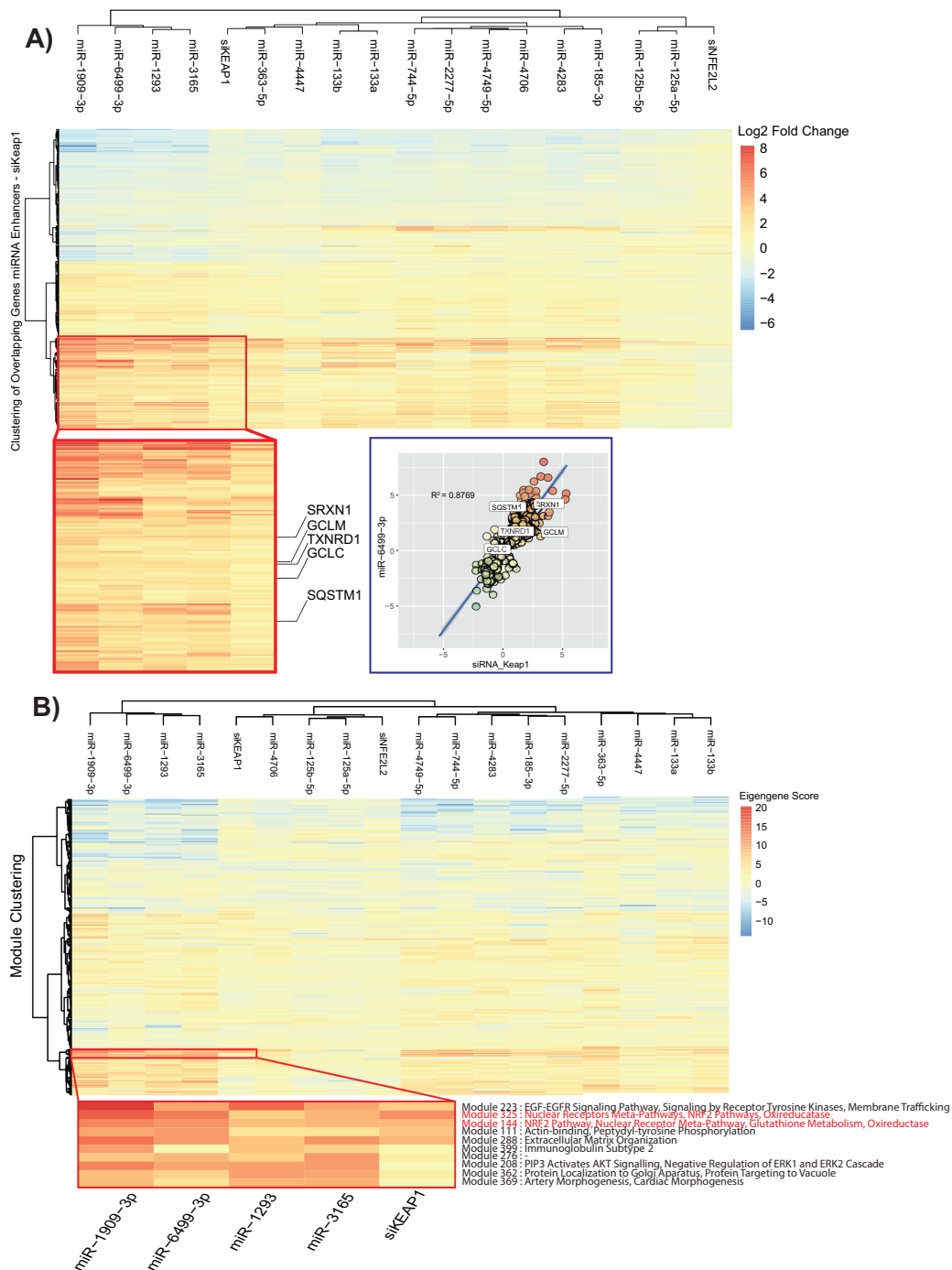


Figure 6. Overview of Nrf2 pathway specific overlapping genes.

A) Flow diagram used to create the two gene sets used in figure B,C, and D. **B)** Overlapping DE genes downregulated after siNFE2L2 transfection and upregulated after siKEAP1 transfection. **C)** Overlapping DE genes downregulated with siKEAP1 transfection and upregulated with siNFE2L2 transfection. **D)** Venn diagram showing the overlap between four gene sets: common genes top 4 inhibitors, common genes top 4 enhancers, siKEAP1 upregulated and siNFE2L2 downregulated genes, and siKEAP1 downregulated and siNFE2L2 upregulated genes. **E)** Overlapping genes top 4 enhancers with DE genes after siKEAP1 transfection. **F)** Overlapping genes top 4 inhibitors with DE genes after siNFE2L2 transfection.



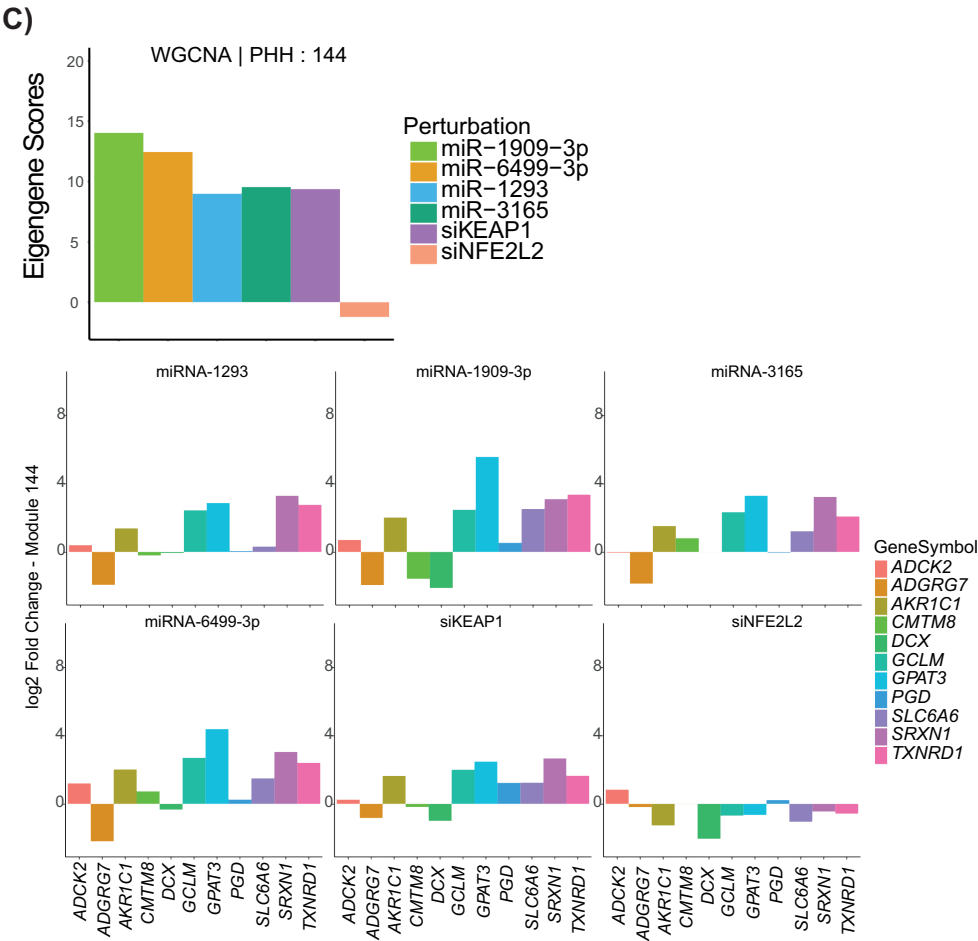


Figure 7. Profiling overlapped genes between microRNA enhancers and siKEAP1.

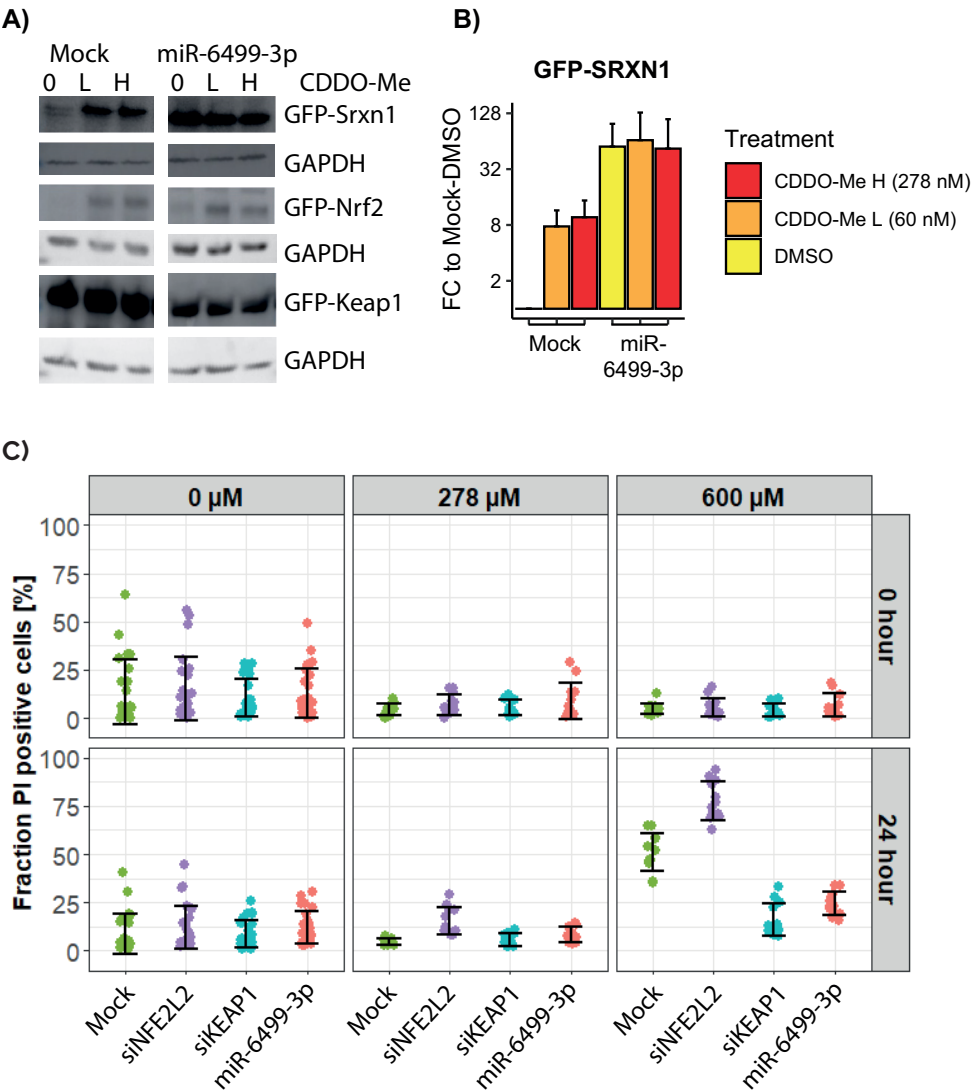
A) A heatmap showing log2 fold change values of overlapped genes between microRNA (miRNA) enhancers and siKEAP1. Hierarchical clustering of the miRNAs, siKEAP1 and siNFE2L2 shows a cluster of 4 strongest miRNA enhancers (miR-1909-3p, miR-6499-3p, miR-1293, and miR-3165) identical to the miRNAs exhibiting strong capacity of inducing SRXN1. An enriched area (red box) is identified in the responses of these strong miRNA and siKEAP1 showing high log 2 fold change > 2 of oxidative stress related genes. Correlation analysis exhibit high Pearson correlation value (0.87) between the strongest miRNA enhancer, miR-6499-3p with siKEAP1. **B)** Pathway enrichment analysis of overlapped genes utilizing TXG-MAPr-PHH showing strong activation of oxidative stress pathways (Module 144 and Module 325) among the other 8 highest activated pathways upon the perturbation of miRNA enhancers. A correlation plot of miR-6499-3p and siKEAP1 at the module (gene network) level shows poor correlation (0.32) with more prominent responses upon miR-6499-3p perturbation. **C)** The eigengene score of Module 144 and the log 2 fold change values of its gene memberships in 4 miRNA enhancers, siKEAP1, and siNFE2L2.

miR-6499-3p affects KEAP1 expression and susceptibility to oxidative stress-induced cell death

Finally, we aimed at understanding the mechanism of Nrf2 pathway modulation of candidate microRNAs. Given that the seed region of a microRNA is important for target recognition (Bartel 2009), as a further validation of our microRNA screen we anticipated that our candidate microRNAs would share the seed region and would therefore have a similar mode-of-action on Nrf2 pathway modulation. We looked at a seed region of 7 nucleotides (Bartel 2009; Mullany et al. 2016). Intriguingly, we found that three of the ten inhibiting microRNAs had the same seed region sequence (miR-25-3p, miR-363-3p, miR-92b-3p; AUUGCAC). Also two of the sixteen selected enhancing microRNAs have the same seed region sequence (miR-4749-5p, miR-4706; GCGGGGA). For miR-25-3p, miR-363-3p and miR-92b-3p we observed considerable overlap in the differential expressed genes (Suppl. Figure 8A). 85 % of the genes differently expressed with miR-4706 overlap with the genes differently expressed by miR-4749-5p, which is 33% of the total genes differentially expressed by miR-4749-5p. This might indicate a similar mode-of-action of the seed region and did involve the Nrf2 pathway modulation (Suppl. Figure 8B). We also anticipated that our candidate microRNAs would directly target Nrf2 pathway components. Therefore we specifically evaluated the effect of our candidate microRNAs on *NFE2L2* and *KEAP1* as well as *SRXN1* using microRNA target prediction tools from IPA, MiRDB, and Targetscan. Only one suppressing microRNA, miR-129-5p, was predicted to target Nrf2, suggesting a direct inhibition of Srxn1 activation due to lack of Nrf2. Three of the enhancing microRNAs, miR-6499-3p, miR-505-5p and miR-4283, were predicted to target *KEAP1*. Counter intuitively all three *KEAP1* targeting microRNAs were also predicted to target *SRXN1*, yet did not block Srxn1-GFP induction. Other *SRXN1* targeting microRNA predictions involved miR-185-3p and miR-200a-5p, an enhancing and suppressing microRNA, respectively. None of the other candidate microRNAs were predicted to target *KEAP1*, *Nrf2/NFE2L2* or *SRXN1*.

We selected miR-6499-3p for some final validation studies since miR-6499-3p showed strong downregulation of Keap1-GFP in conjunction with strong induction of Nrf2 levels and Srxn1-GFP induction (Fig. 2). Moreover, miR-6499-3p correlated highly with siKEAP1 at the transcriptional level. Expression of miR-6499-3p in the reporter cell lines also strongly reduced the expression of GFP-Keap1 at protein level which was consistent with upregulation of Srxn1 and Nrf2 to a maximal level such that further induction by CDDO-Me was not detected (Fig. 8A and B). Given this maximal induction of the Nrf2 response, we then wondered whether miR-6499-3p could be protective for oxidative stress-induced cell death. For this purpose we exposed wild type HepG2 cells to nitrofurantoin (NTF) that causes formation of oxidative stress in hepatocytes that leads to cell death (Wijaya et al. 2021). While siNFE2L2 treatment

highly sensitized cells to NTF treatment, miR-6499-3p was protective against NTF-induced cell death in a similar manner as siKEAP1 treatment. This indicates that the activation of the Nrf2 pathway by miR-6499-3p provides a powerful cytoprotection.



D)

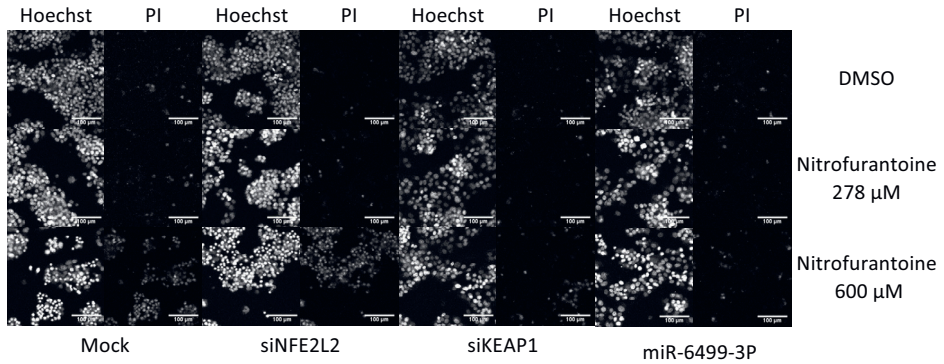


Figure 8. Effect of miR-6499-3p on cytoprotection.

Respective GFP-Keap1, GFP-Nrf2 and GFP-Srxn1 HepG2 reporter cell lines with mock or miR-6499-3p transfection were treated with two different concentrations of CDDO-Me followed by Western blotting for GFP-Srxn1, GFP-Nrf2 and GFP-Keap1 **A)** and quantification of the bands from three independent Western blots **B).** **C)** Wild type HepG2 transfected with miR-6499-3p, siNFE2L2 or siKEAP1 were treated with nitrofurantoin followed by high content imaging of onset of cell death based on propidium iodide (PI) staining. Fraction of PI positive cells after exposure to 0, 278 or 600 μ M nitrofurantoin is shown for the different treatments. Data are derived from 3 independent experiments. For each treatment x concentration x transfection combination, 1 well was imaged at 4 different positions. Error bars indicate the standard deviation around the mean. The viability is expressed in cell fraction PI positive. **(D)** Microscopic images of wild type HepG2 cells stained with Hoechst 33342 and PI after transfection with miR-6499-3p and exposure to nitrofurantoin. Scale bar is equivalent to 100 μ m.

DISCUSSION

Here we applied a systematic microRNA mimic screen to uncover the microRNA landscape that modulates Nrf2 activation. For this purpose we used an established Srxn1-GFP BAC reporter HepG2 cell line that is under full control by Nrf2, in combination with live cell confocal microscopy to evaluate Nrf2 activity in individual cells at the population level. We used CDDO-Me (bardoxolone methyl) as activator of the Nrf2-mediated Srxn1-GFP expression and discerned microRNAs that either inhibit or enhance the induction of Srxn1-GFP by CDDO-Me. We successfully uncovered ten microRNAs that inhibit and sixteen microRNAs that enhance Nrf2 pathway activation. Transcriptome analysis identified that these microRNAs mimicked the activity of either siNFE2L2 or siKEAP1. miR-6499-3p was validated by microRNA target prediction as a candidate microRNA that targets *KEAP1*, and closely mimicked the effect of *KEAP1* knockdown at the transcriptional level as well as cytoprotective level.

Our microRNA mimic screen has identified various microRNAs that can modulate the expression of the Nrf2 target *Srxn1*. Although the effect of this set of twenty-six microRNAs on *Srxn1* expression was in various cases highly comparable with the effect of siKEAP1 and siNFE2L2, there was no consistent modulation of Nrf2 and Keap1 expression based on the Nrf2-GFP and Keap1-GFP reporters (see Figure 3). Thus, miR-6499-3p showed clear correlation between strong *Srxn1*-GFP induction and increased levels of Nrf2-GFP and reduced levels of Keap1-GFP, in concordance with targeting *KEAP1* by this microRNA (Figure 3 and 8). A similar pattern was observed for miR-3165. Yet, in contrast, while miR-4749-5p showed a similar strong induction of *Srxn1*-GFP and a transcriptome modulation similar to miR-6499-3p and siKEAP1, the regulation of Nrf2-GFP was not affected, suggesting other mechanism of enhanced *Srxn1*-GFP expression independent from Nrf2 modulation. Importantly, miR-6499-3p closely mimicked the effect of siKEAP1 at various levels including protection against a high concentration of nitrofurantoin, a drug that can cause oxidative stress-induced cell death in hepatocytes (Wijaya et al. 2021).

We used CDDO-Me (bardoxolone-methyl) in our screen to identify Nrf2-modulating microRNAs. CDDO-Me is a known, potent, inducer of the Nrf2 pathway. CDDO-Me is able to activate the Nrf2 pathway by direct binding to Cys151 of Keap1 and therefore inhibiting Keap1 function (Cleasby et al. 2014). Moreover, CDDO-Me was used in different clinical trials for modulation of the antioxidant response (Wang et al. 2014). We systematically validated that our candidate microRNAs also impacted on the *Srxn1*-GFP induction by other potent pro-oxidants, DEM and tBHQ, that also modulate *Srxn1*-GFP levels through Nrf2 activation (Bischoff et al. 2019). This indicates that our candidate microRNAs are genuine modulators of the Nrf2 pathway and may have implications in diverse pro-oxidant conditions.

We could clearly classify candidate Nrf2 pathway modulating microRNAs into two groups, those that either enhance or inhibit the *Srxn1* response. *Hmox1* has been a classical oxidative stress marker for various tissues. We observed no induction of *Hmox1* reporter activity by CDDO-Me or siKEAP1. Also the microRNAs that enhanced the *Srxn1*-GFP response did themselves not impact on *HMOX1* gene expression, while *GCLM* gene expression was clearly enhanced by enhancer microRNAs. Some other microRNAs did impact on *Hmox1*-GFP activity, but this could not be related back to specific patterns of either Nrf2-GFP, Keap1-GFP and *Srxn1*-GFP modulation. Similarly, while some candidate microRNAs did affect either the unfolded protein response pathway or the DNA damage response pathway, with Chop-GFP and p21-GFP as respective biomarkers, these effects were not directly associated with potency of *Srxn1*-GFP reporter activity. These observations indicate that i) overexpression of these microRNAs does not lead to an overt general cellular perturbation creating a

state of overwhelming “general” cellular stress, consequently leading to apoptosis and/or cell death, and ii) the delicate balance of how different microRNAs can modulate one or multiple stress response signaling pathways.

Activation of the Nrf2 pathway is divided into two mechanisms: canonical and non-canonical (Silva-Islas and Maldonado 2018). The canonical pathway is defined by the Keap1/Nrf2/ARE axes activated by electrophilic compounds and ROS. The non-canonical pathway involves the activation of the Nrf2 pathway by proteins also capable of disrupting the Keap1-Nrf2 interaction. Using three different prediction tools we determined how our candidate microRNAs would target the canonical Nrf2 pathway components. We found miR-4283 to directly target *Srxn1*. Surprisingly, we found miR-4283 to enhance *Srxn1*. miR-129-5p, was predicted to target Nrf2, suggesting a direct inhibition of *Srxn1* activation due to lack of Nrf2. Three of the enhancing miRNAs, miR-6499-3p, miR-505-5p and miR-4283, were predicted to target *KEAP1*. Loss of Keap1-GFP levels was indeed observed in the Keap1-GFP reporter cell line, confirming the target prediction. Previous studies have reported individual Nrf2 pathway modulating microRNAs, including miR-122, miR-144, miR-155, miR-196, miR34a/b/c and miR-200a (reviewed in (Cheng et al. 2013)). In our study only miR-200a-5p was found to suppress *Srxn1* activity. However in other studies, miR-200a is described to target *KEAP1*, leading to Nrf2 induction (Sun et al. 2016; Zhao et al. 2018) which was not observed in our hands. miR-7 activates *HMOX1* and *GCLM*, two downstream targets of the Nrf2 pathway, by direct targeting *KEAP1* in the human neuroblastoma cell SH-SY5Y (Kabaria et al. 2015). In our study, we found miR-7-5p to suppress *GCLM*, but to induce HO-1 on protein level. These different observations are possibly due to cell type differences.

We have identified both positive and negative microRNA regulators of the Nrf2 pathway. Since we did not observe overt cytotoxic responses of these candidate microRNA, we anticipate that such microRNAs that target the Nrf2 pathway could be used for therapeutic approaches. *KEAP1* mutations in cancer are critical drivers in cancer progression as well as drug resistance, in particular in lung cancer (Cuadrado et al. 2019). Such mutations lead to constitutive Nrf2 activation, hence, microRNA that would inhibit the Nrf2 pathway could possibly impact on cancer progression. Similarly, various pathophysiology situations, such as ischemic reperfusion injury of tissues that highly depend on oxidative phosphorylation and involve severe oxidative stress, could benefit from Nrf2 pathway activation (Cuadrado et al. 2019); microRNAs that activate the Nrf2 pathway, such as miR-6499-3p, could be promising therapeutic modulators to protect cells from detrimental oxidative stress cell injury. This would require systematic studies on the efficacy and safety of such microRNA therapeutic approaches.

In conclusion, our study for the first time elucidate the spectrum of microRNAs that target the Nrf2 signaling pathway. The Nrf2 pathway is of critical importance in cancer development and progression, with various *KEAP1* and Nrf2 mutations that act as cancer drivers, as well as in various degenerative disease settings. Therefore, we anticipate that our selected enhancing and inhibiting microRNA might be interesting as putative biomarkers and/or microRNA therapeutics to generically modulate the Nrf2 pathway.

ACKNOWLEDGEMENTS

This work was supported by the Ministry of Defence of the Netherlands and the European Commission Horizon2020 EU-ToxRisk project (grant nr 681002).

REFERENCES

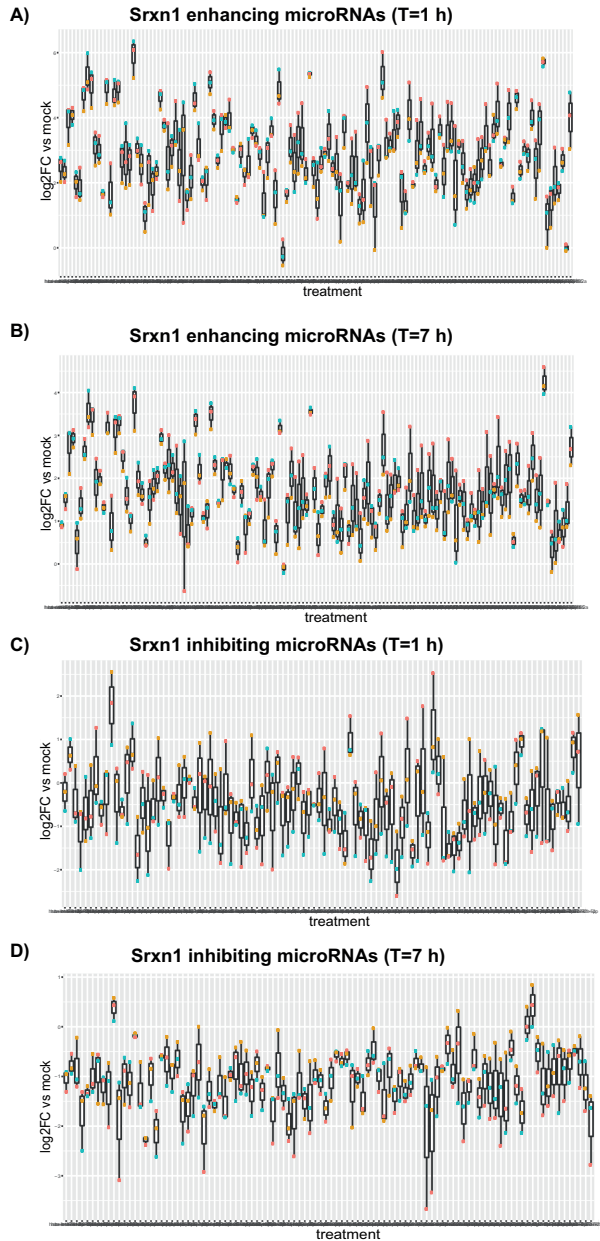
- Agarwal V, Bell GW, Nam JW, Bartel DP (2015) Predicting effective microRNA target sites in mammalian mRNAs. *Elife* 4 doi:10.7554/eLife.05005
- Almeida MI, Reis RM, Calin GA (2011) MicroRNA history: discovery, recent applications, and next frontiers. *Mutat Res* 717(1-2):1-8 doi:10.1016/j.mrfmmm.2011.03.009
- Baird L, Yamamoto M (2020) The Molecular Mechanisms Regulating the KEAP1-NRF2 Pathway. *Molecular and Cellular Biology* 40(13):e00099-20 doi:10.1128/MCB.00099-20
- Balasubramanian S, Gunasekaran K, Sasidharan S, Jeyamanickavel Mathan V, Perumal E (2020) MicroRNAs and Xenobiotic Toxicity: An Overview. *Toxicol Rep* 7:583-595 doi:10.1016/j.toxrep.2020.04.010
- Bartel DP (2009) MicroRNAs: target recognition and regulatory functions. *Cell* 136(2):215-33 doi:10.1016/j.cell.2009.01.002
- Bartoszewska S, Kochan K, Madanecki P, et al. (2013) Regulation of the unfolded protein response by microRNAs. *Cell Mol Biol Lett* 18(4):555-578 doi:10.2478/s11658-013-0106-z
- Bischoff LJM, Kuijper IA, Schimming JP, et al. (2019) A systematic analysis of Nrf2 pathway activation dynamics during repeated xenobiotic exposure. *Arch Toxicol* 93(2):435-451 doi:10.1007/s00204-018-2353-2
- Borchert GM, Lanier W, Davidson BL (2006) RNA polymerase III transcribes human microRNAs. *Nat Struct Mol Biol* 13(12):1097-101 doi:10.1038/nsmb1167
- Brennecke J, Stark A, Russell RB, Cohen SM (2005) Principles of microRNA-target recognition. *PLoS Biol* 3(3):e85 doi:10.1371/journal.pbio.0030085
- Callegaro G, Kunnen SJ, Trairatphisan P, et al. (2021) The human hepatocyte TXG-MAPr: WGCNA transcriptomic modules to support mechanism-based risk assessment. *bioRxiv*:2021.05.17.444463 doi:10.1101/2021.05.17.444463
- Cheng X, Ku CH, Siow RC (2013) Regulation of the Nrf2 antioxidant pathway by microRNAs: New players in micromanaging redox homeostasis. *Free Radic Biol Med* 64:4-11 doi:10.1016/j.freeradbiomed.2013.07.025
- Cleasby A, Yon J, Day PJ, et al. (2014) Structure of the BTB domain of Keap1 and its interaction with the triterpenoid antagonist CDDO. *PLoS One* 9(6):e98896 doi:10.1371/journal.pone.0098896
- Copple IM, den Hollander W, Callegaro G, et al. (2019) Characterisation of the NRF2 transcriptional network and its response to chemical insult in primary human hepatocytes: implications for prediction of drug-induced liver injury. *Arch Toxicol* 93(2):385-399 doi:10.1007/s00204-018-2354-1
- Cuadrado A, Manda G, Hassan A, et al. (2018) Transcription Factor NRF2 as a Therapeutic Target for Chronic Diseases: A Systems Medicine Approach. *Pharmacol Rev* 70(2):348-383 doi:10.1124/pr.117.014753
- Cuadrado A, Rojo AI, Wells G, et al. (2019) Therapeutic targeting of the NRF2 and KEAP1 partnership in chronic diseases. *Nature reviews Drug discovery* 18(4):295-317 doi:10.1038/s41573-018-0008-x
- Djuranovic S, Nahvi A, Green R (2012) miRNA-Mediated Gene Silencing by Translational Repression Followed by mRNA Deadenylation and Decay. *Science* 336(6078):237 doi:10.1126/science.1215691
- Dodson M, de la Vega MR, Cholanians AB, Schmidlin CJ, Chapman E, Zhang DD (2019) Modulating NRF2 in Disease: Timing Is Everything. *Annu Rev Pharmacol Toxicol* 59:555-575 doi:10.1146/annurev-pharmtox-010818-021856

- Filipowicz W, Bhattacharyya SN, Sonenberg N (2008) Mechanisms of post-transcriptional regulation by microRNAs: are the answers in sight? *Nature Reviews Genetics* 9(2):102-114 doi:10.1038/nrg2290
- Hayes JD, McMahon M, Chowdhry S, Dinkova-Kostova AT (2010) Cancer Chemoprevention Mechanisms Mediated Through the Keap1-Nrf2 Pathway. *Antioxidants & Redox Signaling* 13(11):1713-1748 doi:10.1089/ars.2010.3221
- Herpers B, Wink S, Fredriksson L, et al. (2016) Activation of the Nrf2 response by intrinsic hepatotoxic drugs correlates with suppression of NF-kappaB activation and sensitizes toward TNFalpha-induced cytotoxicity. *Arch Toxicol* 90(5):1163-79 doi:10.1007/s00204-015-1536-3
- Hiemstra S, Ramaiahgari SC, Wink S, et al. (2019) High-throughput confocal imaging of differentiated 3D liver-like spheroid cellular stress response reporters for identification of drug-induced liver injury liability. *Archives of Toxicology* 93(10):2895-2911 doi:10.1007/s00204-019-02552-0
- Hou L, Wang D, Baccarelli A (2011) Environmental chemicals and microRNAs. *Mutat Res* 714(1-2):105-12 doi:10.1016/j.mrfmmm.2011.05.004
- Itoh K, Wakabayashi N, Katoh Y, et al. (1999) Keap1 represses nuclear activation of antioxidant responsive elements by Nrf2 through binding to the amino-terminal Neh2 domain. *Genes & Development* 13(1):76-86 doi:10.1101/gad.13.1.76
- Kabaria S, Choi DC, Chaudhuri AD, Jain MR, Li H, Junn E (2015) MicroRNA-7 activates Nrf2 pathway by targeting Keap1 expression. *Free Radic Biol Med* 89:548-56 doi:10.1016/j.freeradbiomed.2015.09.010
- Keum YS, Choi BY (2014) Molecular and chemical regulation of the Keap1-Nrf2 signaling pathway. *Molecules* 19(7):10074-89 doi:10.3390/molecules190710074
- Kobayashi A, Kang MI, Okawa H, et al. (2004) Oxidative stress sensor Keap1 functions as an adaptor for Cul3-based E3 ligase to regulate proteasomal degradation of Nrf2. *Mol Cell Biol* 24(16):7130-9 doi:10.1128/MCB.24.16.7130-7139.2004
- Lam JK, Chow MY, Zhang Y, Leung SW (2015) siRNA Versus miRNA as Therapeutics for Gene Silencing. *Mol Ther Nucleic Acids* 4:e252 doi:10.1038/mtna.2015.23
- Langfelder P, Horvath S (2008) WGCNA: an R package for weighted correlation network analysis. *BMC Bioinformatics* 9(1):559 doi:10.1186/1471-2105-9-559
- Lee RC, Feinbaum RL, Ambros V (1993) The *C. elegans* heterochronic gene *lin-4* encodes small RNAs with antisense complementarity to *lin-14*. *Cell* 75(5):843-54 doi:10.1016/0092-8674(93)90529-y
- Lee Y, Kim M, Han J, et al. (2004) MicroRNA genes are transcribed by RNA polymerase II. *EMBO J* 23(20):4051-60 doi:10.1038/sj.emboj.7600385
- Lewis BP, Shih IH, Jones-Rhoades MW, Bartel DP, Burge CB (2003) Prediction of mammalian microRNA targets. *Cell* 115(7):787-98 doi:10.1016/s0092-8674(03)01018-3
- Lin S, Gregory RI (2015) MicroRNA biogenesis pathways in cancer. *Nat Rev Cancer* 15(6):321-33 doi:10.1038/nrc3932
- Love MI, Huber W, Anders S (2014) Moderated estimation of fold change and dispersion for RNA-seq data with DESeq2. *Genome Biol* 15(12):550-550 doi:10.1186/s13059-014-0550-8
- McMahon M, Thomas N, Itoh K, Yamamoto M, Hayes JD (2006) Dimerization of substrate adaptors can facilitate cullin-mediated ubiquitylation of proteins by a "tethering" mechanism: a two-site interaction model for the Nrf2-Keap1 complex. *J Biol Chem* 281(34):24756-68 doi:10.1074/jbc.M601119200
- Medina MV, Sapochnik D, Garcia Sola M, Coso O (2020) Regulation of the Expression of Heme Oxygenase-1: Signal Transduction, Gene Promoter Activation, and Beyond. *Antioxid Redox Signal* 32(14):1033-1044 doi:10.1089/ars.2019.7991

- Mendell JT, Olson EN (2012) MicroRNAs in stress signaling and human disease. *Cell* 148(6):1172-87 doi:10.1016/j.cell.2012.02.005
- Mullany LE, Herrick JS, Wolff RK, Slattery ML (2016) MicroRNA Seed Region Length Impact on Target Messenger RNA Expression and Survival in Colorectal Cancer. *PLoS One* 11(4):e0154177 doi:10.1371/journal.pone.0154177
- Peter ME (2010) Targeting of mRNAs by multiple miRNAs: the next step. *Oncogene* 29(15):2161-2164 doi:10.1038/onc.2010.59
- Poser I, Sarov M, Hutchins JR, et al. (2008) BAC TransgeneOmics: a high-throughput method for exploration of protein function in mammals. *Nat Methods* 5(5):409-15 doi:10.1038/nmeth.1199
- Riffo-Campos AL, Riquelme I, Brebi-Mieville P (2016) Tools for Sequence-Based miRNA Target Prediction: What to Choose? *Int J Mol Sci* 17(12) doi:10.3390/ijms17121987
- Sangokoya C, Doss JF, Chi JT (2013) Iron-responsive miR-485-3p regulates cellular iron homeostasis by targeting ferroportin. *PLoS Genet* 9(4):e1003408 doi:10.1371/journal.pgen.1003408
- Schimming JP, Ter Braak B, Niemeijer M, Wink S, van de Water B (2019) System Microscopy of Stress Response Pathways in Cholestasis Research. *Methods in molecular biology* (Clifton, NJ) 1981:187-202 doi:10.1007/978-1-4939-9420-5_13
- Silva-Islas CA, Maldonado PD (2018) Canonical and non-canonical mechanisms of Nrf2 activation. *Pharmacol Res* 134:92-99 doi:10.1016/j.phrs.2018.06.013
- Starega-Roslan J, Krol J, Koscianska E, et al. (2010) Structural basis of microRNA length variety. *Nucleic Acids Research* 39(1):257-268 doi:10.1093/nar/gkq727
- Sun X, Zuo H, Liu C, Yang Y (2016) Overexpression of miR-200a protects cardiomyocytes against hypoxia-induced apoptosis by modulating the kelch-like ECH-associated protein 1-nuclear factor erythroid 2-related factor 2 signaling axis. *Int J Mol Med* 38(4):1303-11 doi:10.3892/ijmm.2016.2719
- Sutherland JJ, Webster YW, Willy JA, et al. (2018) Toxicogenomic module associations with pathogenesis: a network-based approach to understanding drug toxicity. *The Pharmacogenomics Journal* 18(3):377-390 doi:10.1038/tpj.2017.17
- Wang YY, Yang YX, Zhe H, He ZX, Zhou SF (2014) Bardoxolone methyl (CDDO-Me) as a therapeutic agent: an update on its pharmacokinetic and pharmacodynamic properties. *Drug Des Devel Ther* 8:2075-88 doi:10.2147/DDDT.S68872
- Wijaya LS, Rau C, Braun TS, et al. (2021) Stimulation of de novo glutathione synthesis by nitrofurantoin for enhanced resilience of hepatocytes. *Cell Biol Toxicol* doi:10.1007/s10565-021-09610-3
- Wink S, Hiemstra S, Herpers B, van de Water B (2017) High-content imaging-based BAC-GFP toxicity pathway reporters to assess chemical adversity liabilities. *Arch Toxicol* 91(3):1367-1383 doi:10.1007/s00204-016-1781-0
- Wink S, Hiemstra SW, Huppelschoten S, Klip JE, van de Water B (2018) Dynamic imaging of adaptive stress response pathway activation for prediction of drug induced liver injury. *Arch Toxicol* 92(5):1797-1814 doi:10.1007/s00204-018-2178-z
- Wong N, Wang X (2015) miRDB: an online resource for microRNA target prediction and functional annotations. *Nucleic Acids Res* 43(Database issue):D146-52 doi:10.1093/nar/gku1104
- Wu S, Huang S, Ding J, et al. (2010) Multiple microRNAs modulate p21Cip1/Waf1 expression by directly targeting its 3' untranslated region. *Oncogene* 29(15):2302-2308 doi:10.1038/onc.2010.34

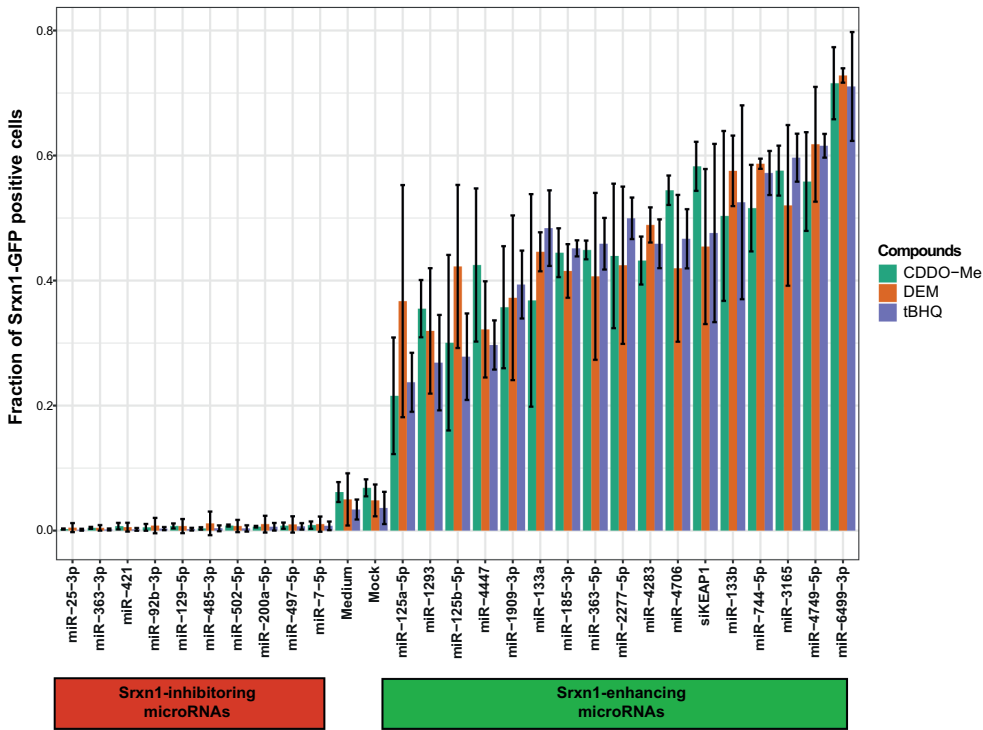
- Yamamoto M, Kensler TW, Motohashi H (2018) The KEAP1-NRF2 System: a Thiol-Based Sensor-Effector Apparatus for Maintaining Redox Homeostasis. *Physiol Rev* 98(3):1169-1203 doi:10.1152/physrev.00023.2017
- Yeakley JM, Shepard PJ, Goyena DE, VanSteenhouse HC, McComb JD, Seligmann BE (2017) A trichostatin A expression signature identified by TempO-Seq targeted whole transcriptome profiling. *PLoS One* 12(5):e0178302 doi:10.1371/journal.pone.0178302
- Zhang DD, Lo SC, Cross JV, Templeton DJ, Hannink M (2004) Keap1 is a redox-regulated substrate adaptor protein for a Cul3-dependent ubiquitin ligase complex. *Mol Cell Biol* 24(24):10941-53 doi:10.1128/MCB.24.24.10941-10953.2004
- Zhang Y, Gordon GB (2004) A strategy for cancer prevention: Stimulation of the Nrf2-ARE signaling pathway. *Molecular Cancer Therapeutics* 3(7):885
- Zhao XJ, Yu HW, Yang YZ, et al. (2018) Polydatin prevents fructose-induced liver inflammation and lipid deposition through increasing miR-200a to regulate Keap1/Nrf2 pathway. *Redox Biol* 18:124-137 doi:10.1016/j.redox.2018.07.002
- Zipper LM, Mulcahy RT (2002) The Keap1 BTB/POZ dimerization function is required to sequester Nrf2 in cytoplasm. *J Biol Chem* 277(39):36544-52 doi:10.1074/jbc.M206530200

SUPPLEMENTAL MATERIALS



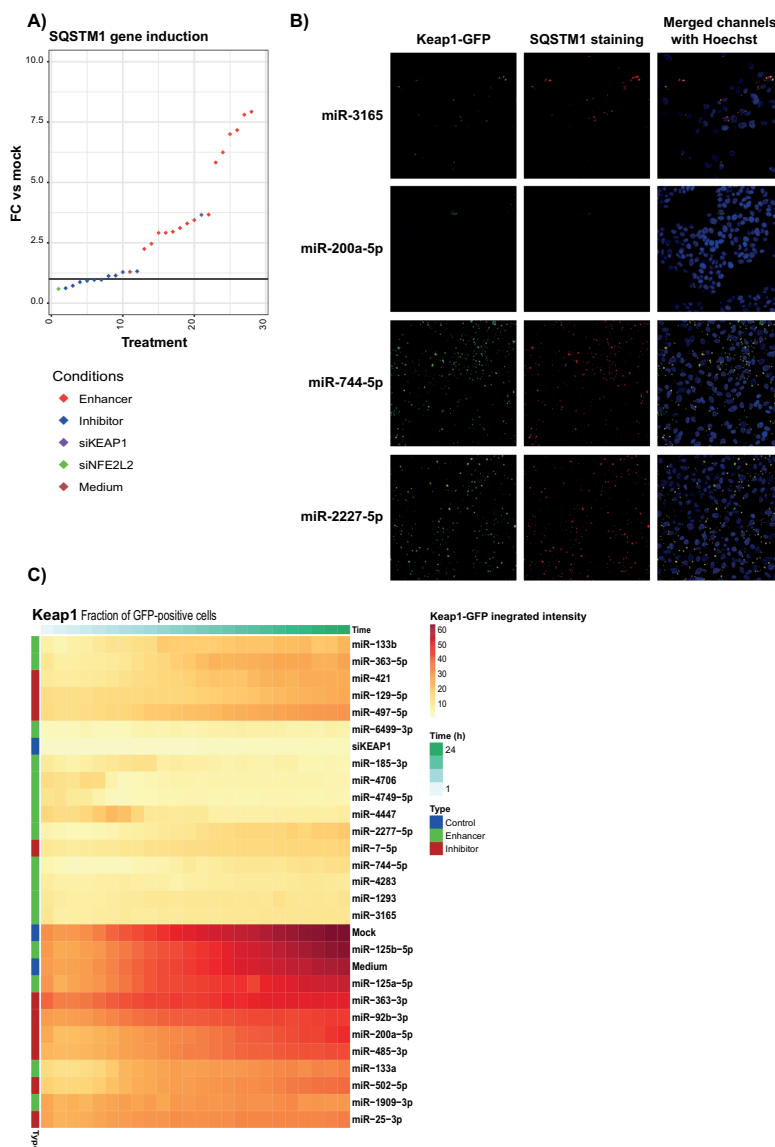
Supplemental Figure 1. Overview of the distribution of the three measurements of the secondary screen.

A) Srxn1 enhancing microRNAs measured 1 h after 30 nM CDDO-Me exposure. **B)** Srxn1 enhancing microRNAs measured 7 h after 30 nM CDDO-Me exposure. **C)** Srxn1 inhibiting microRNAs measured 1 h after 30 nM CDDO-Me exposure. **D)** Srxn1 inhibiting microRNAs measured 7 h after 30 nM CDDO-Me exposure. Three replicates are shown with different color (red, blue, yellow). Log2FC vs mock condition is plotted for the different microRNAs.



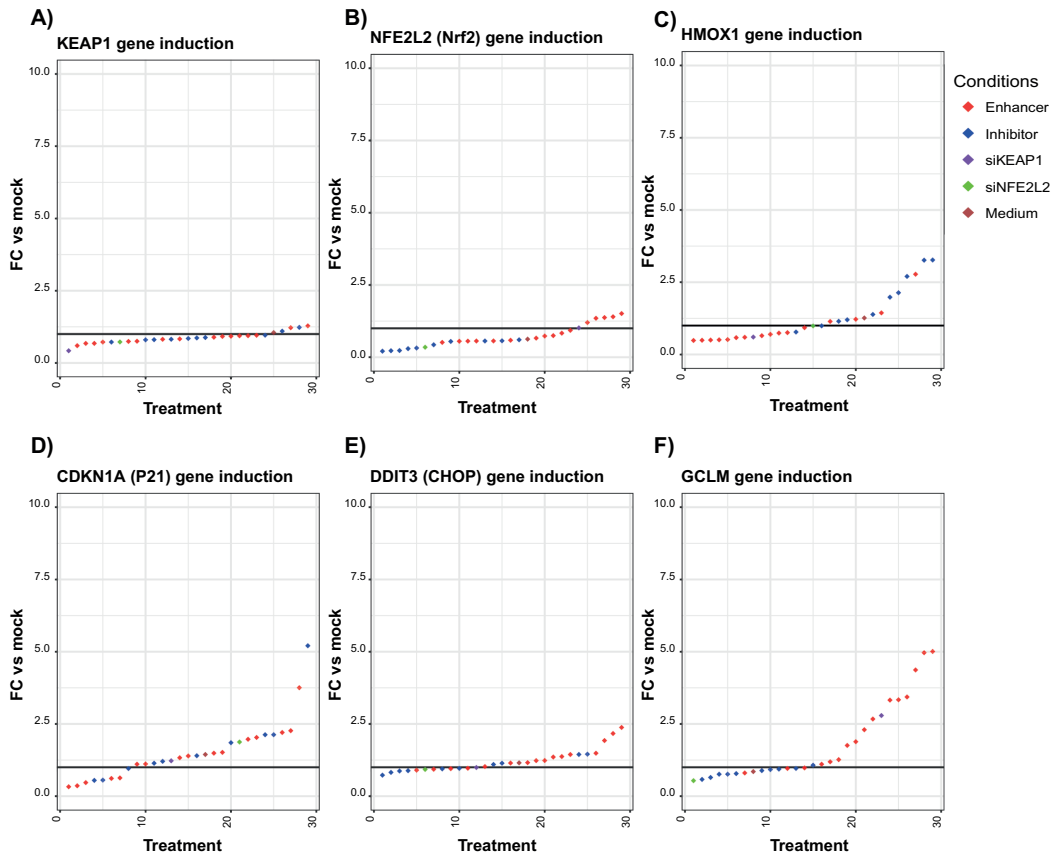
Supplemental Figure 2. Comparison of the effect of different Nrf2-activating compounds.

Comparison of the fraction of Srxn1-GFP positive cells after microRNA transfection and exposure to CDDO-Me (30nM), DEM (100µM), or tBHQ (100µM). Error bars represent the SD (n=3).



Supplemental Figure 3. Effect of microRNAs on Keap1-GFP and SQSTM1 mediated autophagosome formation.

A) Ranked distribution of SQSTM1 gene induction (Fold change vs mock). Srxn1 enhancing microRNAs are shown in red, Srxn1 inhibiting microRNAs are shown in blue, siKEAP1 transfection is shown in purple, siNFE2L2 transfection is shown in green, and the medium condition is shown in brown. Values are the mean of three different experiments. The top 4 enhancers are represented in the top 5 SQSTM1 upregulating microRNAs (enhancers) **B)** Microscope images (confocal) after transfection of 4 different microRNAs in HepG2-keap1-GFP cells. Green = Keap1-GFP, red = SQSTM1 staining, Blue = nucleus staining (Hoechst). Pictures are taken 24 h after microRNA transfection and exposure to 30 nM CDDO-Me. **C)** Keap1-GFP-integrated intensity (mean of three different experiments) is shown over time (1-24 h) after microRNA transfection, siKEAP1 transfection, mock, and medium condition after exposure to 30 nM CDDO-Me.

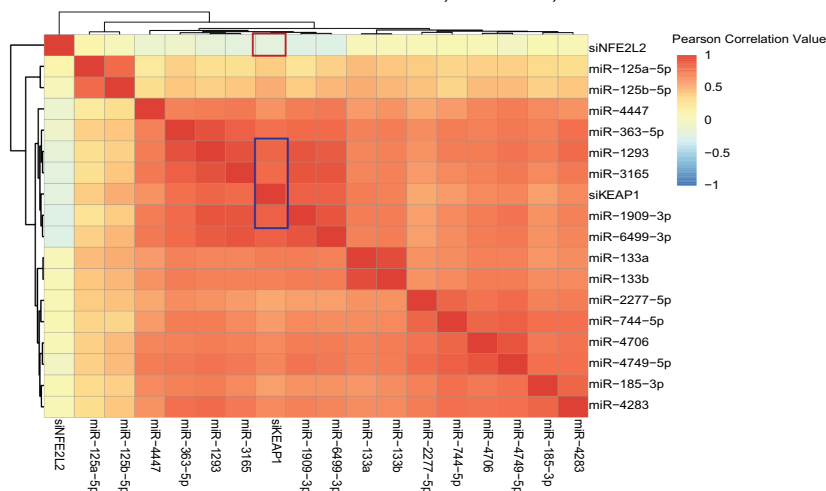


Supplemental Figure 4. Expression of different stress pathway related genes.

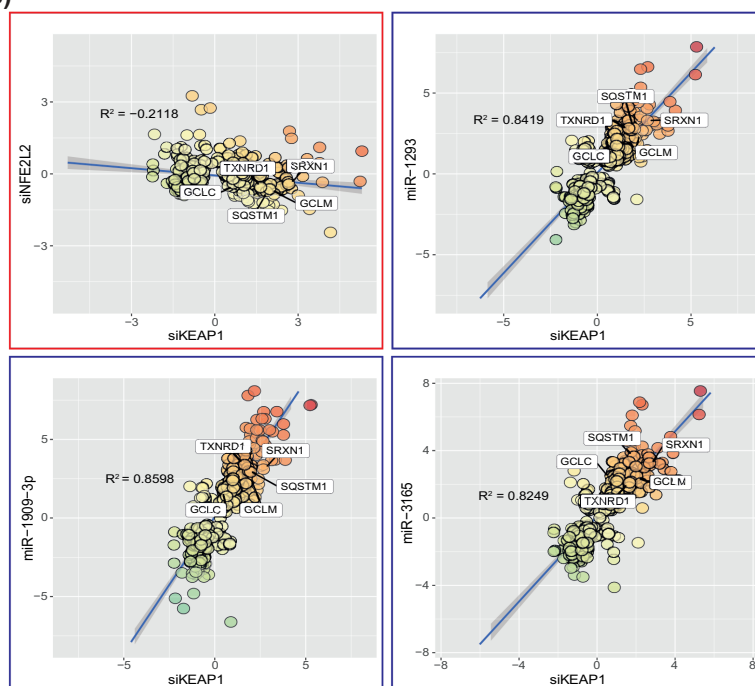
A) Ranked distribution of KEAP1 gene induction (Fold change vs mock). miR-6499-3p can be found directly after siKEAP1. **B)** Ranked distribution of NFE2L2 gene induction (Fold change vs mock). **C)** Ranked distribution of HMOX1 gene induction (Fold change vs mock). **D)** Ranked distribution of CDKN1A gene induction (Fold change vs mock). miR-6499-3p is the most CDKN1A suppressing microRNA. miR-25-3p and miR-744 the most CDKN1A enhancing microRNAs. **E)** Ranked distribution of DDIT3 gene induction (Fold change vs mock). **F)** Ranked distribution of GCLM gene induction (Fold change vs mock). Top 4 microRNA enhancers found with GCLM are the top 4 microRNA enhancers found with SRXN1.

A)

Correlation Matrix of miRNA Enhancers, siKEAP1, and siNFE2L2



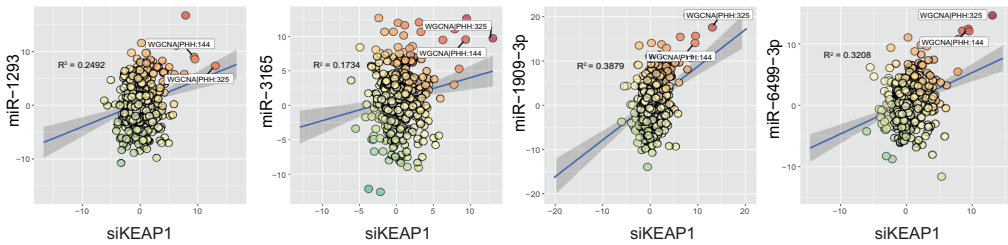
B)



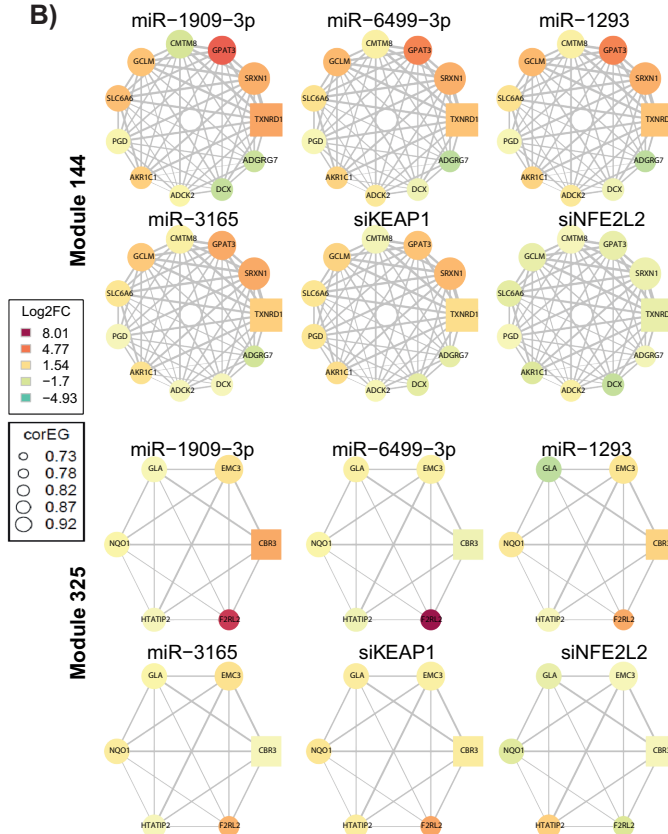
Supplemental Figure 5. Correlation analysis between siKEAP1, miRNA enhancer, and siNFE2L2 based on the overlapping genes of siKEAP1 with miRNA enhancer.

A) A heatmap illustrating the correlation matrix of miRNA enhancers at the gene levels. An enriched area highlighted in the blue box shows high Pearson correlation values (>0.8) between siKEAP1 and 4 strongest microRNA enhancers mentioned in Figure 1A. **B)** Correlation plots between microRNA enhancers and siKEAP1 showing high correlation value (>0.8).

A)

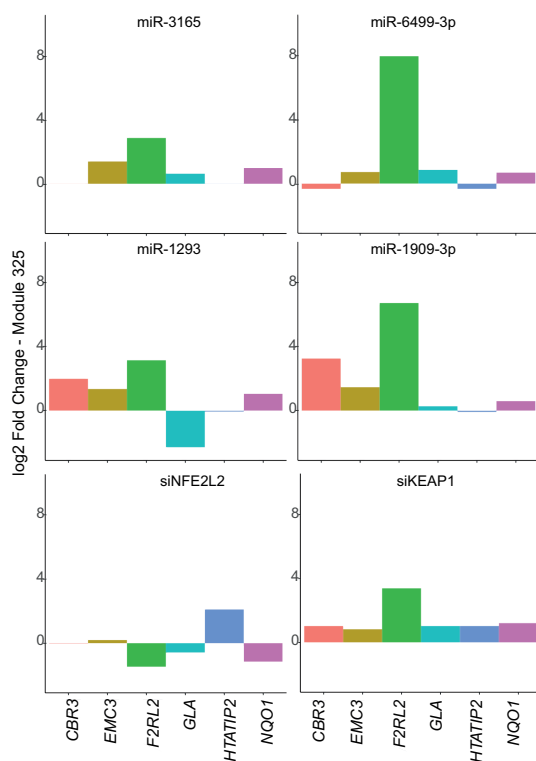
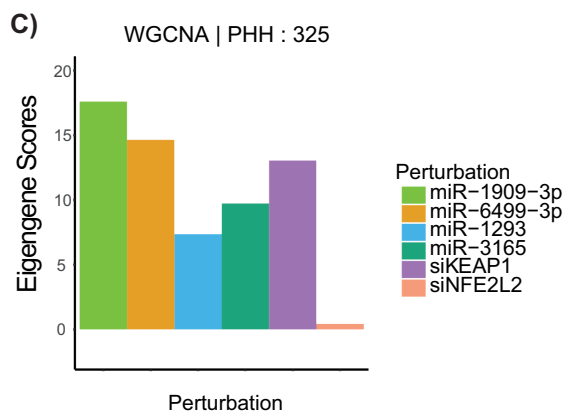


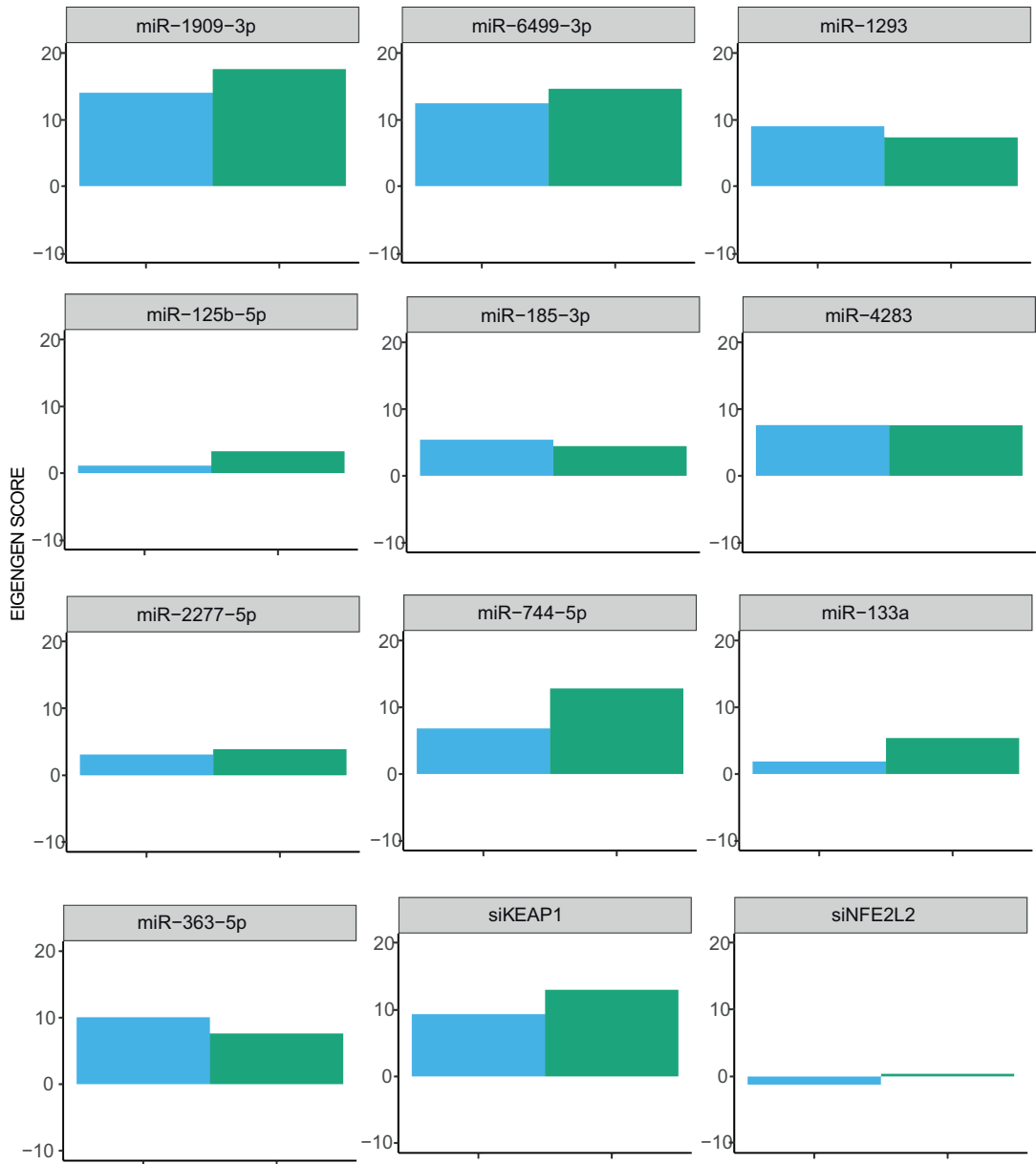
B)



Supplemental Figure 6. Pathway enrichment analysis utilizing PHH TXG-MAPr platform.

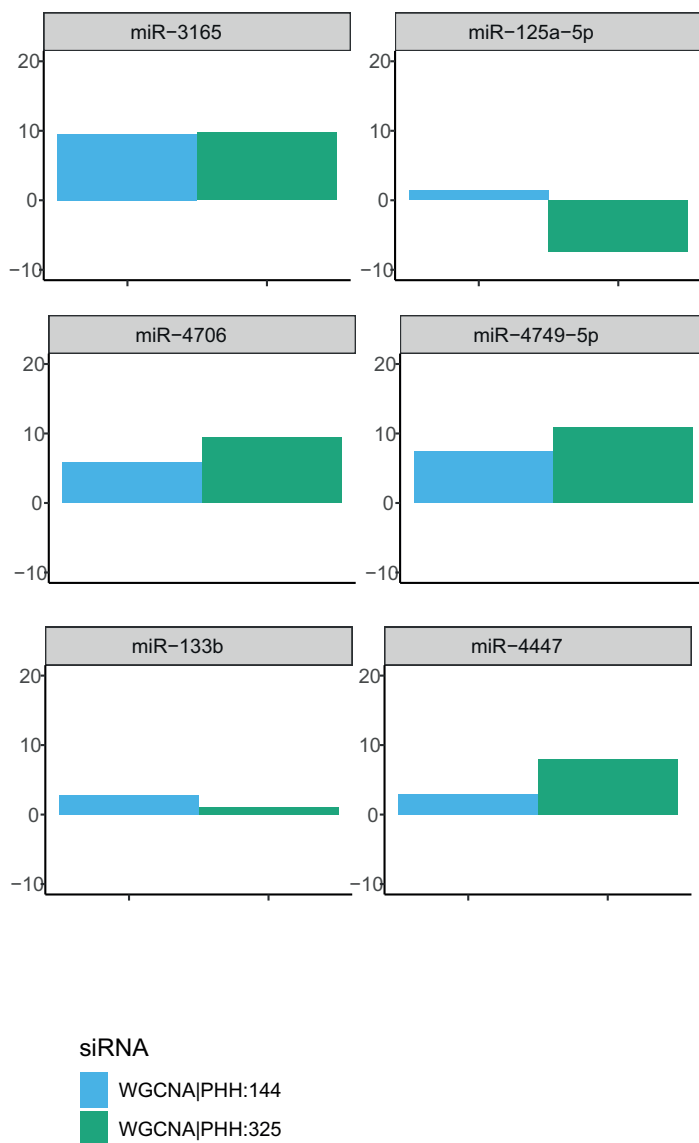
A) Correlation plots between microRNA enhancers and siKEAP1 at the module level show poor correlation (< 0.4) with broader responses of microRNA activating multiple pathways. **B)** The expression of module membership of Module 144 and Module 325 upon the perturbation of microRNA enhancers, siKEAP1, and siNFE2L2. **C)** The Eigengene score of Module 325 and the log 2 fold change values of its gene memberships in 4 microRNA enhancers, siKEAP1, and siNFE2L2.

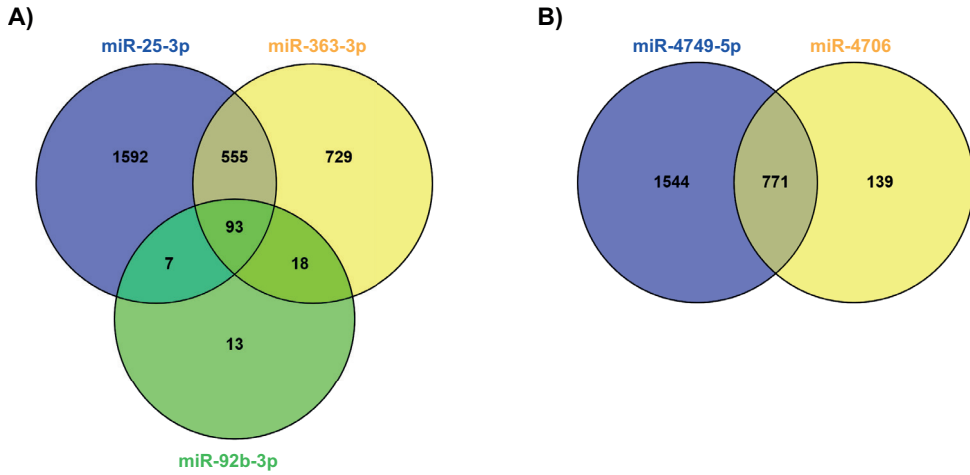




Supplemental Figure 7. Eigengene scores of Module 144 and Module 325 of microRNA enhancers, siKEAP1 and siNFE2L2.

The Eigengene score of Module 144 and 325 upon the perturbation of microRNA enhancers (besides the 4 strongest microRNA enhancers), siKEAP1, and siNFE2L2.





Supplemental Figure 8. MicroRNAs with the same seed region have overlap in transcriptome modulation.

A) Overlapping genes of the inhibiting microRNAs miR-25-3p, miR-363-3p and miR-92b-3p with seed region AUUGCAC. **B)** Overlapping genes of the enhancing microRNAs miR-4706 and miR-4749-5p with seed region GCGGGGA.

Supplemental Table 1. 33 Differentially expressed genes overlapping between the top 4 microRNAs that either enhance or inhibit the Srxn1-GFP response.

Probe_ID	miR-1293			miR-3615			miR-1909-3p		
	padj	log2FC	lfcSE	padj	log2FC	lfcSE	padj	log2FC	lfcSE
ADD3_16935	0.00	-0.55	0.15	0.00	-1.08	0.16	0.00	0.67	0.14
ANXA3_16294	0.00	2.16	0.25	0.00	2.73	0.25	0.00	3.81	0.24
DNAJC18_18335	0.00	1.36	0.20	0.00	1.75	0.20	0.00	1.46	0.20
EMP3_18953	0.00	3.37	0.21	0.00	1.53	0.22	0.00	4.10	0.21
FRMD4B_12533	0.00	2.07	0.21	0.00	2.34	0.21	0.00	2.86	0.20
GBP3_16959	0.00	3.55	0.38	0.00	3.75	0.38	0.00	5.09	0.37
GDF15_18329	0.00	3.22	0.27	0.00	4.23	0.27	0.00	1.21	0.27
GDF15_2621	0.00	2.26	0.24	0.00	2.99	0.24	0.00	0.96	0.24
GEMIN5_22827	0.00	-1.29	0.18	0.00	-1.32	0.18	0.00	-1.33	0.18
GOT1_2737	0.00	-0.62	0.17	0.00	0.93	0.16	0.00	1.13	0.16
IER3_3214	0.00	0.94	0.28	0.00	1.97	0.28	0.00	2.14	0.28
IQCJ-SCHIP1_13265	0.00	2.59	0.31	0.00	1.87	0.32	0.00	3.58	0.30
LEAP2_26340				0.01	-3.92	1.35	0.01	-4.00	1.35
LEAP2_28319	0.00	-2.04	0.30	0.00	-2.12	0.30	0.00	-3.12	0.33
LMO7_27443	0.01	0.65	0.20	0.00	1.61	0.20	0.00	1.08	0.20
MCM3_4072	0.00	-1.79	0.16	0.00	-1.67	0.16	0.00	-1.97	0.16
MGST2_15529	0.00	-1.72	0.31	0.00	-2.02	0.31	0.00	-1.88	0.31
MGST2_27509	0.00	-0.63	0.18				0.00	-1.81	0.20
MGST2_27508							0.01	-1.14	0.36
MIXL1_15283	0.00	-1.64	0.31	0.00	-1.69	0.31	0.00	-2.84	0.31
NBPF14_33921	0.00	1.59	0.22	0.00	1.38	0.22	0.00	1.63	0.22
NSMF_14995	0.00	-1.87	0.45	0.00	-2.03	0.46	0.01	-1.35	0.45
NSMF_4729	0.00	-1.40	0.18	0.00	-1.52	0.18	0.03	-0.46	0.17
NT5C3A_11648	0.00	-0.98	0.18	0.01	-0.53	0.18	0.00	-0.96	0.18
NTN4_11596	0.01	1.51	0.46	0.00	2.67	0.43	0.00	2.42	0.43
RAB5B_22829	0.00	1.06	0.14	0.00	0.84	0.14	0.04	0.35	0.14
SCN9A_17603	0.00	1.56	0.35	0.00	2.42	0.34	0.00	2.20	0.34
SLC25A10_6388				0.03	-2.97	1.13			
SLC25A10_21880	0.00	-1.94	0.21	0.00	-1.92	0.21	0.00	-2.13	0.21
SLC40A1_20629	0.00	1.02	0.15	0.00	2.07	0.15	0.00	1.31	0.15
SLC6A14_6512	0.00	-1.72	0.23	0.00	-0.93	0.23	0.00	-1.71	0.23
SPP1_6720	0.00	-0.97	0.24	0.04	0.60	0.24	0.01	0.72	0.24
TEP1_18252	0.00	2.12	0.22	0.00	2.64	0.22	0.00	1.79	0.22

Probe_ID	miR-1293			miR-3615			miR-1909-3p		
	padj	log2FC	lfcSE	padj	log2FC	lfcSE	padj	log2FC	lfcSE
TMEM214_24547	0.00	-0.96	0.16	0.00	-1.12	0.16	0.00	-1.24	0.16
TRIM28_20524	0.00	-0.65	0.12	0.00	-1.01	0.12	0.00	-1.12	0.12
TRO_28012	0.03	2.50	0.95	0.00	3.43	0.93			
TRO_26673	0.01	2.39	0.80	0.00	3.00	0.79	0.01	2.57	0.80
TRO_7352	0.00	1.90	0.32	0.00	2.00	0.32	0.00	1.64	0.32
UBXN7_22634	0.00	1.66	0.25	0.00	1.42	0.26	0.00	1.67	0.25
VPS13C_24266	0.00	1.52	0.20	0.00	1.28	0.21	0.02	0.61	0.21
ZMYND19_11392	0.00	-0.85	0.16	0.00	-0.78	0.16	0.00	-0.59	0.16

Probe_ID	miR-6499-3p			miR-502-5p			miR-200a-5p		
	padj	log2FC	lfcSE	padj	log2FC	lfcSE	padj	log2FC	lfcSE
ADD3_16935	0.00	1.35	0.14	0.00	-0.66	0.18	0.00	1.50	0.14
ANXA3_16294	0.01	0.85	0.25	0.00	1.22	0.29	0.01	-1.09	0.30
DNAJC18_18335	0.00	0.98	0.20	0.00	1.01	0.23	0.00	0.94	0.20
EMP3_18953	0.00	1.98	0.22	0.01	0.81	0.25	0.02	-0.80	0.25
FRMD4B_12533	0.00	1.94	0.21	0.00	1.37	0.24	0.00	1.12	0.23
GBP3_16959	0.00	4.21	0.37	0.00	2.56	0.43	0.01	1.51	0.41
GDF15_18329	0.00	3.56	0.27				0.00	-1.19	0.27
GDF15_2621	0.00	2.93	0.24	0.03	-0.83	0.29	0.00	-1.49	0.27
GEMIN5_22827	0.00	-0.94	0.18	0.00	-1.03	0.20	0.00	-0.97	0.18
GOT1_2737	0.00	1.00	0.16	0.00	-0.85	0.20	0.01	-0.60	0.17
IER3_3214	0.00	2.18	0.28	0.00	-1.48	0.34	0.00	-1.90	0.31
IQCJ-SCHIP1_13265	0.00	2.82	0.30	0.00	2.23	0.34	0.00	1.86	0.33
LEAP2_26340	0.01	-4.26	1.35						
LEAP2_28319	0.00	-2.73	0.31	0.00	1.44	0.31	0.00	1.38	0.27
LMO7_27443	0.02	0.57	0.20	0.00	1.12	0.23	0.02	0.66	0.20
MCM3_4072	0.00	-2.11	0.16	0.00	-1.11	0.19	0.04	-0.47	0.16
MGST2_15529	0.02	-0.85	0.30	0.03	0.97	0.34			
MGST2_27509	0.01	-0.55	0.18				0.00	-0.71	0.19
MGST2_27508							0.03	-1.13	0.37
MIXL1_15283	0.00	-1.27	0.31	0.00	-1.29	0.36	0.00	-1.38	0.31
NBPF14_33921	0.00	1.21	0.22	0.00	1.13	0.25	0.03	0.70	0.23
NSMF_14995	0.05	-1.13	0.45						
NSMF_4729				0.00	-0.75	0.20	0.00	-1.46	0.18
NT5C3A_11648	0.01	-0.59	0.18	0.01	-0.68	0.21	0.01	-0.65	0.18

Probe_ID	miR-6499-3p			miR-502-5p			miR-200a-5p		
	padj	log2FC	lfcSE	padj	log2FC	lfcSE	padj	log2FC	lfcSE
NTN4_11596	0.00	1.87	0.44	0.00	2.36	0.48	0.00	1.97	0.45
RAB5B_22829	0.00	0.98	0.14	0.02	0.48	0.16	0.00	1.11	0.14
SCN9A_17603	0.00	1.97	0.34	0.00	2.72	0.38	0.04	1.07	0.37
SLC25A10_6388									
SLC25A10_21880	0.00	-1.44	0.21	0.00	-1.16	0.24	0.00	-0.79	0.21
SLC40A1_20629	0.00	3.09	0.15	0.00	1.51	0.18	0.00	1.32	0.15
SLC6A14_6512	0.00	-1.26	0.23	0.00	-1.15	0.26	0.00	-1.75	0.23
SPP1_6720	0.00	1.46	0.24	0.00	1.01	0.28	0.00	-0.99	0.24
TEP1_18252	0.00	1.61	0.22	0.03	0.72	0.26	0.00	-0.97	0.26
TMEM214_24547	0.01	-0.47	0.15	0.00	-0.95	0.18	0.00	-0.68	0.15
TRIM28_20524	0.00	-1.21	0.12	0.00	-0.67	0.14	0.00	-0.46	0.12
TRO_28012				0.00	3.16	0.88			
TRO_26673				0.05	2.81	1.05			
TRO_7352	0.00	1.24	0.33	0.00	2.05	0.35	0.03	1.02	0.34
UBXN7_22634	0.00	1.25	0.26	0.00	1.31	0.29	0.01	0.94	0.27
VPS13C_24266	0.00	0.99	0.21	0.00	1.43	0.23	0.00	0.89	0.21
ZMYND19_11392	0.00	-0.61	0.16	0.00	-0.78	0.18	0.00	-0.69	0.16

Probe_ID	miR-363-3p			miR-25-3p		
	padj	log2FC	lfcSE	padj	log2FC	lfcSE
ADD3_16935	0.00	1.01	0.14	0.00	0.90	0.14
ANXA3_16294	0.00	1.65	0.25	0.00	1.56	0.25
DNAJC18_18335	0.00	1.18	0.20	0.00	1.40	0.20
EMP3_18953	0.00	2.42	0.21	0.00	1.84	0.22
FRMD4B_12533	0.01	0.77	0.22	0.03	0.67	0.23
GBP3_16959	0.00	2.12	0.39	0.00	2.48	0.39
GDF15_18329				0.00	-1.02	0.27
GDF15_2621	0.00	-0.98	0.25	0.00	-1.39	0.26
GEMIN5_22827	0.00	-0.84	0.18	0.00	-0.69	0.18
GOT1_2737	0.00	-0.82	0.17	0.01	-0.60	0.17
IER3_3214	0.00	-1.64	0.30	0.00	-2.09	0.31
IQCJ-SCHIP1_13265	0.00	2.44	0.31	0.00	2.35	0.31
LEAP2_26340						
LEAP2_28319	0.00	-1.46	0.28	0.00	-1.78	0.29

Probe_ID	miR-363-3p			miR-25-3p		
	padj	log2FC	lfcSE	padj	log2FC	lfcSE
LMO7_27443	0.04	0.58	0.20	0.00	0.77	0.20
MCM3_4072	0.01	-0.57	0.16	0.02	-0.48	0.16
MGST2_15529	0.04	-0.86	0.30			
MGST2_27509				0.00	-0.88	0.19
MGST2_27508				0.02	-1.10	0.36
MIXL1_15283	0.00	-2.66	0.31	0.00	-2.13	0.31
NBPF14_33921	0.00	0.90	0.22	0.00	1.30	0.22
NSMF_14995	0.01	-1.52	0.45			
NSMF_4729	0.00	-1.05	0.17	0.00	-1.72	0.18
NT5C3A_11648	0.02	-0.58	0.18	0.00	-1.26	0.18
NTN4_11596	0.01	1.50	0.44	0.00	2.10	0.44
RAB5B_22829	0.01	0.46	0.14	0.00	0.91	0.14
SCN9A_17603	0.01	1.22	0.35	0.03	1.02	0.36
SLC25A10_6388				0.03	2.16	0.78
SLC25A10_21880	0.00	-1.22	0.21	0.00	-1.19	0.21
SLC40A1_20629	0.00	1.70	0.15	0.00	1.76	0.15
SLC6A14_6512	0.00	-3.15	0.24	0.00	-3.56	0.24
SPP1_6720	0.00	-1.50	0.24	0.00	-1.44	0.24
TEP1_18252	0.00	0.87	0.22	0.00	0.85	0.23
TMEM214_24547	0.00	-0.71	0.15	0.00	-1.05	0.16
TRIM28_20524	0.01	-0.41	0.12	0.00	-0.42	0.12
TRO_28012				0.02	2.79	0.95
TRO_26673	0.04	2.30	0.80	0.01	2.72	0.80
TRO_7352	0.00	1.41	0.32	0.00	1.87	0.32
UBXN7_22634	0.02	0.82	0.26	0.02	0.80	0.27
VPS13C_24266	0.00	1.06	0.20	0.00	0.78	0.21
ZMYND19_11392	0.00	-0.63	0.16	0.00	-0.85	0.16

Supplemental Table 2. Common 37 genes of siKEAP1 upregulated genes/ siNFE2L2 downregulated genes and effects of Nrf2 pathway enhancing and inhibiting microRNAs.

Probe_ID	siKEAP1			siNFE2L2		
	padj	log2FC	lfcSE	padj	log2FC	lfcSE
ABCC2_26620	1.1E-32	1.9E+00	1.5E-01	4.4E-02	-5.1E-01	1.6E-01
ACTG1_85	2.6E-03	4.0E-01	1.0E-01	4.9E-02	-3.4E-01	1.0E-01
AKR1B10_19908	4.0E-33	3.1E+00	2.5E-01	1.1E-08	-1.9E+00	2.8E-01
AKR1C1_199	6.1E-14	1.6E+00	2.0E-01	1.5E-07	-1.3E+00	2.0E-01
AKR1C2_28246	1.0E-16	2.1E+00	2.4E-01	6.1E-04	-1.2E+00	2.5E-01
AKR1C3_26820	1.2E-08	1.3E+00	2.1E-01	4.3E-04	-1.0E+00	2.1E-01
AMPD3_16428	1.1E-07	1.9E+00	3.2E-01	8.9E-03	-1.7E+00	4.4E-01
ARG2_19025	1.1E-04	6.9E-01	1.5E-01	2.1E-05	-8.2E-01	1.5E-01
B3GNT3_22416	1.6E-10	2.1E+00	3.0E-01	1.5E-02	-1.3E+00	3.5E-01
CDA_11848	6.1E-14	1.9E+00	2.4E-01	2.1E-04	-1.3E+00	2.7E-01
CTSB_23180	1.1E-10	7.7E-01	1.1E-01	3.6E-03	-4.4E-01	1.1E-01
CYP24A1_11891	7.3E-20	1.9E+00	2.0E-01	1.9E-11	-1.5E+00	2.0E-01
DUSP18_15067	1.8E-03	9.1E-01	2.3E-01	1.9E-02	-9.2E-01	2.6E-01
DUSP5_24241	8.6E-06	1.4E+00	2.8E-01	8.5E-04	-1.4E+00	3.0E-01
FILIP1L_12646	3.9E-05	8.9E-01	1.8E-01	2.4E-02	-6.5E-01	1.8E-01
GCLM_2615	2.0E-16	1.5E+00	1.7E-01	2.8E-05	-9.0E-01	1.7E-01
GCNT2_20683	3.4E-02	6.3E-01	2.2E-01	3.0E-02	-7.5E-01	2.2E-01
GDF15_2621	8.9E-06	1.1E+00	2.0E-01	2.3E-02	-7.3E-01	2.1E-01
GPX2_2766	2.3E-02	1.0E+00	3.4E-01	3.4E-04	-1.6E+00	3.4E-01
MVP_4379	4.3E-06	1.5E+00	2.8E-01	2.4E-02	-1.2E+00	3.3E-01
NDRG4_14331	1.2E-11	1.8E+00	2.5E-01	2.7E-02	-9.8E-01	2.8E-01
NOS3_4638	2.5E-06	1.9E+00	3.4E-01	7.4E-04	-2.2E+00	4.8E-01
NQO1_26473	2.8E-13	1.2E+00	1.5E-01	1.2E-09	-1.1E+00	1.5E-01
PLXND1_10528	7.1E-03	5.4E-01	1.5E-01	2.2E-03	-6.7E-01	1.6E-01
RGS3_27783	1.5E-10	9.3E-01	1.3E-01	5.1E-03	-5.3E-01	1.3E-01
RNF8_15649	2.9E-03	6.8E-01	1.8E-01	1.7E-02	-6.6E-01	1.8E-01
S100A11_23914	3.4E-11	1.6E+00	2.2E-01	1.5E-03	-9.9E-01	2.2E-01
SAT1_6103	1.7E-12	1.6E+00	2.0E-01	8.5E-03	-7.8E-01	2.0E-01
SH3BGR13_12496	5.4E-05	1.0E+00	2.1E-01	1.2E-02	-8.1E-01	2.2E-01
SLC7A11_14100	1.8E-07	1.7E+00	2.9E-01	2.6E-02	-1.2E+00	3.4E-01
SPATS2L_12688	1.8E-02	4.9E-01	1.5E-01	2.9E-02	-5.3E-01	1.5E-01
SPINT1_13261	3.4E-10	2.2E+00	3.1E-01	1.1E-02	-1.2E+00	3.2E-01
SPP1_6720	2.6E-17	1.8E+00	2.0E-01	1.5E-19	-1.9E+00	2.0E-01
TGIF1_27951	7.5E-07	6.7E-01	1.2E-01	1.7E-02	-4.3E-01	1.2E-01
TIMP1_13877	8.0E-06	1.1E+00	2.0E-01	2.6E-02	-7.1E-01	2.1E-01
TMEM45B_11590	1.4E-02	1.2E+00	3.7E-01	4.0E-03	-1.9E+00	4.5E-01
UGDH_7525	1.0E-05	1.1E+00	2.1E-01	6.1E-03	-8.2E-01	2.1E-01

Supplemental Table 3. Common 20 genes of siKEAP1 downregulated genes/ siNFE2L2 upregulated genes and effects of Nrf2 pathway enhancing and inhibiting microRNAs.

Probe_ID	siKEAP1			siNFE2L2		
	padj	log2FC	lfcSE	padj	log2FC	lfcSE
A1BG_25586	6.6E-05	-1.0E+00	2.1E-01	1.5E-14	1.6E+00	1.9E-01
ACSM2A_20941	4.4E-03	-8.1E-01	2.2E-01	1.9E-55	3.3E+00	2.0E-01
ALB_217	1.1E-04	-5.0E-01	1.1E-01	9.9E-23	1.1E+00	1.1E-01
APOH_21123	2.1E-02	-6.7E-01	2.2E-01	2.6E-02	7.3E-01	2.1E-01
C3_886	4.5E-07	-6.6E-01	1.1E-01	4.3E-04	5.3E-01	1.1E-01
CYP3A7-CYP3AP1_24430	3.1E-03	-6.7E-01	1.8E-01	8.7E-06	8.8E-01	1.6E-01
FABP1_11582	1.8E-02	-7.1E-01	2.3E-01	2.1E-04	1.1E+00	2.2E-01
FBXO4_21873	8.7E-04	-5.7E-01	1.4E-01	9.8E-03	5.0E-01	1.3E-01
FGB_2397	4.3E-03	-4.7E-01	1.3E-01	1.3E-03	5.6E-01	1.3E-01
HMGCR_3029	8.4E-09	-9.9E-01	1.5E-01	1.2E-03	6.5E-01	1.5E-01
IDH3A_15224	3.6E-02	-3.0E-01	1.0E-01	2.9E-02	3.5E-01	1.0E-01
IGF2_3255	3.2E-05	-1.2E+00	2.3E-01	3.0E-04	1.1E+00	2.2E-01
LEAP2_28319	8.1E-10	-1.7E+00	2.5E-01	1.3E-05	1.2E+00	2.2E-01
MBL2_16596	2.0E-02	-5.6E-01	1.8E-01	4.8E-06	9.3E-01	1.6E-01
NFATC2_12248	1.7E-06	-1.3E+00	2.4E-01	9.8E-03	7.9E-01	2.1E-01
ONECUT1_4810	4.2E-03	-1.7E+00	4.7E-01	3.6E-02	1.1E+00	3.2E-01
PAQR9_18440	1.6E-02	-4.8E-01	1.5E-01	3.7E-03	5.5E-01	1.3E-01
PECR_27673	2.1E-04	-7.5E-01	1.7E-01	6.8E-03	5.9E-01	1.5E-01
SLC30A10_20231	1.6E-08	-1.1E+00	1.6E-01	1.5E-07	9.8E-01	1.5E-01
TMEM97_7217	2.7E-02	-3.6E-01	1.2E-01	2.6E-03	5.0E-01	1.2E-01

Supplemental Table 4. 397 overlapping genes between the common genes of the 4 Top enhancing microRNAs and siKEAP1.

TOP2A	GCLC	DSCC1	HIST1H3F	APOA5	KIF15	MYL9
AP1S1	GCLM	KLF12	SPAG5	RAB5B	KLF6	TMEM214
ATP6V0C	GOT1	MPP7	RAB2B	FOXF2	RPS27L	HPX
DEPDC1B	HMG2	SH3BGRL3	CCDC150	SPDL1	MCM6	
FHL2	HNRNP	FILIP1L	SDCBP	TROAP	ANG	
FOSL1	HSPB8	SPATS2L	RAD23B	CTSB	ARHGAP11A	
HIST1H1C	CXCL8	CAPN2	IL6R	APOBEC3F	ASAP2	
HIST1H2BC	LOC728554	KCTD21	CLIP1	ACSL5	ATXN7L1	
HIST1H2BM	MAP2K1	AP1S3	SUSD1	PSMB9	C18orf32	
HIST1H4E	MAPK13	NCF2	HIST1H2BD	NCAPH2	CHMP1B	
HIST1H4J	MASTL	TMEM59L	SH3RF1	MTMR10	EID3	
LRP10	MLLT11	RBM39	ESYT2	RTKN2	FYTTD1	
SPC25	MMP3	CSDC2	PPP2R5B	BATF	LMNB1	
TMSB10	MOB1B	ABHD2	DNAJC18	FGG	MICAL1	
ALDH4A1	NQO1	GCNT3	TFR2	BUB1	MYL12B	
LURAP1L	NUP35	IQCJ-SCHIP1	PAQR9	DUSP1	SHB	
MCL1	PEG10	BORA	WDR45	DUSP5	TUBGCP3	
NDRG1	PSRC1	SRSF2	DHFR	CCDC138	GADD45A	
PNN	RAB5A	MND1	DTL	PIP4K2C	MSH6	
PRNP	RAD51	HECA	KLB	SLC26A1	NDC1	
S100P	RIT1	EPHA1	CYP2S1	CYP3A7-CYP3AP1	NTN4	
SASS6	RPS6	GLIPR1	MLXIPL	FHL3	PCYT2	
SKP2	RRM2	ZWILCH	ZFAND5	OPTN	ESAM	
ABCG2	S100A6	NRCAM	PALLD	KIF2A	EMC3	
NR1I2	SAT1	GIN54	EMP3	ANKRD1	CD63	
CDA	SERPINE1	CHPF	PANX1	IDS	C19orf33	
OSGIN1	SERPINE2	KANK4	ARG2	TMOD1	PPM1H	
TMC7	SH3KBP1	KIF20B	ZNF280A	TGIF1	TEP1	
YWHAZ	SLC6A14	GLUD2	HIST1H4D	SUV39H2	RBP1	
TMSB4X	SLC7A11	KIF3A	SLC16A6	VEGFB	SLC40A1	
ANXA2P2	SQSTM1	RMND1	GAB2	PTPN3	ZNF714	
CDT1	TCFL5	CREB5	LRCH1	HPN	ACSM2A	
CENPU	TDP2	C4orf32	KRT15	RCN1	HELLS	
NCEH1	TERF2IP	RALBP1	MSH2	SYT11	SERPINA4	
ANLN	TMEM97	KIAA0430	GPAM	SRPX2	B3GNT3	
SDC4	TRIB1	TM4SF19	SERPINB8	RTN4	AKAP12	

SRXN1	TXNRD1	LGALS3	OIP5	NAV3	CENPI
NR1H4	VMP1	IQCC	GLUL	MIS18A	SLC16A5
PAH	YPEL5	CENPQ	KIF3C	AGR2	FLNA
PBK	MYOF	ZDHH18	KLHL4	MAP2	MAX
AMPD3	C1QBP	DUSP18	QSOX1	CDC42EP2	EIF5A2
BIRC3	EFCAB11	MIXL1	PFKP	SKA1	STBD1
BCL2L11	GPAT3	ASAH2	SLC30A10	TPM4	C3ORF52
CASP1	KRT19	MAP1LC3B	MCCC1	AKR1C3	THOC3
CASP8	PIGA	SNRPF	KLRK1	CCNDBP1	HIST2H3A
DEPDC1	IGFBP1	ONECUT1	IDH1	CYP24A1	CLIP4
FLNB	ZNF331	PARPBP	NEK2	RELL1	NPIPA1
KIAA1217	TSNAX	MGST2	KLF5	A1BG	AKR1C1
LMO7	SECTM1	RP2	CADM1	AGTR1	IER3
NBPF15	SLC7A9	ATP9A	ASPH	MCTP1	RFC5
RRAS2	F2RL2	SEPHS1	KLC1	AGXT	COL26A1
ABCC2	SERPINC1	MMP14	GSR	S100A3	DFNA5
ABCC3	PIK3R2	RAB30	IGFBP2	ACTR3	NSMF
ANXA1	RGS10	CAP2	DGKK	DSTN	ADD3
ANXA2	C1orf109	NASP	INHBB	HNRNPA1	HMGCS2
ANXA3	GBE1	CTPS1	FBXL2	PCK1	SLC25A32
ARL6IP5	HIST1H4B	MRPL1	SEPT10	GSTA1	BACE1
ATAD5	HIST1H4F	ZC3H13	PTGR1	PDLIM3	FAM111A
ATP10D	FABP1	SLC13A5	FBXO4	SMIM24	BDH2
ATP6V1D	TMPO	ZCCHC14	XPR1	IL1R2	IDH3A
AURKA	HIST1H3A	CLIC1	ATAD2	ALB	STMN3
BID	HIST2H3D	VRK1	SLAIN2	C1orf131	ITIH1
CCNB1	SMIM14	GBP3	CENPN	CCNA2	BMF
CCNB2	HARS	TLR6	EAF2	CD3D	ACO1
DLGAP5	GIN51	ZBTB10	TAF13	CENPW	RBP2
EGR1	HIST1H2BB	RPL22L1	AGPAT5	EGF	REEP2
FGB	KLRC2	TNS4	RRP15	HMGCR	ADGRD1
FN1	NFATC2	ADAM9	SMOX	IQGAP1	SLC6A11

Metadata online on request

Supplemental Table 5. 24 overlapping genes between the common genes of the 4 top inhibiting microRNAs and siNFE2L2.

Probe_ID	siNFE2L2			miR-502-5p			miR-200a-5p			miR-363-3p			miR-25-3p		
	padj	log2FC	lfcSE	padj	log2FC	lfcSE	padj	log2FC	lfcSE	padj	log2FC	lfcSE	padj	log2FC	lfcSE
ACO1_20595	0.03	0.50	0.14	0.01	0.67	0.20	0.01	0.61	0.18	0.04	0.51	0.18	0.04	0.48	0.18
ADD3_16935	0.01	0.44	0.12	0.00	-0.66	0.18	0.00	1.50	0.14	0.00	1.01	0.14	0.00	0.90	0.14
ADGRD1_25401	0.00	2.68	0.63	0.01	2.59	0.76	0.03	2.21	0.73	0.00	3.79	0.67	0.00	5.67	0.66
BACE1_13077	0.05	0.57	0.18	0.00	0.88	0.23	0.00	1.08	0.21	0.02	0.64	0.20	0.00	0.96	0.21
BDH2_14883	0.00	0.67	0.12	0.00	1.18	0.16	0.00	1.62	0.14	0.00	0.62	0.14	0.00	0.52	0.14
BMF_16921	0.03	1.16	0.33	0.01	1.53	0.43	0.00	2.87	0.37	0.00	2.78	0.75	0.00	3.22	0.36
BMF_26899							0.03	2.32	0.77	0.00	3.17	0.36	0.01	2.42	0.76
FAM111A_13619	0.02	1.05	0.29	0.01	1.36	0.39	0.04	1.04	0.35	0.00	1.28	0.34	0.00	1.66	0.34
FRMD4B_12533	0.03	0.68	0.19	0.00	1.37	0.24	0.00	1.12	0.23	0.01	0.77	0.22	0.03	0.67	0.23
GDF15_2621	0.02	-0.73	0.21	0.03	-0.83	0.29	0.00	-1.49	0.27	0.00	-0.98	0.25	0.00	-1.39	0.26
GDF15_18329							0.00	-1.19	0.27				0.00	-1.02	0.27
HMGCS2_16503	0.00	2.75	0.44	0.00	3.89	0.55	0.00	2.33	0.52	0.00	2.61	0.50	0.00	3.20	0.50
HPX_25984	0.01	1.02	0.26	0.00	1.85	0.34	0.01	1.08	0.31	0.00	1.36	0.30	0.00	1.64	0.30
IDH3A_15224	0.03	0.35	0.10	0.00	-0.60	0.14	0.01	-0.43	0.13	0.03	-0.37	0.12	0.00	-0.67	0.13
ITIH1_16511	0.00	1.64	0.25	0.00	1.89	0.34	0.00	2.52	0.29	0.01	1.05	0.30	0.04	0.83	0.31
LEAP2_28319	0.00	1.22	0.22	0.00	1.44	0.31	0.00	1.38	0.27	0.00	-1.46	0.28	0.00	-1.78	0.29
MYL9_4413	0.01	1.25	0.33	0.04	1.20	0.44	0.00	1.53	0.39	0.04	1.10	0.39	0.00	2.16	0.38
NSMF_4729	0.02	-0.52	0.14	0.00	-0.75	0.20	0.00	-1.46	0.18	0.00	-1.05	0.17	0.00	-1.72	0.18
NSMF_14995										0.01	-1.52	0.45			
RBP2_22383	0.00	1.65	0.40	0.00	2.34	0.50	0.00	2.41	0.45	0.00	2.29	0.44	0.02	1.38	0.47
REEP2_24279	0.04	0.64	0.20	0.00	1.51	0.27	0.01	0.84	0.24	0.00	1.85	0.23	0.00	2.19	0.23
SLC25A32_6403	0.01	-0.56	0.15	0.01	-0.69	0.21	0.00	-0.73	0.19	0.00	-0.96	0.19	0.00	-1.49	0.19
SLC6A11_26630	0.03	0.49	0.15	0.03	-0.59	0.21	0.00	-0.80	0.18	0.00	-1.32	0.18	0.00	-1.32	0.18
SPP1_6720	0.00	-1.94	0.20	0.00	1.01	0.28	0.00	-0.99	0.24	0.00	-1.50	0.24	0.00	-1.44	0.24
STMN3_15411	0.00	0.99	0.22	0.01	-1.14	0.33	0.00	1.38	0.27	0.00	1.45	0.27	0.00	1.73	0.27
TMEM214_24547	0.04	0.41	0.12	0.00	-0.95	0.18	0.00	-0.68	0.15	0.00	-0.71	0.15	0.00	-1.05	0.16
TRO_7352	0.05	0.91	0.28	0.00	2.05	0.35	0.03	1.02	0.34	0.00	1.41	0.32	0.00	1.87	0.32
TRO_28012				0.05	2.81	1.05				0.04	2.30	0.80	0.02	2.79	0.95
TRO_26673				0.00	3.16	0.88							0.01	2.72	0.80

4

A systematic analysis of Nrf2 pathway activation dynamics during repeated xenobiotic exposure

Luc J.M. Bischoff^{1,3}, Isoude A. Kuijper^{1,3}, Johannes P. Schimming¹, Liesanne Wolters¹, Bas ter Braak¹, Jan P. Langenberg², Daan Noort², Joost B. Beltman¹, Bob van de Water¹

¹Division of Drug Discovery and Safety, Leiden Academic Centre for Drug Research, Leiden University, Leiden, The Netherlands

²Department of CBRN Protection, TNO Defence, Safety and Security, Rijswijk, The Netherlands

³These authors contributed equally to the work.

Based on:

Bischoff LJM, Kuijper IA, Schimming JP, et al. (2019) A systematic analysis of Nrf2 pathway activation dynamics during repeated xenobiotic exposure. Arch Toxicol 93(2):435-451
doi:10.1007/s00204-0182353-2

ABSTRACT

Oxidative stress leads to the activation of the Nuclear factor-erythroid-2-related factor 2 (Nrf2) pathway. While most studies have focused on the activation of the Nrf2 pathway after single chemical treatment, little is known about the dynamic regulation of the Nrf2 pathway in the context of repeated exposure scenarios. Here we employed single cell live imaging to quantitatively monitor the dynamics of the Nrf2 pathway during repeated exposure, making advantage of two HepG2 fluorescent protein reporter cell lines, expressing GFP tagged Nrf2 or sulfiredoxin 1 (Srxn1), a direct downstream target of Nrf2. High throughput live confocal imaging was used to measure the temporal dynamics of these two components of the Nrf2 pathway after repeated exposure to an extensive concentration range of diethyl maleate (DEM) and tert-butylhydroquinone (tBHQ). Single treatment with DEM or tBHQ induced Nrf2 and Srxn1 over time in a concentration-dependent manner. The Nrf2 response to a second treatment was lower than the response to the first exposure with the same concentration, indicating that the response is adaptive. Moreover, a limited fraction of individual cells committed themselves into the Nrf2 response during the second treatment. Despite the suppression of the Nrf2 pathway, the second treatment resulted in a three-fold higher Srxn1-GFP response compared to the first treatment, with all cells participating in the response. While after the first treatment Srxn1-GFP response was linearly related to Nrf2-GFP nuclear translocation, such a linear relationship was less clear for the second exposure. siRNA-mediated knockdown demonstrated that the second response is dependent on the activity of Nrf2. Several other, clinically relevant, compounds (i.e., sulphorophane, nitrofurantoin and CDDO-Me) also enhanced the induction of Srxn1-GFP upon two consecutive repeated exposure. Together the data indicate that adaptation towards pro-oxidants lowers the Nrf2 activation capacity, but simultaneously primes cells for the enhancement of an antioxidant response which depends on factors other than just Nrf2. These data provide further insight in the overall dynamics of stress pathway activation after repeated exposure and underscore the complexity of responses that may govern repeated dose toxicity.

INTRODUCTION

Chemical exposure leads to the activation of various cellular stress response pathways (Jennings et al. 2013; Souza et al. 2017). These cellular stress response pathways are typically activated to initiate repair of cell injury and/or to adapt cells to possible subsequent harmful situations (Baird and Dinkova-Kostova 2011; Kensler et al. 2007). Alternatively, cell injury may initiate the activation of cell death programs to switch on self-demise of cells (Danial and Korsmeyer 2004; Fulda et al. 2010). Although these are realistic conceptual considerations, so far there is little data on how individual cells within an entire population respond upon repeated exposure. This is largely related to the experimental limitations that prohibit a high dimensional analysis of the cellular stress responses at different concentrations and time points in populations of individual cells. To improve our basic understanding of cellular responses to repeated dosing scenarios, we here apply time-resolved live cell imaging of cellular stress response activation, focusing on the Nuclear factor-erythroid-2-related factor 2 (Nrf2) mediated antioxidant stress response signaling pathway.

The Nrf2 pathway plays a role in protection against chemicals with soft electrophile properties and that propagate the generation of reactive oxygen species (ROS), which may lead to oxidative stress with cell death as an ultimate outcome (Ryter et al. 2007). Such enhanced oxidative stress is typically counteracted through activation of the adaptive antioxidant cellular stress response pathway (Deshmukh et al. 2017; Ma 2013) which involves the activation of the Nrf2 pathway as the most critical component (Itoh et al. 1997; Meakin et al. 2014; Vomund et al. 2017). Nrf2 itself is a 'Cap 'n' Collar' (CNC) basic-region leucine zipper transcription factor. Under basal unstressed cellular conditions, a single Nrf2 protein is bound to two Kelch-like ECH-associated proteins (Keap1) (Keum and Choi 2014; Zipper and Mulcahy 2002). Keap1-bound Nrf2 is poly-ubiquitinated, targeting it for degradation (Kobayashi et al. 2004; Zhang et al. 2004). In response to oxidative stress and soft-electrophilic chemical exposure Keap1 is modified (Baird and Dinkova-Kostova 2013). Modification of Keap1 happens on a subset of its 27 cysteine residues (Holland and Fishbein 2010). For example, the chemicals diethyl maleate (DEM) and tert-butylhydroquinone (tBHQ) can bind to cysteine residue 151; This leads to ubiquitination of Keap1, therefore degradation of Nrf2 cannot take place (Holland and Fishbein 2010; Kobayashi et al. 2009). Current models indicate that modified Keap1 remains occupied by Nrf2, driving accumulation of newly translated Nrf2, its translocation into the nucleus and binding and activating the antioxidant response element (ARE) in various target genes (Bryan et al. 2013; Itoh et al. 1997). Nrf2 downstream genes encode for a diverse set of adaptive programs to protect against the oxidative stress environment, exemplified by the upregulation of glutamate-cysteine ligase modifier (*GCLM*), heme oxygenase 1 (*HMOX1*), NAD(P)H quinone oxidoreductase

1 (*NQO1*) and sulfiredoxin1 (*SRXN1*). Here, we focus on the regulation of *Srxn1*, a bona fide Nrf2 target protein that is involved in the reduction of oxidized peroxiredoxin, a family of peroxidases which catalyzes the reduction of H_2O_2 and alkyl hydroperoxides (Chang et al. 2004; Keum et al. 2006; Soriano et al. 2008). Nrf2 pathway activation is thought to lead to an overall protection against oxidative stress, with the expectation that a similar repeated exposure would limit the antioxidant response, since sufficient protection is already available. Indeed, Nrf2 pathway activation typically leads to protection against pro-oxidant response (Itoh et al. 1997; Kensler et al. 2007; Wu et al. 2012). However, so far little is known on the dynamic modulation of Nrf2 under such repeated exposure conditions and whether limitations in the anticipated adaptation exist. Moreover, it remains unclear whether such adaptation is reflected by suppression of Nrf2 pathway activation in general or, alternatively, potential priming of the Nrf2 pathway leading to stronger pathway activation upon a repeated exposure. Understanding the outcome of diverse exposure scenarios is important for rational decision making on the safety assessment of repeated exposure.

A few reports exist on repeated exposure to known Nrf2 inducers. Mathew et al. found a stronger induction of Nrf2-dependent gene expression in primary human skin fibroblasts after repeated exposure to sulphoraphane compared to single exposure. Interestingly, an optimal concentration for repeated sulphoraphane exposure was determined that provided maximal protection against radiation injury (Mathew et al. 2014). In addition, Bergström et al. showed an ongoing accumulation of Nqo1 protein, a downstream target of the Nrf2 pathway, in astrocytes treated with 10 μ M sulphoraphane for 4 h per day over a time span of 4 days (Bergström et al. 2011). While these findings support different outcomes of single exposure compared to repeated exposure to Nrf2 activating agents, these studies have provided little insight in the actual behavior of Nrf2 or downstream Nrf2 target activity during repeated exposure at a single cell level.

We have previously reported the systematic characterization and application of a panel of fluorescent protein reporters to follow individual components of the Nrf2 pathway: Keap1, Nrf2, and *Srxn1* (Hiemstra et al. 2017; Wink et al. 2017; Wink et al. 2018). We used BAC transgenomics to tag these components with GFP and follow their behavior in individual cells over time using high throughput confocal imaging (Wink et al. 2017). Here we applied these reporter cell lines to investigate the effect of two earlier mentioned, well-known inducers of the Nrf2 pathway, DEM and tBHQ, on the dynamics of Nrf2 and *Srxn1* activation under different repeat exposure scenarios. DEM is an alkylating agent able to deplete cellular glutathione (GSH) levels by direct conjugation with GSH or via glutathione S-transferase (Casey et al. 2002; Priya et al. 2014; Yamauchi et al. 2011). tBHQ is the metabolite of butylated hydroxyanisole, a synthetic phenolic antioxidant, that

acts as a redox cycler to generate ROS (Imhoff and Hansen 2010). In the present study, we used DEM and tBHQ to unravel the dynamics of Nrf2 pathway activation during repeated exposure. Our current data provide direct evidence for distinct dynamics of Nrf2 activation during a first and second treatment regimen as well as for priming of the pathway initiated during the first treatment, thus promoting an enhanced activation of the Nrf2 target gene *SRXN1* during a second treatment regimen.

METHODS

Chemicals

Tert-butylhydroquinone (tBHQ, CAS: 1948-33-0), diethyl maleate (DEM, CAS: 141-05-9), L-sulphoraphane (CAS: 142825-10-3) and nitrofurantoin (CAS: 67-20-9) were both obtained from Sigma-Aldrich. Bardoxolone methyl (CDDO-Me, CAS: 218600-53-4) was obtained from Cayman Chemicals/Bio-Connect. All compounds were dissolved in 100 % dimethyl sulfoxide (DMSO, CAS: 67-68-5) from Sigma-Aldrich, to obtain aliquots with stock concentrations of 0.1 M.

Cell culture

The human hepatoma HepG2 cell line was obtained from American Type Culture Collection (ATCC® HB-8065™, Wesel, Germany). Previously, HepG2-GFP reporter cells were developed and characterized for Nrf2 and *Srxn1* (Wink et al. 2017). Briefly, cell lines were constructed with GFP reporter genes located on bacterial artificial chromosomes (BACs) that encode C-terminal GFP-tagged fusion proteins, following a selection with 500 µg/mL G-418. For more information see (Poser et al. 2008). Cells were grown in Dulbecco's Modified Eagle Medium (DMEM) high glucose, supplemented with 10 % (v/v) fetal bovine serum (FBS), 25 U/mL penicillin and 25 µg streptomycin. Cells were used for experiments until passage 20. Cells were seeded in 384-well plates (7,000 cells/well), 2 days before exposure. Cells were exposed to concentrations in the range of 12.5 – 200 µM of DEM or tBHQ, 2.5– 50 µM sulphoraphane, 15.6 – 250 µM nitrofurantoin, and 25 – 500 nM CDDO-Me. DMSO (0.1 % v/v) and DMEM were used as negative controls.

Cell treatment and repeated exposure scenarios

Two different repeated exposure scenarios were used. In scenario 1, 8-h first exposure, was followed by 8-h second exposure, i.e., in total 16 h of live cell imaging. In scenario 2, 24-h first exposure was followed by 24-h second exposure, i.e., in total 48 h of live cell imaging (Figure 1A). For both scenarios we used 9 different concentrations of DEM and tBHQ (12.5, 25, 50, 75, 100, 125, 150, 175, 200 µM). All possible combinations of concentrations in the first and second exposure

were tested. Furthermore, scenario 2 was also used to test the effect of repeated exposures for five different concentrations of sulphoraphane (2.5, 5, 10, 25, 50 μM), nitrofurantoin (15.6, 31.3, 62.5, 125, 250 μM), and CDDO-Me (25, 50, 100, 250, 500 nM). In these experiments, we employed the same concentration of the compound during the second as during the first exposure.

siRNA transfection

siGENOME SMARTpool siRNAs were obtained from Dharmacon: siKEAP1, siNFE2L2, siSRXN1, siMAFF, and siMAFG. Upon arrival, siRNAs were resuspended following the manufacture's description. siRNAs were diluted in 1x siRNA buffer (Dharmacon, USA) to a final concentration of 1 μM . 5 μL siRNA solution/well (96-well plate) was used. Interferin (Westburg/PolyPlus, NL) was used as a transfection agent. Srxn1-GFP HepG2 cells were seeded and transfected in a 96-well plate (23,000 cells/well). 72 h after transfection, cells were exposed to the different chemicals as described above followed by high content imaging.

Confocal microscopy

Live cell confocal imaging was performed on a Nikon Eclipse Ti confocal microscope equipped with four lasers: 408, 488, 561 and 633 nm. A 20x dry PlanApo VC NA 0.75 was used. 384-well microclear imaging plates (microclear, Greiner) were seeded with 7,000 cells/well. Prior to exposure, Hoechst₃₃₃₄₂ 100 ng/mL was added to the wells to stain nuclei. Subsequently, Hoechst-containing medium was washed away and medium (25 μL) that contained 100 nM propidium iodide (PI) was added to allow measurement of cell death during imaging. 25 μL /well of compound containing medium was added to wells. Images were taken every hour for the indicated time periods.

TempO-Seq transcriptome analysis

HepG2-WT cells were plated in 96-well plates (70,000 cells/well) and exposed to 100 μM DEM or tBHQ, with three independent biological replicates. After 24-h exposure, the plates were washed with 200 μL PBS and lysed with 50 μL BioSpyder 1x lysis buffer for 15 min at room temperature. After this step, plates were frozen at -80°C . Next, the lysate plates were shipped on dry ice to BioSpyder technologies where the TempO-Seq assay was conducted (Yeakley et al. 2017). Returned gene transcription data was further analyzed using the Deseq2 package in R allowing to calculate the log2fold change and the corresponding standard error (*lfcSE*) respectively to the base line value (medium only, no treatment).

Image processing and analysis

Cell segmentation and quantification was performed with CellProfiler version 2.1.1 (Hiemstra et al. 2017; Kametsky et al. 2011). To segment the nuclei from

the background and each other, we used an ImageJ plugin for CellProfiler based on watershed masked clustering (WMC) as described before (Yan and Verbeek 2012). In brief, the method consists of three steps. First, the image is divided into intensity regions and starting from local maximum intensities, the watershed region is expanded. Second, a weighted fuzzy C-means clustering algorithm is applied to find an optimal threshold that separates background and nucleus for this region. Third, to correct nuclei that were erroneously subdivided in two different regions (i.e., that were actually a single nucleus), the algorithm merges nuclei from adjacent regions having the same orientation. We used the output of the WMC module, i.e., the segmented nuclei areas, to quantify the intensity of nuclear Nrf2-GFP and PI. To determine the intensity of Srxn1-GFP in the cytoplasm, we applied the propagation setting in CellProfiler ("identify-secondary-objects module"), employing the nuclei as seeds. This implies that CellProfiler takes the outer border of the nuclei as starting points to go outwards in a recursive manner until pixels are no longer positive for GFP or belong to a neighboring cell. In cases with high background levels that precluded correct cytoplasmic segmentation employing the propagation setting, we used the 'distance B' setting in CellProfiler ("identify-secondary-objects module"). In this setting, the nucleus is expanded by a fixed amount of pixels (using 30 pixels for our case), and in this region the background and GFP signal is distinguished.

Nrf2-GFP intensities of single cells are calculated by taking the mean of all the pixels in a segmented nucleus. For Srxn1, the integrated GFP intensity in the cytoplasm, calculated with the propagation or distance B setting. We employed min-max normalization to these values, i.e., we scaled the mean GFP-intensities of individual cells per experiment between 0 and 1, to be able to compare the biological replicates. A cell was considered GFP-positive, when its normalized GFP-intensity exceeded a threshold equal to the third quartile of the GFP-intensity distribution of cells treated with medium (negative control) during the first exposure. To determine this GFP-intensity distribution, all cells were individually included as were all time points of the first exposure. The PI-intensity within the segmented nuclei was used to decide whether a cell was considered dead or alive, based on an analysis of PI- and Srxn1-GFP-intensities. Cells with a PI-intensity of 0.2 or higher never reached a high level of Srxn1-intensity (not shown). Therefore, 0.2 was chosen as a cut-off value, and cells above this PI-intensity were considered dead. Note that the same PI-intensity threshold was applied for the Nrf2-GFP reporter cell line.

To allow comparison of the cellular response during the first exposure with that during the second exposure, we first subtracted the mean intensity of the last time point of the first exposure from the mean intensity of the second exposure. To visualize the strength of the response, we focused on the maximum value (Max), i.e.,

the highest mean intensity at any time point (Figure 1B). To quantify the speed of the response, the time to reach half of the Max value (thMax) was calculated. We used linear interpolation to estimate the time it takes to reach the half-maximal value (hMax). Significance is determined using a one-sided welch two sample t-test.

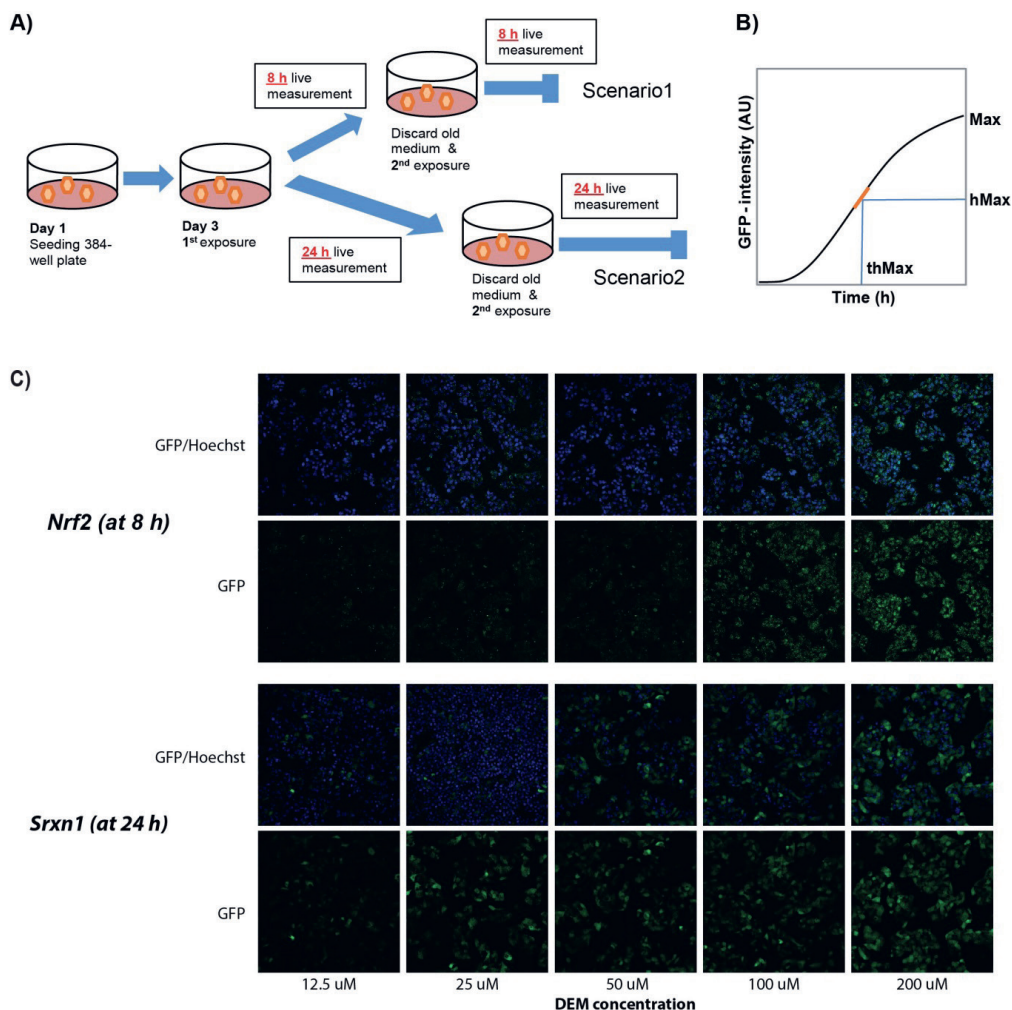


Figure 1. Schematic representation of the *in vitro* exposure scenarios and metrics.

A) Schematic overview of the two exposure scenarios. **B)** Illustration of the metrics used for comparison of the dynamic behaviour between the first and second exposure: **Max**: highest value reached within experimental time frame. **hMax**: half of the Max value; **thMax**: time to reach hMax. The thMax is calculated by interpolating the two data points closest to half of the Max value (illustrated by orange line). **C)** Confocal microscopy images of the Nrf2-GFP signal (at 8 h) and the Srtn1-GFP signal (at 24 h) after exposure to different concentrations of DEM with and without nuclear staining (Hoechst). Data are normalized per experiment and error bars depict the SEM; based on n=3 (for Nrf2-GFP) and n=4 (for Srtn1-GFP) experiments. AU = Arbitrary Units.

RESULTS

Dynamics of Nrf2 and Srxn1 activation after single treatment with DEM and tBHQ

To assess the dynamics of Nrf2 pathway activation we used two model compounds, DEM and tBHQ, two small molecules that target cysteine residues in Keap1, leading to activation of the Nrf2 pathway (Holland and Fishbein 2010; Kobayashi et al. 2009). Here, we first systematically compared the dynamics of Nrf2 activation by DEM and tBHQ upon a single dosing regimen by using confocal microscopy to monitor the stabilization and nuclear translocation of Nrf2-GFP and subsequent induction of Srxn1-GFP, a direct target gene of Nrf2 (Figure 1C). HepG2 Nrf2-GFP and HepG2 Srxn1-GFP reporter-cells were exposed to different concentrations (12.5-200 μ M) of DEM and tBHQ followed by live cell imaging for 24 h (Figure 2A-B). Both compounds caused Nrf2-GFP stabilization and translocation into the nucleus in a concentration-dependent manner (Figure 2A). Nrf2 reaches its hMax after approximately 2 hours of exposure to DEM or tBHQ, independent of the concentration (Figure 2C). Overall maximal values of nuclear Nrf2-GFP were similar for DEM and tBHQ, although at high concentrations of tBHQ a sustained nuclear presence of Nrf2-GFP was observed (Figure 2A). As anticipated, Srxn1-GFP was activated later than Nrf2-translocation to the nucleus (Figure 2A-C). We observed slightly higher maximum values of Srxn1-GFP-intensity after treatment with tBHQ, likely due to the sustained Nrf2 activation at high tBHQ concentration. The Srxn1-response reaches its thMax consistently after approximately 8 h of exposure, 6 h later than the thMax of Nrf2 nuclear entry (Figure 2C). We observed a linear relationship between the maximal Nrf2- Srxn1-GFP-intensities (Figure 2D). Moreover, this relation was compound-specific, with different slopes for DEM (slope = 0.48) and tBHQ (slope = 0.71).

Dynamics of Nrf2 and Srxn1 activation after repeated dosing

There is little understanding on how prior activation of Nrf2 allows adaptation of the cell physiology and adjustment to a secondary Nrf2 activation response. We considered two different scenarios: 1) A secondary exposure at a time point when the Nrf2 response was not yet back to baseline levels, and adaptation not yet fully maximal; 2) a secondary exposure at a time point when the Nrf2 response as well as the adaptation program are largely completed (see Figure 1A, 2AB). We first systematically evaluated the first scenario and treated cells for 8 h with different concentrations of DEM or tBHQ followed by a second exposure matrix at identical concentrations (Figure 3). As for our initial experiment with single dosing (see Figure 2), the Nrf2-GFP response showed a peak after approximately 2 h and subsequently slightly declined (Figure 3A-B). Interestingly, a second treatment after 8 h caused a further (re)activation of the Nrf2-GFP response, in particular when the first concentration was lower than the second

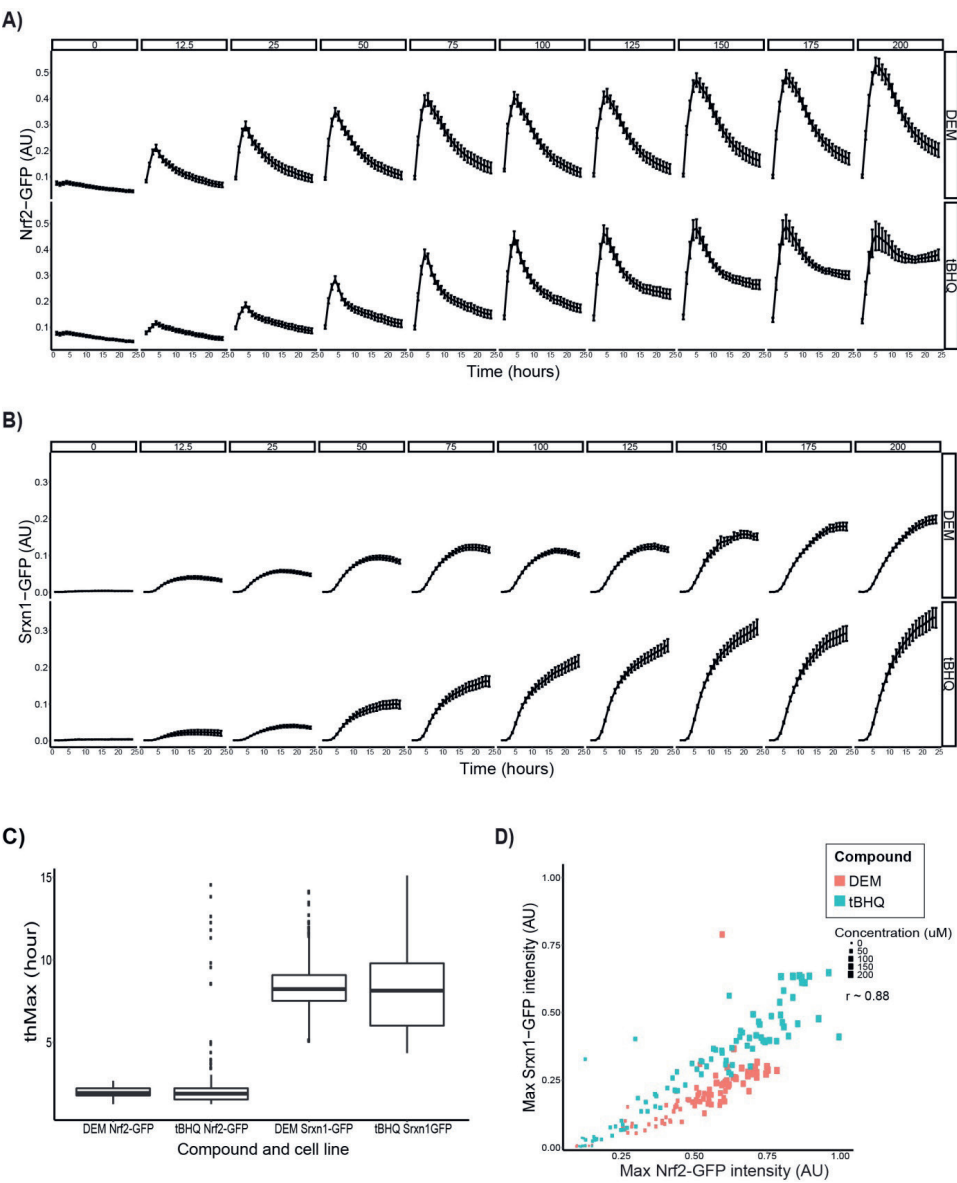


Figure 2. Time-response curves of Nrf2 and Srxn1 activation during 24 h exposure to DEM or tBHQ in a dose range of 12.5-200 μM .

A) Average Nrf2-GFP signal in the nucleus over time. **B)** Average Srxn1-GFP signal in the cytoplasm over time. **C)** thMax for Nrf2 and Srxn1, for both DEM and tBHQ. **D)** Comparison of the maximal Nrf2-GFP and Srxn1-GFP intensity reached after 24 h treatment with different concentrations of DEM or tBHQ (concentration indicated by symbol size).

concentration. However, this was not so strongly observed when the cells were first treated with the highest concentration of 200 μM , suggesting that the physiological response to activate the Nrf2 pathway was already saturated under this condition (Figure 3A-B). The enhanced activation of Nrf2-GFP after a second exposure did not have major consequences for the activation of the downstream target Srxn1 (Figure 3C-D). Thus, although after 8 h from the first treatment the Srxn1-GFP induction was already initiated, a second treatment only marginally affected the Srxn1-GFP induction, in spite of the doubling of the Nrf2-GFP response for some concentration pairs (e.g., the 50-200 μM combination for DEM). These data suggest that the 8-h repeated exposure scenario does not initiate clear adaptation, neither for DEM nor for tBHQ treatment.

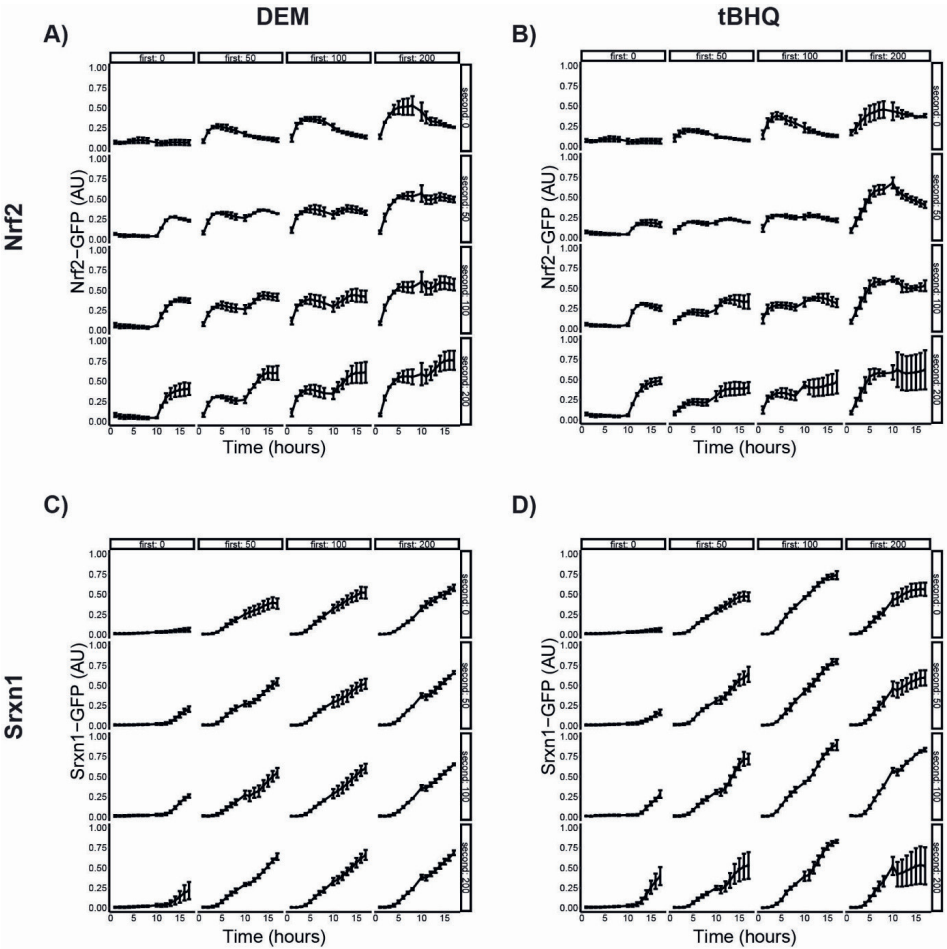


Figure 3. Time response curves of Nrf2 and Srxn1 activation for short repeat exposure scenario (8 h + 8 h).

Cells were exposed to DEM or tBHQ at the start and re-exposed after 8 hours with indicated concentrations. **A-B)** Average Nrf2-GFP intensity in the nucleus over time after exposure to DEM (A) and tBHQ (B). **C-D)** Average Srxn1-GFP intensity in the cytoplasm over time after exposure to DEM (C) and tBHQ (D). Data are normalized per experiment and error bars depict the SEM; based on n=3 experiments.

Next, we determined the effect of repeated exposure at 24 h intervals (scenario 2). We monitored the Nrf2-GFP and Srxn1-GFP response for 48 h, with second treatment initiation at 24 h. The same concentration matrix for the first and second treatment was used as for scenario 1. For both DEM and tBHQ we observed a suppression of the Nrf2-GFP response when identical concentrations for first and second treatment were considered (see e.g. 50 μ M/50 μ M and 100 μ M/100 μ M repeat dosing scenarios in Figure 4A-B). When the concentration of the second treatment was higher than for the first treatment, a Nrf2-GFP response equal to or higher than the first response was observed. This was in particular the case for tBHQ, where the highest concentration of tBHQ caused a sustained activation of Nrf2-GFP during the second exposure (Figure 4B). This response of Nrf2-GFP was not reflected in the behavior of its target Srxn1-GFP. In general, despite the suppression of the Nrf2-GFP response, the Srxn1-GFP of the second treatment was stronger compared to the first treatment, both with respect to response rate as well as the amplitude of the Srxn1-GFP response (Figure 4C and 4D). Only the highest concentration of tBHQ did not demonstrate such a strong secondary Srxn1-GFP response (Figure 4D). This was likely related to the fact that a secondary treatment with 200 μ M tBHQ caused cell death in ~25% of the cells (Supplementary Figure 1), indicating that this concentration was close to the tipping point towards onset of cell death. This coincided with the sustained accumulation of Nrf2-GFP in the nucleus. In conclusion, these data suggest that activation of the Nrf2 pathway response results in an adaptation of Nrf2 activation, in particular at late time points. In addition, such adaptation of Nrf2 activation does not imply suppression of downstream target genes of Nrf2. Intriguingly, the observed adaptation is in fact associated with an enhanced induction of Srxn1-GFP, irrespective of suppression of Nrf2-GFP activation.

Population dynamics of Nrf2 and Srxn1 activation during repeated exposure

So far, our results have demonstrated the effect of repeated treatment at the entire population level. The strength of our live cell imaging approach is that we can determine the commitment of individual cells within the entire population during both the first and second treatment with DEM and tBHQ. Therefore, next we asked whether a difference in the response during the repeated exposure was related to differences in the overall commitment of individual cells into the stress response activation. For this purpose, we determined a background GFP-threshold value based on measurements under control situations. We considered cells to be committed to the response when the GFP-values exceed this background threshold. We observed that there was a drastic commitment of more than 90 % of the cells with respect to Nrf2-GFP activation within the first 2 h after the first treatment with the various concentrations of DEM and tBHQ. The fraction of committing cells

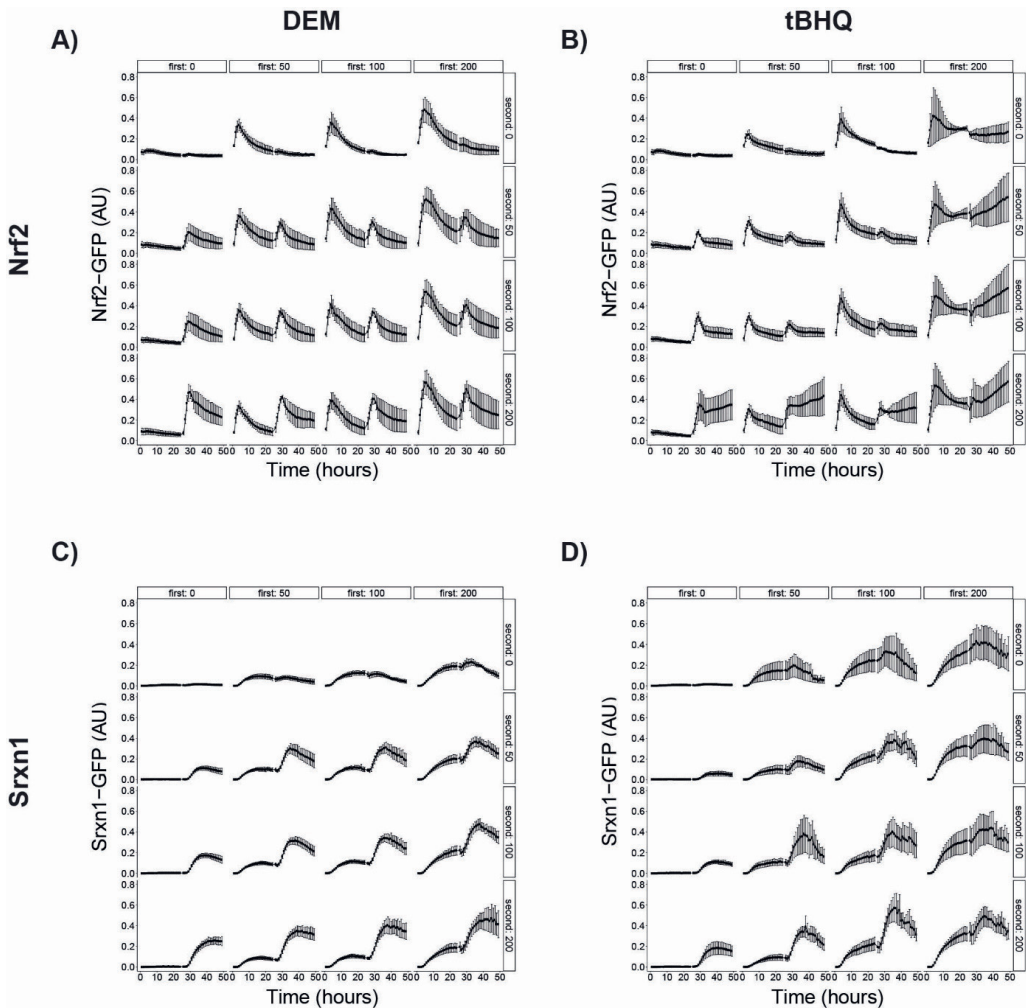


Figure 4. Time response curves of Nrf2 and Srxn1 activation for long repeat exposure scenario (24 h + 24 h).

Cells were exposed to DEM or tBHQ at the start and re-exposed after 24 h. **A-B)** Average Nrf2-GFP signal in the nucleus over time after exposure to DEM (A) and tBHQ (B). **C-D)** Average Srxn1-GFP signal in the cytoplasm over time after exposure to DEM (C) and tBHQ (D). Data are normalized per experiment and error bars depict the SEM; based on $n=3$ (for Nrf2-GFP) and $n=4$ (for Srxn1-GFP) experiments.

then slowly declined to baseline levels over time if there was no second exposure. For the second treatment we observed an equally fast increase in individual cell commitment, and prior treatment hardly affected the commitment of cells (Figure 5), despite that the population-level amplitude of activation was lower compared to the first treatment (see Figure 4). The commitment to Nrf2-GFP activation was typically shorter in duration for the second than for the first exposure (Figure 5A-B).

Interestingly, for high concentrations of tBHQ the overall commitment of Nrf2-GFP activation remained high.

With respect to the Nrf2-mediated activation of the Srnx1-GFP response, almost all cells committed already during the first treatment period, with a lag phase of up to four hours (Figure 5C-D). The second treatment did not further affect the commitment of individual cells into the response, besides that the overall amplitude of the Srnx1-GFP response was higher (compare Figure 4 and 5). Together, these data indicate that at the individual cell level a clear adaptation of Nrf2-GFP activation occurs, where the overall commitment to Nrf2-GFP activation is sustained for a shorter period in the second treatment compared to the first treatment period.

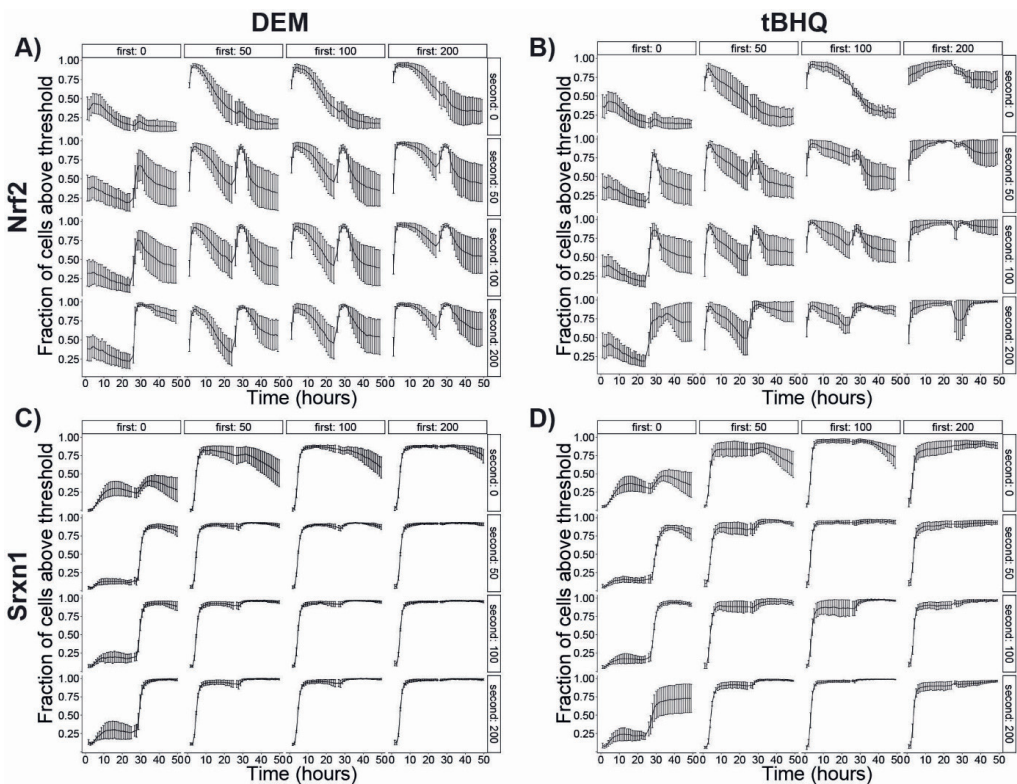


Figure 5. Commitment of individual cells into the Nrf2 and Srnx1 response during long repeat exposure scenario.

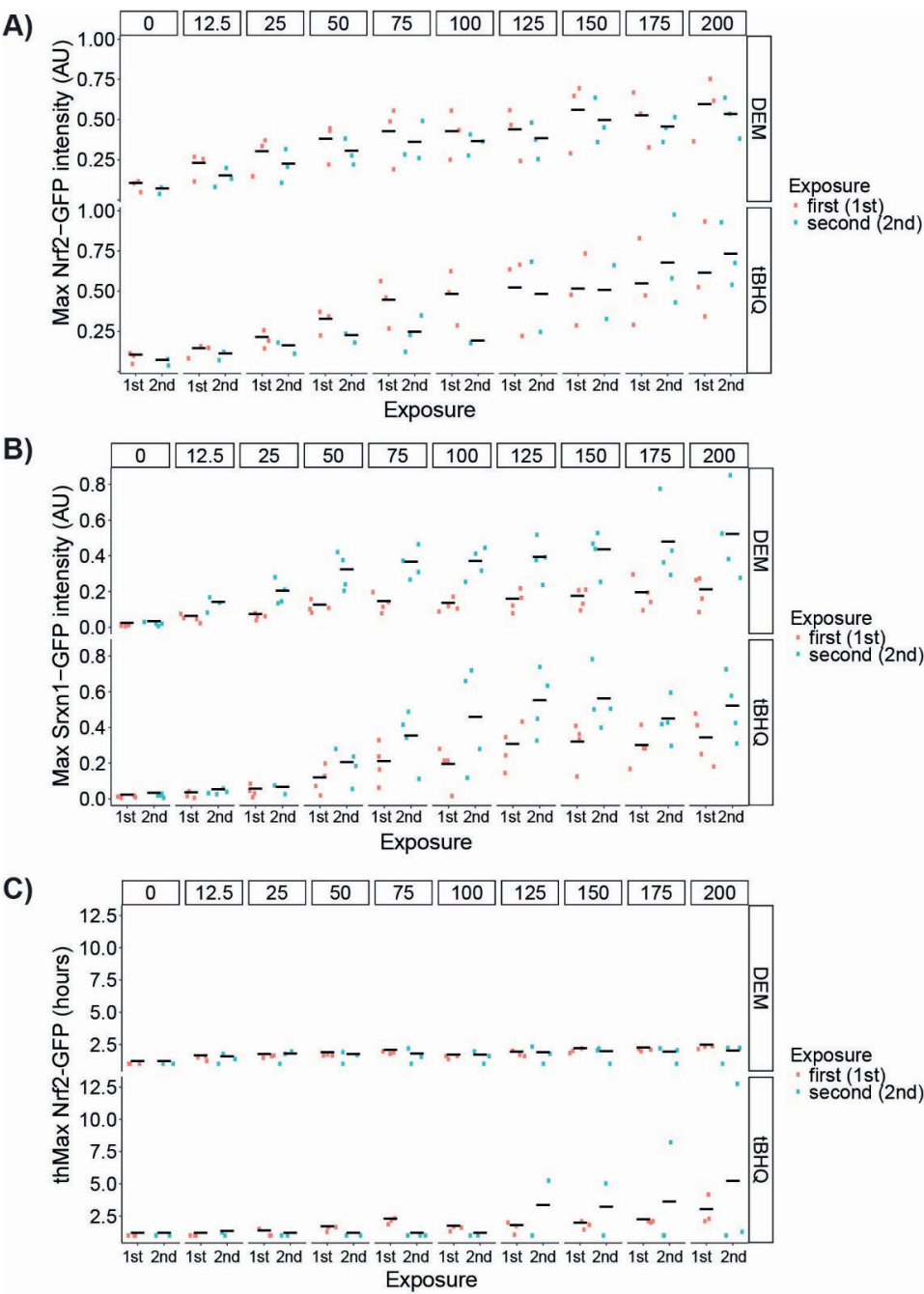
Cells were exposed to DEM or tBHQ at the start and re-exposed after 24 hours. **A-B)** Fraction of cells whose nuclear Nrf2-GFP levels exceed background levels over time, after exposure to DEM (A) and tBHQ (B). **C-D)** Fraction of cells whose cytoplasmic Srnx1-GFP levels exceed background levels, after exposure to DEM (C) and tBHQ (D). Data are normalized per experiment and error bars depict the SEM; based on n=3 (for Nrf2) and n=4 (for Srnx1) experiments.

Differential activation dynamics for Nrf2 and Srxn1 activation for first and second treatment regimens

The analysis above indicated differences in the commitment of cells with respect to Nrf2 activation. Since in our experimental setup we recorded the reporter activities for all treatment conditions with ~1-h time resolution, we next extracted the maximal Nrf2-GFP and Srxn1-GFP activation and the speed of activation onset during the first and second exposure. The maximum intensity of Nrf2-GFP for the first 24 h exposure was slightly higher than for the second 24 h, supporting adaptation of the Nrf2 response (Figure 6A). In contrast, the maximum response for Srxn1-GFP was up to three times higher after the second treatment (Figure 6B). We also considered potential differences in the dynamics of both Nrf2-GFP and Srxn1-GFP activation. The *thMax* was hardly affected by concentration or compound, except for the highest repeat concentrations of tBHQ at which the Nrf2 pathway does not recover and the concentration of Nrf2 in the nucleus increases for the entire 48 h treatment duration (Figure 6C-D). Interestingly, despite similar Nrf2-GFP dynamics between the first and second exposure, the *thMax* for Srxn1-GFP activation declined by almost a factor two, from ~8 h to ~4 h. This is consistent with the notion that the enhanced Srxn1 upregulation is part of an adaptation programme to control prolonged exposure to soft electrophiles such as DEM and tBHQ. Because of the opposite direction of the response, i.e. the reduced response of Nrf2-GFP and the increased response of Srxn1-GFP during the second treatment condition, the linear relationship between Nrf2-GFP and Srxn1-GFP activation that we observed for the first exposure was less clearly present for the second treatment period (Figure 6E). Moreover, the slope difference between DEM and tBHQ was no longer apparent. These data together indicate that during repeated treatment with soft electrophilic chemicals, different mechanisms take part in the cellular stress response activation of the Nrf2 pathway for the first and for subsequent exposures.

Secondary enhanced activation of Srxn1 expression is dependent on the Keap1/Nrf2 pathway

We next investigated the underlying mechanism of the Srxn1 induction during repeated exposure. Because *SRXN1* is a well-described Nrf2 target gene (Soriano et al. 2008), we investigated whether both the first and second induction of Srxn1-GFP expression depended on the Keap1/Nrf2 pathway using siRNA knockdown experiments. *siSRXN1* inhibited the induction of *SRXN1* during both the first and the second exposure to DEM and tBHQ (Figure 7A-B), indicating that our knockdown condition was effective. Since Keap1 targets Nrf2 for degradation, we anticipated that knockdown of *KEAP1* would enhance Nrf2 activity and promote Srxn1-GFP expression. Indeed, *siKEAP1* enhanced both the first and second induction of Srxn1-GFP by DEM and tBHQ (Figure 7A-B). Finally, knockdown of Nrf2 itself through



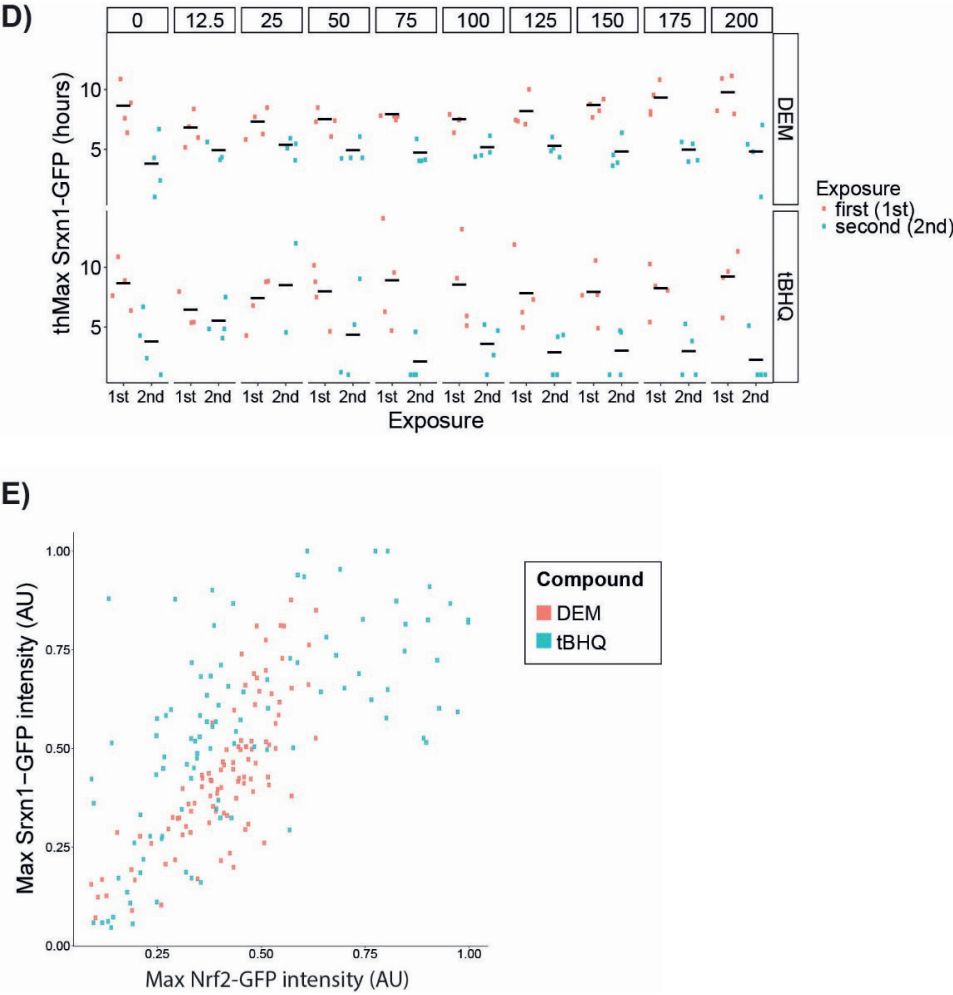


Figure 6. Quantitative analysis of Nrf2 and Srxn1 activation dynamics during first and second treatment periods.

A-B) The maximal values reached within 24 hours after the first or second exposure to DEM or tBHQ for Nrf2-GFP (A) and Srxn1-GFP (B). **C-D)** thMax after the first or second exposure to DEM or tBHQ for Nrf2-GFP (C) and Srxn1 (D). **E)** Comparison of the maximal Nrf2-GFP and Srxn1-GFP values reached within 24 hours after second exposure to DEM or tBHQ.

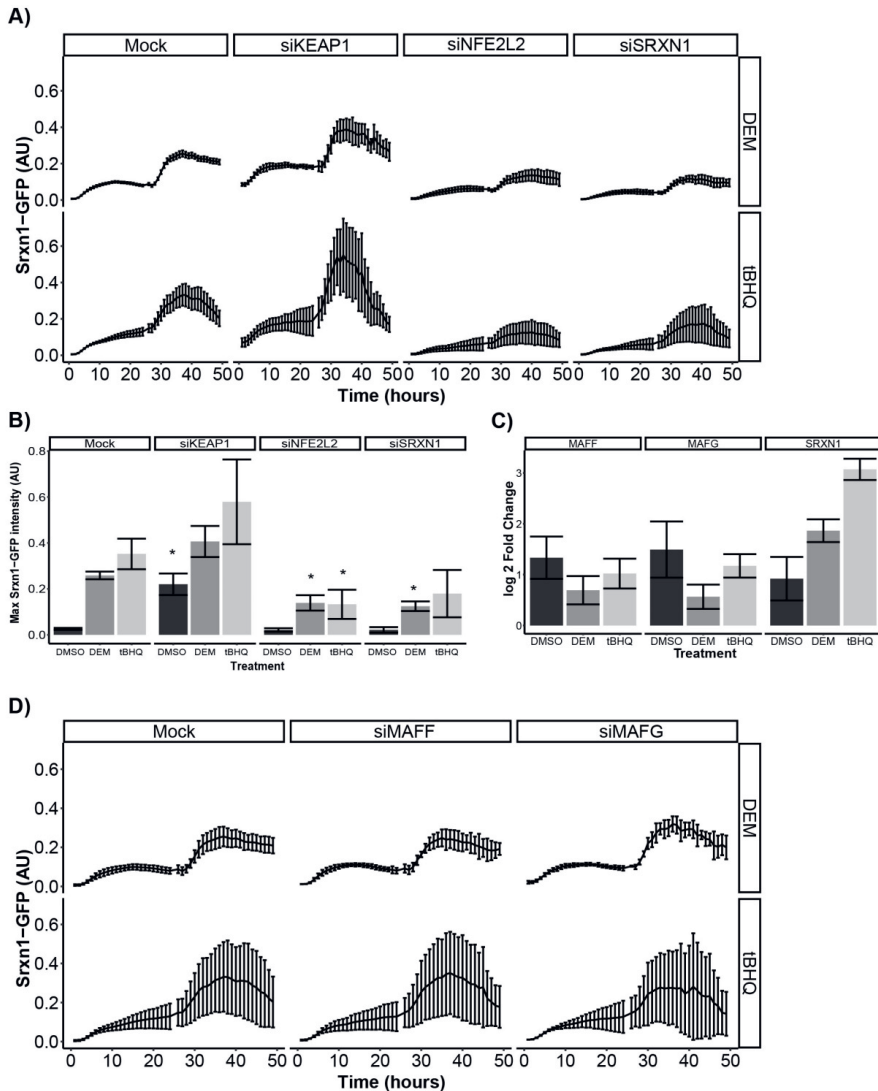


Figure 7. siRNA mediated knockdown of different Nrf2 pathway proteins.

A) Time response curves of Srnx1-GFP induction after treatment with DEM (100 μ M) or tBHQ (100 μ M) in mock condition or with siKEAP1, siNFE2L2 or siSRXN1. **B)** Maximal Srnx1-GFP intensity at 24 h after exposure to DMSO (0.1%), DEM (100 μ M) or tBHQ (100 μ M) and in mock condition or transfection with mock condition, siKEAP1, siNFE2L2 or siSRXN1. Significance is shown with a * based on a $p < 0.05$ comparing the same treatment in the mock condition, hypothesizing that the siKEAP1 knockdown gives a higher Srnx1-GFP intensity, while the other si-knockdowns have a lower Srnx1-GFP intensity compared to mock. **C)** Gene expression changes of MAFF, MAFG and SRXN1 vs baseline (i.e., medium sample just before treatment) 24 h after exposure to DMSO (0.1 %), DEM (100 μ M) or tBHQ (100 μ M). **D)** Time response curves of Srnx1-GFP induction after treatment with DEM (100 μ M) or tBHQ (100 μ M) in mock condition or with siMAFF or siMAFG. Results are in all cases based on $n=3$ experiments, with error bars depicting the SEM (A, B, D) or the lfcSE (C).

siNFE2L2 led to inhibition of *Srxn1* induction during first and second exposure (Figure 7A-B), demonstrating that the strong induction of *Srxn1* during the second response depends primarily on Nrf2.

MAF-transcription factors are co-activators of Nrf2 as well as downstream targets of Nrf2, offering a potential explanation for the increased *Srxn1* induction during repeated exposure. However, we did not observe an induction of either *MAFF* or *MAFG* gene expression at 24 h after the first treatment with DEM or tBHQ (Figure 7C). Moreover, knockdown of neither *MAFF* nor *MAFG* inhibited the induction of *Srxn1*-GFP during either the first or second exposure (Figure 7D), suggesting that MAFs do not provide an explanation for the enhanced *Srxn1* induction in the second exposure. Altogether, these data indicate a primary role for Nrf2 in the regulation of secondary *Srxn1* induction.

Enhancement of secondary *Srxn1* induction by other compounds including drugs that activate the Nrf2 pathway

Finally, we evaluated whether the enhanced secondary response was also observed for compounds where Nrf2 activation is related to the direct pharmacology or off-target effects. Specifically, we included bardoxolone methyl (CDDO-Me) (Cleasby et al. 2014; Wang et al. 2017), sulphoraphane (Alumkal et al. 2015; Lynch et al. 2017) and nitrofurantoin (Herpers et al. 2016; Tsuchiya et al. 2018), each of which activates the Nrf2 pathway at a different concentration range. Evaluation of *Srxn1*-GFP expression through imaging at 24 and 48 hours post exposure with CDDO-Me (250 nM), sulphoraphane (10 μ M) and nitrofurantoin (250 μ M) demonstrated that *Srxn1* was induced at 24 h, and that this induction was further enhanced by a second exposure from 24-48 h, similar as for exposure to DEM (Figure 8A and B). In contrast, a continuous single treatment with these drugs for 48 h did not lead to a similar high *Srxn1*-GFP level, except for CDDO-Me, which is likely due to the prolonged response this compound causes (Wink et al. 2017). These data indicate that the enhancement of *Srxn1* expression during a secondary Nrf2 response is in general relevant for drugs that can activate the Nrf2 pathway.

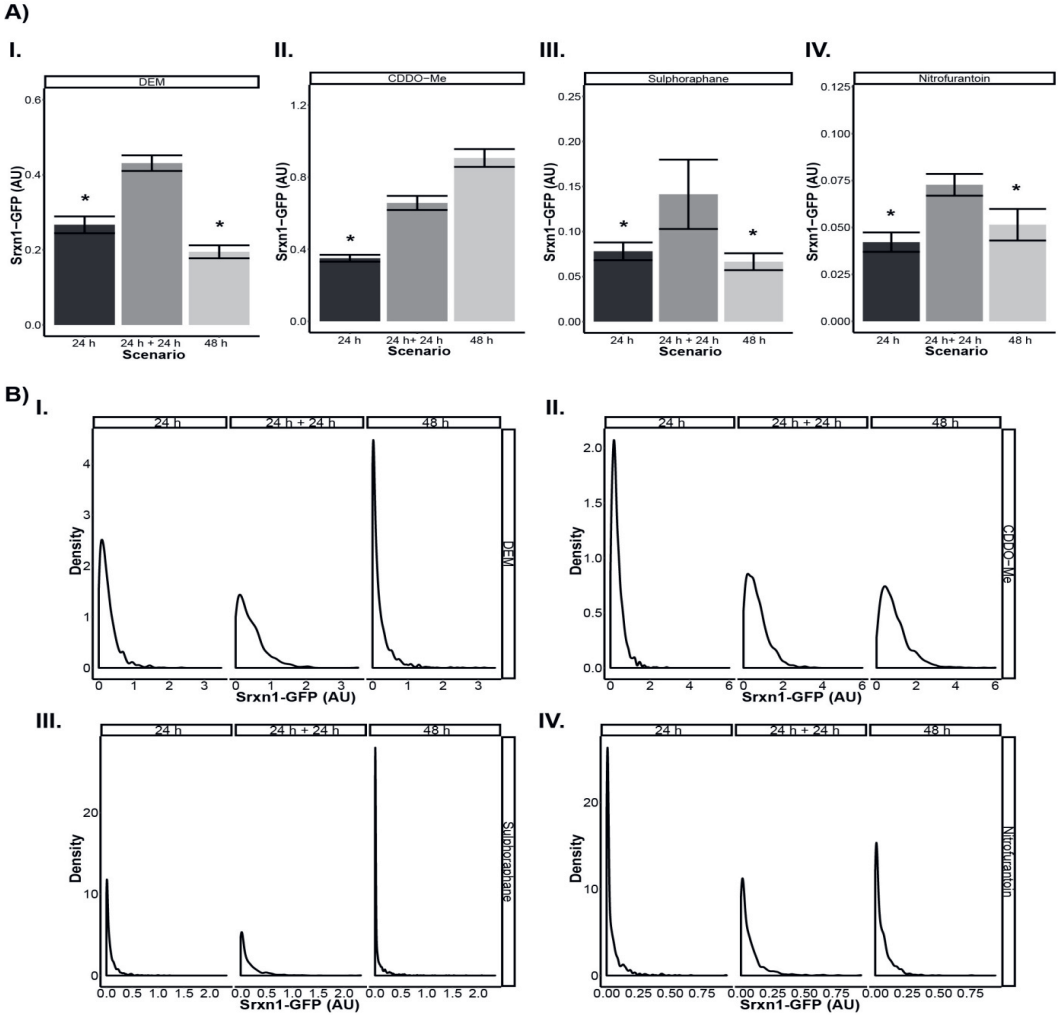


Figure 8. Srnx1 induction following repeated exposure to various drugs.

Srnx1-GFP reporter cells were exposed for either 24 h, or exposed for two time periods of 24 h, or for a single time period of 48 h to CDDO-Me (0.25 μ M), DEM (50 μ M), Nitrofurantoin (250 μ M), Sulphoraphane (10 μ M) or DMSO (0.1 %). **A)** Srnx1-GFP expression after chemical exposure. Significance is shown with a * based on a < 0.05 p value comparing 24 h exposure or 48 h exposure to the repeated 24 h exposure, hypothesizing that the repeated exposure has always the highest Srnx1-GFP intensity **B)** Population commitment to Srnx1 induction presented as density plot, plotted as fraction of cells (y-axis) expressing the Srnx1-GFP levels (x-axis). Shown is average data of $n=3$ experiments.

DISCUSSION

Our general understanding of the dynamics of cellular stress response pathway activation in repeated treatment scenarios is limited. Here, we systematically mapped the Nrf2 pathway adaptive response landscape of repeated exposure to two different soft electrophiles, DEM and tBHQ. We took advantage of two biologically relevant fluorescent HepG2 reporter cell lines that allowed us to monitor the activation of Nrf2 and its downstream target Srxn1 in individual cells over time using live cell confocal imaging. Our data indicate that cells adapted to oxidative stress: During a second treatment they have limited Nrf2 activation and a relatively short-lasting commitment, yet cells are primed to exhibit enhanced activation of Nrf2 downstream target Srxn1.

Our high throughput analysis of Nrf2-GFP and Srxn1-GFP activation for diverse concentrations demonstrated that there is a linear and compound-dependent relationship between the maximal amount of Nrf2 in the nucleus after single exposure and the subsequent maximal amount of Srxn1 in the cytoplasm. Single exposure to DEM and tBHQ resulted in a concentration-dependent activation of both Nrf2 and Srxn1, with slightly different dynamics for both compounds. The different dynamics observed, and the different correlation between Nrf2 and Srxn1 might be due to the different manners in which both compounds activate the Nrf2 pathway, involving both Keap1-dependent and -independent activation mechanisms (Bryan et al. 2013; Lee et al. 2001). Moreover, the half-life of DEM and tBHQ in the culture conditions may differ, offering a potential explanation for differential activation dynamics of Nrf2, although this does not explain why there is a different Nrf2 to Srxn1 ratio. The latter was in particular apparent for very high tBHQ concentrations.

For the first exposure, Nrf2-GFP reached hMax activation levels within 2 h, which was associated with an overall commitment to Nrf2 activation of >90 % of the cells. Interestingly, when a second exposure was initiated after 8 h both DEM and tBHQ could further promote Nrf2-GFP accumulation, despite the fact that the response had not yet returned to baseline. Apparently, the machinery to produce newly synthesized Nrf2-GFP was not yet at its maximum capacity, and/or there was still remaining Keap1 to be targeted by the electrophiles, further suppressing Nrf2 ubiquitination. Regardless, the increased amount of Nrf2-GFP did not equally enhance Srxn1 activation, as the amount of Srxn1-GFP hardly changed. Thus, adaptation to electrophiles takes longer than 8 h, which is relevant for the design of repeated dose scenarios in the context of pharmacological modulation of the Nrf2 pathway, yet also for toxicant exposure scenarios in daily life that may cause Nrf2 pathway activation.

Two main observations indicate that adaptation at the level of Nrf2-GFP activation occurs during long-term (24 h) repeated treatment scenarios. Firstly, the Nrf2-GFP nuclear accumulation was lower for the second treatment than for the first treatment. This effect was strongest when the same concentration was applied during the first and second treatment, but was also visible when the concentration of the second treatment was higher. Secondly, the overall time period that individual cells remained committed to Nrf2-GFP nuclear accumulation was shorter for the second treatment. This effect was observed both for DEM and tBHQ, although for tBHQ the overall commitment of the population after the second treatment did not reach the levels of the first exposure. The stabilization and nuclear accumulation of Nrf2 is known to reflect the activation of the oxidative stress sensing machinery (Kobayashi et al. 2006). Thus, if pro-oxidants affect the Cys residues of Keap1 more strongly, the degradation of Nrf2 is also more difficult. Because we observed less Nrf2-GFP in the nucleus and a shorter commitment period for cells in the second compared to the first exposure, this suggests a limited targeting of the sensing machinery. Hence, during the second exposure both DEM and tBHQ may be more rapidly detoxified by the action of downstream Nrf2 targets, including *Srxn1*.

The adaptation to both DEM and tBHQ resulted in an unanticipated further upregulation of *Srxn1*-GFP. Thus, despite the relatively low response of Nrf2 after the second treatment, *Srxn1*-GFP showed a three-fold increased induction. Given the critical role of *Srxn1* in the antioxidant response (Baek et al. 2012; Soriano et al. 2008; Zhou et al. 2015), we presume that this phenomenon is a critical component of an adaptation program that primes cells to subsequent exposures and improves protection against oxidative stress. The Keap1/Nrf2 interaction was the main component responsible for the enhanced secondary response, since knockdown of *NFE2L2* strongly inhibited this response and knockdown of *KEAP1* promoted it. Still, this enhanced response of *Srxn1*-GFP is likely not driven by Nrf2 alone, since the Nrf2-GFP nuclear activity was lower during the second exposure than during the first exposure. In our hands, knock-down of MAF-family transcriptional regulators *MAFF* and *MAFG* that can modulate Nrf2 transcriptional activity did not affect the enhanced *Srxn1* induction. We therefore anticipate that other factors are involved in the secondary response, that also themselves might be modulated as part of the primary response.

In the literature, some evidence has been presented for the accumulation of downstream targets of Nrf2 during repeated exposure. For example, Bergström et al. (2011) showed a daily accumulation of NQO1 mRNA and protein in astrocytes treated with 10 μ M sulphoraphane for 4 h per day over a time span of 4 days. Interestingly, they did not find the same for HMOX1, which only exhibited an increase after the first

exposure, but no further accumulation after repeated exposure. Similar conclusions with respect to NQO1 and HMOX1 were obtained by Mathew et al. (2014), who treated human fibroblasts with different concentrations of sulphoraphane for 4 h per day over a time span of 3 days. To what extent these effects are related to activity of Nrf2 and/or other factors remains unclear. Factors that govern Nrf2 activity itself may also be relevant for the observed priming effects at the level of Srxn1-GFP induction. This could be related to post-translational modification of Nrf2 through for example phosphorylation or acetylation (Huang et al. 2000; Sun et al. 2009) or through the induction of transcriptional co-regulators that act in concert with Nrf2 to target specific genes, including for example p21 (Chen et al. 2009; Katsuoka et al. 2005). Alternatively, given the role of Keap1 in modulating Nrf2 changes in the overall Keap1/Nrf2 interactome, modifications in this interactome may also effect Nrf2 activity. Keap1 is found as a homodimer associated with Cullin-3, which binds to the BTB (Bric a brac) domain of Keap1, and is anchored to the actin cytoskeleton (Wakabayashi et al. 2004). In addition, some proteins are able to bind to the free site at Keap1, like the p62 protein (Jiang et al. 2015), thereby competing with Nrf2 for this binding site. Because of such binding, the closed conformational state cannot be formed. Altered expression of proteins that interact with the Keap1/Nrf2 complex during the first treatment may have consequences for the complex activity during a second treatment phase. Further work is required to identify the priming factors that drive an enhanced secondary anti-oxidant response and whether this response would occur for other bona fide Nrf2 target genes as well.

We set out to improve our fundamental understanding of cellular responses to repeat dosing scenarios. Altogether, our results demonstrate that cells previously exposed to pro-oxidants exhibit an altered response pattern compared to 'naive' cells. Importantly, such responses are also observed for drug molecules that are currently used in the clinic and show a severe-DILI liability (nitrofurantoin) or are in clinical trials (CDDO-Me). This involves both suppression of the activity of the transcription factor Nrf2 and priming for an enhanced upregulation of anti-oxidant molecules. Our findings could imply that a 'memory' mechanism is in place within the Nrf2 pathway in which cells previously exposed to xenobiotics are better protected against similar future exposures. These results have implications for the comprehension and translation of stress response activation for chemical safety assessment in daily life and drug treatment situations which typically involve repeat dose exposure scenarios.

ACKNOWLEDGEMENTS

This work was supported by the Ministry of Defence of the Netherlands and the European Commission Horizon2020 EU-ToxRisk project (grant nr 681002).

REFERENCES

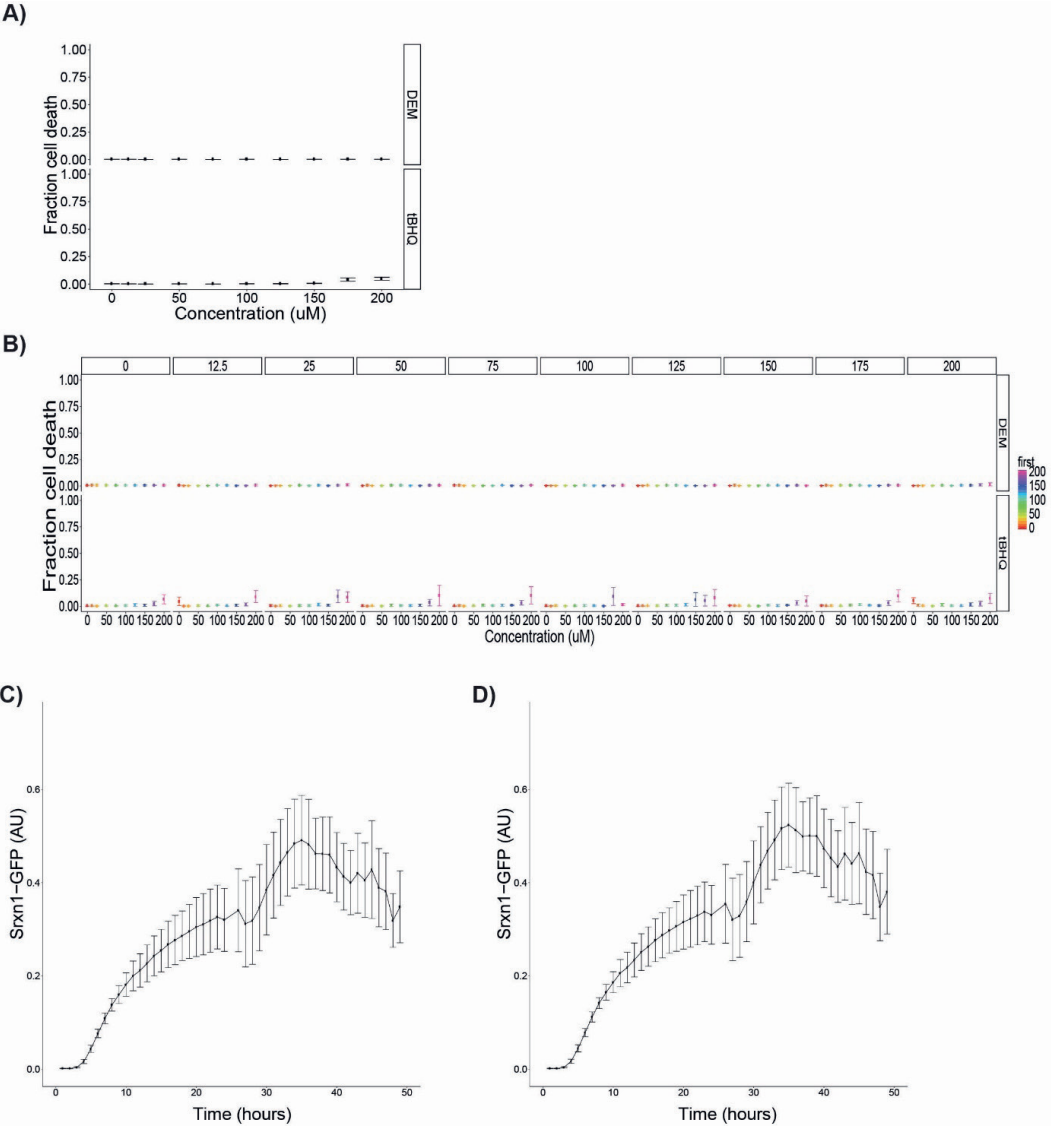
- Alumkal JJ, Slottke R, Schwartzman J, et al. (2015) A phase II study of sulforaphane-rich broccoli sprout extracts in men with recurrent prostate cancer. *Investigational New Drugs* 33(2):480-489 doi:10.1007/s10637-014-0189-z
- Baek JY, Han SH, Sung SH, et al. (2012) Sulfiredoxin protein is critical for redox balance and survival of cells exposed to low steady-state levels of H₂O₂. *J Biol Chem* 287(1):81-9 doi:10.1074/jbc.M111.316711
- Baird L, Dinkova-Kostova AT (2011) The cytoprotective role of the Keap1-Nrf2 pathway. *Arch Toxicol* 85(4):241-72 doi:10.1007/s00204-011-0674-5
- Baird L, Dinkova-Kostova AT (2013) Diffusion dynamics of the Keap1-Cullin3 interaction in single live cells. *Biochem Biophys Res Commun* 433(1):58-65 doi:10.1016/j.bbrc.2013.02.065
- Bergström P, Andersson HC, Gao Y, et al. (2011) Repeated transient sulforaphane stimulation in astrocytes leads to prolonged Nrf2-mediated gene expression and protection from superoxide-induced damage. *Neuropharmacology* 60(2-3):343-53 doi:10.1016/j.neuropharm.2010.09.023
- Bryan HK, Olayanju A, Goldring CE, Park BK (2013) The Nrf2 cell defence pathway: Keap1-dependent and -independent mechanisms of regulation. *Biochem Pharmacol* 85(6):705-17 doi:10.1016/j.bcp.2012.11.016
- Casey W, Anderson S, Fox T, Dold K, Colton H, Morgan K (2002) Transcriptional and physiological responses of HepG2 cells exposed to diethyl maleate: time course analysis. *Physiological genomics* 8(2):115-22 doi:10.1152/physiolgenomics.00064.2001
- Chang TS, Jeong W, Woo HA, Lee SM, Park S, Rhee SG (2004) Characterization of mammalian sulfiredoxin and its reactivation of hyperoxidized peroxiredoxin through reduction of cysteine sulfinic acid in the active site to cysteine. *J Biol Chem* 279(49):50994-1001 doi:10.1074/jbc.M409482200
- Chen W, Sun Z, Wang XJ, et al. (2009) Direct interaction between Nrf2 and p21(Cip1/WAF1) upregulates the Nrf2-mediated antioxidant response. *Mol Cell* 34(6):663-73 doi:10.1016/j.molcel.2009.04.029
- Cleasby A, Yon J, Day PJ, et al. (2014) Structure of the BTB domain of Keap1 and its interaction with the triterpenoid antagonist CDDO. *PLoS One* 9(6):e98896 doi:10.1371/journal.pone.0098896
- Danial NN, Korsmeyer SJ (2004) Cell death: critical control points. *Cell* 116(2):205-19
- Deshmukh P, Unni S, Krishnappa G, Padmanabhan B (2017) The Keap1–Nrf2 pathway: promising therapeutic target to counteract ROS-mediated damage in cancers and neurodegenerative diseases. *Biophysical Reviews* 9(1):41-56 doi:10.1007/s12551-016-0244-4
- Fulda S, Gorman AM, Hori O, Samali A (2010) Cellular stress responses: cell survival and cell death. *International journal of cell biology* 2010:214074 doi:10.1155/2010/214074
- Herpers B, Wink S, Fredriksson L, et al. (2016) Activation of the Nrf2 response by intrinsic hepatotoxic drugs correlates with suppression of NF- κ B activation and sensitizes toward TNF α -induced cytotoxicity. *Arch Toxicol* 90:1163-1179 doi:10.1007/s00204-015-1536-3
- Hiemstra S, Niemeijer M, Koedoot E, et al. (2017) Comprehensive Landscape of Nrf2 and p53 Pathway Activation Dynamics by Oxidative Stress and DNA Damage. *Chem Res Toxicol* 30(4):923-933 doi:10.1021/acs.chemrestox.6b00322
- Holland R, Fishbein JC (2010) Chemistry of the Cysteine Sensors in Kelch-Like ECH-Associated Protein 1. *Antioxidants & Redox Signaling* 13(11):1749-1761 doi:10.1089/ars.2010.3273
- Huang HC, Nguyen T, Pickett CB (2000) Regulation of the antioxidant response element by protein kinase C-mediated phosphorylation of NF-E2-related factor 2. *Proc Natl Acad Sci U S A* 97(23):12475-80 doi:10.1073/pnas.220418997

- Imhoff BR, Hansen JM (2010) Tert-butylhydroquinone induces mitochondrial oxidative stress causing Nrf2 activation. *Cell Biol Toxicol* 26(6):541-51 doi:10.1007/s10565-010-9162-6
- Itoh K, Chiba T, Takahashi S, et al. (1997) An Nrf2/small Maf heterodimer mediates the induction of phase II detoxifying enzyme genes through antioxidant response elements. *Biochem Biophys Res Commun* 236(2):313-22
- Jennings P, Limonciel A, Felice L, Leonard MO (2013) An overview of transcriptional regulation in response to toxicological insult. *Arch Toxicol* 87(1):49-72 doi:10.1007/s00204-012-0919-y
- Jiang T, Harder B, Rojo de la Vega M, Wong PK, Chapman E, Zhang DD (2015) p62 links autophagy and Nrf2 signaling. *Free Radic Biol Med* 88(Pt B):199-204 doi:10.1016/j.freeradbiomed.2015.06.014
- Kamentsky L, Jones TR, Fraser A, et al. (2011) Improved structure, function and compatibility for CellProfiler: modular high-throughput image analysis software. *Bioinformatics* 27(8):1179-80 doi:10.1093/bioinformatics/btr095
- Katsuoka F, Motohashi H, Engel JD, Yamamoto M (2005) Nrf2 transcriptionally activates the mafG gene through an antioxidant response element. *J Biol Chem* 280(6):4483-90 doi:10.1074/jbc.M411451200
- Kensler TW, Wakabayashi N, Biswal S (2007) Cell survival responses to environmental stresses via the Keap1-Nrf2-ARE pathway. *Annu Rev Pharmacol Toxicol* 47:89-116 doi:10.1146/annurev.pharmtox.46.120604.141046
- Keum YS, Choi BY (2014) Molecular and chemical regulation of the Keap1-Nrf2 signaling pathway. *Molecules* 19(7):10074-89 doi:10.3390/molecules190710074
- Keum YS, Han YH, Liew C, et al. (2006) Induction of heme oxygenase-1 (HO-1) and NAD[P]H: quinone oxidoreductase 1 (NQO1) by a phenolic antioxidant, butylated hydroxyanisole (BHA) and its metabolite, tert-butylhydroquinone (tBHQ) in primary-cultured human and rat hepatocytes. *Pharm Res* 23(11):2586-94 doi:10.1007/s11095-006-9094-2
- Kobayashi A, Kang MI, Okawa H, et al. (2004) Oxidative stress sensor Keap1 functions as an adaptor for Cul3-based E3 ligase to regulate proteasomal degradation of Nrf2. *Mol Cell Biol* 24(16):7130-9 doi:10.1128/MCB.24.16.7130-7139.2004
- Kobayashi A, Kang MI, Watai Y, et al. (2006) Oxidative and electrophilic stresses activate Nrf2 through inhibition of ubiquitination activity of Keap1. *Mol Cell Biol* 26(1):221-9 doi:10.1128/MCB.26.1.221-229.2006
- Kobayashi M, Li L, Iwamoto N, et al. (2009) The antioxidant defense system Keap1-Nrf2 comprises a multiple sensing mechanism for responding to a wide range of chemical compounds. *Mol Cell Biol* 29(2):493-502 doi:10.1128/MCB.01080-08
- Lee JM, Moehlenkamp JD, Hanson JM, Johnson JA (2001) Nrf2-dependent activation of the antioxidant responsive element by tert-butylhydroquinone is independent of oxidative stress in IMR-32 human neuroblastoma cells. *Biochem Biophys Res Commun* 280(1):286-92 doi:10.1006/bbrc.2000.4106
- Lynch R, Diggins EL, Connors SL, et al. (2017) Sulforaphane from Broccoli Reduces Symptoms of Autism: A Follow-up Case Series from a Randomized Double-blind Study. *Global Advances in Health and Medicine* 6:2164957X17735826 doi:10.1177/2164957X17735826
- Ma Q (2013) Role of nrf2 in oxidative stress and toxicity. *Annu Rev Pharmacol Toxicol* 53:401-26 doi:10.1146/annurev-pharmtox-011112-140320
- Mathew ST, Bergström P, Hammarsten O (2014) Repeated Nrf2 stimulation using sulforaphane protects fibroblasts from ionizing radiation. *Toxicol Appl Pharmacol* 276(3):188-94 doi:10.1016/j.taap.2014.02.013

- Meakin PJ, Chowdhry S, Sharma RS, et al. (2014) Susceptibility of Nrf2-null mice to steatohepatitis and cirrhosis upon consumption of a high-fat diet is associated with oxidative stress, perturbation of the unfolded protein response, and disturbance in the expression of metabolic enzymes but not with insulin resistance. *Mol Cell Biol* 34(17):3305-20 doi:10.1128/MCB.00677-14
- Poser I, Sarov M, Hutchins JR, et al. (2008) BAC TransgeneOmics: a high-throughput method for exploration of protein function in mammals. *Nat Methods* 5(5):409-15 doi:10.1038/nmeth.1199
- Priya S, Nigam A, Bajpai P, Kumar S (2014) Diethyl maleate inhibits MCA+TPA transformed cell growth via modulation of GSH, MAPK, and cancer pathways. *Chem Biol Interact* 219:37-47 doi:10.1016/j.cbi.2014.04.018
- Ryter SW, Kim HP, Hoetzel A, et al. (2007) Mechanisms of cell death in oxidative stress. *Antioxid Redox Signal* 9(1):49-89 doi:10.1089/ars.2007.9.49
- Soriano FX, Léveillé F, Papadia S, et al. (2008) Induction of sulfiredoxin expression and reduction of peroxiredoxin hyperoxidation by the neuroprotective Nrf2 activator 3H-1,2-dithiole-3-thione. *Journal of neurochemistry* 107(2):533-43 doi:10.1111/j.1471-4159.2008.05648.x
- Souza TM, Kleinjans JCS, Jennen DGJ (2017) Dose and Time Dependencies in Stress Pathway Responses during Chemical Exposure: Novel Insights from Gene Regulatory Networks. *Front Genet* 8:142 doi:10.3389/fgene.2017.00142
- Sun Z, Chin YE, Zhang DD (2009) Acetylation of Nrf2 by p300/CBP augments promoter-specific DNA binding of Nrf2 during the antioxidant response. *Mol Cell Biol* 29(10):2658-72 doi:10.1128/mcb.01639-08
- Tsuchiya T, Kijima A, Ishii Y, et al. (2018) Role of oxidative stress in the chemical structure-related genotoxicity of nitrofurantoin in Nrf2-deficient gpt delta mice. *Journal of Toxicologic Pathology* 31(3):169-178 doi:10.1293/tox.2018-0014
- Vomund S, Schafer A, Parnham MJ, Brune B, von Knethen A (2017) Nrf2, the Master Regulator of Anti-Oxidative Responses. *Int J Mol Sci* 18(12) doi:10.3390/ijms18122772
- Wakabayashi N, Dinkova-Kostova AT, Holtzclaw WD, et al. (2004) Protection against electrophile and oxidant stress by induction of the phase 2 response: Fate of cysteines of the Keap1 sensor modified by inducers. *Proc Natl Acad Sci U S A* 101(7):2040-2045 doi:10.1073/pnas.0307301101
- Wang X-Y, Zhang X-H, Peng L, et al. (2017) Bardoxolone methyl (CDDO-Me or RTA402) induces cell cycle arrest, apoptosis and autophagy via PI3K/Akt/mTOR and p38 MAPK/Erk1/2 signaling pathways in K562 cells. *American Journal of Translational Research* 9(10):4652-4672
- Wink S, Hiemstra S, Herpers B, van de Water B (2017) High-content imaging-based BAC-GFP toxicity pathway reporters to assess chemical adversity liabilities. *Arch Toxicol* 91(3):1367-1383 doi:10.1007/s00204-016-1781-0
- Wink S, Hiemstra SW, Huppelschoten S, Klip JE, van de Water B (2018) Dynamic imaging of adaptive stress response pathway activation for prediction of drug induced liver injury. *Arch Toxicol* doi:10.1007/s00204-018-2178-z
- Wu KC, Cui JY, Klaassen CD (2012) Effect of graded Nrf2 activation on phase-I and -II drug metabolizing enzymes and transporters in mouse liver. *PLoS One* 7(7):e39006 doi:10.1371/journal.pone.0039006
- Yamauchi S, Kiyosawa N, Ando Y, et al. (2011) Hepatic transcriptome and proteome responses against diethyl maleate-induced glutathione depletion in the rat. *Arch Toxicol* 85(9):1045-56 doi:10.1007/s00204-010-0632-7
- Yan K, Verbeek FJ Segmentation for High-Throughput Image Analysis: Watershed Masked Clustering. In, Berlin, Heidelberg, 2012. Leveraging Applications of Formal Methods, Verification and Validation. Applications and Case Studies. Springer Berlin Heidelberg, p 25-41

- Yeakley JM, Shepard PJ, Goyena DE, VanSteenhouse HC, McComb JD, Seligmann BE (2017) A trichostatin A expression signature identified by TempO-Seq targeted whole transcriptome profiling. *PLoS One* 12(5):e0178302-e0178302 doi:10.1371/journal.pone.0178302
- Zhang DD, Lo SC, Cross JV, Templeton DJ, Hannink M (2004) Keap1 is a redox-regulated substrate adaptor protein for a Cul3-dependent ubiquitin ligase complex. *Mol Cell Biol* 24(24):10941-53 doi:10.1128/MCB.24.24.10941-10953.2004
- Zhou Y, Duan S, Zhou Y, et al. (2015) Sulfiredoxin-1 attenuates oxidative stress via Nrf2/ARE pathway and 2-Cys Prdxs after oxygen-glucose deprivation in astrocytes. *J Mol Neurosci* 55(4):941-50 doi:10.1007/s12031-014-0449-6
- Zipper LM, Mulcahy RT (2002) The Keap1 BTB/POZ dimerization function is required to sequester Nrf2 in cytoplasm. *J Biol Chem* 277(39):36544-52 doi:10.1074/jbc.M206530200

SUPPLEMENTAL MATERIALS



Supplementary figure 1. Cell death caused by DEM and tBHQ does not impact GFP responses.

A-B) Fraction of cells that exhibited a nuclear PI intensity above background levels, representing cell death; data shown are from the Srxn1-GFP cell line after treatment with tBHQ or DEM during single exposure (A; measured at 24 h) or repeated exposure (B; measured at 48 h). **C-D)** The dynamic response of Srxn1-GFP exposed to 100 μM of tBHQ at time point 0 h and re-exposed at 24 h. The response is either calculated as the average of all cells in the well (i.e. alive and dead cells) (C) or as the average of only the alive cells (D). Cells are considered alive when they have a PI intensity below background levels in their nuclei. Error bars indicate the SEM (n=4)

5

A systematic high throughput transcriptomics and phenotypic screening approach to classify the pro-oxidant mode-of-action of a large class of phenolic compounds

Luc J.M. Bischoff^{1,4}, Johannes P. Schimming^{1,4}, Wanda van der Stel¹, Marije Niemeijer¹, Sylvia Escher³, Giulia Callegaro¹, Bas ter Braak¹, Jan P. Langenberg², Daan Noort², Bob van de Water¹

¹Division of Drug Discovery and Safety, Leiden Academic Centre for Drug Research, Leiden University, Leiden, The Netherlands

²Department of CBRN Protection, TNO Defence, Safety and Security, Rijswijk, The Netherlands

³Department of Chemical Safety and Toxicology, Fraunhofer Institute for Toxicology and Experimental Medicine, ITEM, Hannover, Germany.

⁴Authors contributed equally to this work

Manuscript in preparation

ABSTRACT

Oxidative stress is an important key event in many disease pathologies like cancer, Alzheimer's disease and liver diseases. Since many chemical substances can induce oxidative stress, characterizing the possibility and potency of chemicals to induce oxidative stress is of great importance for safety assessment. To evaluate the potential of oxidative stress we examined the induction of the Nrf2 response pathway for a biological read across of a diverse panel of 20 phenolic compounds including redox cyclers, non-redox cyclers, and alkylated phenols. We integrated high throughput transcriptomics using targeted RNA sequencing of primary human hepatocytes (PHH) and HepG2 and HepG2 Nrf2-GFP and Srxn1-GFP reporter cell lines. Using a panel of five pro-oxidants, including CDDO-Me, sulforaphane, *tert*-butylhydroperoxide, etacrynic acid and diethyl maleate, we identified a panel of five Nrf2 target genes that could define oxidative stress potential: *AKR1B10*, *SRXN1*, *ABCC2*, *AKR1C3* and *NQO1*. These five genes could discriminate between alkylated, redox-cyclers, and non-redox-cyclers, with strong activation of *AKR1B10* and *SRXN1* at low concentrations of redox-cyclers, and little to no activation for the alkylated phenols and non-redox-cyclers in PHH and HepG2 cells, with PHH being more vulnerable for these compounds. Subsequent high throughput confocal microscopy Nrf2 pathway activation analysis demonstrated that in particular redox-cycling phenols caused an early onset concentration-dependent activation and nuclear accumulation of the Nrf2-GFP reporter activity and subsequent induction of Srxn1-GFP. The Srxn1-GFP response and the *SRXN1* gene expression pattern were highly correlated for all phenols. In conclusion, our study demonstrates the utility to integrate both high throughput transcriptomics data from selected Nrf2 target genes with temporal response data from Nrf2 pathway GFP reporters to quantify oxidative stress induction and qualify mode-of-action of a large panel of structural similar compounds. The combination of test systems and assays might provide an innovative NAM (new approach methodology) approach for the rapid assessment of oxidative stress response to support read across-based chemical safety testing.

INTRODUCTION

Toxicity testing aims to unravel the potency of a chemical, at a certain concentration in a certain time-span to induce an adverse outcome effect. Currently, new approach methodologies (NAMs) are designed to test chemicals, including drugs, in a high throughput manner, as there is a global aim to search for alternatives to animal tests. NAMs include *in vitro* and *in chemico* assays, as well as *in silico* approaches (ECHA, 2016) and are aimed to support regulatory decisions for the use of chemicals. In particular the application of NAMs in read across has been advocated. Furthermore, the use of NAMs will improve our knowledge of the toxicokinetic and toxicodynamic properties of chemicals, making NAMs useful tools to provide input for read-across studies (Escher et al. 2019; Graepel et al. 2019; Parish et al. 2020). The rapid development and broad use of NAMs, including high throughput test systems and the use of integrated approaches e.g. combining *in vitro* and *in silico* models, has led to an increased role and understanding of stress response pathways (toxicity pathways) in modern toxicity testing (Benfenati et al. 2019; Perkins et al. 2019; Wambaugh et al. 2019). As these pathways play an important role in the response to xenobiotic exposure, cellular damage and disease, knowledge of these pathways is of great importance in the development of NAMs for the early detection of toxicity and therefore safety assessment in general. Here we addressed the question whether specific toxicity pathway testing can be applied for read across evaluation based on biological similarity. We focused here on the assessment of NAMs for the assessment of the toxicodynamics of a diverse group of phenolic compounds with a focus on the Nrf2 antioxidant stress signaling pathway named after the transcription factor nuclear factor erythroid 2-related factor 2 (Nrf2), which is the gene product of *NFE2L2*.

Under basal conditions, Nrf2 is bound in the cytoplasm to two Kelch-like ECH-associated protein 1 (Keap1) proteins (Keum and Choi 2014; Zipper and Mulcahy 2002), ubiquitinated and degraded via the ubiquitin-26S proteasomal pathway (Kobayashi et al. 2004). Upon activation by oxidative stress, caused by reactive oxygen species or electrophilic compounds (Figure 1A and 1B) (Takaya et al. 2012), degradation via the ubiquitin-26S proteasomal pathway is prevented and newly produced Nrf2 proteins are now able to translocate to the nucleus. In the nucleus, Nrf2 will bind to the antioxidant response element (ARE), which in turn will lead to the expression of a battery of antioxidant response genes including amongst others sulfiredoxin1 (Srxn1) (Copple et al. 2019; Figure 1B). Srxn1 was first discovered in yeast (Biteau et al. 2003) but is known to be present in all eukaryotes. Srxn1 plays a role in the reduction of oxidized peroxiredoxin and reversal of glutathionylation (Findlay et al. 2006; Jeong et al. 2006). Since endogenous levels of Srxn1 are relatively

low, but are strongly induced by Nrf2 activation, *Srxn1* is an excellent biomarker to determine the potency and dynamics of Nrf2 activation in liver hepatocytes (Bischoff et al. 2019; Wink et al. 2018). Yet other transcriptomic biomarkers are also considered strongly indicative for Nrf2 activation (Copple et al. 2019).

A class of widely used chemical compounds, known to activate the Nrf2 pathway are phenolic compounds (phenols/quinones). In daily life, humans are exposed to phenols/quinones via diet, medicine intake, or environmental chemicals (Kyselova 2011). Despite the fact that these compounds might be beneficial due to their antioxidant properties, they are also related to hepatotoxicity (Kyselova 2011). Quinones are Michael acceptors and are able to covalently bind to cellular nucleophiles such as glutathione (GSH), resulting in depletion of GSH (Attia 2010; Bolton and Dunlap 2017). Quinones can be enzymatically reduced to hydroquinones (two electron reduction) or to semiquinones (one electron reduction) (Monks et al. 1992). Two major toxicity mechanisms are described in literature concerning quinones: ROS formation and arylation/alkylation (Xiong et al. 2014) as displayed in Figure 1C. The redox potential of a quinone is influenced by substituent effects, with addition of an electronegative substitute usually leading to a much stronger oxidant (Monks and Lau 1997). A broad overview of quinone toxicity has been published before (Bolton et al. 2000). The application of high throughput NAMs to classify the mode-of-action as well as the potency of different phenolic compounds has so far not been evaluated.

Here we used a large panel of phenols to characterize their redox-cycling-mediated oxidative stress potential. As NAMs we used high throughput transcriptomics approaches and evaluated the effects of these phenols on oxidative stress pathway activation in primary human hepatocytes as well as HepG2 hepatocarcinoma cells. Moreover, we used our established HepG2-Nrf2-GFP and HepG2-Srxn1-GFP phenotypic reporter system in combination with live cell imaging (Wink et al. 2017) to define the dynamics and potency of phenol-mediated Nrf2 pathway activation.

METHODS

Chemicals

A phenolic compound set was used which consisted of three different classes of phenolic compounds (Figure 1D): 6 hydroquinone like compounds with anticipated redox-cycling potential (redox cyclers); 12 phenolic compounds with alkyl side chain without anticipated redox-cycling potential (alkylated phenols), 2 non-alkylated and redox-cycling negative (non-redox cyclers). Chemicals were purchased from Sigma

Figure 1. Phenol toxicity mechanisms.

A)

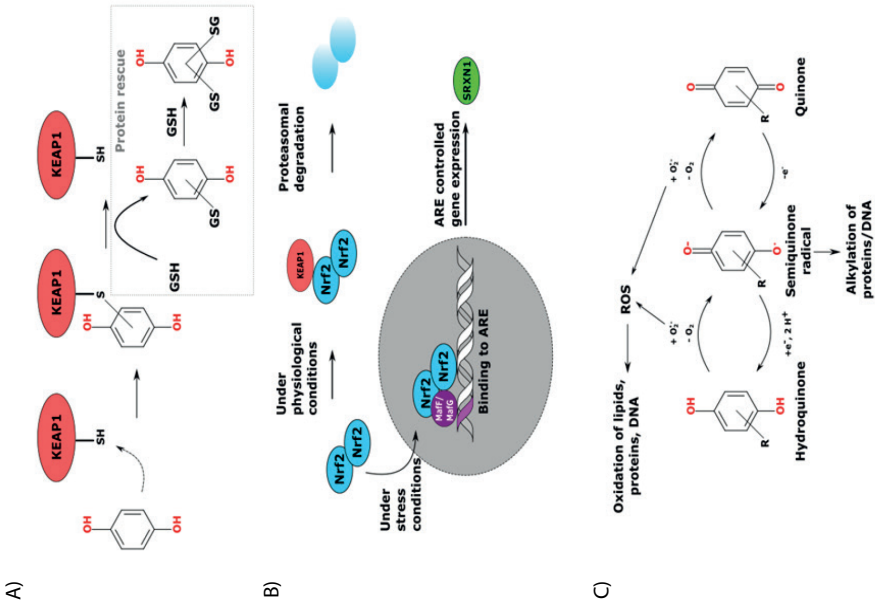
A) Modulation of Keap1 by phenols. **B)** Nrf2 pathway activation and downstream target activation. **C)** Radical formation of phenols. **D)** Chemical structures of the three different classes of phenolic compounds used in this study.

D)

Catechol Cas nr.: 120-80-9	Hydroquinone Cas nr.: 123-31-9	Menadione Cas nr.: 58-27-5
tert-Buthydroquinone Cas nr.: 1948-33-0	Tetramethyl-p-phenylenediamine Cas nr.: 637-01-4	Trimethylbenzene-1,4-diol Cas nr.: 700-13-0

Phenol Cas nr.: 108-95-2	Resorcinol Cas nr.: 108-46-3
------------------------------------	--

2,4-Dimethylphenol Cas nr.: 88-18-6	2,4-Di-tert-butylphenol Cas nr.: 96-76-4
2,3,5-Trimethylphenol Cas nr.: 697-82-5	2,6-Dimethylphenol Cas nr.: 576-26-1
2,6-Di-tert-butyl-4-ethylphenol Cas nr.: 4130-42-1	2,6-Di-tert-butylphenol Cas nr.: 128-39-2
4-Methylphenol Cas nr.: 106-44-5	p-tert-Buylphenol Cas nr.: 98-54-4



Aldrich (Amsterdam, Netherlands), or from TCI (Rotterdam, Netherlands). Upon arrival chemicals were diluted in DMSO (Sigma Aldrich (USA)) to stock concentrations of 500 mM, except for catechol, hydroquinone, resorcinol, phenol, diquat bromide monohydrate and TMPPD which were diluted in PBS to stock concentrations of 50 mM. All stocks were aliquoted and stored at -20 °C for experimental use. Concentration ranges of the compounds used for experiments were derived from literature and pilot experiments with HepG2 cells.

Cell culture

Primary human hepatocytes (PHH) and the human hepatoma cell line HepG2 were used for gene expression analysis. Cryopreserved PHH cells (LiverPool, 10 donor, #X008001 Lot: KCB, BioIVT) were thawed in OptiThaw Hepatocyte medium (Sekisui XenoTech, #K8000) and subsequently seeded at a density of 70,000 cells per well (0.32 cm^2) plating medium in INVITROGRO CP Medium (BioIVT, #Z99029) on Corning BioCoat collagen I coated 96-well plates (Corning, #08-774-5). 6 h after seeding the plating medium was exchanged with maintenance InVitroGro Hi Medium (BioIVT, #Z99029). 24 h after seeding the PHHs were exposed to the test compounds in InVitroGro Hi Medium.

HepG2 cells (ATCC, Wesel, Germany, clone HB8065) were grown in Dulbecco's Modified Eagle Medium (DMEM, GIBCO, #41966-029) high glucose, supplemented with 10 % (v/v) fetal bovine serum (FBS, GIBCO, #10270-106), 25 U/mL penicillin and 25 µg streptomycin (Pen Strep, GIBCO, #15070-063). For fluorescent protein reporter activity analysis we used HepG2-Srxn1-GFP and HepG2-Nrf2-GFP. These fluorescent protein reporter cell lines are bacterial artificial chromosomes (BAC)-based and developed and characterized previously (Wink et al. 2017). HepG2 cells were used for experiments until passage 20. Cells were seeded in a 96-well plate (23.000 cells/well, Greiner Bio One, #655090) for transcriptomic analysis, and exposed 72 h after plating. For GFP reporter measurement, cells were seeded in a 384-well plate (8.000 cells/well, Greiner Bio One, #781091) and exposed to the compounds 48 h after plating.

TempO-Seq assay

For transcriptome analysis, 24 h after treatment the cells were washed with PBS and lysed with 1X BioSpyder Lysis Buffer (BioSpyder, #P/N N041L). The lysate was stored in v-bottom plates on -80 °C until shipment on dry ice to BioClavis (UK) for TempO-Seq analysis. The TempO-Seq assay is a template oligonucleotide annealing and ligation assay combined with a sequencing readout for high-throughput targeted RNAseq transcriptomics (Yeakley et al. 2017). We used this technology to measure gene expression patterns after compound exposure in HepG2-WT cells and PHHs.

Therefore the cells were seeded and allowed to attach for 24 h before exposure to the test compounds. After 24h of treatment, wells were washed with 200 μ L PBS and lysed with 50 μ L BioSpyder 1x lysis buffer for 5 minutes at ambient temperature (20 to 24 $^{\circ}$ C). Lysate plates were sealed and immediately frozen at -80 $^{\circ}$ C. The lysate plates were shipped on dry ice to BioClavis for TempO-Seq analysis using the EU-ToxRisk S1500+ v2 gene set, an extension of the S1500+ gene set developed by the US NIEHS-National Toxicology Program. Briefly, a set of genes were identified on the basis of their diversity, co-expression and pathway coverage as found in publicly available transcriptomic data sets. Combined with the nominated genes by a Tox21 expert panel, this formed the S1500 gene set (Mav et al. 2018). Next, the gene set was used to extrapolate the whole transcriptome and genes were added to reach optimal performance resulting in the S1500+ gene set (Bushel et al. 2018). An additional group of genes was added by experts of the EU-ToxRisk consortium to meet scientific application for the project resulting in the EU-ToxRisk S1500+ v2 gene set (Daneshian et al. 2016). To cover this gene set of 3257 genes, 3561 different TempO-Seq probes were used.

Nrf2 gene set

To acquire a liver specific gene set regulated by the Nrf2 pathway, we overlapped the EU-ToxRisk S1500+ v2 gene set with the experimentally derived Nrf2 target gene list of human liver hepatocytes (Copple et al. 2019). The latter gene list is based on a siRNA knockdown (KD) screen of primary human hepatocytes with siKEAP1 and siNFE2L2 whole transcriptome analysis. All genes identified showed a significant upregulation under siKEAP1 KD and a significant downregulation under siNFE2L2 KD as compared to a scrambled siRNA control resulting in a list of 108 genes of which 36 overlap with the EU-ToxRisk S1500+ v2 gene set. The overlapping gene list is annexed in Suppl. Table 1.

Live confocal imaging

Fluorescent protein reporter activity was determined by live cell confocal imaging using a Nikon Eclipse Ti confocal microscope equipped with four lasers: 366, 408, 488 and 561 nm. A 20x dry PlanApo VC NA 0.75 with 1x zoom was used. Prior to exposure, Hoechst₃₃₃₄₂ 100 ng/mL was added to the wells to stain nuclei and propidium iodide (PI) was added to measure cell death. Images were taken on specific time points or for a period of 24 h (1 image per hour).

Transcriptomics and imaging data analysis

The differentially expressed genes (padj <0.05) were identified by the DESeq2 method (Love et al. 2014) using the therein described R package DESeq2. The cutoff for sample exclusion was a total count of 100,000. The dose response modelling was

conducted in BMDExpress version 2.2 (Phillips et al. 2018). For the identification of a dose response, BMDExpress fitted several different curves following continuous functions towards the fold change dose response of every probe. Specifically, a linear function, exponential functions of the order 2, 3, 4 and 5, polynomial functions of second degree, hill model functions and power model functions. For each probe and function type maximal 250 iterations were done and as a cutoff for the benchmark response one standard deviation above or below baseline (confidence interval of 0.95).

Microscopy images were analyzed at the single cell level using Cell Profiler and R as previously described (Schimming et al. 2019). The fraction of GFP-positive cells were calculated by counting the amount of cells with a GFP-value two times above baseline (DMSO control) level.

RESULTS

Determination of the liver specific oxidative stress response gene panel

We firstly systematically identified the relevant oxidative stress response genes that are represented in the targeted EU-ToxRisk S1500+ V2 TempO-Seq gene panel. As a first step we treated HepG2 cells with five different well known Nrf2 pathway inducing compounds: bardoxolone methyl (CDDO-Me), diethyl maleate (DEM), *tert*-butylhydroperoxide (tBHP), etacrynic acid and sulforaphane. For each of these compounds the number of significantly ($\text{padj} < 0.05$) up- and down-regulated genes in the EU-ToxRisk S1500+ v2 gene panel was calculated after exposing HepG2 cells to different concentrations for 24 hours. We observed an increased number of differentially expressed genes with exposure to an increasing concentration of all five pro-oxidants (Figure 2A). For DEM and etacrynic acid the number of differentially expressed genes is lower after exposure to the highest concentrations, which is likely due to onset of cell death at these high concentration. Next, we investigated the effect on genes related to the Nrf2 oxidative stress response pathway. We selected a set of 36 genes that are affected by *KEAP1* and *NFE2L2* knockdown in primary human hepatocytes and are in overlap with our targeted gene panel (Copple et al. 2019). For the entire gene set we rank ordered the absolute maximum expression changes after compound exposure across all concentrations, and projected the 36 Nrf2-related genes in red ($\text{padj} < 0.05$) (Figure 2B). We observed that two of the Nrf2 target genes, *AKR1B10* and *SRXN1*, demonstrated the strongest activation for all five compounds and were consistently the two most responsive genes of the 36-gene set. Other Nrf2 target genes did not show any apparent different pattern from other

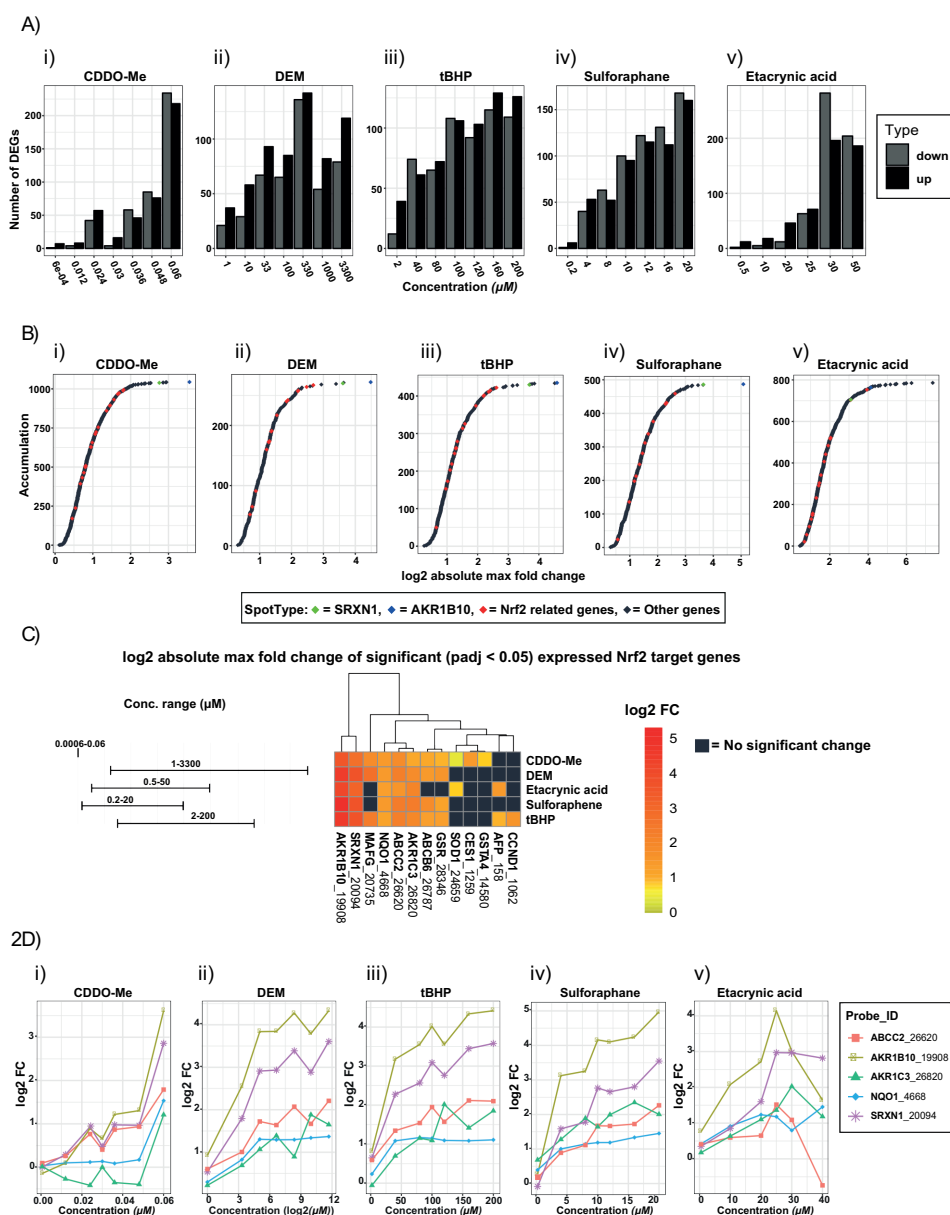


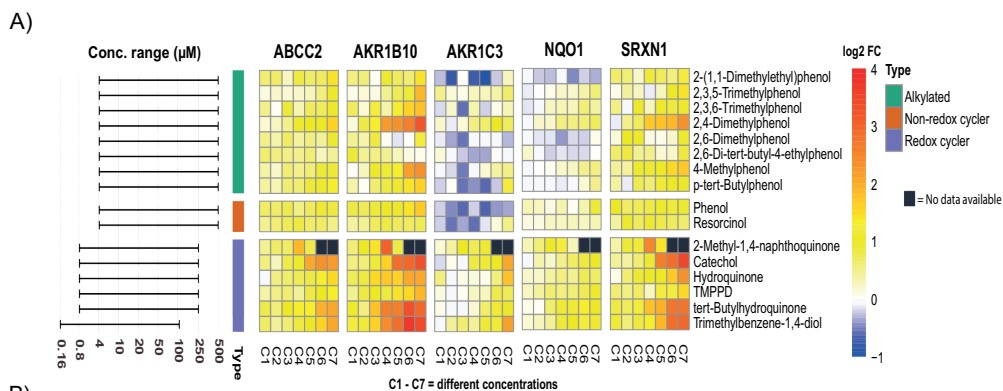
Figure 2. Gene expression response upon treatment with the selected positive controls.

A) Number of significant ($\text{padj} < 0.05$) differently expressed genes (up/down regulated) at different compound concentrations. **B)** Accumulation plots of the significant ($\text{padj} < 0.05$) expressed genes ranked to the \log_2 absolute maximal fold change. Green = SRXN1, blue is AKR1B10, red = selected Nrf2 related genes, and black = other significant expressed genes after exposure to the different positive controls. **C)** Heatmap of the maximal \log_2 FC of significant ($\text{padj} < 0.05$) expressed Nrf2 related genes (gene_probe combination). Column clustering is based on Euclidean method. **D)** Dose-response (\log_2 FC) curves of the positive controls for the five highest significantly ($\text{padj} < 0.05$) differentially expressed Nrf2 related genes after exposure to the different positive controls.

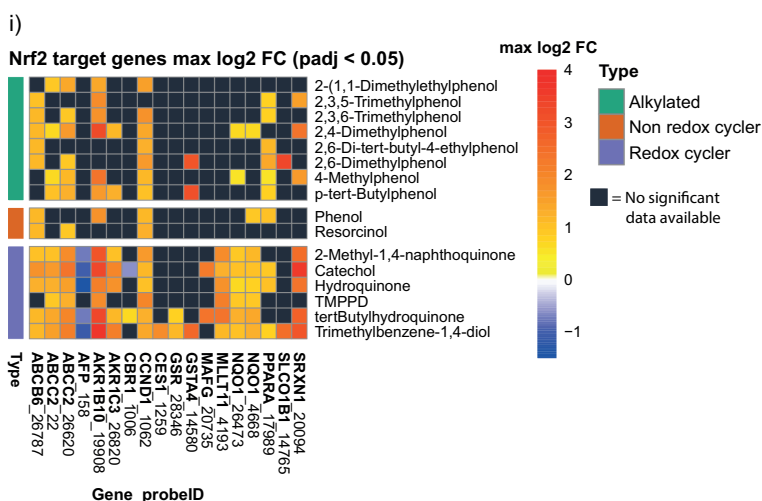
differentially expressed genes. It should be noted that the concentration at which the maximal fold change was reached is not taken into account as we only looked at the maximum fold change that could be reached over the entire concentration range. As a next step, we wondered which of the Nrf2 target genes were significantly ($p_{adj} < 0.05$) differently expressed (\log_2 FC) after exposure to the five different pro-oxidants. We found 13 of the 36 Nrf2 target genes to be significantly differently expressed by at least one compound across the full concentration range. The highest fold changes across all five compounds were found for *AKR1B10* and *SRXN1*, followed by *ABCC2*, *AKR1C3* and *NQO1* (Figure 2C). All of these five Nrf2 target genes showed a concentration dependent induction, with *AKR1B10* and *SRXN1* being the most sensitive across the entire concentration range (Figure 2D). These data indicate that this selective panel of five Nrf2 target genes is a good representative for pro-oxidant Nrf2 activation in HepG2 cells.

Nrf2 target gene expression patterns in HepG2 cells and primary human hepatocytes after exposure to the different phenolic compounds

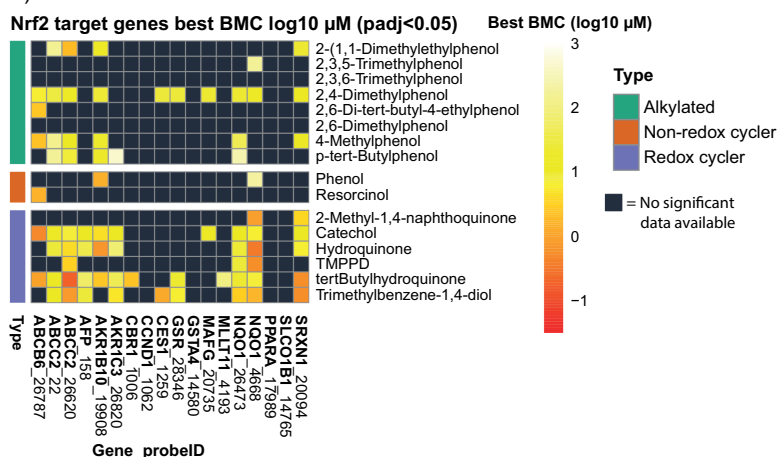
Next, we investigated the potency of activation of the Nrf2 pathway of the different phenolic compounds belonging to one of the three different groups: redox cyclers, non-redox cyclers, and alkylated phenols. We first focused on activation of the five selected Nrf2 target genes (Figure 3A). In general, we found higher activation of these genes after exposure to the redox cyclers, with trimethylbenzene-1,4-diol being the most potent. *SRXN1* and *AKR1B10* showed the strongest response after exposure to the redox cyclers. No response was observed for the two highest concentrations of 2-methyl-1,4-naphthoquinone due to cell death after 24 h exposure. Interestingly, also some alkylated compounds, in particular 2,4-dimethylphenol, demonstrated activation of Nrf2 target genes, albeit at higher concentrations. As expected, the two non-redox cyclers (phenol and resorcinol) showed hardly any response. Next, we compared the maximum fold change (\log_2 FC) of all the Nrf2 target genes ($p_{adj} < 0.05$) and included only those genes for which at least a significant differential expression was observed for one compound. The redox-cycling phenols resulted in a higher response of these genes, compared to the non-redox cyclers and alkylated phenolic compounds (Figure 3B). Also other genes, including *MTLL11* and *CCND1* were activated. So far, these data only indicated a possibility to activate these Nrf2 target genes, but did not provide information on the potency. Therefore we also determined the bench mark concentration (BMC) for all compounds for the set of significantly affected Nrf2 target genes. We observed that redox-cycling phenols did activate the Nrf2-related genes at lower concentrations than alkylated phenols (Figure 3C); 2,4-dimethylphenol was the exception as the most responsive alkylated phenol. Next, we wondered whether we could classify the three classes of phenolic compounds only based the FC and BMC information of the five Nrf2



B)



ii)



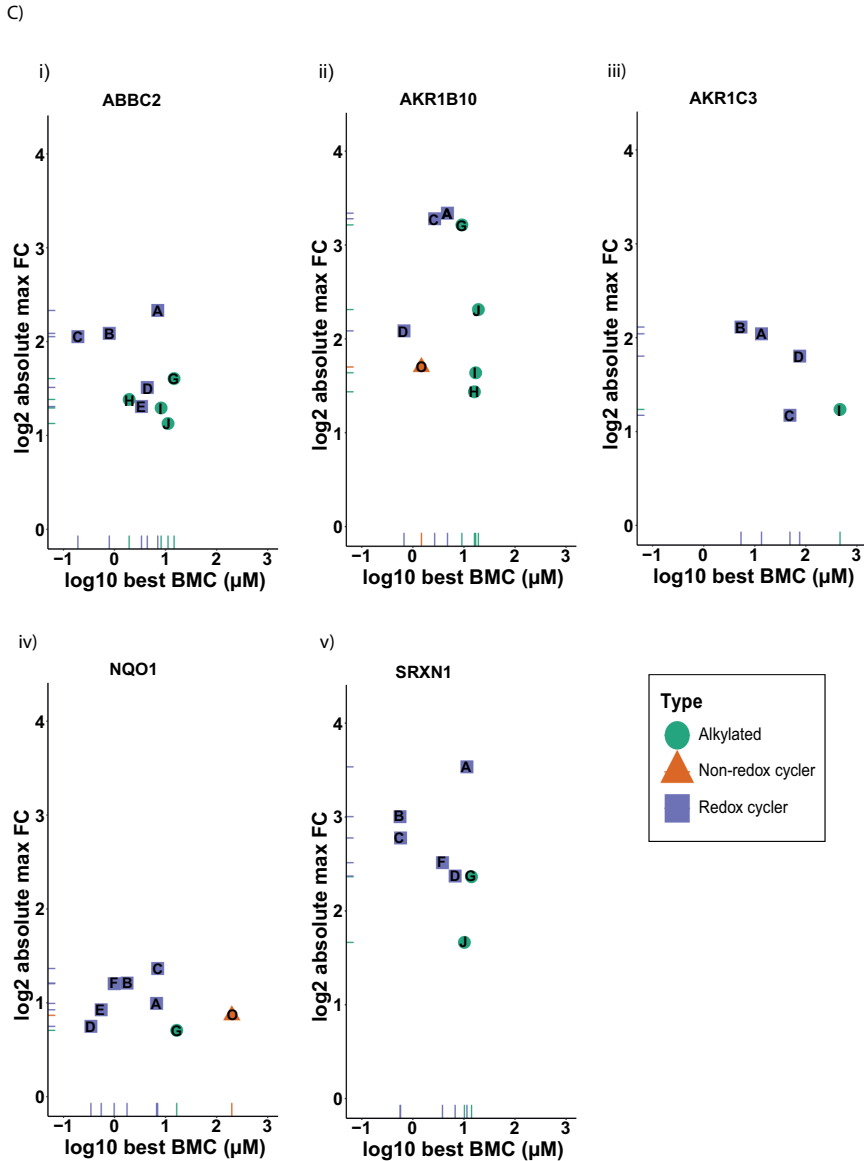


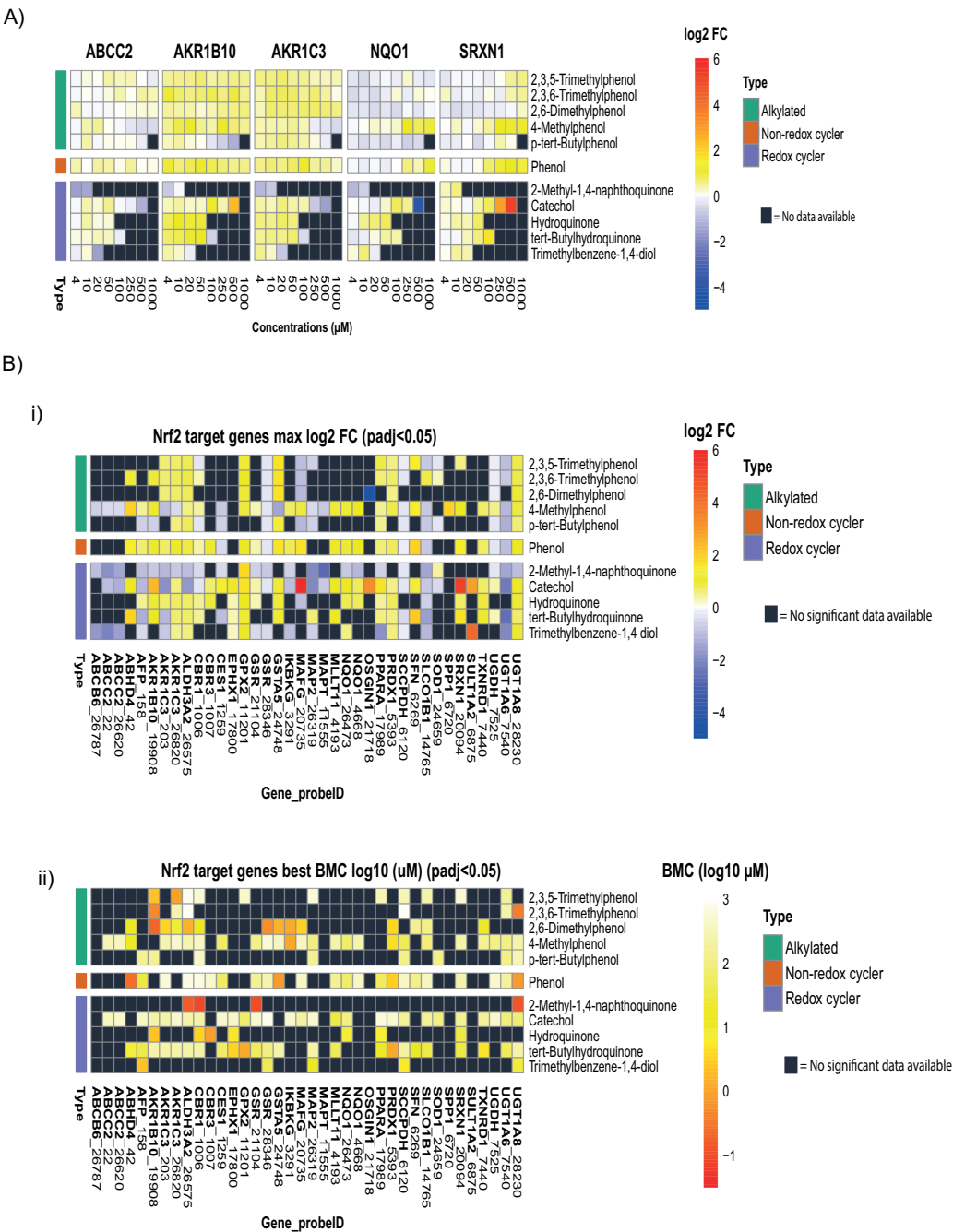
Figure 3. Nrf2 related gene expression of HepG2 cells after exposure to different phenolic compounds.

A) Heatmap showing the dose response of the five most responsive Nrf2 related genes. Note the different concentration ranges for the various phenols. **B)** i) Heatmap showing the significant ($p_{adj} < 0.05$) max (highest positive value (upregulation) and otherwise highest negative value (down regulation)) log₂ maximal fold changes of all the Nrf2 target genes across the entire concentration range. ii) Heatmap showing the significant ($p_{adj} < 0.05$) best BMC (benchmark concentration) of the Nrf2 related genes **C)** Scatterplot best log₁₀ BMC vs log₂ max absolute FC for the five most response Nrf2 related genes for the three different classes of phenolic compounds. A = Catechol, B = Trimethylbenzene-1,4-diol, C = tert-Butylhydroquinone, D = Hydroquinone, E = TMPPD, F = 2-Methyl-1,4-naphthoquinone, G = 2,4-Dimethylphenol, H = 2-(1,1-Dimethylethyl)phenol, I = p-tert-Butylphenol, J = 4-Methylphenol, K = 2,3,6-Trimethylphenol, L = 2,3,5-Trimethylphenol, M = 2,6-Dimethylphenol, N = 2,6-Di-tert-butyl-4-ethylphenol, O = Phenol, P = Resorcinol.

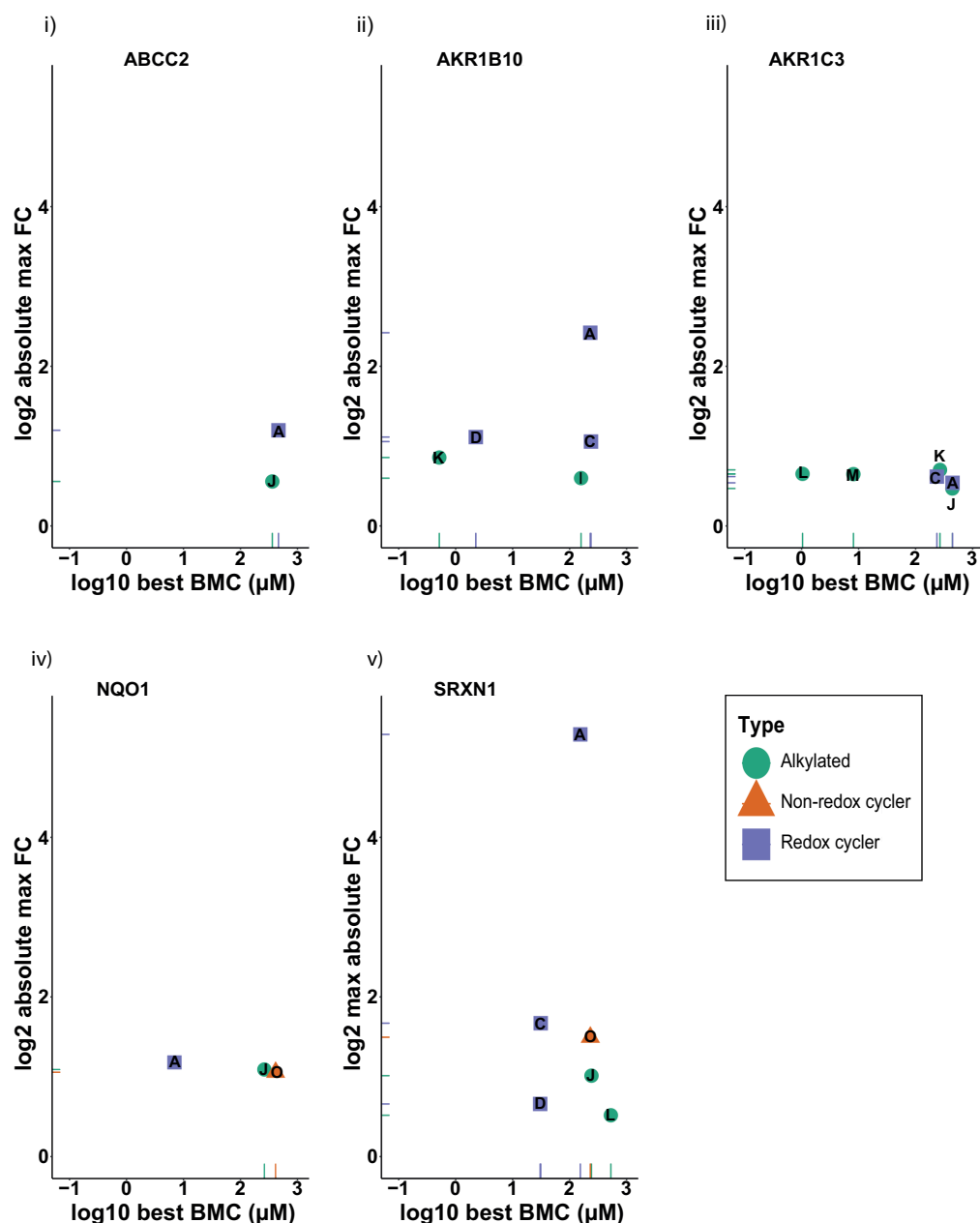
target genes (Figure 3C). We observed the same pattern for all five genes, as redox-cycling phenols present in the upper left corner (high max absolute log2 FC and a low best log10 BMC) and alkylated compounds present in the lower right corner. The non-redox cycling phenols did not show a significant response for most of the five genes except for *AKR1B10* and *NQO1*. These data support the notion that this panel of five Nrf2 target genes provides a good basis for classifying the phenolic compounds based oxidative stress activation. Based on the responses of these five genes we were largely able to separate the active redox cycling phenols from the other phenolic compound classes.

As a next step, we wondered whether we would observe the similar Nrf2 target gene activation in primary cultured human hepatocytes (PHH) based on a pool of 10 different donors. Therefore, PHH were exposed for 24 hours to a selected set of different phenolic compounds used for the HepG2 cells; we included all redox cycling phenols, yet reduced the number of alkylated phenols and non-redox cycling phenols. Viability assays showed a high sensitivity of the PHH to redox cycling phenols with a steep concentration response (Suppl. Figure 1). Limited cytotoxicity was observed for the alkylated phenols and phenol. This indicates that PHH are more sensitive for onset of cell death by redox cycling phenols than HepG2 cells, with 2-methyl-1,4-naphtoquinone being most potent. Cytotoxicity was associated with low number of total Tempo-Seq read counts; due to the cytotoxicity we could not determine the activation of Nrf2 target genes at these cytotoxic concentration. Regardless, at the non-cytotoxic concentrations we did observe activation of Nrf2 target genes, with *SRXN1* and *AKR1B10* being most prominent (Figure 4A), albeit that the maximum fold change induction was limited compared to HepG2 cells.

We extended our analysis to all the differential expressed Nrf2 target genes. Irrespective of the limitation on the dose response information due to the cytotoxicity, we determined the max log2 FC values for all other Nrf2 target genes as well as the log10 best BMC (Figure 4B). Other Nrf2 target genes also showed induction depending on phenol compound treatment, including *CBR3*, *ADHB4*, *MAFG*, *OSGIN1* and *SULT1A2*, but the overall max log2 FC values could not discriminate between redox-cycling and alkylated phenolic compounds. Similarly, the log10 best BMC did not show drastic lower BMC values for redox-cycling phenols, with the caveat that the cytotoxicity of redox cycling phenols prohibited accurate BMC calculation due to loss of full dose response information. In particular for the most cytotoxic phenol compound 2-methyl-1,4-naphtoquinone this hampered determination of realistic BMC values. Further plotting of the log10 best BMC against the max absolute log2 FC for *Srxn1* showed the best separation of the redox-cyclers from the alkylated phenolic compounds. Overall, comparing the transcriptomics response of HepG2 cells with

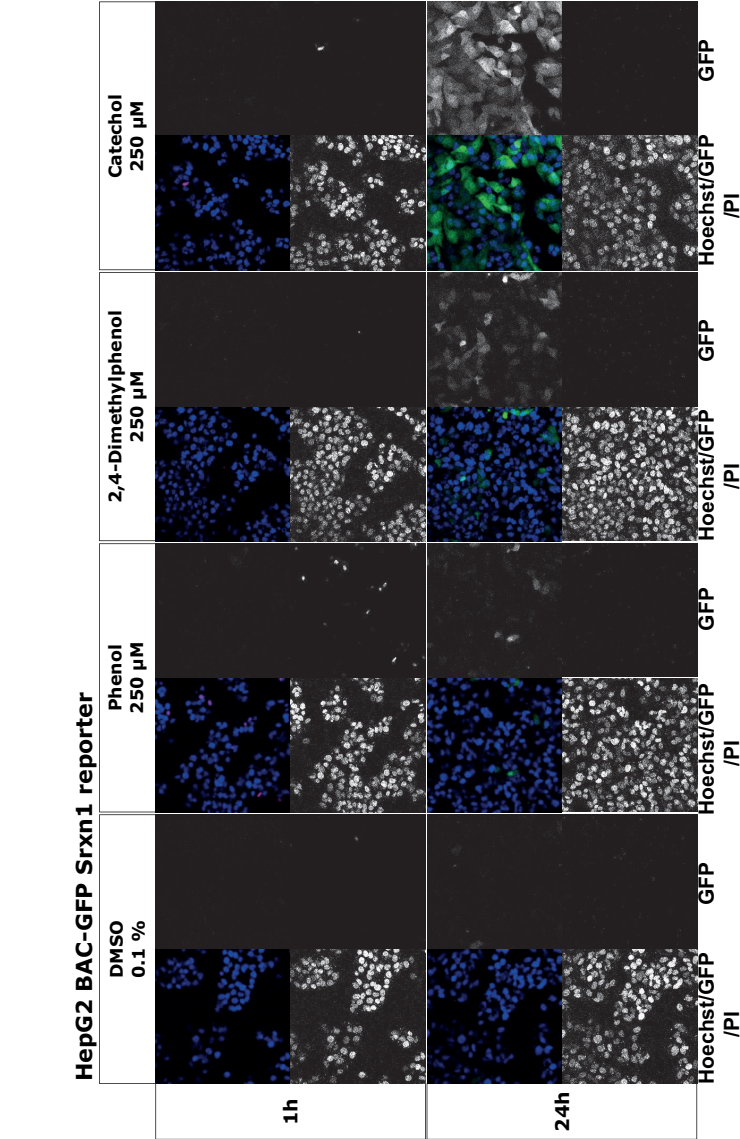


C)



best BMC (benchmark concentration) (log₁₀μM) of the Nrf2 target genes in Bi. **C)** Scatterplots of best log₁₀ BMC vs log₂ max absolute FC for the five selected Nrf2 target genes for the three different classes of phenolic compounds; only compounds with quantifiable values are depicted. A = Catechol, B = Trimethylbenzene-1,4-diol, C = tert-Butylhydroquinone, D = Hydroquinone, E = TMPPD, F = 2-Methyl-1,4-naphthoquinone, G = 2,4-Dimethylphenol, H = 2-(1,1-Dimethylethyl)phenol, I = p-tert-Butylphenol, J = 4-Methylphenol, K = 2,3,6-Trimethylphenol, L = 2,3,5-Trimethylphenol, M = 2,6-Dimethylphenol, N = 2,6-Di-tert-butyl-4-ethylphenol, O = Phenol, P = Resorcinol.

the PHH regarding the assessment of the effect of different phenolic compounds on the modulation of the Nrf2 pathway demonstrated that PHH had a smaller window of response due to increased sensitivity for the onset of cytotoxicity. Regardless of this increased sensitivity of PHH, we identified *Srxn1* as the most optimal marker that can inform on activation of the Nrf2 pathway in both HepG2 and PHH.

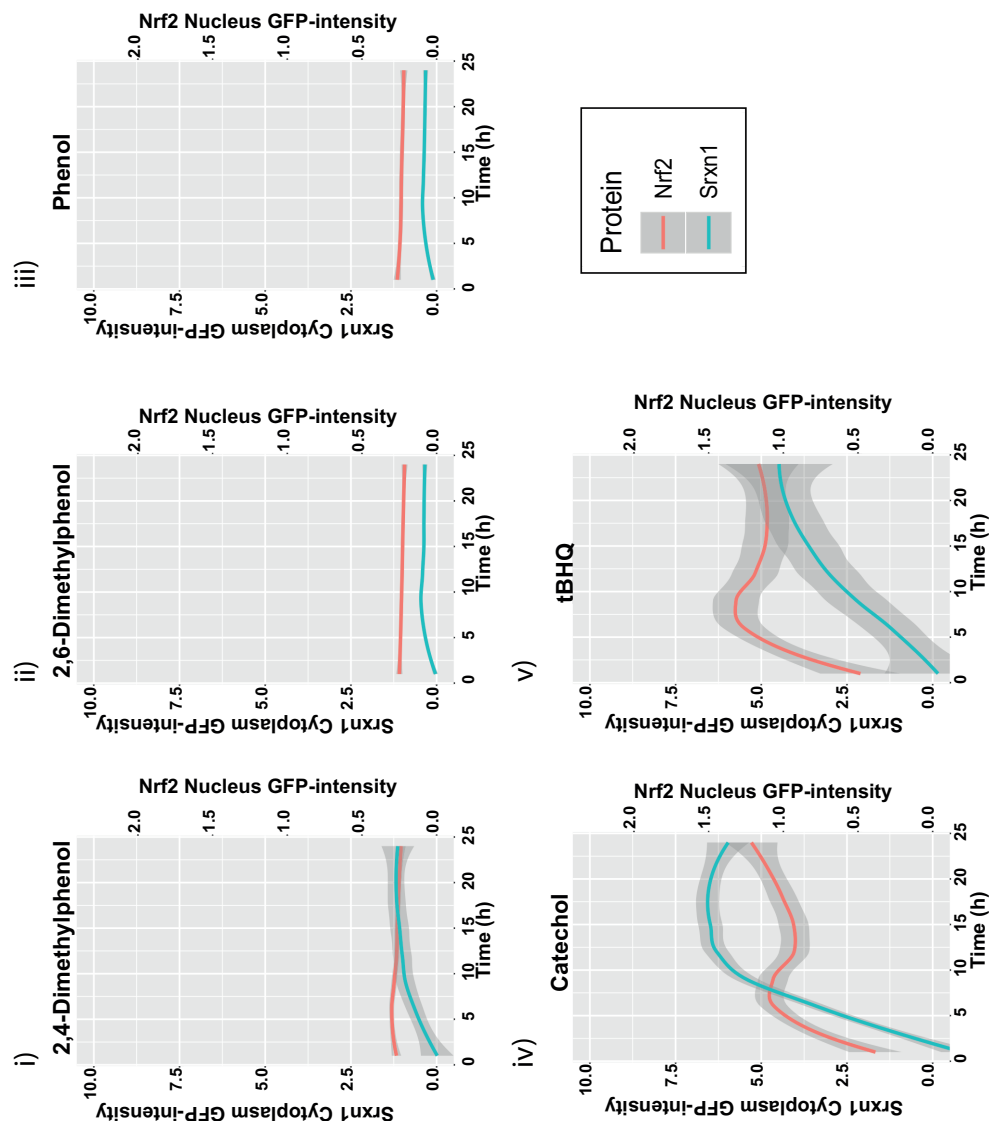


B)

Figure 5. Effect of different phenolic compounds on Nrf2 activation and Srxn1 induction in HepG2 GFP-reporter cell lines.

A) Effect of various phenolic compounds on GFP-Srxn1 induction in the HepG2 GFP-Srxn1 reporter cell line based on confocal microscopy at 1 and 24 hour after treatment. Each subpanel contains a composite image (upper left), Hoechst33342 picture (lower left), GFP picture (upper right) and propidium iodide (lower right). All images have same brightness/contrast settings. Note that no cell death was observed up till 24 hour treatment. Scale bar = 50 μ m.

B) Time response curves of Srxn1-GFP activation and Nrf2-GFP translocation to the nucleus after exposure to 250 μ M of different phenolic compounds.



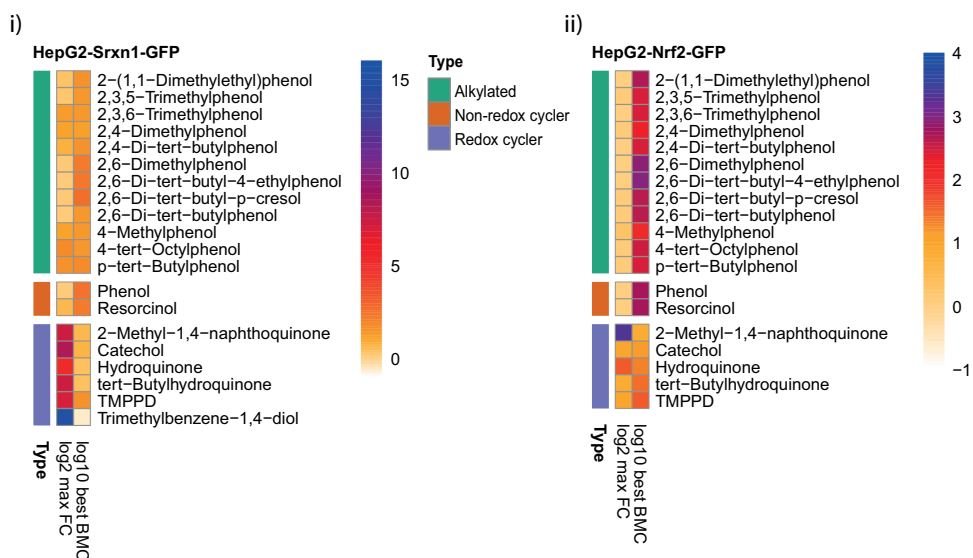
Srxn1 as biomarker to discriminate different phenolic compounds

The transcriptomics data above indicate that *Srxn1* is the most optimal sensitive biomarker to determine Nrf2 pathway activation in both HepG2 and PHH. Next we aimed to translate transcriptomics information to protein level and relate this to Nrf2 activity. We previously established HepG2-GFP-reporter cell lines for Nrf2 and its downstream target *Srxn1* (Wink et al. 2017) that allow the high throughput imaging-based quantitative assessment of Nrf2 stabilization and nuclear translocation and *Srxn1* activation. These reporters are strongly activated by prototypical Keap1 modulators (Wink et al. 2017). Reporter cells were exposed to all the phenolic compounds that were used for transcriptomics in HepG2 and PHH, and we further expanded the number of alkylated phenols. Then Nrf2-GFP translocation to the nucleus and cytoplasmic *Srxn1*-GFP induction was measured every hour for 24 hours using quantitative live cell confocal microscopy (Figure 5A; see Figure 1D for all phenolic compounds). We observed clear dose response early activation of Nrf2-GFP followed by a later induction of *Srxn1*-GFP for the redox cycling phenols catechol and tBHQ (Figure 5B). The alkylated phenols such as 2,6-dimethylphenol and non-redox cycling phenols did not show a response. Yet, 2,4-dimethylphenol caused a mild induction *Srxn1*-GFP expression, which was corresponding to the *Srxn1* mRNA expression observed with the transcriptomics analysis in the parental HepG2 cells. Next, for all the phenolic compounds tested we determined the maximal absolute log2 FC for the entire concentration time course data as well as the best log10 BMC. Redox cycling phenols showed the best absolute log2 FC accompanied with a lower best log10 BMC for both Nrf2-GFP activation and *Srxn1*-GFP induction (Figure 6A; and see Suppl. Table 2 for summary). None of the alkylating phenols was a strong activator of the Nrf2 pathway reporters. We explored further if we could integrate the FC and BMC information from our transcriptomics and GFP reporter assays. When comparing the expression changes (best absolute log2 FC) of *Srxn1* protein expression to *SRXN1* gene expression changes, we observed a clear separation of the redox cyclers and alkylating phenols (Figure 6B). Similarly, the same pattern was found when comparing *Srxn1*-GFP log10 best BMC to the *SRXN1* gene log10 best BMC (Figure 6B).

DISCUSSION

Here we systematically determined a testing strategy for assessment of Nrf2 pathway activation for application in a read across approach. The present study describes the application of a high throughput transcriptomics analysis in HepG2 and PHH in combination with high throughput single cell imaging of GFP-*Srxn1* reporter system. As a proof of concept, we aimed to identify whether certain classes

A)



B)

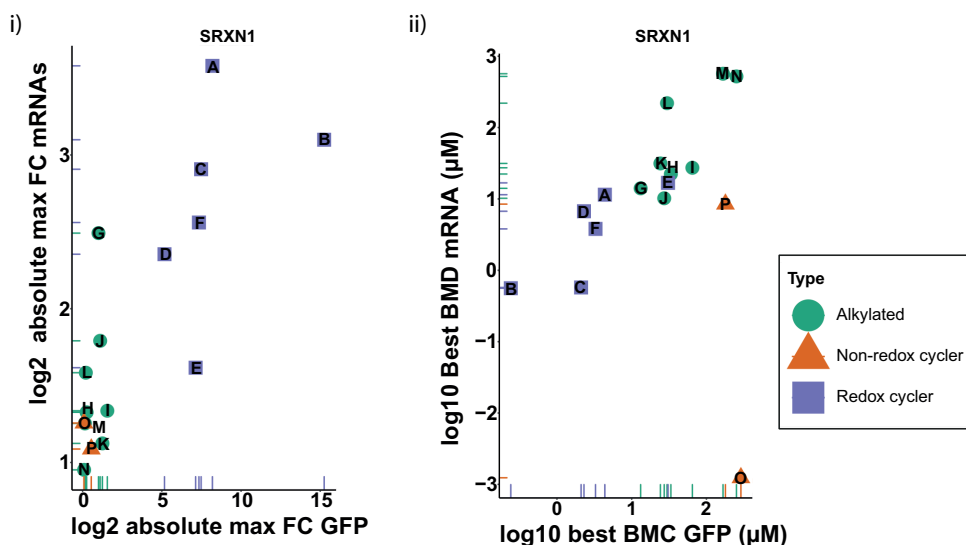


Figure 6. Effect of Nrf2 and Srxn1 response in HepG2 fluorescent protein reporter cells after phenolic compound exposure and relation with gene expression.

A) Heatmap of **i)** Srxn1-GFP response (max log₂ FC and log₁₀ best BMC (μM)) and **ii)** Nrf2-GFP response (max log₂ FC and log₁₀ best BMC) after exposure to different concentrations of phenolic compounds to HepG2 cells after 24h exposure.

B) Scatterplot of: **i)** max absolute log₂ FC-Srxn1-GFP versus max absolute log₂ FC-SRXN1 gene expression and **ii)** log₁₀ best BMC-Srxn1-GFP versus log₁₀ best BMC-SRXN1 gene expression after 24h exposure of different classes of phenolic compounds. A = Catechol, B = Trimethylbenzene-1,4-diol, C = tert-Butylhydroquinone, D = Hydroquinone, E = TMPPD, F = 2-Methyl-1,4-naphthoquinone, G = 2,4-Dimethylphenol, H = 2-(1,1-Dimethylethyl)phenol, I = p-tert-Butylphenol, J = 4-Methylphenol, K = 2,3,6-Trimethylphenol, L = 2,3,5-Trimethylphenol, M = 2,6-Dimethylphenol, N = 2,6-Di-tert-butyl-4-ethylphenol, O = Phenol, P = Resorcinol.

of phenolic compounds (redox cyclers, non-redox cyclers, and alkylated phenols) can be classified based on their potential to induce the oxidative stress response. Based on exposure to different compounds which are known to induce the Nrf2-pathway, we identified the five most responsive genes out of a set of 36 Nrf2 related genes: *ABCC2*, *AKR1B10*, *AKR1C3*, *NQO1*, and *SRXN1*. The same genes also stood out for most phenolic redox cyclers.

Comparison of the Nrf2 target genes responses between HepG2 and PHH demonstrated that *SRXN1* showed the strongest resemblance in response. *SRXN1* plays a critical role in counteracting ROS (Findlay et al. 2006; Jeong et al. 2006; Ross and Siegel 2017; Siegel et al. 2018). We have previously reported on the dependence of *Srxn1* expression on Nrf2 activation (Wink et al. 2017). The induction of *Srxn1* gene expression by both our training pro-oxidants as well as the redox cycling phenols was highly sensitive. This sensitivity was also reflected by the GFP-*Srxn1* induction in the reporter cell line. The latter reporter responses also allowed single cell time-resolved analysis of Nrf2 activation to also define similarity in temporal responses, thereby providing further support for biological similarity for read across.

AKR1B10 and *AKR1C3* were two genes found in the top 5 of most response Nrf2 targets and are members of the superfamily of the aldo-keto reductases (AKRs). AKRs can reduce carbonyl substrates, including quinones (Penning 2015), and play an important role in the detoxification of chemicals. Our previous studies using siKEAP1 and siNFE2L2 indicated the dependence on Nrf2 pathway activation for the induction of both *AKR1B10* and *AKR1C3* (Copple et al. 2019). *AKR1B10* was much more sensitive for induction by our pro-oxidants and followed a similar pattern as *SRXN1*. *AKR1C3* and *AKR1B10* are expressed at higher levels in HepG2 cells compared to other cell lines (Ebert et al. 2011) and therefore might be picked up easily in our studies. This may be related to the fact that *AKR1B10* is overexpressed in early stages of hepatocellular carcinoma (HCC), but down regulated in advanced tumor stages (Heringlake et al. 2010). Interestingly, also *AKR1C3* plays a role in the cytoprotection and is involved in the detoxification of ROS in association with resistance to radiotherapy in esophageal carcinoma cells (Xiong et al. 2014). Since *AKR1B10* induction was very strong in both HepG2 and PHH and activated by various pro-oxidants, we propose that *AKR1B10* could be an additional relevant sensitive reporter for Nrf2 pathway activation and, thereby, contributing to weight-of-evidence in read across when used in combination with the GFP-*Srxn1* reporter.

We observed higher sensitivity in HepG2 cells to distinguish redox cyclers and non-redox cyclers/alkylated phenolic compounds than PHH. This might be due to a higher

biotransformation capacity of PHH, and therefore the ability of converting alkylated/non-redox cyclers into redox cyclers like quinone species. HepG2 cells are known for the inferior phase I and II biotransformation enzyme expression levels, that can impair their ability to successfully metabolize alkylated/non-redox cyclers (Jennen et al. 2010). However, it is also known that PHH lose their metabolic capacity rapidly in culture and therefore lose their close resemblance to the physiological situation in humans. Of relevance is that PHH were more sensitive towards redox cycling induced cell death, which might indicate a high hepatic vulnerability towards oxidative stress induced by redox cycling phenolic compounds. This was successfully substantiated in the HepG2 reporter with the ability to detect this redox-cycling activity as mode of action.

Although most alkylated phenolic compounds showed no or only a minor response in activating Nrf2 related genes, 2,4-dimethylphenol was found as one of the most active alkylated phenolic compounds in HepG2 cells as assessed by transcriptomic analysis. A similar observation was made in PHH. Interestingly 2,6-dimethylphenol gave a far lower response indicating that minor differences in the phenols can have major impact on biological effects. Hence, care should be taken with sole evaluation of read across on structural similarity, but also involve a systematic evaluation of similarity of biological effects including potency evaluation such as using transcriptomic analysis.

Recently we have evaluated the experimental requirements to study phenols in relation to volatility (Tolosa et al. 2021). Based on these studies, here we used membranes to prevent loss of volatile phenolic compounds. We cannot exclude that we have lost some parent compounds in our HepG2 and PHH test systems during the 24 h exposure through other routes, including metabolism or degradation. Given that the phenols have a direct effect on Nrf2-GFP activation within the first 8 hours as well as the direct subsequent induction of Srxn1-GFP, we anticipate that we can faithfully determine differences in the proximal mode-of-action of the entire panel of phenols used in this study. This underscores the applicability of these reporter systems, since we can monitor the temporal response of the Nrf2 pathway activation at the individual cell level over time, including early time points. The transcriptomics responses were determined 24 hour after treatment and largely correlated with the anticipated effects of redox-cycling and alkylated phenols, in particular in HepG2 cells. However, we cannot exclude that some of the transcriptomics responses at the late 24 h time point are partially related to metabolites derived from the parent phenols.

In summary, we demonstrate that integration of high throughput HepG2 Nrf2 pathway reporter cell line data in combination with transcriptomics data from HepG2 and PHH, provides valuable mechanistic information on mode-of-action of structural similar phenols and their biological similarity. We anticipate that integration of these strategies, in combination with further information on toxicokinetics of these compounds, will provide a valuable approach for a read across assessment. Therefore, we foresee the use of this new approach methodology as a major part of an integrated approach for chemical safety testing with respect to a compounds potential to induce oxidative stress.

ACKNOWLEDGMENTS

This work was supported by the Ministry of Defence of the Netherlands and the European Commission Horizon2020 EU-ToxRisk project (grant nr 681002).

REFERENCES

- Attia SM (2010) Deleterious effects of reactive metabolites. *Oxid Med Cell Longev* 3(4):238-53 doi:10.4161/oxim.3.4.13246
- Benfenati E, Chaudhry Q, Gini G, Dorne JL (2019) Integrating in silico models and read-across methods for predicting toxicity of chemicals: A step-wise strategy. *Environ Int* 131:105060 doi:10.1016/j.envint.2019.105060
- Bischoff LJM, Kuijper IA, Schimming JP, et al. (2019) A systematic analysis of Nrf2 pathway activation dynamics during repeated xenobiotic exposure. *Arch Toxicol* 93(2):435-451 doi:10.1007/s00204-018-2353-2
- Biteau B, Labarre J, Toledano MB (2003) ATP-dependent reduction of cysteine-sulphinic acid by *S. cerevisiae* sulphiredoxin. *Nature* 425(6961):980-984 doi:10.1038/nature02075
- Bolton JL, Dunlap T (2017) Formation and Biological Targets of Quinones: Cytotoxic versus Cytoprotective Effects. *Chem Res Toxicol* 30(1):13-37 doi:10.1021/acs.chemrestox.6b00256
- Bolton JL, Trush MA, Penning TM, Dryhurst G, Monks TJ (2000) Role of Quinones in Toxicology. *Chemical Research in Toxicology* 13(3):135-160 doi:10.1021/tx9902082
- Bushel PR, Paules RS, Auerbach SS (2018) A Comparison of the TempO-Seq S1500+ Platform to RNA-Seq and Microarray Using Rat Liver Mode of Action Samples. *Front Genet* 9:485-485 doi:10.3389/fgene.2018.00485
- Copple IM, den Hollander W, Callegaro G, et al. (2019) Characterisation of the NRF2 transcriptional network and its response to chemical insult in primary human hepatocytes: implications for prediction of drug-induced liver injury. *Arch Toxicol* 93(2):385-399 doi:10.1007/s00204-018-2354-1
- Daneshian M, Kamp H, Hengstler J, Leist M, van de Water B (2016) Highlight report: Launch of a large integrated European in vitro toxicology project: EU-ToxRisk. *Archives of toxicology* 90(5):1021-1024 doi:10.1007/s00204-016-1698-7
- Ebert B, Kisiela M, Wsol V, Maser E (2011) Proteasome inhibitors MG-132 and bortezomib induce AKR1C1, AKR1C3, AKR1B1, and AKR1B10 in human colon cancer cell lines SW-480 and HT-29. *Chem Biol Interact* 191(1-3):239-49 doi:10.1016/j.cbi.2010.12.026
- ECHA (2016) New Approach Methodologies in Regulatory Science: Proceedings of a Scientific Workshop, April 2016. Available at: https://echa.europa.eu/documents/10162/21838212/scientific_ws_proceedings_en.pdf/a2087434-0407-4705-9057-95d9c2c2cc57. In.
- Escher SE, Kamp H, Bennekou SH, et al. (2019) Towards grouping concepts based on new approach methodologies in chemical hazard assessment: the read-across approach of the EU-ToxRisk project. *Arch Toxicol* 93(12):3643-3667 doi:10.1007/s00204-019-02591-7
- Findlay VJ, Townsend DM, Morris TE, Fraser JP, He L, Tew KD (2006) A novel role for human sulfiredoxin in the reversal of glutathionylation. *Cancer Res* 66(13):6800-6 doi:10.1158/0008-5472.CAN-06-0484
- Graepel R, Ter Braak B, Escher SE, et al. (2019) Paradigm shift in safety assessment using new approach methods: The EU-ToxRisk strategy. *Current Opinion in Toxicology* 15:33-39 doi:10.1016/j.cotox.2019.03.005
- Heringlake S, Hofdmann M, Fiebler A, Manns MP, Schmiegeler W, Tannapfel A (2010) Identification and expression analysis of the aldo-ketoreductase1-B10 gene in primary malignant liver tumours. *Journal of Hepatology* 52(2):220-227 doi:https://doi.org/10.1016/j.jhep.2009.11.005
- Jennen DG, Magkoufopoulou C, Ketelslegers HB, van Herwijnen MH, Kleinjans JC, van Delft JH (2010) Comparison of HepG2 and HepaRG by whole-genome gene expression analysis for the purpose of chemical hazard identification. *Toxicol Sci* 115(1):66-79 doi:10.1093/toxsci/kfq026

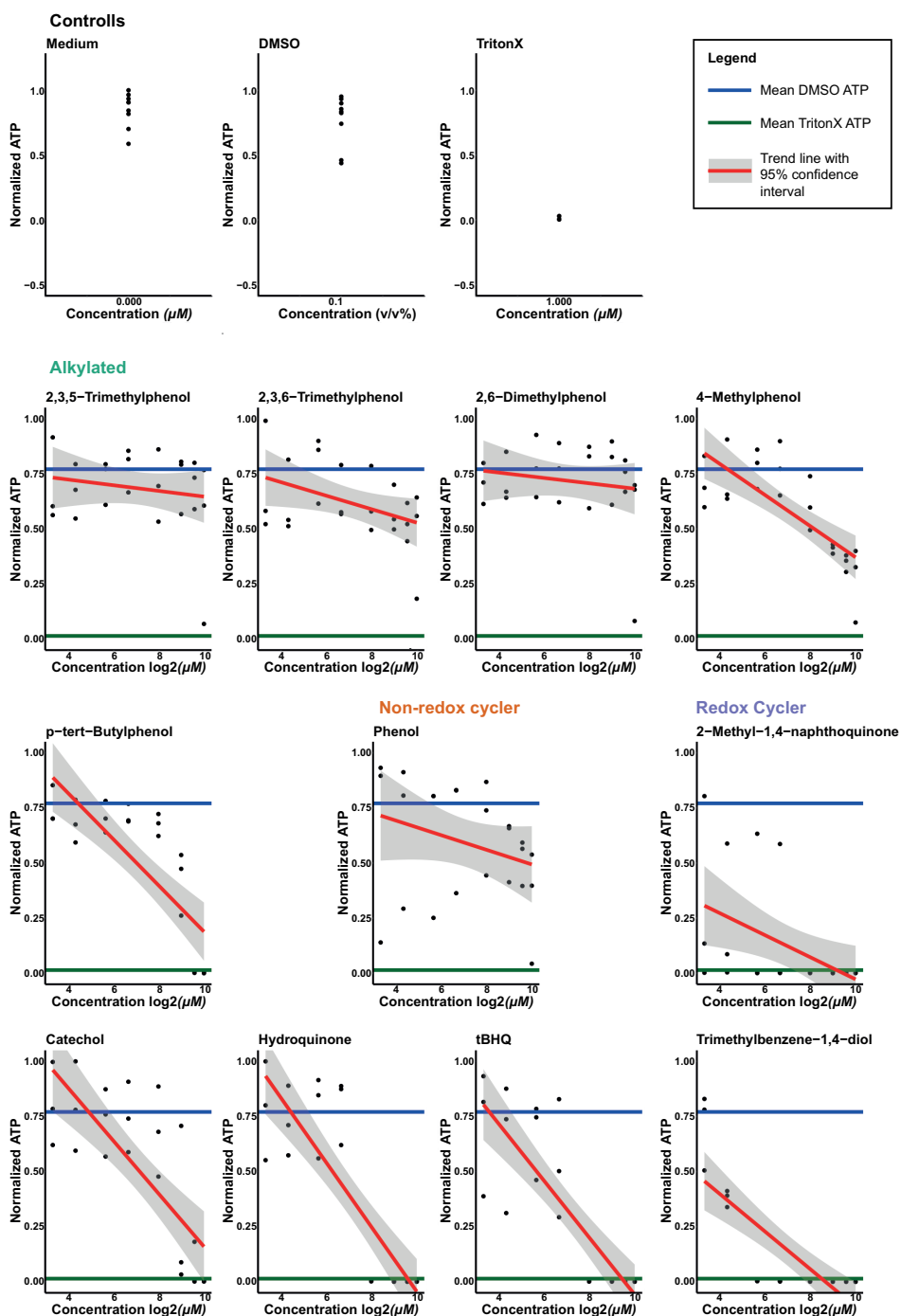
- Jeong W, Park SJ, Chang TS, Lee DY, Rhee SG (2006) Molecular mechanism of the reduction of cysteine sulfinic acid of peroxiredoxin to cysteine by mammalian sulfiredoxin. *J Biol Chem* 281(20):14400-7 doi:10.1074/jbc.M511082200
- Keum YS, Choi BY (2014) Molecular and chemical regulation of the Keap1-Nrf2 signaling pathway. *Molecules* 19(7):10074-89 doi:10.3390/molecules190710074
- Kobayashi A, Kang MI, Okawa H, et al. (2004) Oxidative stress sensor Keap1 functions as an adaptor for Cul3-based E3 ligase to regulate proteasomal degradation of Nrf2. *Mol Cell Biol* 24(16):7130-9 doi:10.1128/MCB.24.16.7130-7139.2004
- Kyselova Z (2011) Toxicological aspects of the use of phenolic compounds in disease prevention. *Interdiscip Toxicol* 4(4):173-83 doi:10.2478/v10102-011-0027-5
- Love MI, Huber W, Anders S (2014) Moderated estimation of fold change and dispersion for RNA-seq data with DESeq2. *Genome Biol* 15(12):550-550 doi:10.1186/s13059-014-0550-8
- Mav D, Shah RR, Howard BE, et al. (2018) A hybrid gene selection approach to create the S1500+ targeted gene sets for use in high-throughput transcriptomics. *PLoS One* 13(2):e0191105 doi:10.1371/journal.pone.0191105
- Monks TJ, Hanzlik RP, Cohen GM, Ross D, Graham DG (1992) Quinone chemistry and toxicity. *Toxicology and Applied Pharmacology* 112(1):2-16 doi:https://doi.org/10.1016/0041-008X(92)90273-U
- Monks TJ, Lau SS (1997) Biological reactivity of polyphenolic-glutathione conjugates. *Chem Res Toxicol* 10(12):1296-313 doi:10.1021/tx9700937
- Parish ST, Aschner M, Casey W, et al. (2020) An evaluation framework for new approach methodologies (NAMs) for human health safety assessment. *Regul Toxicol Pharmacol* 112:104592 doi:10.1016/j.yrtph.2020.104592
- Penning TM (2015) The aldo-keto reductases (AKRs): Overview. *Chem Biol Interact* 234:236-46 doi:10.1016/j.cbi.2014.09.024
- Perkins EJ, Ashauer R, Burgoon L, et al. (2019) Building and Applying Quantitative Adverse Outcome Pathway Models for Chemical Hazard and Risk Assessment. *Environ Toxicol Chem* 38(9):1850-1865 doi:10.1002/etc.4505
- Phillips JR, Svoboda DL, Tandon A, et al. (2018) BMDEExpress 2: enhanced transcriptomic dose-response analysis workflow. *Bioinformatics* 35(10):1780-1782 doi:10.1093/bioinformatics/bty878
- Priya S, Nigam A, Bajpai P, Kumar S (2014) Diethyl maleate inhibits MCA+TPA transformed cell growth via modulation of GSH, MAPK, and cancer pathways. *Chem Biol Interact* 219:37-47 doi:10.1016/j.cbi.2014.04.018
- Ross D, Siegel D (2017) Functions of NQO1 in Cellular Protection and CoQ10 Metabolism and its Potential Role as a Redox Sensitive Molecular Switch. *Front Physiol* 8:595 doi:10.3389/fphys.2017.00595
- Schimming JP, ter Braak B, Niemeijer M, Wink S, van de Water B (2019) System Microscopy of Stress Response Pathways in Cholestasis Research. In: Vinken M (ed) *Experimental Cholestasis Research*. Springer New York, New York, NY, p 187-202
- Siegel D, Dehn DD, Bokatzian SS, et al. (2018) Redox modulation of NQO1. *PLoS One* 13(1):e0190717 doi:10.1371/journal.pone.0190717
- Takaya K, Suzuki T, Motohashi H, et al. (2012) Validation of the multiple sensor mechanism of the Keap1-Nrf2 system. *Free Radic Biol Med* 53(4):817-27 doi:10.1016/j.freeradbiomed.2012.06.023
- Tolosa L, Martínez-Sena T, Schimming JP, et al. (2021) The in vitro assessment of the toxicity of volatile, oxidisable, redox-cycling compounds: phenols as an example. *Archives of toxicology* 95(6):2109-2121 doi:10.1007/s00204-021-03036-w

- Wambaugh JF, Bare JC, Carignan CC, et al. (2019) New approach methodologies for exposure science. *Current Opinion in Toxicology* 15:76-92 doi:10.1016/j.cotox.2019.07.001
- Wink S, Hiemstra S, Herpers B, van de Water B (2017) High-content imaging-based BAC-GFP toxicity pathway reporters to assess chemical adversity liabilities. *Arch Toxicol* 91(3):1367-1383 doi:10.1007/s00204-016-1781-0
- Wink S, Hiemstra SW, Huppelschoten S, Klip JE, van de Water B (2018) Dynamic imaging of adaptive stress response pathway activation for prediction of drug induced liver injury. *Arch Toxicol* doi:10.1007/s00204-018-2178-z
- Xiong R, Siegel D, Ross D (2014) Quinone-induced protein handling changes: implications for major protein handling systems in quinone-mediated toxicity. *Toxicol Appl Pharmacol* 280(2):285-95 doi:10.1016/j.taap.2014.08.014
- Yeakley JM, Shepard PJ, Goyena DE, VanSteenhouse HC, McComb JD, Seligmann BE (2017) A trichostatin A expression signature identified by TempO-Seq targeted whole transcriptome profiling. *PLoS One* 12(5):e0178302 doi:10.1371/journal.pone.0178302
- Zipper LM, Mulcahy RT (2002) The Keap1 BTB/POZ dimerization function is required to sequester Nrf2 in cytoplasm. *J Biol Chem* 277(39):36544-52 doi:10.1074/jbc.M206530200

SUPPLEMENTAL MATERIALS

Supplemental Table 1: Gene list overlap between Nrf2 regulated genes EU-ToxRisk S1500+ V2 TempO-Seq gene panel (= 36 Nrf2 related genes).

Gene symbol	Ensembl ID	Gene symbol	Ensembl ID
ABCB6	ENSG00000115657	MAP2	ENSG00000078018
ABCC2	ENSG00000023839	MAPT	ENSG00000186868
ABHD4	ENSG00000100439	MLLT11	ENSG00000213190
AFP	ENSG00000081051	NQO1	ENSG00000181019
AKR1B10	ENSG00000198074	OSGIN1	ENSG00000140961
AKR1C3	ENSG00000196139	PPARA	ENSG00000186951
ALDH3A2	ENSG00000072210	PRDX1	ENSG00000117450
CBR1	ENSG00000159228	SCCPDH	ENSG00000143653
CBR3	ENSG00000159231	SFN	ENSG00000175793
CCND1	ENSG00000110092	SLCO1B1	ENSG00000134538
CES1	ENSG00000198848	SOD1	ENSG00000142168
EPHX1	ENSG00000143819	SPP1	ENSG00000118785
GPX2	ENSG00000176153	SRXN1	ENSG00000271303
GSR	ENSG00000104687	SULT1A2	ENSG00000197165
GSTA4	ENSG00000170899	TXNRD1	ENSG00000198431
GSTA5	ENSG00000182793	UGDH	ENSG00000109814
IKBKG	ENSG00000269335	UGT1A6	ENSG00000167165
MAFG	ENSG00000197063	UGT1A8	ENSG00000242366



Supplemental Figure 1. Effect of phenolic compounds on PHH viability.

Viability was determined by ATP content of PHH. Three measurements per concentration are shown and six for the controls. ATP levels were measured 24 h after exposure.

Supplemental Table 2. Effect of Nrf2 and Srxn1 response in HepG2 fluorescent protein reporter cells after phenolic compound exposure and relation with gene expression.

Srxn1-GFP response (max log2 FC and log10 best BMC (μM)) and Nrf2-GFP response (max log2 FC and log10 best BMC (μM)) after exposure to different concentrations of phenolic compounds to HepG2 cells after 24 h exposure.

Compound	Type	SRXN1		NRF2	
		log2_FC	log10_BMC	log2_FC	log10_BMC
2-(1,1-Dimethylethyl)phenol	Alkylated	0.254064686	1.524681663	0.0477701	2.688186593
2,3,5-Trimethylphenol	Alkylated	0.203229098	1.473098486	0.1017354	2.454340176
2,3,6-Trimethylphenol	Alkylated	1.250000243	1.38433549	0.0348152	2.421794711
2,4-Dimethylphenol	Alkylated	1.002061115	1.120096603	0.101833	2.280921937
2,4-Di-tert-butylphenol	Alkylated	0.692341787	1.582353175	0.0348152	2.421794711
2,6-Dimethylphenol	Alkylated	0.144863275	2.22224291	0.0303122	2.91131105
2,6-Di-tert-butyl-4-ethylphenol	Alkylated	0.09451427	2.401963724	0.0279593	2.958588249
2,6-Di-tert-butyl-p-cresol	Alkylated	0.159260826	2.594364923	0.066368	2.599238791
2,6-Di-tert-butylphenol	Alkylated	0.102174362	1.380393969	0.066368	2.599238791
4-Methylphenol	Alkylated	1.10856306	1.435627802	0.2853099	2.166684636
4-tert-Octylphenol	Alkylated	1.763377625	1.364596017	0.0686018	2.466499871
p-tert-Butylphenol	Alkylated	1.559155564	1.812247373	0.0980131	2.411845211
Phenol	Non redox cycler	0.08445872	2.461722069	0.0345162	2.754764081
Resorcinol	Non redox cycler	0.546179954	2.254463482	0.0347753	2.743064267
2-Methyl-1,4-naphthoquinone	Redox cycler	7.343117656	0.516101524	3.2964561	0.868288159
Catechol	Redox cycler	8.192966392	0.640883743	0.9853045	1.143102275
Hydroquinone	Redox cycler	5.167800943	0.361644746	1.60402	1.324950878
tert-Butylhydroquinone	Redox cycler	7.479745856	0.323076696	0.829921	1.462285666
TMPPD	Redox cycler	7.133384638	1.486129982	0.9502092	1.599766299
Trimethylbenzene-1,4-diol	Redox cycler	15.24768824	-0.617410283	NA	NA

6

General discussion and future prospects

As we are constantly exposed to a broad spectrum of chemicals, which may lead to adverse health effects, developing human relevant mechanistic biomarkers which provide information regarding the type of exposures and its (predicted) effect are from utmost importance.

THE EVOLUTION OF BIOMARKERS: FROM A SINGLE MOLECULE TOWARDS A BIOMARKER FINGERPRINT

As described in **Chapter 1**, the perspective of a biomarker is changing over time. This process is driven by new technologies enabling us to measure a wide spectrum of, for example, genes, proteins and metabolites in a short amount of time as well as increased effort to reduce the number of animal tests. Moreover, techniques like for example high content high throughput microscopy in combination with GFP-reporter cell lines makes it possible to study biological responses over time, providing us valuable information concerning the onset, magnitude and progression of the stress response pathway. Furthermore, spatial-temporal analysis provide information regarding the place and time of the molecules in the signal transduction cascade that is specific for a type of chemical stress. The large amount of data created by these techniques enables us to search for the interactions in biological processes which in turn provides opportunities for biological network analysis. Biological network analysis, like for example gene-gene interaction networks, co-regulation / co-expression networks, Bayesian networks, and weighted gene co-expression analysis (WGCNA) makes it possible to enhance our understanding of these molecular interactions and to identify the molecules which play a central role in a biological network (Charitou et al. 2016; Saelens et al. 2018), and therefore may be promising candidate biomarkers of chemical exposure and disease. Moreover, WGCNA approaches combining gene expression data with histology and clinical chemistry data can be used to predict adverse and non-adverse outcomes of chemical exposure and allows translation from animal to human (Callegaro et al. 2021; Sutherland et al. 2018). Recently, WGCNA was also conducted on microRNA data to find new biomarkers (Qin et al. 2019; Soleimani Zakeri et al. 2020). Interestingly, integrating microRNA data (microRNA and mRNA co-expression modules) also makes it possible to examine the regulatory roles that microRNAs have on their target genes (Mamdani et al. 2015). Therefore, including microRNA data into WGCNA modules show great promise, making it possible to obtain a more comprehensive coverage to elucidate the underlying mechanisms of toxicity as cannot be achieved by using gene expression data as the only source of data (Ma et al. 2019).

MICRORNAS AS BIOMARKERS OF EXPOSURE AND DISEASE

As described above, microRNAs are new players which might be part of a biological fingerprint. In **Chapter 2**, the use of microRNAs as biomarkers of chemical exposure and disease are described. Interestingly, we found several microRNAs to be differently expressed after exposure to different chemicals, like for example miR-21 and miR-26. Of course a change in, for example, miR-21 does not provide any information about a change in health state. However, we must be careful to link a change in expression of only one or two microRNAs to a particular chemical exposure or effect. Most of the biomarkers identified in the various studies have analyzed microRNA changes in the cells, either in cell culture *in vitro* or tissue *in vivo*. It remains unclear whether these microRNAs can be detected in the blood and thereby represent a mechanistic biomarker that could reflect on the mode of action of a particular chemical exposure. So far biomarkers measured in the blood have not per se been discovered in relation to their mode of action. Therefore, the question still has to be answered whether or not the rise of certain microRNAs found in the blood has indeed a functional role, or that the change in expression is just the result of tissue damage. However, microRNAs which are known to be strongly related to a specific organ, like miR-122 for the liver, can provide valuable information about which organ is damaged upon exposure to a chemical or during disease, as miR-122 makes up for 70% of the total pool of microRNAs in the liver (Jopling 2012) and is linked to e.g. cholesterol/lipid metabolism, iron homeostasis, and differentiation of hepatocytes. However, the rise of miR-122 levels measured in blood on its own has no relation to the type of toxic liver injury (Madboly et al. 2019). Interestingly, hepatocellular carcinoma cells, like HepG2 cells, have lower levels of miR-122 as compared to normal liver cells. The loss of miR-122 is related to downregulation of tumor cell apoptosis, hepatic cell invasion, interhepatic metastasis and reduced sensitivity towards drugs (Ha et al. 2019; Xing et al. 2013) making miR-122 restoration as a treatment interesting for the clinic (Ha et al. 2019). Defining whether the candidate microRNA biomarkers play an integral functional role in disease mechanism is a difficult task. One single microRNA might have hundreds of different targets and the role of the microRNA might differ between different tissues. Furthermore, a microRNA can both increase or diminish the stress response depending on their involvement in the inhibition of negative regulators in a positive feedback loop or as part of a negative feedback loop, respectively (Emde and Hornstein 2014).

New emerging techniques to measure microRNAs in *in vitro* and *ex-vivo* derived biological samples, like for example droplet digital PCR, makes it possible to quantify microRNA copy number of multiple microRNAs in a single sample (Stein et al. 2017). Moreover, the measurement of microRNAs derived from extracellular vesicles (EVs) is

growing in popularity as EVs might in some cases provide a more consistent source of microRNAs compared to circulating-free microRNAs associated with proteins (Endzelins et al. 2017). However, robust and high throughput isolation of specific groups of EVs is still challenging (Buschmann et al. 2018).

MIMICKING THE OVEREXPRESSION OF CERTAIN MICRORNAS CAN ENHANCE OR INHIBIT THE SRXN1 RESPONSE IN HEPG2 CELLS

Investigating the role of microRNAs in a stress response pathway might be accomplished by using microRNA inhibitors or mimics. In **Chapter 3**, research is presented making use of microRNA mimics, so mimicking overexpression of a particular microRNA in a cell. Making use of different HepG2-GFP reporter cells in combination with live cell confocal microscopy, we were able to study the effect of almost all individual microRNA directly on GFP-reporter protein level at the single cell level. We identified several microRNAs which, when overexpressed, are able to enhance or reduce the expression of sulfiredoxin (Srxn1), a sensitive biomarker for the induction of oxidative stress that is a direct downstream target of the transcription factor Nrf2 (Soriano et al. 2008). The same pattern was observed in gene expression changes of sulfiredoxin. However, the microRNAs found to alter the expression of sulfiredoxin in this study, are not selective for the Nrf2 pathway as they were also able to regulate the expression of other genes that are part of other (stress response) pathways, such as the unfolded protein response. Of course this might be explained by the fact that those microRNAs have hundreds of different targets. However, we also have to keep in mind that most stress-response pathways are linked to each other (Bhattarai et al. 2021) and that, *in vivo*, multiple different microRNAs can “work together” by targeting the same gene, where the change in expression is the resultant of all the different microRNAs (Peter 2010). Therefore, to obtain information concerning the primary response upon microRNA expression changes, there is a need to perform further temporal analysis of the transcriptional changes after microRNA transfection. High throughput transcriptomics based on TempO-seq is a preferred cost effective method for this.

Interestingly, some of our most potent microRNA candidates would have been missed by various online target prediction tools. This suggests the limitations in the prediction of these *in silico* tools and indicates that biological microRNA screens as performed during our studies is of high importance. The microRNAs found in

our study that enhance or inhibit the Nrf2 pathway might provide opportunities for microRNA therapeutics that target the Nrf2 pathway. Enhanced Nrf2 pathway activation is considered as a pro-oncogenic pathway. This is exemplified by the high penetrance of *KEAP1* mutations in e.g. lung cancer that prohibit Nrf2 ubiquitination and enhance an antioxidant stress response and resistance to anticancer therapy (Jaramillo and Zhang 2013). However, findings indicate that not changes in the genes e.g. somatic mutations in either *KEAP1* and/or *NFE2L2* itself are responsible for high Nrf2 activity, but are rather the consequence of deregulation of the transcription of Nrf2 by epigenetic factors like hypermethylation of the *KEAP1* promoter and microRNAs linked to the cell-detoxifying network (Fabrizio et al. 2018; Shah et al. 2013). Therefore, microRNAs which are able to inhibit the Nrf2 pathway might be used to make cancer cells more vulnerable for chemo- and radiotherapy. Furthermore, oxidative stress plays a central role in various acute and chronic pathologies including ischemia/reperfusion injury and neurodegenerative diseases (Arshad et al. 2017). Therefore, microRNAs enhancing the Nrf2 pathway might be used to enhance a person's protection against oxidative stress. As a consequence, drug delivery strategies to target microRNAs to specific target tissues are currently being development (Vassalle et al. 2020), providing improved strategies for Nrf2-modulating therapeutic approaches through microRNAs. Additional research on the dose response and long term safety profile of our candidate Nrf2 modulating microRNAs is required.

Caution however has to be made to link microRNAs which alter the Nrf2 response directly to Nrf2. As described by Ashrafizadeh et al. 2020, microRNAs can regulate the Nrf2 pathway via different ways: 1) by affecting the nuclear translocation of Nrf2, 2) by influencing the expression of Nrf2, regulating the upstream mediators of Nrf2 and modulation of *KEAP1* (Ashrafizadeh et al. 2020). Interestingly, also redox stress itself can alter the microRNA biogenesis and processing pathway leading, for example, to altered redox signaling an disease mechanisms (Cheng et al. 2013). Furthermore, Mendell and Olson describe five different mechanisms by which microRNAs can regulate signaling pathways in general, depending on the cellular and functional context, as a single microRNA is not limited to one of these mechanisms: stress signal mediation, stress signal modulation, negative feedback, positive feedback, and buffering (Mendell and Olson 2012).

CELLS PREVIOUSLY EXPOSED TO PRO-OXIDANTS EXHIBIT AN ALTERED RESPONSE PATTERN COMPARED TO 'NAIVE' CELLS

Biology is equipped with adaptive responses that allow cells and tissues to cope with altering environmental conditions, such as exposure to toxic substances. This also holds true for cellular stress response programs, including the Nrf2 pathway. Therefore, we studied the dynamics of the Nrf2 pathway over time and were wondering what the effect would be of a second exposure given at different stages of the response. In **Chapter 4**, we describe the outcome of this study. Interestingly, we found that the Nrf2 response after a second treatment after 24 h, was lower than the response to the first exposure with the same concentration, indicating that the Nrf2 is adaptive. However, sulfiredoxin, a downstream target of Nrf2, showed a three-fold higher response compared to the first treatment, with all cells participating in the response. Although more research is needed to unravel the precise mechanism, it is clear that repeated exposure testing will add valuable information in testing the safety of a chemical or drug. As indicated in **Chapter 4**, several aspects are important to consider in future research. First of all characteristics of the chemical compound used to induce the Nrf2 pathway, like mode of action and half-life, as these aspects determine the speed and duration of the response. Other molecules playing a role in the modulation of Nrf2 transcriptional activity might be incorporated in the study as well as other downstream targets which might behave differently upon repeated chemical exposure (Bergström et al. 2011; Mathew et al. 2014). siRNA-mediated knockdown of single or combinations of Nrf2 pathway-related molecules can be used to elucidate their role in the first and second response. Also the time between the first and second exposure can be changed, however, *in vitro*, caution has to be taken not to induce cytotoxicity. Moreover, the role of microRNAs have to be investigated in this matter as they may play a role in the induction of the second response as they are able to block the expression of genes playing a role in controlling, e.g. inhibiting the Nrf2 response (see **Chapter 3**). As indicated by several studies, preconditioning might be used for therapeutic approaches using low non-toxic concentrations (Mathew et al. 2014). However, challenge remains in finding the optimum dosing regimen: dose per treatment, time between treatments and number of repeated treatments.

TESTING STRATEGIES FOR CELLULAR STRESS RESPONSE ACTIVATION

As activation of the Nrf2 pathway upon chemical exposure might indicate oxidative damage, we hypothesized that our high throughput microscopy reporter and transcriptomics toolbox might be suitable to characterize the ability of chemicals to cause oxidative stress and activation of the Nrf2 pathway. To test this hypothesis, a panel of different phenolic compounds was used that were either redox cycling phenols, alkylated phenols, and non-redox cycling phenols. Outcomes of this study are described in **Chapter 5**. Interestingly we were able to discriminate between redox-cyclers that induce the oxidative stress response and non-redox-cyclers that lack this ability, at least at lower concentrations. Moreover, although the concentration of a compound needed to induce the Nrf2 pathway was different in HepG2 cells compared to primary hepatocytes, we were still able to discriminate between these two compound classes. This indicates that the onset of downstream targets like sulfiredoxin can indeed provide information concerning the mode of action of a compound.

Besides *SRXN1*, we also found *AKR1B10* to be a sensitive marker to discriminate between redox-cyclers and non-redoxcyclers. The Nrf2 pathway is known to be one of the major regulatory systems for *AKR1B10* gene regulation (Endo et al. 2021; Rooney et al. 2020) and therefore it was not a surprise that we found *AKR1B10* to be induced by our set of oxidative stress inducing compounds. However, we have to keep in mind that activation of the Nrf2 pathway, or a stress response pathway in general, is not a direct indication for an adverse outcome leading towards toxicity, although a harmful event is needed to activate the stress response pathway. Activation, as a consequence, may lead towards cellular protection against more harmful stimuli, as protection due to induction of a stress response pathway is not specific for the event which activated the pathway. For example, sulforaphane, a known inducer of the Nrf2 pathway present in e.g. broccoli sprouts, was found to provide cellular protection against radiation (Mathew et al. 2014). The same of course is true for phenolic compounds as used in **Chapter 5** which were chosen based on knowledge obtained in animal studies and compound structure similarity. Furthermore, Castañeda-Arriaga et al. 2018, identified the presence of redox metals, the pH, and the possibility of the formation of benzoquinones as key aspects regarding the pro-versus anti-oxidant effects of phenolic compounds and therefore these aspects have to be taken into account future research (Castañeda-Arriaga et al. 2018).

A parameter often used in toxicity testing is the point of departure (PoD) which is defined as the lowest concentration at which a response can be detected. As *SRXN1* and *AKR1B10* were found to be the most responsive, they also had the lowest PoD (Hatherell et al. 2020). Care should be taking when a marker is too sensitive, since the potential of a compound to induce for example the Nrf2 pathway and results in adversity might be overestimated. An early response might be linked to the primary mode-of-action of the compound and be indicative that targeting the Nrf2 pathway is the primary event of the exposure at low concentrations, but not part of a general toxicity response that may involve other pathways and seen at high concentrations. Therefore, activation of protective pathways at low concentrations would be indicative of a beneficial effect of the compound *in vivo* rather than an adverse health effect. As a consequence, the use of a single marker or only stress-response pathway information is not enough to fully predict the ultimate adverse effect of a chemical. For example, some organophosphate (OP) pesticides we tested for Nrf2 pathway activation potential, did only activate the Nrf2 pathway at very high concentrations; yet at lower concentrations, the toxic effect of these compounds, acetylcholinesterase inhibition, might already occur *in vivo*. As the liver is the most prominent target tissue for adverse drug reactions, most test systems used in drug safety evaluation are focused on the liver to assess novel chemical drug entities for the liability to induce drug-induced liver injury. In other areas, especially in the field of environmental safety testing, efforts are made to establish test systems to measure the toxicity of a chemical compound in multiple organs like multiorgan-on-a-chip (multi-OoC) platforms as reviewed by Picollet-D'hahan et al. (Picollet-D'hahan et al. 2021).

FUTURE PROSPECTS

As technical abilities and knowledge regarding stress response pathways is growing, future biomarkers will probably consist of different key-players of these pathways. These biomarkers will be proteins, genes, microRNAs as well as several combinations of these markers together forming a biomarker fingerprint. Combining these markers enables us to make use of the strengths of each of these molecules and to overcome the weaknesses they have when used as a single biomarker. Recent advancement in measurement technologies enables the simultaneous detection of combinations of small molecules, proteins and microRNAs in one sample. Wang and Walt (2020), for example describe the simultaneous detection of interleukin 6 and miR-141 making use of single molecule arrays (Simoa). In this assay, Dye-encoded beads modified with specific capture probes were used to quantify each analyte (Wang and Walt 2020). These multiplex detection methods make it possible to measure multiple

markers in a single assay and therefore decrease the amount of sample needed (Cai et al. 2021; Jet et al. 2021; Nagarajan et al. 2020). Therefore, combining multiplex assays combined with e.g. lateral-flow immunoassays, makes these tools suited for point of care testing in clinical settings (Huang et al. 2020).

The greatest challenge however will be the usability/accessibility of the biomarker fingerprint in the *in vivo* situation. Biomarkers intended to be used as biomarkers for disease or biomarkers of exposure established *in vitro* should preferably have applicability *in vivo*. Therefore, all members of the biomarker panel should be easily obtained, preferable in blood, urine or saliva. Second, the marker should have the same function *in vivo* as established *in vitro*. This is especially challenging for microRNAs, as microRNAs might have different functions in different tissues. Subsequently, a microRNA mechanistically linked to a stress response pathway *in vitro* cannot necessarily be linked to its established mechanistic link to the stress response pathway *in vivo*. Therefore, simultaneous detection with other biomarkers that are reflective of the same biological perturbation might underpin the *in vivo* function of the microRNA. At this stage more research is necessary to obtain information regarding the different functions of microRNAs in different settings of disease and chemical exposure.

Recently, CRISPR-Cas9 based techniques are used to aid microRNA research. A CRISPR-Cas9 based “stoplight” reporter system is described by de Jong et al. (2020), which allows direct functional study of EV-mediated transfer of small noncoding RNA molecules at single-cell resolution. Data obtained can contribute to increase our understanding of the regulatory pathways that dictate the underlying processes by which microRNA function (de Jong et al. 2020). Furthermore, Wang et al. (2019) created a miRNA sensor that can measure microRNA activity at cellular levels by using a microRNA-mediated single guide RNA (sgRNA)-releasing strategy, which can be used to monitor the differentiation status of stem cells (Wang et al. 2019). Altogether this indicates the wide use of microRNAs and the new possibilities of combining microRNA knowledge with novel state of the art technologies, like CRISPR-Cas9, in different fields of research. In turn this could pave the way towards an improved understanding to discover novel mechanistic microRNA biomarkers of chemical exposure as well as novel disease modifying biomarkers.

REFERENCES

- Arshad AR, Sulaiman SA, Saperi AA, Jamal R, Mohamed Ibrahim N, Abdul Murad NA (2017) MicroRNAs and Target Genes As Biomarkers for the Diagnosis of Early Onset of Parkinson Disease. *Front Mol Neurosci* 10:352 doi:10.3389/fnmol.2017.00352
- Ashrafizadeh M, Ahmadi Z, Samarghandian S, et al. (2020) MicroRNA-mediated regulation of Nrf2 signaling pathway: Implications in disease therapy and protection against oxidative stress. *Life Sci* 244:117329 doi:10.1016/j.lfs.2020.117329
- Bergström P, Andersson HC, Gao Y, et al. (2011) Repeated transient sulforaphane stimulation in astrocytes leads to prolonged Nrf2-mediated gene expression and protection from superoxide-induced damage. *Neuropharmacology* 60(2-3):343-53 doi:10.1016/j.neuropharm.2010.09.023
- Bhattarai KR, Riaz TA, Kim H-R, Chae H-J (2021) The aftermath of the interplay between the endoplasmic reticulum stress response and redox signaling. *Experimental & Molecular Medicine* 53(2):151-167 doi:10.1038/s12276-021-00560-8
- Buschmann D, Kirchner B, Hermann S, et al. (2018) Evaluation of serum extracellular vesicle isolation methods for profiling miRNAs by next-generation sequencing. *Journal of extracellular vesicles* 7(1):1481321 doi:10.1080/20013078.2018.1481321
- Cai S, Pataillot-Meakin T, Shibakawa A, et al. (2021) Single-molecule amplification-free multiplexed detection of circulating microRNA cancer biomarkers from serum. *Nat Commun* 12(1):3515 doi:10.1038/s41467-021-23497-y
- Callegaro G, Kunnen SJ, Trairatphisan P, et al. (2021) The human hepatocyte TXG-MAPr: WGCNA transcriptomic modules to support mechanism-based risk assessment. *bioRxiv*:2021.05.17.444463 doi:10.1101/2021.05.17.444463
- Castañeda-Arriaga R, Pérez-González A, Reina M, Alvarez-Idaboy JR, Galano A (2018) Comprehensive Investigation of the Antioxidant and Pro-oxidant Effects of Phenolic Compounds: A Double-Edged Sword in the Context of Oxidative Stress? *The journal of physical chemistry B* 122(23):6198-6214 doi:10.1021/acs.jpcc.8b03500
- Charitou T, Bryan K, Lynn DJ (2016) Using biological networks to integrate, visualize and analyze genomics data. *Genet Sel Evol* 48:27 doi:10.1186/s12711-016-0205-1
- Cheng X, Ku CH, Siow RC (2013) Regulation of the Nrf2 antioxidant pathway by microRNAs: New players in micromanaging redox homeostasis. *Free Radic Biol Med* 64:4-11 doi:10.1016/j.freeradbiomed.2013.07.025
- de Jong OG, Murphy DE, Mager I, et al. (2020) A CRISPR-Cas9-based reporter system for single-cell detection of extracellular vesicle-mediated functional transfer of RNA. *Nat Commun* 11(1):1113 doi:10.1038/s41467-020-14977-8
- Emde A, Hornstein E (2014) miRNAs at the interface of cellular stress and disease. *Embo j* 33(13):1428-37 doi:10.15252/embj.201488142
- Endo S, Matsunaga T, Nishinaka T (2021) The Role of AKR1B10 in Physiology and Pathophysiology. *Metabolites* 11(6) doi:10.3390/metabo11060332
- Endzelins E, Berger A, Melne V, et al. (2017) Detection of circulating miRNAs: comparative analysis of extracellular vesicle-incorporated miRNAs and cell-free miRNAs in whole plasma of prostate cancer patients. *BMC Cancer* 17(1):730 doi:10.1186/s12885-017-3737-z
- Fabrizio FP, Sparaneo A, Trombetta D, Muscarella LA (2018) Epigenetic versus Genetic Deregulation of the KEAP1/NRF2 Axis in Solid Tumors: Focus on Methylation and Noncoding RNAs. *Oxidative medicine and cellular longevity* 2018:2492063-2492063 doi:10.1155/2018/2492063

- Ha SY, Yu JI, Choi C, et al. (2019) Prognostic significance of miR-122 expression after curative resection in patients with hepatocellular carcinoma. *Sci Rep* 9(1):14738 doi:10.1038/s41598-019-50594-2
- Hatherell S, Baltazar MT, Reynolds J, et al. (2020) Identifying and Characterizing Stress Pathways of Concern for Consumer Safety in Next-Generation Risk Assessment. *Toxicol Sci* 176(1):11-33 doi:10.1093/toxsci/kfaa054
- Huang L, Tian S, Zhao W, Liu K, Ma X, Guo J (2020) Multiplexed detection of biomarkers in lateral-flow immunoassays. *Analyst* 145(8):2828-2840 doi:10.1039/c9an02485a
- Jaramillo MC, Zhang DD (2013) The emerging role of the Nrf2-Keap1 signaling pathway in cancer. *Genes Dev* 27(20):2179-91 doi:10.1101/gad.225680.113
- Jet T, Gines G, Rondelez Y, Taly V (2021) Advances in multiplexed techniques for the detection and quantification of microRNAs. *Chem Soc Rev* 50(6):4141-4161 doi:10.1039/d0cs00609b
- Jopling C (2012) Liver-specific microRNA-122: Biogenesis and function. *RNA Biol* 9(2):137-42 doi:10.4161/rna.18827
- Ma X, Tao R, Li L, et al. (2019) Identification of a 5microRNA signature and hub miRNA-mRNA interactions associated with pancreatic cancer. *Oncol Rep* 41(1):292-300 doi:10.3892/or.2018.6820
- Madboly AG, Alhusseini NF, Abd El Rahman SM, El Gazzar WB, Idris AMM (2019) Serum miR-122 and miR-192 as biomarkers of intrinsic and idiosyncratic acute hepatotoxicity: A quantitative real-time polymerase chain reaction study in adult albino rats. *Journal of Biochemical and Molecular Toxicology* 33(7):e22321 doi:https://doi.org/10.1002/jbt.22321
- Mamdani M, Williamson V, McMichael GO, et al. (2015) Integrating mRNA and miRNA Weighted Gene Co-Expression Networks with eQTLs in the Nucleus Accumbens of Subjects with Alcohol Dependence. *PLoS One* 10(9):e0137671 doi:10.1371/journal.pone.0137671
- Mathew ST, Bergström P, Hammarsten O (2014) Repeated Nrf2 stimulation using sulforaphane protects fibroblasts from ionizing radiation. *Toxicol Appl Pharmacol* 276(3):188-94 doi:10.1016/j.taap.2014.02.013
- Mendell JT, Olson EN (2012) MicroRNAs in stress signaling and human disease. *Cell* 148(6):1172-87 doi:10.1016/j.cell.2012.02.005
- Nagarajan MB, Tentori AM, Zhang WC, Slack FJ, Doyle PS (2020) Spatially resolved and multiplexed MicroRNA quantification from tissue using nanoliter well arrays. *Microsyst Nanoeng* 6:51 doi:10.1038/s41378-020-0169-8
- Peter ME (2010) Targeting of mRNAs by multiple miRNAs: the next step. *Oncogene* 29(15):2161-2164 doi:10.1038/onc.2010.59
- Picollet-D'hahan N, Zuchowska A, Lemeunier I, Le Gac S (2021) Multiorgan-on-a-Chip: A Systemic Approach To Model and Decipher Inter-Organ Communication. *Trends in Biotechnology* 39(8):788-810 doi:https://doi.org/10.1016/j.tibtech.2020.11.014
- Qin D, Wei R, Liu S, Zhu S, Zhang S, Min L (2019) A Circulating miRNA-Based Scoring System Established by WGCNA to Predict Colon Cancer. *Anal Cell Pathol (Amst)* 2019:1571045 doi:10.1155/2019/1571045
- Rooney JP, Chorley B, Hiemstra S, et al. (2020) Mining a human transcriptome database for chemical modulators of NRF2. *PLoS One* 15(9):e0239367 doi:10.1371/journal.pone.0239367
- Saelens W, Cannoodt R, Saeys Y (2018) A comprehensive evaluation of module detection methods for gene expression data. *Nat Commun* 9(1):1090 doi:10.1038/s41467-018-03424-4
- Shah NM, Rushworth SA, Murray MY, Bowles KM, MacEwan DJ (2013) Understanding the role of NRF2-regulated miRNAs in human malignancies. *Oncotarget* 4(8):1130-42 doi:10.18632/oncotarget.1181

- Soleimani Zakeri NS, Pashazadeh S, MotieGhader H (2020) Gene biomarker discovery at different stages of Alzheimer using gene co-expression network approach. *Scientific Reports* 10(1):12210 doi:10.1038/s41598-020-69249-8
- Soriano FX, Léveillé F, Papadia S, et al. (2008) Induction of sulfiredoxin expression and reduction of peroxiredoxin hyperoxidation by the neuroprotective Nrf2 activator 3H-1,2-dithiole-3-thione. *Journal of neurochemistry* 107(2):533-43 doi:10.1111/j.1471-4159.2008.05648.x
- Stein EV, Duewer DL, Farkas N, Romsos EL, Wang L, Cole KD (2017) Steps to achieve quantitative measurements of microRNA using two step droplet digital PCR. *PLoS One* 12(11):e0188085 doi:10.1371/journal.pone.0188085
- Sutherland JJ, Webster YW, Willy JA, et al. (2018) Toxicogenomic module associations with pathogenesis: a network-based approach to understanding drug toxicity. *The Pharmacogenomics Journal* 18(3):377-390 doi:10.1038/tpj.2017.17
- Vassalle C, Maltinti M, Sabatino L (2020) Targeting Oxidative Stress for Disease Prevention and Therapy: Where Do We Stand, and Where Do We Go from Here. *Molecules* 25(11) doi:10.3390/molecules25112653
- Wang X, Walt DR (2020) Simultaneous detection of small molecules, proteins and microRNAs using single molecule arrays. *Chem Sci* 11(30):7896-7903 doi:10.1039/d0sc02552f
- Wang XW, Hu LF, Hao J, et al. (2019) A microRNA-inducible CRISPR-Cas9 platform serves as a microRNA sensor and cell-type-specific genome regulation tool. *Nat Cell Biol* 21(4):522-530 doi:10.1038/s41556-019-0292-7
- Xing TJ, Xu HT, Yu WQ, Jiang DF (2013) Methylation regulation of liver-specific microRNA-122 expression and its effects on the proliferation and apoptosis of hepatocellular carcinoma cells. *Genetics and molecular research: GMR* 12(3):3588-97 doi:10.4238/2013.September.13.3

7

Appendices

LIST OF ABBREVIATIONS

A	ABCC2	ATP binding cassette subfamily C member 2
	AKR1B10	Aldo-keto reductase family 1 member B10
	AKR1C3	Aldo-keto reductase family 1 member C3
	ARE	Antioxidant response element
B	BAC	Bacterial artificial chromosomes
	BMC	Bench mark concentration
C	CDDO-Me	Bardoxolone methyl
D	DEM	Diethyl maleate
	DMEM	Dulbecco's modified eagle medium
	DMSO	Dimethyl sulfoxide
E	EGS	Eigengene scores
	ERS	Endoplasmic reticulum stress
F	FBS	Fetal bovine serum
G	GCLM	Glutamate-cysteine ligase modifier subunit
	GFP	Green fluorescent protein
	GSH	Glutathione
H	HepG2	Hepatoma G2 / human liver cancer cell line
	Hmox1	Hemeoxygenase 1
K	Keap1	Kelch-like ECH-associated protein 1
M	miR / miRNA	MicroRNA
N	NAM	New approach methodology
	Nqo1	NAD(P)H-quinone oxidoreductase 1
	Nrf2	Nuclear factor erythroid 2-related factor 2
P	PHH	Primary human hepatocytes
	PI	Propidium iodide
R	RISC	RNA-Induced Silencing Complex
	NS	Reactive nitrogen species
	ROS	Reactive oxygen species
S	SQSTM1	Sequestosome 1 / p62
	Srxn1	Sulfiredoxin1
T	tBHP	<i>Tert</i> -butylhydroperoxide
	tBHQ	<i>Tert</i> -butylhydroquinone
U	UPR	Unfolded protein response
W	WMC	Watershed masked clustering

ENGLISH SUMMARY

There is an increasing number of chemicals that enter the society, including drugs, environmental chemicals and cosmetics, combined also referred to as the chemical exposome. Likewise there is an increased hazard for chemically-induced health effects. Chemicals can interfere with biological systems and induce compound-specific responses, either related to the pharmacological on- or off-target effects. In particular compounds with (in)direct electrophilic reactivity are of direct harm to cells. Such compounds will interfere with normal cellular physiological processes and activate adaptive cellular stress responses that try to repair the cellular injury. Understanding the fundamental relationship between activation of these cellular stress responses and ultimate onset of cytotoxicity can be used for constructing mechanism-based biomarkers.

In this study we focused on the oxidative stress response, also known as the Nrf2 pathway named after its transcription factor, nuclear factor erythroid 2-related factor 2 (Nrf2). The Nrf2 pathway plays a role in protection against chemicals with soft electrophile properties and that propagate the generation of reactive oxygen species (ROS), which may lead to oxidative stress with cell death as an ultimate outcome. Recently it became clear that besides genes and proteins also microRNA, a type of small non-coding RNA, play an important role in the regulation of stress response pathways.

A literature study was conducted to obtain information related to microRNA up/down regulation after exposure to a diverse panel of chemicals. Results of this study are presented in **Chapter 2**. We found that the microRNAs most frequently found to be dysregulated are also found to play a role in various diseases linked to chemical exposure. Although microRNA expression changes show great potential as biomarkers, questions concerning biomarker robustness, biological functionality and adverse outcome causality of the response still remain. It remains unclear whether these microRNAs detected in the blood or other body fluids, represent a mechanistic biomarker that could reflect on the mode of action regarding the toxicity of a chemical compound. So far, biomarkers measured in the blood have not per se been discovered in relation to their mode of action. Therefore, the question still has to be answered whether or not the rise of certain microRNAs found in the blood has indeed a functional role, or that the change in expression is just the result of tissue damage. However, microRNAs which are known to be strongly related to a specific organ, like miR-122 for the liver, can provide valuable information about which organ is damaged upon exposure to a chemical or during disease.

Defining whether the candidate microRNA biomarkers play an integral functional role in disease mechanism is a difficult task. One single microRNA might have hundreds of different targets and, as a consequence, the role of the microRNA might differ between different tissues. Furthermore, a microRNA can both increase or diminish the stress response depending on their involvement in the inhibition of negative regulators in a positive feedback loop or as part of a negative feedback loop, respectively. New emerging techniques like droplet digital PCR and measurements in different biological matrices like extracellular vesicles enable more in depth research on microRNAs.

In order to investigate the role of microRNAs on the Nrf2 pathway, we screened a panel of ~2600 individual microRNA mimics using an endogenous Nrf2 target *Srxn1*-GFP HepG2 reporter cell line in combination with high throughput live confocal imaging after treatment with CDDO-Me. In this research, presented in **Chapter 3**, we identified a panel of 16 microRNAs that enhance (including miR-3165, miR-1909-3p, miR-1293, and miR-6499-3p) and 10 microRNAs that inhibit (including miR-200a-3p, miR-363-3p, miR-502-5p, and miR-25-3p) CDDO-Me-induced *Srxn1*-GFP expression. These microRNAs might be relevant biomarkers and/or provide alternative therapeutic modalities to modulate Nrf2 pathway activity in health and disease. In conclusion, this study for the first time elucidated the spectrum of microRNAs that target the Nrf2 signalling pathway.

The microRNAs found in our study that enhance or inhibit the Nrf2 pathway might provide opportunities for microRNA therapeutics that target the Nrf2 pathway. Enhanced Nrf2 pathway activation is considered as a pro-oncogenic pathway. Therefore, to obtain information concerning the primary response upon microRNA expression changes, there is a need to perform further temporal analysis of the transcriptional changes after microRNA transfection. MicroRNAs which are able to inhibit the Nrf2 pathway might be used to make cancer cells more vulnerable for chemo- and radiotherapy. MicroRNAs enhancing the Nrf2 pathway might be used to enhance a person's protection against oxidative stress. Additional research on the dose response and long term safety profile of our candidate Nrf2 modulating microRNAs is required. Caution, however, has to be made to link microRNAs which alter the Nrf2 response directly to Nrf2, as microRNAs can regulate the Nrf2 pathway via different ways: 1) by affecting the nuclear translocation of Nrf2, and 2) by influencing the expression of Nrf2, regulating the upstream mediators of Nrf2 and modulation of *KEAP1*. Furthermore, also redox stress itself can alter the microRNA biogenesis and processing pathway leading, for example, to altered redox signaling and disease mechanisms.

As in daily life not only single exposure to a chemical takes place, but also repeated exposure to a chemical substance may occur. However, our general understanding of the dynamics of cellular stress response pathway activation in repeated treatment scenarios is limited. In order to study the dynamics of the Nrf2 pathway upon repeated exposure we used confocal microscopy in combination with HepG2-GFP reporter cells. These cells were repeatedly exposed to a concentration range of diethyl maleate (DEM) and tert-butylhydroquinone (tBHQ). The outcome of this study is described in **Chapter 4**. Interestingly, we found that the amount of Nrf2 in the nucleus after a second treatment after 24 h was lower than the amount measured after the first exposure with the same concentration, indicating that the Nrf2 response is adaptive. However, the amount of Srxn1 measured in the cell was three-fold higher compared to the first treatment. Although more research is needed to unravel the precise mechanism, it is clear that repeated exposure testing will add valuable extra information in testing the safety of a chemical or drug. Furthermore, as indicated by several studies, preconditioning might be used for therapeutic approaches using low non-toxic concentrations of a Nrf2-pathway inducing chemical to protect against exposure to a toxic concentration. However, challenge remains in finding the optimum dosing regimen: dose per treatment, time between treatments and number of repeated treatments.

As activation of the Nrf2 pathway upon chemical exposure might indicate oxidative damage, we hypothesized that the ability of chemical compounds to induce oxidative stress and to stimulate a Nrf2 mediated oxidative stress response can be determined by the temporal dynamics of the stress response proteins combined with transcriptomic expression profiles.

To test this hypothesis, a panel of different phenolic compounds was used that were either redox cycling phenols, alkylated phenols, or non-redox cycling phenols. Outcomes of this study are described in **Chapter 5**. We integrated high throughput transcriptomics using targeted RNA sequencing of primary human hepatocytes (PHH) and HepG2-WT and HepG2 Nrf2-GFP and Srxn1-GFP reporter cell lines. Using a panel of five pro-oxidants, including CDDO-Me, sulforaphane, tert-butylhydroperoxide, etacrynic acid and diethyl maleate, we identified a panel of five Nrf2 target genes that could define oxidative stress potential: *AKR1B10*, *SRXN1*, *ABCC2*, *AKR1C3* and *NQO1*. Next, we measured the response of these five genes after exposure to different concentrations of the three types of phenols. We found that measurement of these five genes could be used to discriminate between the three types of phenolic compounds. Furthermore, we demonstrated that integration of high throughput HepG2 Nrf2 pathway reporter cell line data with transcriptomics data from HepG2 and PHH, provides valuable mechanistic information on mode-of-action of structural similar phenolic compounds and their biological similarity.

In summary, the research described in this thesis provides additional information concerning the dynamics of the Nrf2 pathway upon single and repeated exposure and the use of key players involved in this pathway as, part of a panel of, mechanistic biomarkers of chemical exposure as well as disease. Especially microRNAs might add value to these biomarker panels. Furthermore, obtaining more knowledge concerning their role in stress response pathways enables elucidation of the exact mode of action of these stress response pathways.

NEDERLANDSE SAMENVATTING

Er is een toenemend aantal chemische stoffen in de samenleving, waaronder geneesmiddelen, milieugevaarlijke stoffen en cosmetica, samen ook wel aangeduid als het “chemisch exposoom”. Evenzo is er een verhoogd gevaar voor chemisch geïnduceerde gezondheidseffecten. Chemische stoffen kunnen interfereren met biologische systemen en stof specifieke reacties induceren gerelateerd aan de farmacologische on- of off-target-effecten. In het bijzonder chemische stoffen met een (in)directe elektrofiële reactiviteit zijn rechtstreeks schadelijk voor cellen. Dergelijke chemische stoffen interfereren met normale cellulaire fysiologische processen en zorgen voor activatie van adaptieve cellulaire stressreacties die de cellulaire schade trachten te herstellen. Inzicht in de fundamentele relatie tussen activering van deze cellulaire stressreacties en het uiteindelijke ontstaan van cytotoxiciteit kan worden gebruikt voor het construeren van mechanistische biomarkers.

In deze studie hebben we ons gericht op de adaptive respons die een rol speelt bij de bescherming tegen chemische stoffen met “zachte” elektrofiële eigenschappen en stoffen die de aanmaak van reactieve zuurstofcomponenten (reactive oxygen species (ROS)) bevorderen, de oxidative stress response. De oxidatieve stress respons staat ook bekend als de Nrf2 gemedieerde oxidatieve stress respons genoemd naar zijn transcriptiefactor, nuclear factor erythroid 2-related factor 2 (Nrf2). Onlangs werd duidelijk dat naast genen en eiwitten, microRNA, een type kort, niet coderend RNA, een belangrijke rol speelt bij de regulering van stress responsen.

Blootstelling aan een chemische stof kan leiden tot verstoring in de regulatie van microRNA's.

Om meer inzicht te krijgen in het de verschillen in expressie van microRNA, in verschillende biologische matrices, na chemische blootstelling werd een literatuurstudie uitgevoerd. De resultaten van deze studie worden gepresenteerd in **Hoofdstuk 2**. We ontdekten dat de microRNA's die het meest frequent ontregeld bleken te zijn, ook een rol bleken te spelen bij verschillende ziekten die verband houden met blootstelling aan chemische stoffen. Hoewel veranderingen in de expressie van microRNA's een groot potentieel hebben om als biomarker gebruikt te worden, blijven er vragen bestaan over de robuustheid van microRNA als biomarker, de biologische functionaliteit en de causaliteit van de respons. Het blijft onduidelijk of microRNA's die in het bloed, of eventueel een ander lichaamsvocht, kunnen worden gedetecteerd gebruikt kunnen worden als een mechanistische biomarker die informatie verschaffen over het werkingsmechanisme achter de toxiciteit van een bepaalde chemische stof. Tot dusver zijn in het bloed gemeten biomarkers

nog niet eenduidig te linken aan hun werkingsmechanisme. Het is nog steeds onduidelijk of de verandering in expressie van bepaalde microRNA's gemeten in het bloed, inderdaad een functionele rol heeft, dan wel of de verandering in expressie gewoon het gevolg is van weefselschade. MicroRNA's waarvan bekend is dat zij sterk gerelateerd zijn aan een specifiek orgaan, zoals miR-122 voor de lever, kunnen in ieder geval waardevolle informatie verschaffen over welk orgaan beschadigd is bij blootstelling aan een chemische stof of tijdens ziekte.

Het is ingewikkeld om te bepalen of kandidaat-microRNA biomarkers een functionele rol spelen in het ziektemechanisme. Eén enkele microRNA kan honderden verschillende targets hebben waardoor de rol van een microRNA in verschillende weefsels verschillend kan zijn. Een microRNA kan de stressrespons zowel versterken, als het onderdeel is van een positieve feedback loop, als verzwakken. Dit laatste gebeurt als de microRNA betrokken is bij de remming van negatieve regulatoren (negatieve feedback loop).

Het is nog steeds een uitdaging om microRNA goed te meten. Nieuwe meettechnieken, zoals droplet digital PCR en nieuwe strategieën om samples te verkrijgen, zoals het kunnen scheiden van microRNA bevattende extracellulaire vesicles, maken vervolg stappen op het gebied van microRNA onderzoek mogelijk. Om de rol van microRNA's in de Nrf2 gemedieerde oxidatieve stress respons te onderzoeken, hebben we gekeken naar het effect van van ~2600 individuele microRNA mimics op de activatie van GFP-gelabeld *Srxn1*, een Nrf2 target, na blootstelling aan de electrofiele stof CDDO-Me. In dit onderzoek, gepresenteerd in **Hoofdstuk 3**, identificeerden we een panel van 16 microRNA's die de CDDO-Me-geïnduceerde *Srxn1*-GFP expressie versterken (waaronder miR-3165, miR-1909-3p, miR-1293, en miR-6499-3p) en 10 microRNA's die de CDDO-Me-geïnduceerde *Srxn1*-GFP expressie remmen (waaronder miR-200a-3p, miR-363-3p, miR-502-5p, en miR-25-3p). Deze microRNA's zouden relevante biomarkers kunnen zijn en/of alternatieve therapeutische targets kunnen bieden om de activiteit van de Nrf2 gemedieerde oxidatieve stress respons in gezondheid (preventief) en ziekte te moduleren. Concluderend, deze studie laat voor het eerst het geheel aan microRNA's zien die de Nrf2 gemedieerde oxidatieve stress respons als target hebben.

De microRNA's die volgens onze studie de Nrf2 gemedieerde oxidatieve stress respons versterken of remmen, zouden gebruikt kunnen worden als microRNA therapeutica die zich richten op de Nrf2 gemedieerde oxidatieve stress respons. Verhoogde activering van de Nrf2 gemedieerde oxidatieve stress respons wordt beschouwd als een pro-oncogene respons. Daarom, om informatie te verkrijgen

over de primaire respons op microRNA expressie veranderingen, is er behoefte aan verdere temporele analyse van de transcriptionele veranderingen na microRNA transfectie. MicroRNA's die in staat zijn de Nrf2 gemedieerde oxidatieve stress respons te remmen, kunnen worden gebruikt om kankercellen kwetsbaarder te maken voor chemo- en radiotherapie. MicroRNA's die de Nrf2 gemedieerde oxidatieve stress respons versterken, zouden gebruikt kunnen worden om de bescherming tegen oxidatieve stress te ondersteunen. Aanvullend onderzoek is nodig om inzicht te krijgen in de dosis-respons relatie van onze kandidaat Nrf2 modulerende microRNA's en hoe veilig (lange termijn) gebruik van microRNA is als therapie. Voorzichtigheid is echter geboden om microRNA's die de Nrf2 respons veranderen als direct target van Nrf2 te bestempelen. MicroRNA's kunnen de Nrf2 route namelijk op verschillende manieren reguleren: 1) door de nucleaire translocatie van Nrf2 te beïnvloeden, en 2) door de expressie van Nrf2 te beïnvloeden door de upstream mediators van Nrf2 te reguleren en middels de modulatie van *KEAP1*. Verder kan ook redox stress op zichzelf de aanmaak van microRNA's beïnvloeden, wat bijvoorbeeld kan leiden tot veranderde redox signalering en ziekte mechanismen.

In het dagelijks leven vindt niet alleen eenmalige blootstelling aan een chemische stof plaats, maar wordt je ook herhaaldelijk blootgesteld aan chemische stoffen. Desondanks is onze kennis betreffende de dynamiek van de oxidatieve stress respons bij herhaalde blootstelling klein. Om deze dynamiek bij herhaalde blootstelling te bestuderen, gebruikten we confocaal microscopie in combinatie met HepG2-GFP reporter cellen. Deze cellen werden herhaaldelijk blootgesteld aan verschillende concentraties diethylmaleaat (DEM) en tert-butylhydroquinone (tBHQ). Het resultaat van deze studie wordt beschreven in **Hoofdstuk 4**. Interessant is de bevinding dat na een tweede behandeling na 24 uur er minder Nrf2 in de kern werd gemeten dan na de eerste blootstelling met dezelfde concentratie. Dit geeft aan dat de Nrf2 gemedieerde oxidatieve stress respons adaptief is. Echter, de hoeveelheid *Srxn1* in de cel was driemaal zo hoog in vergelijking met de eerste behandeling. Hoewel meer onderzoek nodig is om het precieze mechanisme te ontrafelen, is het duidelijk dat herhaalde blootstellingstesten waardevolle extra informatie kunnen verschaffen bij het beoordelen van de veiligheid van een chemische stof of geneesmiddel. Bovendien zou, zoals uit verschillende studies blijkt, preconditionering kunnen worden gebruikt voor therapeutische benaderingen waarbij lage niet-toxische concentraties van een chemische stof die de oxidatieve stress respons activeert kan worden gebruikt om bescherming op te bouwen tegen een toxische concentratie. Het blijft echter een uitdaging om het optimale doseringsschema te vinden: dosis per behandeling, tijd tussen de behandelingen en aantal herhaalde behandelingen.

Aangezien activering van de Nrf2 gemedieerde oxidatieve stress respons bij chemische blootstelling zou kunnen wijzen op oxidatieve schade, formuleerde we de hypothese dat het vermogen van chemische stoffen om oxidatieve stress te veroorzaken en een Nrf2 gemedieerde oxidatieve stress respons te stimuleren kan worden afgeleid aan de hand van de temporele dynamiek van stress respons eiwitten gecombineerd met transcriptoom expressie profielen.

Om deze hypothese te testen werd een panel van verschillende fenolen gebruikt: redox cyclische fenolen, gealkyleerde fenolen, of niet-redox cyclische fenolen. De resultaten van deze studie worden beschreven in **Hoofdstuk 5**. We integreerden high throughput transcriptomics met behulp van gerichte RNA sequencing van primaire menselijke hepatocyten (PHH) en HepG2 Nrf2-GFP en Srxn1-GFP reporter cellijnen. Gebruikmakend van een panel van vijf pro-oxidanten, waaronder CDDO-Me, sulforafaan, tert-butylhydroperoxide, etacrynic acid en diethylmaleaat, identificeerden we een panel van vijf Nrf2 target genen die het oxidatieve stresspotentieel zouden kunnen bepalen: *AKR1B10*, *SRXN1*, *ABCC2*, *AKR1C3* en *NQO1*. Vervolgens werd de response van deze vijf genen gemeten na blootstelling aan verschillende concentraties van de drie typen fenolen.

Onze bevinding was dat het meten van deze vijf genen gebruikt kon worden om de drie gedefinieerde typen fenolen van elkaar te onderscheiden. We laten hier ook mee zien dat integratie van high throughput HepG2 gemedieerde oxidatieve stress respons reporter cellijn data met transcriptomics data van HepG2 en PHH cellen, waardevolle mechanistische informatie oplevert over het werkingsmechanisme van structureel verwante fenolen.

Samenvattend, het onderzoek beschreven in dit proefschrift levert aanvullende informatie over de dynamiek van de Nrf2 gemedieerde oxidatieve stress respons bij eenmalige en herhaalde blootstelling en het mogelijke gebruik van belangrijke spelers in deze stress respons als onderdeel van een panel van mechanistische biomarkers voor chemische blootstelling en ziekte. Vooral microRNA's zouden van toegevoegde waarde kunnen zijn in deze biomarkerpanels. Bovendien kan door het vergaren van meer inzicht over de rol van microRNA's in stress responsen het precieze werkingsmechanisme van deze stress responsen worden ontrafeld.

LIST OF PUBLICATIONS

A systematic analysis of Nrf2 pathway activation dynamics during repeated xenobiotic exposure

Luc J. M. Bischoff[‡], Isoude A. Kuijper[‡], Johannes P. Schimming, Liesanne Wolter, Bas ter Braak, Jan P. Langenberg, Daan Noort, Joost B. Beltman, and Bob van de Water.
Arch Toxicol, 2019, 93(2):435-451

[‡]Both authors contributed equally

MicroRNA patterns as biomarkers for chemical exposure and disease

Luc J.M. Bischoff, Jan P. Langenberg, Daan Noort, and Bob van de Water.
Manuscript in preparation.

Screening the microRNA landscape of Nrf2 pathway modulation identifies miR-6499-3p as a novel modulator of the anti-oxidant response through targeting of KEAP1

Luc J.M. Bischoff, Nanette G. Vrijenhoek, Johannes P. Schimming, Anke H.W. Essing, Lukas S. Wijaya, Jan P. Langenberg, Daan Noort, and Bob van de Water
Manuscript in preparation.

A systematic high throughput transcriptomics and phenotypic screening approach to classify the pro-oxidant mode-of-action of a large class of phenolic compounds

Luc J.M. Bischoff[‡], Johannes P. Schimming[‡], Wanda van der Stel, Marije Niemeijer, Sylvia Escher, Giulia Callegaro, Bas ter Braak, Jan P. Langenberg, Daan Noort, and Bob van de Water

[‡]Both authors contributed equally

Manuscript in preparation.

CURRICULUM VITAE

Lucas Jacobus Marie (Luc) Bischoff was born on June 4th, 1984 in Boxmeer, the Netherlands.

From 1996 to 2002 he attended the Christian Huygens College in Eindhoven, where he graduated in 2002. In that same year he went to study medical technical nursing at Fontys University of Applied Sciences in Eindhoven. In 2005 however he left to study at the James Boswell institute in Utrecht to obtain certificates at WO level of chemistry, physics, mathematics and biology to be accepted at a Dutch university.

In 2006 he was admitted at the Radboud University in Nijmegen where he studied biomedical sciences with a major in toxicology and a minor in occupational and environmental health.

During his study he did an internship in the Department of Biochemistry, Nijmegen Centre for Molecular Life Sciences, Department of Blood transfusion and Transplantation Immunology of the Radboud University Nijmegen Medical Centre on the topic "Vesicles of circulating cells as potential biomarkers for human disease".

Fascinated by the topic of biomarkers he conducted a literature study in the CBRN Protection department of TNO Defence, Security and Safety in Rijswijk on the topic: "Biomarkers of physiological responses to chemical exposures that occurred during military operations", followed by an internship on the topic "Model development for an immunological, persistent biomarker of chemical exposure".

After receiving his master degree in 2011, he worked as a research scientist at TNO Defence, Security and Safety in Rijswijk, and contributed to projects involving immunotoxicity, biomarkers, nano-toxicity, *in vitro* cell models, and *in vivo* animal models.

In 2014 he started as a PhD student at the Leiden Academic Center for Drug Research (LACDR) at the Leiden University, on the project "Dynamics and regulation of the oxidative stress response upon chemical exposure", which was sponsored by TNO and the Dutch Ministry of Defence.

In 2018 he worked with great enthusiasm in the department of Systems Biomedicine & Pharmacology of the LACDR, where he worked on a project aimed at finding early biomarkers of Alzheimer's Disease, which included the measurement of microRNAs in blood samples.

Since 2019 he is employed by the Dutch Ministry of Defence as chemical safety advisor.